Nitrogen cycling in technical water systems

Dissertation

zur Erlangung des akademischen Grades eines Doktors der Naturwissenschaften

– Dr. rer. nat. –

vorgelegt von

Julia Heise

geboren in Warburg

Fakultät für Chemie der Universität Duisburg-Essen

2020

Die vorliegende Dissertation wurde im Zeitraum von März 2015 bis September 2018 im Arbeitskreis von Prof. Dr. Rainer Meckenstock am Biofilm Centre der Universität Duisburg-Essen durchgeführt.

Gutachter: Prof. Dr. Rainer Meckenstock

Prof. Dr. Martin Denecke

Tag der Disputation: 04.03.2021

Vorsitzende: PD Dr. Ursula Telgheder

DOI: 10.17185/duepublico/74169
URN: urn:nbn:de:hbz:464-20210419-101545-7

For my Family.

Table of contents

Abbreviations

°C	degree Celsius (unit)
ΔG^0	Gibb's free energy
A	Ampere (unit)
AMO	ammonia monooxygenase
anammox	anaerobic ammonium oxidation
asv	amplicon sequencing variant(s)
BES	bioelectrochemical system(s)
bp	base pairs (unit)
CO_2	carbon dioxide
comammox	complete ammonium oxidation
Cq	threshold cycle(s)
DGGE	denaturing gradient gel electrophoresis
DNA	deoxyribonucleic acid
dNTP	2´-desoxyribonucleosid-5´-triphosphate
EPS	extracellular polymeric substances
g	gram (unit)
h	hour (unit)
hao	hydroxylamine dehydrogenase gene
hcp	hydroxylamine reductase gene
HDH	hydrazine dehydrogenase
HZS	hydrazine synthase
J	Joule, 1 V A s (unit)
k (prefix)	kilo, 10^3 (unit)
L	litre (unit)
µ (prefix)	micro, 10^{-6} (unit)
m (prefix)	milli, 10^{-3} (unit)
min	minute (unit)
mmo	methane monooxygenase gene
mol	mole (unit)
n (prefix)	nano, 10^{-9} (unit)
n.a.	not available, not detected
N_2	elemental nitrogen
N_2H_4	hydrazine

N_2O	nitrous oxide
NAP	(periplasm-bound) nitrate reductase
NAR	(membrane-bound) nitrate reductase
NH_2OH	hydroxylamine
NH_3	ammonia
NH_4^+	ammonium ion
NIR	nitrite reductase
NO	nitric oxide
NO_2^-	nitrite
NO_2^--N	nitrite-nitrogen, referring to the nitrogen atom in nitrite
NO_3^-	nitrate
NO_3^--N	nitrate-nitrogen, referring to the nitrogen atom in nitrate
NOR	nitric oxide reductase
NOS	nitrous oxide reductase
NXR	nitrite oxidoreductase
OTU(s)	operational taxonomy unit(s)
PMO	particulate methane monooxygenase
(q)PCR	(quantitative) polymerase chain reaction
RAS	recirculating aquaculture system
RF(s)	restriction fragment(s)
RFLP	restriction fragment length polymorphism
RFU	relative fluorescence units (unit)
rpm	rounds per minute (unit)
rRNA	ribosomal ribonucleic acid
s	second (unit)
T-RFLP	terminal restriction fragment length polymorphism
U	unit of enzyme activity, µmol substrate min^{-1}
V vs. Ag/AgCl	Volt versus silver/silver chloride reference electrode (unit)
WHO	World's Health Organisation
WWTP(s)	wastewater treatment plant(s)

1. General Introduction

1.1. **The nitrogen cycle**

Nitrogen is one of the most abundant elements on earth. The atmosphere contains a volume fraction of 78% dinitrogen (N_2). It is also an essential component of many biomolecules, such as nucleic acids and amino acids. For microorganisms, it is one of the major elements in demand together with carbon, oxygen, hydrogen, phosphorous, and sulphur (Madigan & Martinko, 2006). However, dinitrogen is an inert gas and its fixation is highly energy intensive. Only few microorganisms are capable of fixing the molecular nitrogen. The nitrogen available for microorganisms represents a small fraction and is cycled between organic nitrogen found in biomass, dead organic matter and soluble inorganic nitrogen salts in biogeochemical processes (Figure 1.8.1-1) (Maier *et al.*, 2009).

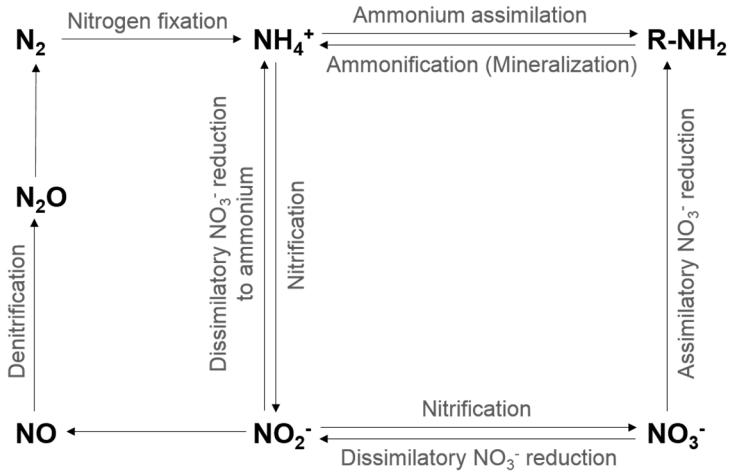

Figure 1.8.1-1 | The nitrogen cycle adapted from (Maier *et al.*, 2009) .

Nitrogen can obtain oxidation states between -3 in ammonium (NH_4^+) and +5 in nitrate (NO_3^-) during fixation, ammonification, assimilation, nitrification, and denitrification processes. While the nitrification process depends on the availability of oxygen, denitrification of nitrate to ammonium and dissimilatory reduction of nitrate to ammonium are carried out under anoxic conditions using nitrogen as electron acceptor (Madigan & Martinko, 2006).

1.2. **The nitrification process**

Nitrification describes the two-step oxidation process of ammonia (NH_4^+) to nitrate (NO_3^-) via the intermediate nitrite (NO_2^-). It is predominantly carried out under aerobic and chemoautotrophic conditions (Maier *et al.*, 2009) and both reaction steps deliver energy (Eq. 1.2-1 – 1.2-3) (van Kessel *et al.*, 2015). Most of the energy is used for CO_2 fixation via the reductive tricarboxylic acid cycle (Klotz *et al.*, 2006, Lücker *et al.*, 2010, Daims *et al.*, 2015). Some species produce carboxysomes for accumulation of the enzyme ribulose-1,5-bisphosphate carboxylase/oxygenase (RuBisCO) to enhance CO_2 fixation (Koops *et al.*, 1991).

$NH_4^+ + 1.5\ O_2 \rightarrow NO_2^- + H_2O + 2\ H^+$	$\Delta G^0 = -274.7$ kJ mol^{-1}	(Eq. 1.2-1)
$NO_2^- + 0.5\ O_2 \rightarrow NO_3^-$	$\Delta G^0 = -74.1$ kJ mol^{-1}	(Eq. 1.2-2)
$NH_4^+ + 2\ O_2 \rightarrow NO_3^- + H_2O + 2\ H^+$	$\Delta G^0 = -348.9$ kJ mol^{-1}	(Eq. 1.2-3)

Depending on the pH in the system, ammonium exists in the form of ammonia (NH_3) or the ammonium ion (NH_4^+). The equilibrium is favoured towards the ionised form at acidic and near-neutral pH. The pH optimum for nitrification is between 6.6 to 8.0. Below pH 4.5 the reaction process seems to be inhibited (Maier *et al.*, 2009). Nevertheless, it was shown that nitrification can also occur at pH 4 in aggregations of chemolithotrophic bacteria due to their protection against nitrous oxide within the cell aggregates (De Boer *et al.*, 1991). At near-neutral pH nitrite might accumulate in the system as it was recently described in soil (Tierling & Kuhlmann, 2018). Ammonia is naturally not or only present in small amounts in groundwater exhibiting a neutral level of 0.2 mg NH_4^+ L^{-1}. The limit value of ammonia in groundwater and in surface waters is 0.3 mg NH_4^+ L^{-1} (TrinkwV, 2001, Wricke, 2014).

The two-step nitrification process is carried out by two physiological distinct groups of microorganisms (Koops *et al.*, 2006). Bacteria performing the first oxidation step from ammonia to nitrite are labelled with the prefix *Nitroso-* (e.g. *Nitrosomonas*), while those responsible for the second step show the prefix *Nitro-* (e.g. *Nitrobacter*, *Nitrospira*). Aerobic ammonia oxidising bacteria and nitrite oxidising bacteria are gram

negative and belong to the *Alpha*-, *Beta*-, *Gamma*-, and *Deltaproteobacteria*. *Nitrospira* comprise their own phylum. They are commonly coexisting in many different terrestrial and aquatic environments (Madigan & Martinko, 2006, Maier *et al.*, 2009).

Ammonium is oxidised by the ammonia monooxygenase (AMO) to hydroxylamine (Norton *et al.*, 2002, Stein *et al.*, 2007). The enzyme ammonia monooxygenase is a copper containing enzyme, which consists of at least three subunits, *amoA*, *amoB*, and *amoC* (Arp *et al.*, 2007). It is also homologous to the particulate methane monooxygenase (PMO) (Norton *et al.*, 2002). Subsequently, hydroxylamine is converted to nitrite in the periplasma via the hydroxylamine dehydrogenase, also referred to as hydroxylamine (oxido-)reductase, which consists of two subunits, *hoaA* and *hoaB* (Arp *et al.*, 2007). There are two cytochromes, c_{554} and c_{M552}, that were shown to be additionally important for the oxidation of ammonium to nitrite (Arp *et al.*, 2002).

The nitrite produced in the first step is further oxidised by the nitrite oxidoreductase (NXR). Nitrite oxidation is a reversible process and the nitrite oxidoreductase can catalyse the reduction of nitrate to nitrite as it was shown for *Nitrobacter winogradskyi* (Bock *et al.*, 1991). The NXR complex is a membrane-associated protein in *Nitrobacter* located at the inner cell membrane and the intracytoplasmic membrane (Spieck *et al.*, 1996, Starkenburg *et al.*, 2006) and it is an iron-sulphur molybdoprotein (Sundermeyer-Klinger *et al.*, 1984, Meincke *et al.*, 1992). The protein consists of two, *nxrA* and *nxrB* (Meincke *et al.*, 1992), to three subunits with an assumed $\alpha_2\beta_2\gamma_1$ stoichiometry (Sundermeyer-Klinger *et al.*, 1984). As *Nitrospira* form their own phyla, the enzymes of these canonical *Nitrospira* are different from those of *Nitrobacter*. The NXR of *Nitrospira* contains molybdenum and is found at the inner cell membrane in contact with the periplasma since an intracytoplasmic membrane is missing (Spieck *et al.*, 1998). The enzymes for nitrite oxidation and the carbon fixation pathway in *Candidatus* Nitrospira defluvii were shown to be different from all other known nitrifying bacteria but were more related to the NRX complex of *Candidatus* Kuenenia stuttgartiensis, an anaerobic ammonium oxidising bacterium (Lücker *et al.*, 2010).

Due to the energy efficiency of the single nitrification steps (Eq. 1.2-1 and 1.2-2), it was postulated that bacteria capable of performing the complete nitrification (Eq. 1.2-3) would exist (Costa *et al.*, 2006). It was in 2015, when two research groups were the first to report *Candidatus* Nitrospira species, which genomes exhibit all necessary genes for complete ammonium oxidation, in short comammox (Daims *et al.*, 2015, van Kessel *et al.*, 2015). The species were isolated from a biofilm found in a hot water pipe used as oil exploration well (Daims *et al.*, 2015) and from a biofilm of a trickling filter used in an anaerobic compartment in a recirculating aquaculture system (RAS) (van Kessel *et al.*, 2015). They were proposed as *Candidatus* Nitrospira nitrosa, *Candidatus* Nitrospira nitrificans (van Kessel *et al.*, 2015), and *Candidatus* Nitrospira inopinata (Daims *et al.*, 2015). Conditions favouring comammox in the environment may be slow, substrate-influx-limited growth in microbial aggregates and biofilms (Costa *et al.*, 2006).

In addition to the NXR complex for nitrite oxidation, the newly discovered *Nitrospira* strains also exhibit the full set of AMO and hydroxylamine dehydrogenase genes necessary for ammonia oxidation. The enzymes resemble but are phylogenetically distinct from those of canonical ammonium-oxidising bacteria (Daims *et al.*, 2015, van Kessel *et al.*, 2015). *Candidatus* Nitrospira inopinata showed two further AMO homologous of the proteins AmoD and AmoE as well as tetraheam c-type chromosomes, which resemble those in ammonia oxidising bacteria (Daims *et al.*, 2015). *Candidatus* Nitrospira nitrosa and *Candidatus* Nitrospira nitrificans were also found to lack enzymes responsible for assimilatory nitrite reduction, which would indicate the adaptation to ammonium containing habitats (van Kessel *et al.*, 2015).

As the *amoA* gene of comammox *Nitrospira* involved in ammonia oxidation are distinct from other ammonium-oxidising bacteria, specific PCR primers for the detection of *amoA* did not detect comammox *Nitrospira* and, thus, were overlooked for a long time (Pjevac *et al.*, 2017). Previously designed PCR primers revealed the abundances of comammox *Nitrospira* in different habitats (Bartelme *et al.*, 2017, Pjevac *et al.*, 2017). Meanwhile, they have been investigated in wastewater treatment plants (Gonzalez-Martinez *et al.*, 2016, Pjevac *et al.*, 2017), drinking water systems (Pinto *et al.*, 2016, Wang *et al.*, 2017), groundwater aquifers (Fowler *et al.*, 2018), agricultural soils (Beeckman *et al.*, 2018), and rivers (Black & Just, 2018).

1.3. **The denitrification process**

The denitrification process is carried out under facultative anaerobic, carbon-limiting, and electron acceptor-rich conditions (Tiedje, 1988). Denitrifying bacteria vary widely in terms of energy and carbon sources as well as electron donors (Maier *et al.*, 2009). Nitrate is reduced by microorganisms to elementary nitrogen (N_2) via the intermediates nitrite (NO_2^-), nitric oxide (NO), and nitrous oxide (N_2O). The single step equations (Eq. 1.3-1 to 1.3.4) and the overall equation (Eq. 1.3-5) are shown below with their respective Gibb's free energies (ΔG^0) (Thauer *et al.*, 1977).

$$2\ NO_3^- + 4\ e^- + 4\ H^+ \rightarrow 2\ NO_2^- + 2\ H_2O$$

$$\Delta G^0 = -326.0\ kJ\ mol^{-1} \qquad \text{(Eq. 1.3-1)}$$

$$2\ NO_2^- + 2\ e^- + 4\ H^+ \rightarrow 2\ NO + 2\ H_2O$$

$$\Delta G^0 = -146.4\ kJ\ mol^{-1} \qquad \text{(Eq. 1.3-2)}$$

$$2\ NO + 2\ e^- + 2\ H^+ \rightarrow N_2O + 2\ H_2O$$

$$\Delta G^0 = -306.3\ kJ\ mol^{-1} \qquad \text{(Eq. 1.3-3)}$$

$$N_2O + 2\ e^- + 2\ H^+ \rightarrow N_2 + H_2O$$

$$\Delta G^0 = -341.4\ kJ\ mol^{-1} \qquad \text{(Eq. 1.3-4)}$$

$$2\ NO_3^- + 10\ e^- + 12\ H^+ \rightarrow N_2 + 6\ H_2O \qquad \text{(Eq. 1.3-5)}$$

In the first step, nitrate is reduced to nitrite by the dissimilatory nitrate reductase, which can be expressed as a membrane-bound reductase (NAR) or a reductase located in the periplasm (NAP) (Philippot, 2002). The membrane-bound nitrate reductase (NAR) consists of three subunits (*narGHI*): a molybdopterin cofactor catalytic subunit (*narG*), a soluble β subunit (*narH*), and a subunit containing two *b*-type haems (*narI*) (Philippot, 2002). The *narGHI* complex is organised in an operon with *narJ*, a gene required for the assembly of the subunits (Blasco *et al.*, 1998). The *narGHJI* operon is often associated with at least one *narK* encoding protein responsible for transmembrane transportation (Marger & Saier Jr, 1993). The

periplasmatic nitrate reductase (NAP) consists of two subunits: a molybdopterin cofactor catalytic subunit (*napA*) and a *c*-type cytochrome (*napB*) (Berks *et al.*, 1995). Also belonging to the operon is the *napC* gene. This gene encodes a membrane-anchored c-type tetra-haem cytochrome, which is supposed to be involved in electron transfer between quinols and the complex (Berks *et al.*, 1995).

The reduction of nitrite to nitric oxide is a key step in denitrification and distinguishes denitrifiers from other nitrate reducing bacteria (Zumft, 1997). There are two different nitrite reductases: a cytochrome cd_1 enzyme encoded by the *nirS* gene (cd_1NIR) and a copper-containing enzyme encoded by the *nirK* gene (Cu-NIR) (Throbäck *et al.*, 2004). Both enzymes are evolutionary unrelated and are different in terms of structure and the containing metal (Philippot, 2002). The soluble cd_1NIR is composed of two identical subunits, each containing a haem *c* and a haem d_1 (Gudat *et al.*, 1973). Haem d_1 enables the binding of nitrite and nitric oxide to its reduced form (Ward, 2015). The Cu-NIR consists of three identical subunits and each subunit contains a type I copper site and one type II copper site (Abraham *et al.*, 1993). They are connected via ligands, a cysteine-histidine bridge, for rapid electron transfer (Li *et al.*, 2015).

The nitric oxide reductase (NOR) catalyses the reduction of nitric oxide to nitrous oxide and it is composed of two subunits encoded by the genes *norC* and *norB* (Arai *et al.*, 1995). The *norC* gene encodes the membrane-anchored *c*-type cytochrome, while the *norB* gene encodes cytochrome *b* (Ward, 2015). There are three types of NOR reported: cNOR, qNOR and qCu_ANOR. The cNOR is an iron-containing enzyme (Hino *et al.*, 2010) and is present in many denitrifying bacteria (Zumft, 2005). The qNOR is usually found in bacteria that are of medical interests (Ward, 2015). It is a single-subunit resembling the NorB subunit in cNOR (Spiro, 2012). The hybrid qCu_ANOR consists of two subunits: the NorB and a membrane-bound subunit containing two copper atoms (Cu_A) (Ward, 2015). It was described in the gram positive *Bacillus azotoformans* (Suharti *et al.*, 2001).

The last step in the denitrification pathway is the reduction of nitrous oxide to elemental nitrogen. The nitrous oxide reductase (NOS) consists of two identical subunits containing eight copper atoms (SooHoo & Hollocher, 1991). They are

arranged as two conserved domains with copper centres, Cu_A and Cu_Z (Brown *et al.*, 2000). The Z-type Nos is encoded by the *nosZ* gene, which is generally linked to other *nos* genes (Spiro, 2012). A c-type Nos additionally consists of a C-terminal mono-haem cytochrome *c* domain and is characterised in Wolinella species (Kern & Simon, 2009).

There are many bacteria capable of denitrification. They are all aerobes with one exception (Shapleigh, 2013) and found throughout more than 50 genera (Zumft, 1997). Among them are *Pseudomonas*, *Beggiatoa*, *Geobacter*, *Rhodobacter*, *Thauera*, *Thiobacillus*, and *Azoarcus*. Studies on denitrifying communities is usually done using primers targeting the genes *nirS*, *nirK*, *norB* as well as *nosZ* (Scala & Kerkhof, 1999, Braker *et al.*, 2000, Braker & Tiedje, 2003, Heylen *et al.*, 2007). However, the nosZ gene is not always representative as some denitrifying bacteria lack this enzyme (Throbäck *et al.*, 2004).

Some bacteria such as *Beggiatoa* species are able to storage nitrate in vacuoles (McHatton *et al.*, 1996). *Beggiatoa* are filamentous, gliding sulphur bacteria (Teske & Salman, 2014). They are chemolithoautotrophic and oxidise sulphide using nitrate as electron acceptor for sulphide oxidation in the absence of oxygen (Sweerts *et al.*, 1990, Sayama *et al.*, 2005, Kamp *et al.*, 2006). In large marine *Beggiatoa* species the vacuoles can rise up to 90% of the cell volume with nitrate concentrations up to 160 mmol L^{-1} (McHatton *et al.*, 1996). Freshwater *Beggiatoa* were shown to have smaller nitrate storing capacities or even lack vacuoles (Teske & Salman, 2014). They form dense, easily recognisable mats of filaments in the sediment-water interface separating the oxygen layer from the sulphidic subzone (Teske & Salman, 2014). In anoxic sediments, where nitrate is depleted, *Beggiatoa* do not form dense mats. They are gliding in the sediments to bridge the spacial separation of electron donors and acceptors (Mußmann *et al.*, 2003, Preisler *et al.*, 2007). The nitrate storage capacity of *Beggiatoa* is, therefore, an advantage over other bacteria since nitrate is taken up in times of substrate influxes into the upper sediment layer and is used as electron acceptor for sulphide oxidation in deeper layers (Mußmann *et al.*, 2003).

1.4. **The anammox process**

The anaerobic ammonia oxidation process, shortly called the anammox process, is another possibility of bacterial ammonia degradation (Mulder *et al.*, 1995, Strous *et al.*, 1997). Ammonium is oxidised by chemolithoautotrophic bacteria in the presence of nitrite under strictly anoxic conditions via the intermediates nitric oxide (NO), hydroxylamine (NH_2OH) or hydrazine (N_2H_4) (Van De Graaf *et al.*, 1997, Strous *et al.*, 1999, Zekker *et al.*, 2015). The single anammox reaction, the nitritation reaction and the overall reactions are given in the following equations (Eq. 1.4-1 to 1.4-3) (Kartal *et al.*, 2010) with their respective Gibb's free energies (Op den Camp *et al.*, 2007):

(I) $NH_4^+ + NO_2^- \rightarrow N_2 + 2\ H_2O$

$\Delta G^0 = -357\ kJ\ mol^{-1}$ (Eq. 1.4-1)

(II) $NH_4^+ + 1.5\ O_2 \rightarrow NO_2^- + 2\ H^+ + H_2O$

$\Delta G^0 = -275\ kJ\ mol^{-1}$ (Eq. 1.4-2)

$2\ NH_4^+ + 1.5\ O_2 \rightarrow N_2 + 2\ H^+ + 3\ H_2O$ (Eq. 1.4-3)

In comparison to the aerobic ammonium oxidation reaction, the anaerobic oxidation is almost equally energetically favourable (Mulder *et al.*, 1995). Since microorganisms usually live in communities, the nitrite required for the anammox reaction can be provided by aerobic ammonium-oxidising bacteria and archaea (Francis *et al.*, 2007). The anammox bacteria utilize CO_2 as their carbon source for growth using the acetyl coenzyme A pathway (Schouten *et al.*, 2004). Therefore, the equation 1.4-1 is often expressed as the following equation 1.4-4 (Kuenen, 2008):

$NH_4^+ + 1.32\ NO_2^- + 0.066\ HCO_3^- + 0.13\ H^+$

$\rightarrow 1.02\ N_2 + 0.26\ NO_3^- + 2.03\ H_2O + 0.066\ CH_2O_{0.5}N_{0.15}$ (Eq. 1.4-4)

So far, the molecular mechanism of anammox is proposed as follows by Kartal *et al.* (2011). In the first step nitrite is converted to nitric oxide by a nitrite reductase

(NIR). In the second step nitric oxide is combined with ammonium to form hydrazine by a hydrazine synthase (HZS). The hydrazine is subsequently converted to dinitrogen gas by a set of hydrazine dehydrogenases (HDH) that resemble the hydroxylamine reductases encoded by *hao* genes in aerobic ammonia oxidisers. The whole process is catalysed by several cytochrome c proteins.

Anammox bacteria are quite distinct from other bacteria as they share some features with all three domains of life, *Bacteria*, *Archaea*, and *Eukarya*. Their membrane lipids, called ladderanes, show ester-linked and ether-linked fatty acids as well as two different ring systems (Damsté *et al.*, 2002, Jetten *et al.*, 2003, Kuypers *et al.*, 2003, Damsté *et al.*, 2005). The ladderanes are very impermeable and assist the anammox process by keeping metabolites such as the toxic hydrazine within a unique cell compartment separated by intracytoplasmic membranes, called the anammoxosome (Damsté *et al.*, 2002). The anammoxosome is assumed to be organelle, where all catabolic processes are carried out (Lindsay *et al.*, 2001, van Niftrik *et al.*, 2008, Jetten *et al.*, 2009, Van Niftrik *et al.*, 2010).

The anammox process can reversibly be inhibited by dissolved oxygen concentrations higher than 0.5% air saturation as well as by organic carbon (Strous *et al.*, 1997). Complete and irreversible inhibition by dissolved oxygen is observed at 18% air saturation (Egli *et al.*, 2001). The oxidation process may also be inhibited by higher concentrations of more than 7.14 mmol NO_2^--N L^{-1}. Nitrite concentrations higher than 15 mmol L^{-1} inhibited the growth of a *Brocadia* species almost completely (Carvajal-Arroyo *et al.*, 2013). Inhibition due to nitrite can be overcome with the addition of hydroxylamine or hydrazine (Strous *et al.*, 1999). Additionally, it was shown for *Brocadia* that elevated concentrations of the intermediates up to 3 mmol L^{-1} may inhibit the anammox process (Carvajal-Arroyo *et al.*, 2013).

Bacterial species that are capable of ammonia oxidation belong to the *Planctomycetes* (Strous *et al.*, 1999). So far, the six genera *Candidatus* Brocadia (Kartal *et al.*, 2004), *Candidatus* Kuenenia (Schmid *et al.*, 2000), *Candidatus* Scalindua (Kuypers *et al.*, 2003), *Candidatus* Jettenia (Quan *et al.*, 2008), *Candidatus* Anammoxoglobus (Kartal *et al.*, 2007), and *Candidatus* Anammoxibacterium (Khramenkov *et al.*, 2013) have been proposed. The discovery of anammox bacteria

was first reported in the 1990's (Van de Graaf *et al.*, 1995, Strous *et al.*, 1999) and subsequent studies showed that these bacteria inhabit a wide range of environments, including wastewater treatment plants (Van de Graaf *et al.*, 1995, Jetten *et al.*, 2003), freshwater bodies (Schubert *et al.*, 2006, Smith *et al.*, 2015), and marine sediments (Schmid *et al.*, 2000, Kuypers *et al.*, 2003). In marine environments, it is assumed that at least 50% of the nitrogen is converted by the anammox process (Arrigo, 2004, Francis *et al.*, 2007) and it can be observed at low and at high temperatures as well as at high and at low salinities (Kartal *et al.*, 2010). The anammox process most likely takes place in oligotrophic systems with low oxygen concentrations and a surplus of ammonium (van Niftrik & Jetten, 2012).

Due to their capability of ammonia oxidation, anammox bacteria find application in wastewater treatment plants as an alternative to conventional techniques (Op den Camp *et al.*, 2006, Van der Star *et al.*, 2007, Kartal *et al.*, 2010). However, anammox bacteria are slow growing with generation times of about 10 to 12 days at 35°C (Kuenen, 2008). The slow growth and activity of anammox bacteria at temperatures below their optimum range of 30 to 40 °C limits wastewater treatment performance (Morales *et al.*, 2015).

1.5. **Environmental impacts of nitrogen**

During the last decades the supply of ionic (reactive) nitrogen species (ammonium and nitrogen oxides (NO_x)) has increased from anthropogenic sources to meet human's needs (Vitousek *et al.*, 1997, Galloway *et al.*, 2003, Erisman *et al.*, 2013). The cultivation of crops and vegetables enhances the biological nitrogen fixation to ammonium. Nitrogen containing fertilizers used in plant cultivation are mostly generated by the Haber-Bosch process, where additional elemental nitrogen is fixed. High ammonium and nitrate concentrations are responsible for acidification, eutrophication, and the loss of biodiversity in soils, lakes, streams, and coastal ecosystems (Dodds *et al.*, 2002, Smith, 2003, Conley *et al.*, 2009). Eutrophication causes the development and proliferation of primary producers (phytoplankton, algae, and macrophytes), which are responsible for the degradation of organic compounds leading to oxygen depletion in the aquatic systems. Hypoxic or anoxic conditions with

subsequent mortality of fishes and invertebrates in the freshwater systems are the result (Anderson *et al.*, 2002, Breitburg, 2002).

Furthermore, the combustion of fossil fuels leads to the production of nitrous oxide (N_2O) and nitric oxide (NO). Both nitrogen oxide species are greenhouse gases, promoting the global climate change and increasing ozone depletion. N_2O is as approximately 300 times stronger greenhouse gas than CO_2 (IPCC Climate Change, 2007) and has a residence time of about 100 years in the atmosphere (Galloway *et al.*, 2003). Furthermore, N_2O emissions also arise from nitrogen-containing fertilizers by soil bacteria (Tierling & Kuhlmann, 2018).

1.6. **Health impacts of nitrogen species**

Although, nitrogen is a vital component for all living beings, inorganic nitrogen compounds are also of public health concern (World Health Organization, 2004). Guideline values for nitrate and nitrite of 50 mg NO_3^- L^{-1} and 0.1 mg NO_2^- L^{-1} were introduced, respectively (TrinkwV, 2001). While the concentration of nitrate must not rise in the drinking water distribution system, the concentration of nitrate may increase to 0.1 mg NO_2^- L^{-1}. Ammonium is not assumed to be directly responsible causing health implications in humans but is regarded as faecal indicator. The guideline value for ammonium is 0.5 mg NH_4^+ L^{-1} (TrinkwV, 2001).

The uptake of elevated nitrate and nitrite concentrations may elicit several health implications in humans (Cissé & Mao, 2008, Ward *et al.*, 2018). Nitrate has been mainly associated with methemoglobinemia in infants (“blue-baby syndrome”) (Fan & Steinberg, 1996, Manassaram *et al.*, 2010, Shuval & Gruener, 2013). Nitrate is reduced to nitrite in the body, which is taken up into the bloodstream. There, nitrite oxidizes the Fe^{2+} present in haemoglobin to Fe^{3+}, a molecule called methaemoglobin (Umbreit, 2007). In contrast to haemoglobin, which binds oxygen reversible, methaemoglobin is unable to transport oxygen through the bloodstream leading to asphyxia (Mansouri & Lurie, 1993). Due to low levels of red cell NADH-cytochrome b5 reductases in infants, methaemoglobin cannot be converted back to haemoglobin (Mansouri & Lurie, 1993). Moreover, studies suggest that nitrate in drinking water is

also associated with preterm delivery and low birth weight (Stayner *et al.*, 2017), and neural tube defects (Brender *et al.*, 2004).

Additionally, nitrate and nitrite were classified as probably cancerogenic (International Agency for Research on Cancer, 2010). Evidences of linkages between nitrate in drinking water and cancer were shown (Inoue-Choi *et al.*, 2012, Espejo-Herrera *et al.*, 2016, Jones *et al.*, 2016). Nitrate can be reduced to nitrite in the human body and nitrite subsequently reacts with certain amines to cancerogenic nitrosamines (Mirvish, 1977, Ward *et al.*, 2005). The risk of cancer due to the uptake of elevated nitrate and nitrite concentrations through food is assumed to be irrelevant as nitrosation (i.e. conversion of organic compounds to nitroso derivatives) is inhibited at high concentrations of ascorbic acid, polyphenols, and other compounds present in most vegetables (International Agency for Research on Cancer, 2010).

1.7. **Biofilms**

At aqueous interfaces to air and solid surfaces, microorganisms form flocs, mats, sludge, and biofilms (Wimpenny, 2000, Flemming & Wingender, 2010). Biofilms have been found in different shapes ranging from flat films to mushroom-like architectures (Tielen *et al.*, 2005). The biofilm matrix consists predominantly of water making up 90% to 97% and a conglomeration of a wide range of biopolymers known as extracellular polymeric substances (EPS), which are primarily produced by the microorganisms themselves (Sutherland, 2001, Flemming & Wingender, 2010). The EPS matrix differs also in its chemical and physical properties and is influenced by intrinsic (i.e. microorganisms) and extrinsic factors (i.e. physico-chemical environment) (Sutherland, 2001). Additionally, enzymes, lipids, polysaccharides, oligonucleotides, and other cell compounds resulting from cell lysis are constituents of the matrix (Flemming & Wingender, 2010).

Within these biofilms, microorganisms are protected against environmental stresses such as oxygen (De Beer *et al.*, 1994), disinfectants (Bridier *et al.*, 2011), surfactants (Simões *et al.*, 2006), and desiccation (Espinal *et al.*, 2012), since the biofilm matrix functions as a diffusion barrier (Flemming & Wingender, 2010). The EPS matrix additionally favours the horizontal gene transfer facilitating the exchange of

DNA between cells (Molin & Tolker-Nielsen, 2003), the ‘communication’ of bacterial cells termed quorum sensing process via small signal molecules (autoinducers) in the biofilm matrix (Nadell *et al.*, 2008), and the production of shuttle molecules used for extracellular electron transfer (Rabaey & Verstraete, 2005). In natural occurring biofilms microbial communities are established containing many different species (Wimpenny, 2000).

1.8. **Bioelectrochemical systems**

1.8.1. The setup of a bioelectrochemical system

A bioelectrochemical system (BES) is an electrochemical cell in which electrochemically active microorganisms form biofilms on either one of the electrodes or both and catalyse oxidation and/or reduction reactions (Larminie and Dicks 2000). A BES consists of a cell containing two electrodes, the anode and the cathode, connected via a circuit so that electrons can travel from the cathode to the anode through a voltmeter or potentiostat (Larminie and Dicks 2000). A schematic overview of a BES is shown in Figure 1.8.1-1. In the presence of attached microorganisms on the anode and the cathode, electrodes are referred to as bioanodes or biocathodes, respectively.

To build up a bioelectrochemical system all components utilized have to be chosen very well. The reactor design, the electrode material and their size in relevance to the size of the chamber, the establishment of biofilms, and living conditions for the microorganisms (e.g. nutrient sources, pH, temperature) determine the efficiency of the system (Call & Logan, 2008, Freguia *et al.*, 2008, Logan, 2010, Patil *et al.*, 2010, Wrighton *et al.*, 2010, Patil *et al.*, 2011, Guo *et al.*, 2015).

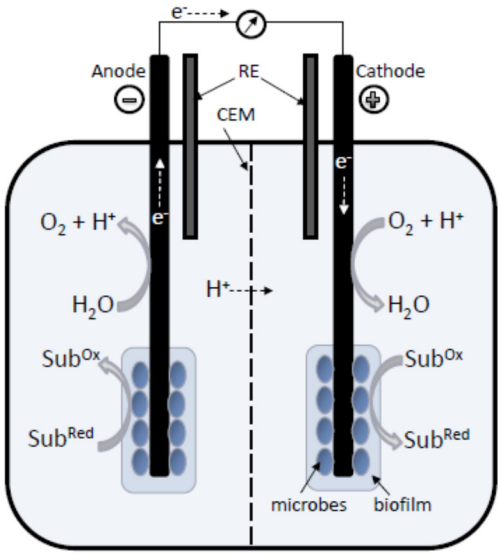

Figure 1.8.1-1 | Schematic overview of a bioelectrochemical system. Substrates (Sub) are oxidised or reduced by microorganisms living in biofilms. Abiotic reactions (e.g. oxidation/reduction of water) also take place. RE = reference electrode. CEM = cation exchange membrane.

Bioelectrical systems can be separated into microbial fuel cells and electrolysis cells (Rozendal *et al.*, 2008). In microbial fuel cells reactions occur spontaneously and energy can be obtained. In electrolysis cells reactions do not occur spontaneously and, therefore, energy has to be provided. Most of the described systems in literature are microbial fuel cells as gaining electricity from bioelectrochemical systems is one of the main aims (Logan *et al.*, 2006). Hydrogen formed in microbial electrolysis cells may be a sustainable energy carrier used as a clean fuel, for instance, in transportation systems (Schrope, 2001, Turner, 2004). However, the main aim regarding microbial electrolysis cells focuses on the removal of contaminants. Bioelectrical systems are mainly applied in wastewater treatment. It is often referred then to a bioremediation system, since waste or contaminants are removed from the electrolyte (Harnisch & Schröder, 2010).

The ability of microorganisms to form biofilms at aqueous surfaces can be used in bioelectrochemical systems. Electrochemically active microorganisms establish a biofilm community directly on the electrode catalysing various redox reactions (Du *et al.*, 2007). Homogenous biofilm communities established on electrodes provide lower current densities in BES than heterogeneous biofilm communities (Rabaey *et al.*, 2008). It is suggested that microbial interactions between species present in the biofilm

lead towards an electrochemically competent biofilm (Rabaey *et al.*, 2007) that fits best the performance of the BES (Wrighton *et al.*, 2010).

1.8.2. Losses decreasing BES performance

The performance of a BES is decreased by electrode potential losses, ohmic losses and membrane pH gradients (Rozendal *et al.*, 2008). The electrode potential losses can be divided into three kinds of losses: (I) activation losses, (II) bacterial metabolism losses, and (III) mass transport or concentration losses (Logan *et al.*, 2006). Activation losses occur during the electron transfer from or to a compound at the electrode in imperfect catalysis of reduction/oxidation reactions (Rabaey *et al.*, 2007). They are dependent on the electrode material (Noren & Hoffman, 2005) and have a great impact on voltage drop in cells working at low temperatures (Larminie *et al.*, 2003). They can be lowered by increasing the electrode surface resulting in a lower current density, by increasing the operating temperature or through the establishment of an enriched biofilm featuring mediated electron transfer (Aelterman *et al.*, 2006, Logan *et al.*, 2006). The bacterial metabolic losses are related to the energy generation of bacteria by transporting electrons from a compound at a low potential through the electron transport chain to the final electron acceptor at a higher potential. The higher the metabolic energy yield for the microorganism is, the lower will be the maximum attainable voltage (Logan *et al.*, 2006). Mass transport or concentration losses occur at high current densities due to limited mass transfer of chemical species by diffusion to the electrode surface leading to an increased ratio of the oxidised to the reduced species at the anode and a decreased ratio at the cathode (Larminie *et al.*, 2003, Logan *et al.*, 2006). It is assumed that mass transfer losses occur predominantly within the biofilm because the losses did not significantly decrease after increasing the recirculation (Aelterman *et al.*, 2006). The mass transfer losses additionally describe the reduced substrate flux to the biofilm that may arise when the system is poorly mixed (Logan *et al.*, 2006).

Moreover, bioelectrical systems suffer from ohmic voltage losses. They describe the potential losses concerning the electrode and the ones related to the electrolyte (Rabaey & Verstraete, 2005) and increase linearly with increasing ohmic resistance and current density (Noren & Hoffman, 2005). The electrode ohmic losses imply the

voltage loss caused by the movement of electrons through the electrodes, the electrical contacts and the wiring. The electrolyte ohmic losses are related to the movement of electrons through the electrolyte and the membrane (Rabaey & Verstraete, 2005). The electrolyte ohmic losses become considerable when electrolytes with low conductivity are applied (Rozendal *et al.*, 2008).

In BES, usually ion exchange membranes are used to ensure efficient transport of cations from one electrode to the other to avoid pH gradients in the compartments. However, the transport of different ions than protons and hydroxyl ions were often observed (Rozendal *et al.*, 2006, Kim *et al.*, 2007, Harnisch *et al.*, 2008). Loop-figurations of BES have been shown to overcome the problem of pH gradients because the electrolyte in the anode compartment (i.e. anolyte) is transferred to the cathode compartment (Freguia *et al.*, 2008, Virdis *et al.*, 2008).

1.8.3. The electron transfer

To catalyse redox reactions, electrons have to be extracellularly transferred between electrodes and the microorganisms. Up to now, different mechanisms were described. Most of them were investigated in anodic systems. It is suggested that the mechanisms of electron transfer from the anode to the microorganism differs from the mechanisms transferring electrons from the microorganism to the cathode (Strycharz *et al.*, 2011). It is also assumed that direct electron transfer may possibly be bidirectional (Rosenbaum *et al.*, 2011). However, it is not yet clarified whether electron transfer is possible from one microorganism to another within the biofilm.

In general, electrons can be transferred through immobilized structures (direct transfer) and through mobile components indirect transfer). For the direct electron transfer through an immobilized structure the microorganisms are in physical contact to the acceptor or donor (Gregory *et al.*, 2004, Pous *et al.*, 2014). The electrons are transferred from the insoluble donor to the microorganism and from the microorganism to the insoluble acceptor, respectively, via membrane associated redox proteins, such as c-type chromosomes (Rabaey *et al.*, 2007). Investigations of the electron transfer in *Geobacter sulfurreducens* revealed that c-type chromosomes as well as other outer-membrane proteins such as OmpJ are involved in the reduction of Fe(III) oxides and

Mn(IV) oxides (Afkar *et al.*, 2005, Mehta *et al.*, 2005). Additionally, the electron transfer through highly conductive pili have been reported in *Geobacter sulfurreducens* (Reguera *et al.*, 2005). With pili, a certain distance can be bridged between the microorganism and the electrode.

Furthermore, extracellular electron transfer can occur without a direct contact between microorganisms and the electrode. This indirect transfer is achieved with the utilization of mobile components. Microorganisms are able to produce soluble molecules that are used as redox mediators. Several compounds have been studied in bioelectrical systems as possible mediators such as hydrogen (Rabaey *et al.*, 2008) or pyocyanin and phenazine in *Pseudomonas aeruginosa*, which significantly enhance electron transfer (Rabaey *et al.*, 2004, Rabaey *et al.*, 2005). Microorganisms are also capable of using redox mediators which are produced by other species (Rabaey *et al.*, 2004). Additionally, artificial substances such as neutral red can be added to enhance electron transfer (Park & Zeikus, 2000).

1.9. **Community analysis**

To investigate main key players in biodegradation processes, different fingerprinting techniques targeting evolutionary conserved marker genes (e.g. 16S rRNA genes) have been developing. Specified regions of bacterial 16S rRNA are amplified by polymerase chain reactions (PCR) and analysed using electrophoresis procedures, such as denaturing gradient gel electrophoresis (DGGE), terminal restriction length polymorphism (T-RFLP) or next-generation sequencing techniques.

The DGGE procedure for the characterization of complex bacterial communities was first reported in 1993 (Muyzer *et al.*, 1993). In this study species that represent only 1% of the total communities have been identified in microbial mats and wastewater treatment reactors. Following in 1997, the T-RFLP technique was introduced (Liu *et al.*, 1997) identifying up to 72 unique terminal restriction fragment lengths in sludge, aquifer sand, and termite gut. Digital data output of the separation patterns facilitated the analysis of complex environmental samples. Both techniques, DGGE and T-RFLP, were subsequently used to investigate microbial community compositions and their changes in e.g. agricultural soils (Lukow *et al.*, 2000, Smalla *et*

al., 2007, Wallis *et al.*, 2010), forest soils (Bäckman *et al.*, 2003, Rich *et al.*, 2003, Agnelli *et al.*, 2004, Kemnitz *et al.*, 2007), marine sediments (Wieringa *et al.*, 2000, Braker *et al.*, 2001, Webster *et al.*, 2007, Schauer *et al.*, 2010), wastewater (Boon *et al.*, 2002, LaPara *et al.*, 2002, Siripong & Rittmann, 2007, Lefebvre *et al.*, 2010), and aquacultures (Sandaa *et al.*, 2003, Michaud *et al.*, 2009, Wietz *et al.*, 2009, Gregory *et al.*, 2012).

Environmental samples, however, are very complex and can consist of millions of different species though only a small number of species are dominant in these community compositions (Curtis *et al.*, 2002, Sogin *et al.*, 2006). High-throughput sequencing methods have been developed and became the method of choice for the characterization of complex community structures as sequencing services are meanwhile available at relative low costs (Sogin *et al.*, 2006, Dong *et al.*, 2017). The two commonly used high-throughput sequencing systems are Roche 454 pyrosequencing and the Illumina MiSeq platform, whereas the Illumina system became the commonly used platform of next-generation sequencing methods in the last years. Extracted DNA from diverse environmental habitats is amplified with PCR using primers that target conserved regions of prokaryotic 16S rRNA genes with lengths of ~400 bp (Dong *et al.*, 2017). The amplicons in each sample are subsequently tagged with “barcode” sequences specific for each sample. After pooling the samples, all amplicons are sequenced in a single run.

For data processing of Illumina sequencing results many software programs have been developing such as MetaAmp (Dong *et al.*, 2017) and mothur (Kozich *et al.*, 2013), or they can be analysed in the R environment (R Core Team, 2018) using additional analysis packages. With the web-based MetaAmp software, Illumina fasta- or fastq-files are uploaded online for analysis. Profonde expertise or training is not required. OTU tables are generated based on the large SILVA databank (Quast *et al.*, 2012). Despite choosing parameter settings in the beginning for the analysis, however, direct influence on the analysis itself is impeded. The Mothur software provides the possibility to monitor calculations done during data processing and to change parameter settings. Unfortunately, Mothur generates large data files and the analysis of large data sets arising from highly complex samples are not doable on home computers or notebooks. Analysis in the R environment, on the contrary, allows direct

influence on the calculations and even larger data sets can be evaluated without the need of additional servers. OTU taxonomy and diversities of many complex samples are analysed and displayed using additional R packages such as phyloseq (McMurdie & Holmes, 2013) and stringr (Wickham, 2019). Since different databanks can be chosen for the taxonomical classification, one must keep in mind that the classification heavily depends on the underlying databank (Dong *et al.*, 2017).

1.10. **Aims of the study**

During the last few decades, environmental problems concerning nitrogen pollution have become evident (Galloway *et al.*, 2003, Camargo & Alonso, 2006, Winiwarter *et al.*, 2015, Boyle, 2017). This thesis addresses fundamental research using bioelectrochemical systems as well as aquaponic systems to provide knowledge for problem-solving approaches in drinking water production, wastewater treatment and food production.

Aquaponic systems combine aquaculture (fish cultivation) and hydroponic systems (vegetable and fruit production) to a recirculating system using the ammonium enriched effluent from the fish tank as fertilizer for the plants in the grow beds. Residual ammonium, which is toxic to fish in high concentration is converted by microorganism into less toxic nitrate. Studying microbial communities in an aquaponic system is rarely done so far. Until now, it is not known, which microorganisms are primarily responsible for the oxidation of toxic ammonium in the system. However, understanding the fundamental principles of such a system can help to improve the overall outcome of sustainable food production. In this thesis, research is based on the microbial community composition in the sump of a backyard aquaponic system to reveal the key microorganisms responsible for ammonium oxidation. Additionally, chemical species will be measured to monitor the efficiency of the system.

In Germany, about 51% of groundwater bodies are contaminated with nitrate due to excessive fertilization on agricultural lands (European Commission, 2018). So far, process steps in drinking water production systems for complete nitrate removal of groundwater water are not implemented yet. Here, batch bioelectrochemical systems (BES) are used to remove nitrate by means of denitrification at the cathode. A large-

scale BES could be added as a step in the existing drinking water production process. Until now, however, the key microorganisms and removal processes at the cathode in BES are not clear. Furthermore, the influence of time-depending potential settings has not been investigated. In this study, the microbial communities at the cathode are studied using continuous and intermittent potential settings.

Wastewater treatment plants deal with highly ammonium concentrated municipal sewage, most likely due to low household drinking water usage. Therefore, BES are used in this study to remove ammonium by combining nitrification and the anammox process at the anode. It is the first attempt to cultivate nitrifying bacteria and anammox bacteria in a BES. Furthermore, little is known about oxygen evolution rates in BES. Oxygen is essential for nitrification, however, the anammox process is inhibited by oxygen. Here, the focus lies on a controlled oxygen production at the anode to ensure constant oxygen concentration for nitrifying bacteria without inhibiting anammox bacteria. So far, using the anammox process in a BES has not been investigated.

Next-generation sequencing techniques meanwhile became quite cheap and reveal detailed information of the whole microbial community composition. However, it takes several days until results are provided by a company. For monitoring systems including the presence of specific bacterial species responsible for the compound degradation of interest, the knowledge of the whole community composition is not even necessary. Here, an easy and rapid method known as restriction fragment length polymorphism (RFLP) for the detection of specific strains within a few days will be tested using capillary electrophoresis for analysis. To our knowledge, this is the first report of carrying out an established method on a regular and already available device such as a capillary electrophoresis.

2. Comammox *Nitrospira* perform ammonia transformation in a backyard aquaponic system

The aquaponic system was build, maintained and sampled by Dr. Rainer U. Meckenstock. The statistical analysis was mainly performed by Dr. Alexander J. Probst. Dr. Huber Müller analysed the metagenomic data. All other work was conducted by Julia Heise. The paper was submitted to the journal Current Microbiology on the 30th of June 2020.

2.1. **Abstract**

Aquaponic systems are sustainable solutions for food production combining fish growth (aquaculture) and production of vegetables (hydroponic) in one recirculating system. In aquaponics, ammonium-enriched wastewater from fish in the aquaculture serves as fertilizer for the plants in the hydroponics, while the ammonium-depleted and detoxified water flows back to the aquaculture. To investigate bacterial nitrogen cycling in such an aquaponic system, measurements of nitrogen species was coupled with time-resolved 16R rRNA gene profiling and the functional capacity of organisms was studied using metagenomics. The aquaponic system was consistently removing ammonia and nitrite below 23 µM and 19 µM, and nitrate to steady state concentrations of about 0.5 mM. 16S rRNA gene amplicon sequencing of sediments exposed in the pump sump revealed that typical signatures of canonical ammonia-oxidising microorganisms were below detection limit. However, one of the most abundant operational taxonomic units (OTU) was classified as a member of the genus *Nitrospira*, for which we also recovered genome scaffolds encoding the only ammonia monooxygenase genes identified in the metagenome. This study indicates that even in highly efficient aquaponic systems, comammox *Nitrospira* rather than canonical nitrifying organisms can be responsible for complete nitrification at low steady-state ammonia concentrations.

2.2. **Introduction**

Over the last 50 years, aquaponic systems became a promising biotechnology for sustainable food production. In aquaponics, aquaculture (fish cultivation) and hydroponics (vegetables production) are integrated into one water-circulating system. One of the main issues in aquaculture is the accumulation of ammonium due to decomposed fish food and fish excrements. Depending on the fish species and the exposure time (USEPA, 2013), ammonia is chronically toxic to fish in concentrations higher than 1.9 mg L^{-1} total ammonia nitrogen at pH 7 and 20 °C. Therefore, the water of aquaculture systems must be replaced regularly or requires cleaning. Aquaponic systems solve the issue of regeneration by pumping water from the fish tank into the grow beds of the hydroponic part, where it serves as fertilizer for vegetables, fruits, or herbs. Plants can use both ammonium and nitrate as nitrogen sources (Xu *et al.*, 2012). However, the essential reaction in the aquaponic system is the nitrification, during which toxic ammonium is oxidised to less harmful nitrate (Stormer *et al.*, 1996, Alonso & Camargo, 2003). Since the complete oxidation of ammonia to nitrate is an essential step for the effective operation in an aquaponic system, the nitrogen turnover in such a system was elucidated in this study.

Until 2015, nitrification was assumed to be exclusively performed in a two-step process carried out by two phylogenetically distinct bacterial lineages. In the first step, ammonium is oxidised to nitrite via hydroxylamine by e.g. *Nitrosomonas*. In the second step, nitrite is oxidised to nitrate by e.g. *Nitrobacter* or *Nitrospira*. This process was discovered in marine (Foesel *et al.*, 2007, Kuhn *et al.*, 2010) and freshwater (Tokuyama *et al.*, 2004, Sugita *et al.*, 2005, Itoi *et al.*, 2006, Pedersen *et al.*, 2009) aquaponic or aquaculture systems by enrichment techniques, fluorescence *in situ* hybridization, or sequence analyses.

In 2015, Daims *et al.* (2015) and van Kessel *et al.* (2015) discovered that nitrification can also be carried out by one single organism affiliated to the genus *Nitrospira*. By showing that this bacterium was capable of oxidising ammonium fully to nitrate, a process called ‘comammox’ (complete ammonia oxidation), the authors overturned the 100-yr old lasting paradigm that nitrification can only be performed by two distinct groups of organisms. Since there discovery, comammox *Nitrospira* have

been frequently detected in aquifers (Fowler *et al.*, 2018), drinking water systems (Pinto *et al.*, 2016), wastewater treatment plants (Pjevac *et al.*, 2017), as well as in recirculating aquaculture systems (Bartelme *et al.*, 2017). Furthermore, 16S rRNA gene analysis of community compositions in different compartments of an aquaponic system showed that nitrification took place on a biofilter located behind the fish tank retaining large particle matter (Schmautz *et al.*, 2017). Since *Nitrospira* was among the most abundant species and other nitrifying bacteria seemed not to be present in the biofilm community of the aquaponic system, the authors assumed that the nitrification process was carried out by *Nitrospira* alone.

So far, all known comammox *Nitrospira* belong to the sublineage II of *Nitrospira* (Daims *et al.*, 2015, van Kessel *et al.*, 2015, Pinto *et al.*, 2016), which comprises comammox *Nitrospira* species and nitrite-oxidising (canonical) *Nitrospira* species (Daims *et al.*, 2001, Koch *et al.*, 2015). Additionally, comammox and canonical *Nitrospira* form mixed phylogenetic clades within this sublineage (Daims *et al.*, 2015, van Kessel *et al.*, 2015, Pinto *et al.*, 2016), suggesting that they cannot be distinguished based on 16S rRNA sequences alone.

Here, we elucidate the type of microbial nitrogen metabolism in an aquaponic system and how the microbial communities develop over time. A combination of 16S rRNA gene sequencing and metagenomic analysis is employed for distinguishing different types of nitrification and to follow the respective functional clades.

2.3. **Experimental procedure**

2.3.1. The aquaponic system

The aquaponic system was build and continuously maintained by Dr. Rainer U. Meckenstock. The fish tank was built from a regular 1200 L plastic intermediate bulk container (IBC) and filled with 1000 L tap water. The hydroponic part consisted of two grow beds, each 100 x 120 cm in size and filled with gravel up to 30 cm in height. The overflow water from the fish tank flew into the grow beds by gravity and was treated by a biofilter made of gauze with 1 mm mesh size to remove larger particles. The particle filter was cleaned daily. The water of the grow beds was periodically released into a sump by a hydraulic siphon system. From there, it was continuously pumped back into the fish tank with an adjusted flow rate of 800 L h^{-1}. The setup of the aquaponic system is schematically shown in Figure 2.3.1-1.

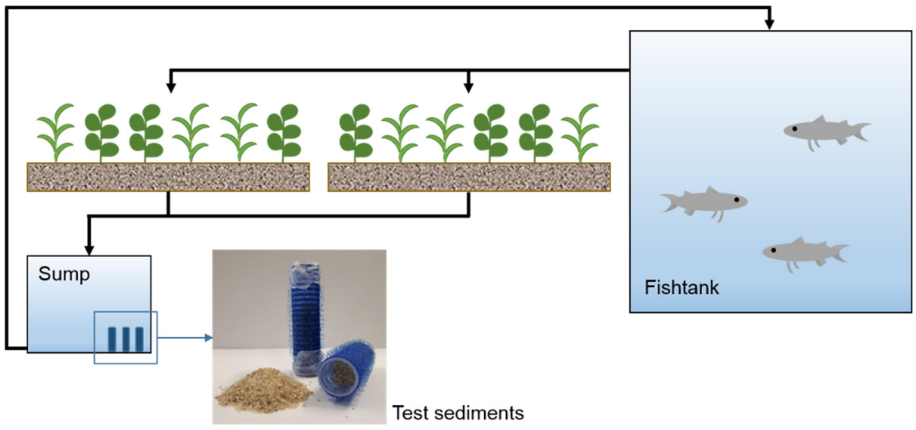

Figure 2.3.1-1 | Schematic view of the backyard aquaponic system (not to scale). The test sediments used for analysing the microbial community were exposed in small cylinders in the sump (hair curlers).

In the beginning of the operation carps (Cyprinus carpio) and wels catfish (Silurus glanis) were grown. After a fish disease killing all the fishes, the water in the aquaponic system was completely exchanged and all system parts cleaned. Only carps were grown then resulting in 15 individuals of 400 g weight each at the end of the experiment. Lettuce, tomatoes, cucumber, and strawberries were grown in the grow beds from May to October.

2.3.2. Test sediments and sampling

Quartz sand (1 mm grain size) was autoclaved for 20 min at 120 °C. Regular plastic hair curlers (6.5 cm in length) with porous walls (1x0.5 mm pore size) were filled with approximately 10 g of the sand and closed with parafilm at both ends. The test sediments were incubated in the aquaponic sump over 17 months. One curler was regularly taken for amplicon sequencing. For metagenome sequencing, DNA was extracted from one test sediment taken at the last day of incubation. Water was sampled regularly to check the system performance and analyses of nitrogen species concentrations (cf. section 2.3.3). The pH was determined on-site using test stripes (pH 4.5-10) [Carl Roth GmbH, Karlsruhe, Germany].

2.3.3. Sample preparation and analyses using ion chromatography

To analyse the concentrations of nitrate, nitrite, and ammonium water samples were regularly taken from the aquaponic sump and triplicates were analysed by ion chromatography. The samples were prepared by 1:2 dilution with 0.01 mM potassium buffer for the analysis of anions and with 20 mM methyl sulfonic acid (70% v/v) (Merck KGaA, Darmstadt, Germany) for the analysis of cations. All samples were centrifuged for 15 min at 16,000 x g to precipitate solids. 200 µL of the supernatants were diluted 1:5 with ultrapure water (18.2 µS, Merck Millipore System, Merck KGaA, Darmstadt, Germany). The samples were stored at -20 °C until analysis.

Anions and cations were measured with an ion chromatograph (Thermo Fisher Scientific, Dreieich, Germany) equipped with a Dionex™ IonPac™ AS23-4µm column and an AERS 500 suppressor (2 mm) for the measurement of anions using 0.8 mM $NaHCO_3$/4.5 mM Na_2CO_3 (Thermo Fisher Scientific, Dreieich, Germany) as eluent at a flow rate of 0.25 mL min^{-1} at 7 mA. Ammonium was measured with a Dionex™ IonPac™ CS12 A column and a CERS 500 suppressor (2 mm) using 20 mM methyl sulfonic acid (70% v/v) (Merck KGaA, Darmstadt, Germany) as eluent at a flow rate of 0.25 mL min^{-1} at 15 mA.

The detection limit was calculated based on the calibration method according to DIN EN 32645. Non-equidistant calibration points (10, 20, 50, 100, 200 µM) were used.

2.3.4. DNA extraction of aquaponic samples

DNA was extracted using the FastDNA^{TM} SPIN Kit for Soil [MP Biomedicals, Heidelberg, Germany]. 460-480 mg of sand (wet weight) were taken and treated as described in the manufacturers' instructions. For the cell lysis the bead-beating system Precellys24 tissue homogenizer [Bertin Instruments, Montigny-le-Bretonneux, France] was used for two times at 65,000 rpm for 30 s each turn. The DNA samples were stored at -20 °C until further usage.

2.3.5. Preparation of 16S rRNA gene amplicon library

The preparation of the amplicon library was adapted from the Illumina 16S sequencing library preparation guide (part no. 15044223 Rev. B). The primers Pro341F/Pro805R (Table 2.3.5-1) (Takahashi *et al.*, 2014) targeting the V3-V4 region of 16S rRNA genes of bacteria and archaea were applied to get 250 bp reads lengths. They were combined with the Illumina overhang adapters [Eurofins Genomics, Ebersberg, Germany].

Table 2.3.5-1 | Primer set used for amplification of 16S rRNA genes for sequencing. The primer sequences (underlined) are shown inclusively the Illumina barcode adapter sequences.

Primer	Sequence
Pro341F	TCGTCGGCAGCGTCAGATGTGTATAAGAGACAGCCTACGGGNBGCASCAG
Pro805R	GTCTCGTGGGCTCGGAGATGTGTATAAGAGACAGGACTACNVGGGTATCTAATCC

For the first stage PCR, 2 µL of extracted DNA was mixed with 1X KAPA HiFi Hot Start Ready Mix [Roche, Basel, Switzerland], 0.25 µmol L^{-1} of each the forward and the reverse primers including the Illumina overhang adapters, and nuclease-free water [Qiagen, Hilden, Germany] to a final reaction volume of 25 µL. Duplicates were

prepared for each sample and pooled after the PCR. The PCR amplification was carried out with an initial denaturation step at 94 °C for 5 min followed by 30 cycles of denaturation at 94 °C for 30 s, annealing at 55 °C for 30 s, and extension at 70 °C for 1 min, and a final extension at 70 °C for 5 min.

The PCR amplicons were purified using MagSi-NGS^{PREP} Plus magnetic beads [Steinbrenner, Wiesenbach, Germany] by thoroughly mixing 32 µL of magnetic beads with 40 µL of samples and following the PCR clean-up instructions given in the Illumina 16S metagenomic sequencing library preparation guide with the exception that the beads were resuspended in 42.5 µL of elution buffer EB [Qiagen, Hilden, Germany]. 40 µL of the supernatants were then taken for further analyses.

The index PCR was performed using the Nextera XT DNA Library Preparation Kit v2 Set D (FC-131-2004) from Illumina [Munich, Germany]. The PCR and the second PCR clean-up were performed as described in the Illumina 16S metagenomic sequencing library preparation guide.

DNA concentrations were measured with a Qubit fluorometer using the Qubit™ dsDNA HS Assay Kit [ThermoFisher Scientific, Dreieich, Germany]. The samples were normalized to a concentration of 2 ng µL^{-1} and 5 µL of all samples were combined into one ready-to-load sample, which was analysed by GATC Biotech AG [Konstanz, Germany] on an Illumina Miseq platform. The 16S rRNA gene sequence reads are deposited in the NCBI's nr database as SUB5504898 in the bioproject PRJNA534201.

2.3.6. Analysing 16S rRNA gene sequencing data

The 16S rRNA sequences were analysed as paired-end run using the MetaAmp Version 2.0 software (Dong et al., 2017). The settings were: similarity cutoff of 0.97, minimum overlap of 35 bp, no mismatches in the overlap region, no differences in primer sequences, max. one expected error and a trim amplicon length of 350 bp. The alignment of reads was conducted using the SILVA 128 database.

Statistical analyses were carried out using the R code described in (Weinmaier et al., 2015). For multivariate statistics, data were rarefied (to the lowest number of sequences in the samples) and a Bray-Curtis distance was calculated. In order to

account for rarefication biases, we repeated this procedure 100 times and averaged the distance across these iterations. Alpha diversity was determined using the Shannon-Wiener-Index. Principle coordinate analysis (PCoA) was used to display the beta diversity of the samples. Relationships between OTUs and environmental factors (time, pH, nitrate, ammonia, sulphate, chloride, sodium, magnesium, and calcium) were calculated using PERMANOVA (Adonis testing).

Identification of OTUs that significantly correlated with time in relative abundance, were selected by applying a Pearson correlation. Only OTUs with a p-value < 0.001 are reported in the manuscript.

2.3.7. Metagenomic sequencing and analysis

For the metagenome sequencing, 390 ng of DNA were extracted from the sand sample on day 508. Library preparation and Illumina HiSeq sequencing of paired-end 150-bps reads were done by GATC Biotech AG (Konstanz, Germany). Raw reads obtained from GATC Biotech were trimmed and quality filtered using bbduk (http://jgi.doe.gov/data-and-tools/bbtools/) and SICKLE version 1.21 (https://github.com/najoshi/sickle). The processed reads were assembled and scaffolded using metaSPADES version 3.10.1 (Nurk et al., 2017). For scaffolds longer than 1 kb genes were predicted using prodigal (Hyatt et al., 2010) and diamond blastp (Buchfink et al., 2015) was used to annotate the genes against the Unifref100 database (Suzek et al., 2014), which contained taxonomy information from UniProt and the NCBI taxonomy database.

Databases of 100 amino acid sequences each for ammonia monooxygenase subunit A (amoA), subunit B (amoB), and subunit C (amoC) and the hydroxylamine reductase were created from highly identical sequences derived from NCBI's nr database. The sequences were aligned using MUSCLE (Edgar, 2004) and maximum likelihood phylogenetic trees were constructed based on the JTT matrix-based model (Jones et al., 1992) using the MEGA7 software (Kumar et al., 2016) by applying default settings.

2.3.8. Quantification of comammox *Nitrospira* using qPCR

The concentration of comammox *Nitrospira* in the aquaponic system were measured with quantitative PCR (qPCR) using the primer sets reported by Pjevac *et al.* (2017) for comammox Nitrospira clade A and clade B (Table 2.3.8-1). The primers were purchased from Eurofins Genomics [Ebersberg, Germany].

Table 2.3.8-1 | qPCR primer sets used for quantification of comammox *Nitrospira*.

		Name	Sequence
Clade A	Forward primer	comaA-244F	TAYAAYTGGGTSAAYTA
	Reverse primer	comaA-659R	ARATCATSGTGCTRTG
Clade B	Forward primer	comaB-244F	TAYTTCTGGACRTTYTA
	Reverse primer	comaB-659R	ARATCCARACDGTGTG

Standards for quantification of comammox *Nitrospira* in qPCR were obtained from 16S rRNA sequences lodged by Pjevac *et al.* (2017) derived in the present study in NCBI's nr database (NZ_LN885086.1 for *comaA* and KY606428.1 for *comaB*) using the primers mentioned above. The standards were purchased from IDT Integrated DNA Technologies [Leuven, Belgium]. They were prepared in gene copies μL^{-1} as serial dilutions in nuclease-free water ranging from 10^6 to 10^1 gene copies μL^{-1}.

The qPCR mix was prepared using the SsoFast™ EvaGreen® supermix [Bio-Rad Laboratories, Munich, Germany] and following the manufacturers' instructions (Table 2.3.8-2). The thermal profile used for quantification is shown in Table 2.3.8-2. A subsequent melting curve was conducted from 60 °C to 96 °C with 0.5 °C per second.

Table 2.3.8-2 | qPCR mix for the quantification of comammox *Nitrospira*.

	Stock conc.	Final conc.	Per reaction
DNA template	-	-	5 µL
Nuclease-free water	-	-	3 µL
SsoFast™ EvaGreen®	10X	1X	10 µL
Forward primer	100 µmol L^{-1}	0.5 µmol L^{-1}	1 µL
Reverse primer	100 µmol L^{-1}	0.5 µmol L^{-1}	1 µL

Table 2.3.8-3 | Thermal profile used for qPCR.

Temperature	Time	
95 °C	3 min	
95 °C	30 s	45 cycles
52 °C	45 s	
72 °C	1 min	
70 °C	5 min	
4 °C	hold	

All samples were measured in duplicates. Nuclease-free water was purchased from Promega GmbH [Mannheim, Germany]. The qPCR was performed in the thermal cycler CFX96^{TM} real-time system [Bio-Rad Laboratories, Munich, Germany]. Analyses of samples were done using the attended software CFX-Manager 3.0. The raw qPCR data are shown in the appendix in Table 2.5.4-3 (*Nitrospira* clade A) and Table 2.5.4-4 (*Nitrospira* clade B).

2.4. **Results**

2.4.1. Nitrogen species in the aquaponic system

The aquaponic system efficiently removed nitrogen from the water. Only nitrate was measurable in low concentrations up to 1.1 mM in the sump of the aquaponic system at the end of the system operation (Figure 2.4.1-1).

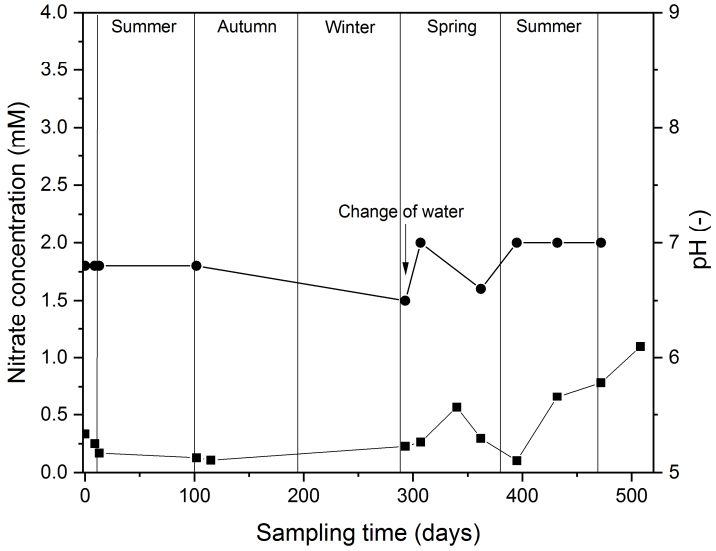

Figure 2.4.1-1 | Concentrations of nitrate (squares) and pH (circles) in the aquaponic system from May 2016 to October 2017. Concentrations of nitrite and ammonium were below 23 µM and 19 µM, respectively, throughout the monitoring time.

Ammonium and nitrite concentrations were always below 23 µM and 19 µM, respectively, indicating that both ammonium and nitrate were taken up by the plants and residual ammonium was completely oxidised by nitrifying microorganisms. In April 2017, the concentration of nitrate raised to 0.6 mM due to the starting metabolism of the fish resulting in a higher nitrogen load of the water. When seedlings were planted in May, nitrate and potentially ammonium were increasingly taken up by the plants leading to a decrease of nitrate concentrations to 0.1 mM in June 2017. The nitrate concentrations increased again from June onwards to 1.1 mM at the end of the operation in October 2017. The absence of ammonium in all samples indicated that a

nitrifying microbial community was established in the aquaponic system. The pH stayed constant between 6.8 and 7 and was not adjusted.

2.4.2. Microbial diversity

Sequencing of 16S rRNA genes revealed a highly diverse community structure in the aquaponic system. A total of 40 bacterial phyla were identified, out of which 15 made up 95.4% of the total microbial community. The most dominant phyla in the aquaponic system were Proteobacteria, Bacteroidetes, Verrucomicrobia, Acidobacteria, Actinobacteria, and Nitrospira (Figure 2.4.2-1). The three most abundant OTUs classified on family level at the end of the operation of the aquaponic system (day 508) were Verrucomicrobiaceae (4.3%), Nitrospiraceae (3.8%), and Comamonadaceae (2.8%), which belong to the phylum Proteobacteria.

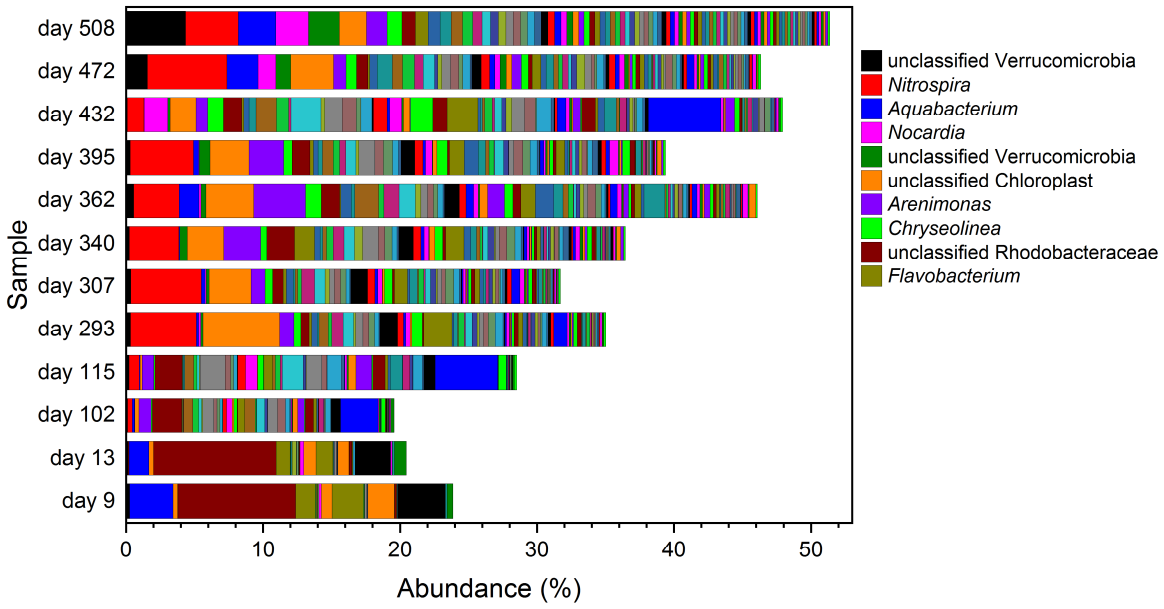

Figure 2.4.2-1 | Relative abundances of taxonomic phyla in the aquaponic system based on 16S rRNA gene sequencing. Taxonomy was sorted based on the total reads of the sample "day 508". Please consider the repetition of colours. The water change was performed on day 293.

In the highly diverse samples, the 100 most abundant genera make up almost 50% of the total community at the end of the operation of the aquaponic system (Figure 3). After a water change on day 293, unclassified *Verrucomicrobia*, unclassified *Chloroplasts*, as well as *Nitrospira*, *Aquabacterium*, and *Arenimonas* were among the

most dominant genera based on OTUs. The dominant OTU classified as *Nitrospira* was found in all samples after the water change. The classical genus of ammonia oxidisers, *Nitrosomonas*, was only found in very low relative abundance (0.03%) suggesting that the detected *Nitrospira* were fully oxidising ammonium to nitrate similar to the previously found *Candidatus* Nitrospira inopinata (Daims *et al.*, 2015, van Kessel *et al.*, 2015).

The microbial diversity in the aquaponic system was described using the Shannon index H_S (Figure 2.4.2-2). During the first year of operation, the diversity was increasing over time from 4.74 (day 9) to 6.30 (day 307). During the second year the Shannon index stagnated between 6.27 and 6.39 indicating a stabilization of the microbial diversity on a very high diversity level. A total water exchange was performed on day 293.

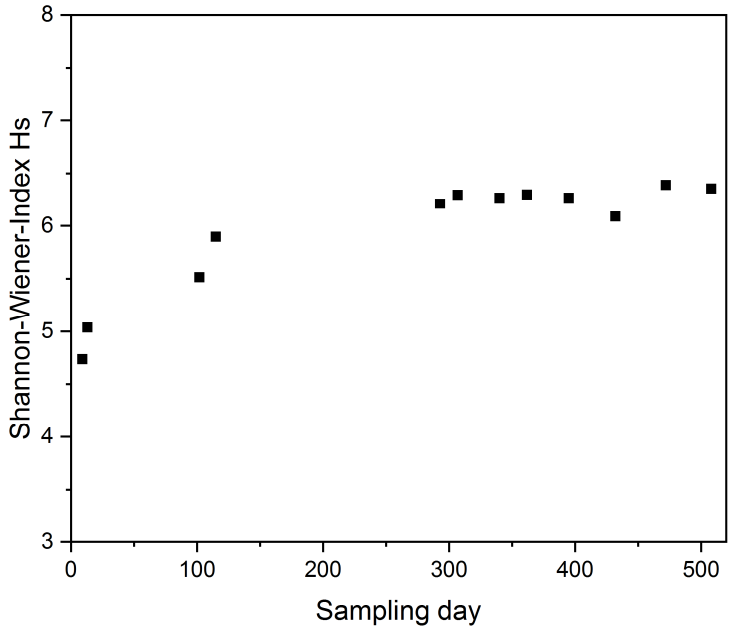

Figure 2.4.2-2 | Shannon indices as measure for microbial alpha diversity calculated from OTU abundances at different time points.

Principal coordinate analysis of the relative abundances of OTUs showed a distinct shift in the microbial community composition over time (Figure 2.4.2-3). Samples taken in the beginning of the operation in spring 2016 (day 9 and day 13) differed significantly from the samples taken at the end of summer (day 102 and day

115). After the change of water in spring 2017 (day 293), the microbial community composition deviated again showing a precedent shift in the winter period. In the last half of the year of operation, the community composition seemed to become more stable and shifted only slightly with seasons.

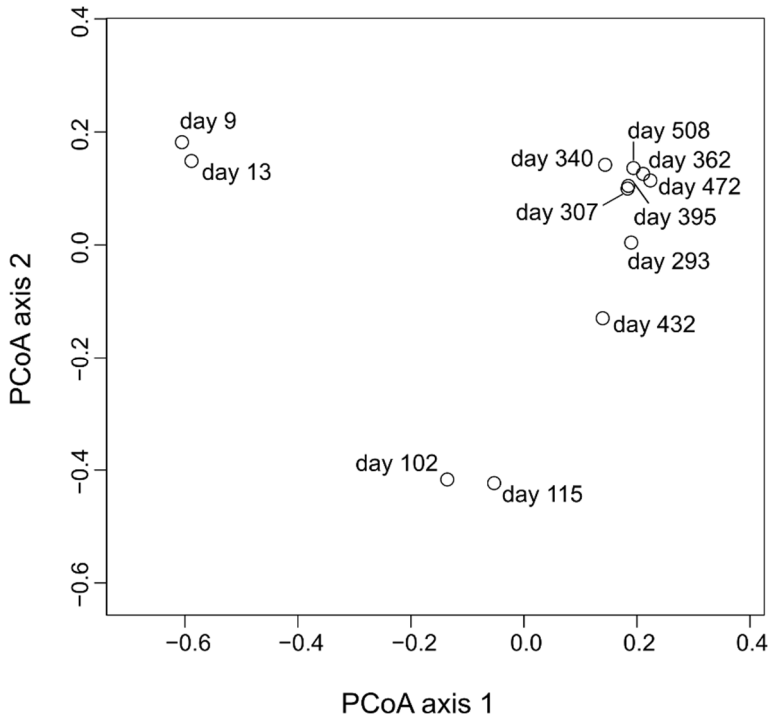

Figure 2.4.2-3 | Principal coordinate analysis diagram showing the beta diversity of OTUs in the microbial community at different sampling days. Principal coordinate analysis axis 1 and axis 2 explained 44.2% and 22.5% of the total variance in the community, respectively.

As indicated in the principal coordinate analysis, time had a substantial impact on the microbial community composition (PERMANOVA p-value 0.001). Interestingly, no other measured parameter showed a significant association with the observed microbiome structure. OTUs classified as members of the genera *Nitrospira*, *Acidobacteria*, *Sphingobacteria* and *Cytophagia* were less abundant or not even detectable in the beginning and increased continuously during the operation time of the aquaponic system (Figure 2.4.2-4). Other genera, mainly belonging to the *Alphaproteobacteria*, decreased in abundances over time. However, even after one and a half years of operation a steady state community had not been reached according to the PERMANOVA test.

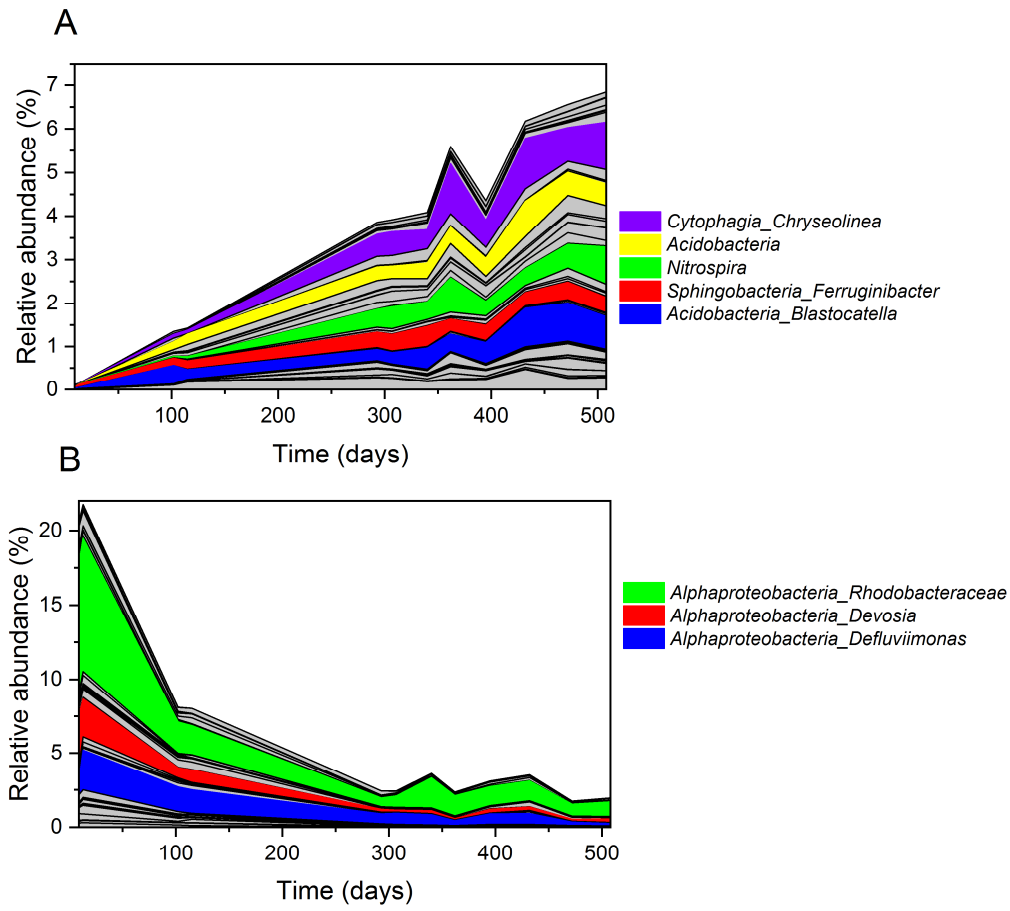

Figure 2.4.2-4 | Correlation of OTUs with the factor time. Relative abundances of 50 OTUs are shown in each panel that changed either most positively (A) or most negatively (B) with time. Note the differences in scales.

2.4.3. Metagenome analyses

Metagenome sequencing was performed from the samples taken at the last sampling day (day 508) to investigate the metabolism of the key players in ammonia oxidation. The assembled metagenome showed that the ammonia monooxygenases genes *amoA*, *amoB*, and *amoC* were only found on scaffolds classified as *Nitrospira*. The ammonia monooxygenase subunits *amoA* (Figure 2.4.3-1), *amoB* (Figure 2.4.3-2), and *amoC* (Figure 2.4.3-3) showed highly identical amino acid sequences to those obtained from reference sequences of comammox *Nitrospira nitrificans* (Table 2.4.3-1). The sequences of amino acids showed highest identities (98% for *amo* subunits and 96% for hydroxylamine reductase) with comammox *Nitrospira* species found on a rapid sand filter and a household sand filter (Wang *et al.*, 2017, Palomo *et*

al., 2018). Two further scaffolds contained *amoA* and *amoC* genes, respectively (Table 2.5.4-1).

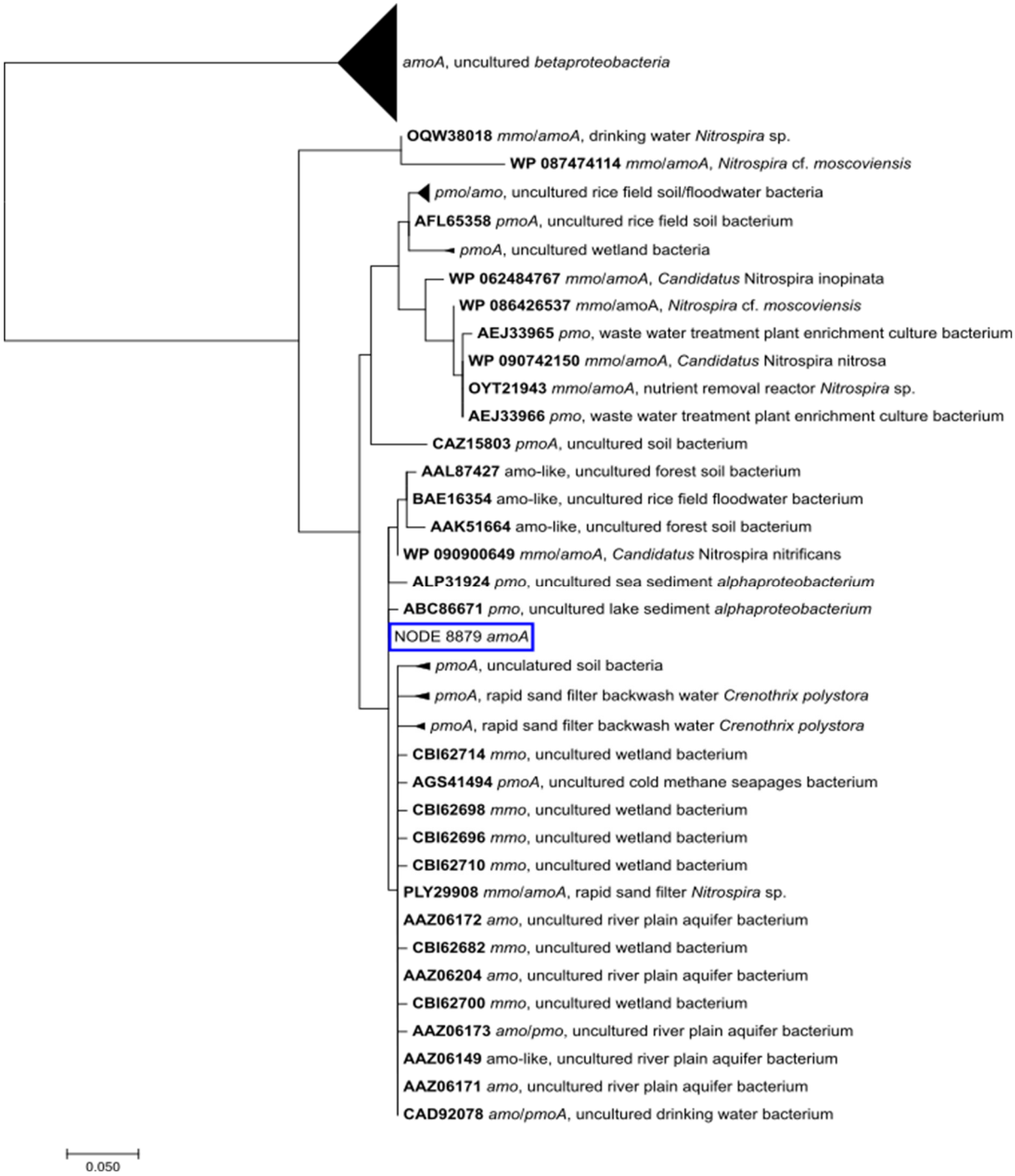

Figure 2.4.3-1 | Phylogenetic tree of *amoA* gene sequences using the maximum likelihood method based on the JTT matrix-based model (Jones *et al.*, 1992). *Amo*: ammonia monooxygenase. *Mmo*: methane monooxygenase. *Pmo*: particulate methane monooxygenase. Scale bar indicates estimated number of substitutions per site.

Figure 2.4.3-2 | Phylogenetic tree of *amoB* gene sequences using the maximum likelihood method based on the JTT matrix-based model (Jones *et al.*, 1992). *Amo*: ammonia monooxygenase. *Mmo*: methane monooxygenase. Scale bar indicates estimated number of substitutions per site.

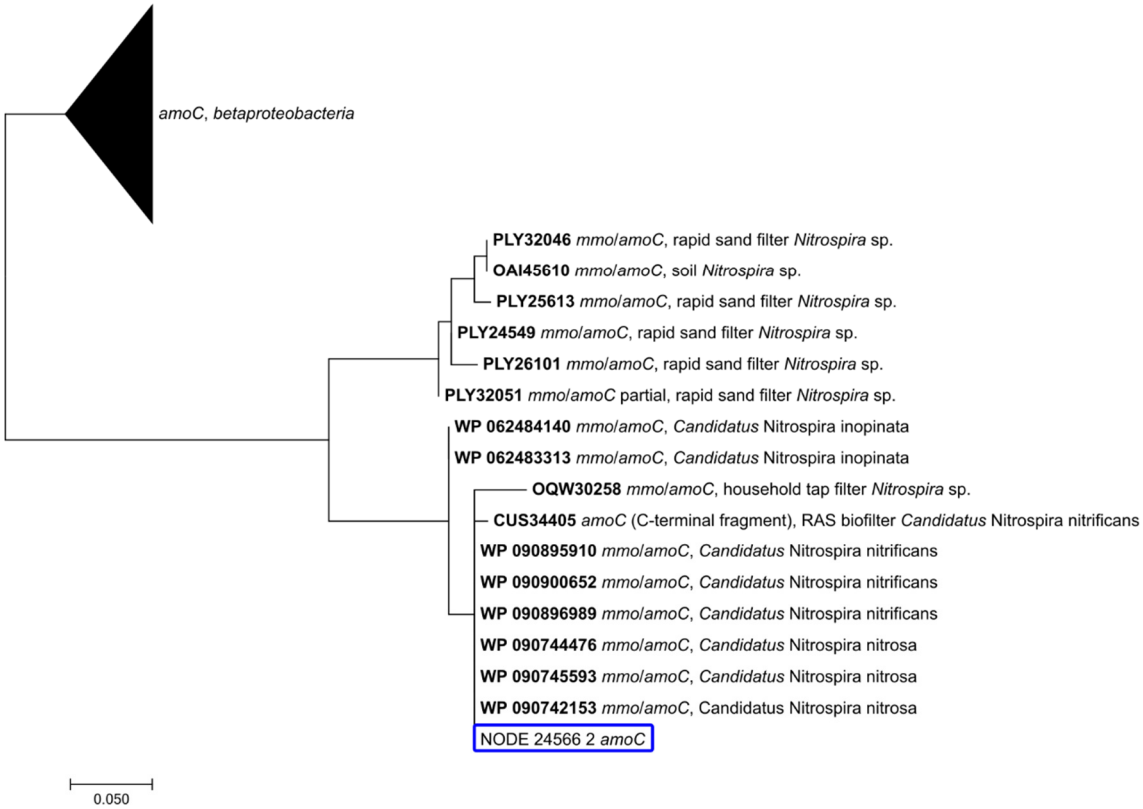

Figure 2.4.3-3 | Phylogenetic tree of *amoC* gene sequences using the maximum likelihood method based on the JTT matrix-based model (Jones *et al.*, 1992). *Amo*: ammonia monooxygenase. *Mmo*: methane monooxygenase. Scale bar indicates estimated number of substitutions per site.

Table 2.4.3-1 | Comparison of genes involved in complete ammonia oxidation obtained in this study and from known strains. Identity and total score were retrieved from a blast search against the NCBI's nr database.

	Nitrospira nitrificans		***Nitrospira nitrosa***		***Nitrospira inopinata***	
	Identity	**Score**	**Identity**	**Score**	**Identity**	**Score**
amoA	WP_090900649.1		WP_090742150.1		WP_062484767.1	
	98%	499	91%	437	90%	443
amoB	WP_090900646.1		WP_090742146.1		WP_062484768.1	
	93%	782	82%	723	82%	734
amoC	WP_090895910.1		WP_090744476.1		WP_062484140.1	
	98%	351	96%	342	95%	340
hcp	WP_090894739.1		WP_090900629.1		WP_062481664.1	
	70%	564	69%	561	70%	566

Moreover, hydroxylamine reductases were only found in *Nitrospira* (Figure 2.4.3-4). Two additional genes were identified for a putative hydroxylamine reductase (Table 2.5.4-1). Consequently, *Nitrospira* was the only significantly abundant genus capable of ammonia oxidation in the backyard aquaponic system.

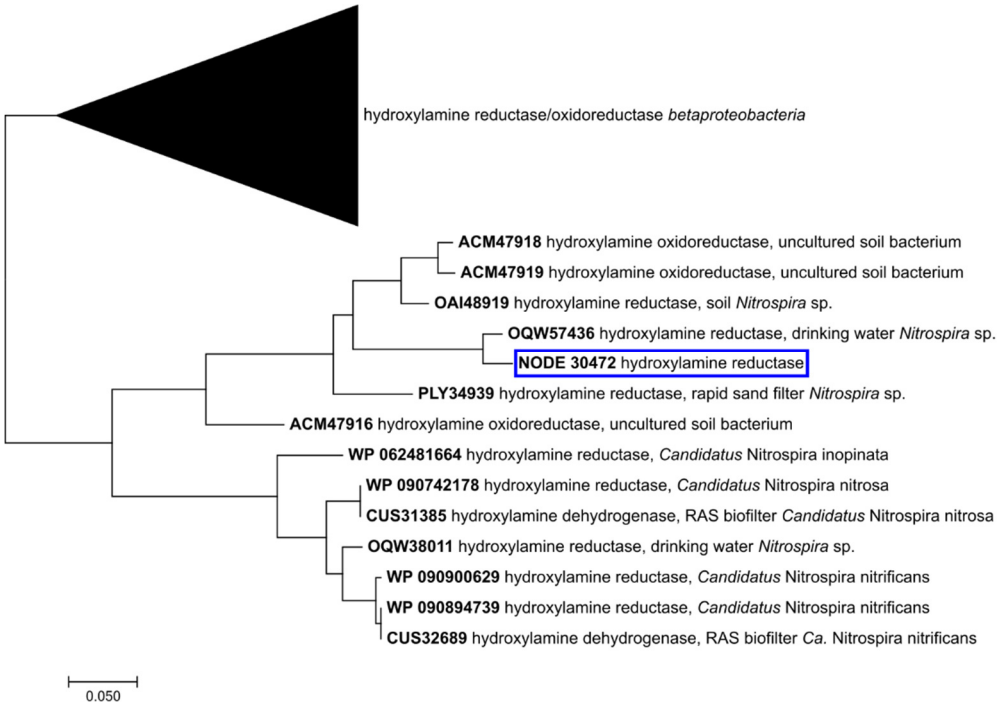

Figure 2.4.3-4 | Phylogenetic tree of hydroxylamine reductase gene sequences using the maximum likelihood method based on the JTT matrix-based model (Jones *et al.*, 1992). RAS: recirculating aquaculture system. Scale bar indicates estimated number of substitutions per site.

2.4.4. Quantification of comammox *Nitrospira* in the aquaponic system

The abundance of comammox *Nitrospira* was investigated via qPCR using primer sets specifically designed for both clades, clade A and clade B (Pjevac *et al.*, 2017). The concentrations given in gene copies μL^{-1} are shown in Table 2.4.4-1. Comammox *Nitrospira* clade A were only detectable at day 102 and day 432. All other samples revealed measurable concentrations in gene copies μL^{-1} for both genes. However, different melting temperatures were obtained showing that different qPCR products might have been amplified. Comammox *Nitrospira* clade B were detectable in 6 out of 12 samples showing additionally a similar melting temperature as the standard. It must also be stated that efficiencies were very low (54.6% and 49.3% in

the case of comammox *Nitrospira* clade A and clade B, respectively) in the qPCR assays.

Table 2.4.4-1 | Quantification of comammox *Nitrospira* clade A and clade B in the aquaponic system. N/A = not available based on melting temperature.

Sample day	**Concentration of comammox *Nitrospira* clade A [gene copies µL^{-1}]**	**Concentration of comammox *Nitrospira* clade B [gene copies µL^{-1}]**
Day 9	N/A	N/A
Day 13	N/A	$9.88 \pm 0.47 \times 10^4$
Day 102	$3.50 \pm 0.74 \times 10^4$	$1.30 \pm 0.08 \times 10^5$
Day 115	N/A	$9.87 \pm 1.49 \times 10^4$
Day 293	N/A	$3.07 \pm 0.51 \times 10^5$
Day 307	N/A	N/A
Day 340	N/A	N/A
Day 362	N/A	$2.36 \pm 0.30 \times 10^5$
Day 395	N/A	N/A
Day 432	$1.05 \pm 0.14 \times 10^5$	N/A
Day 472	N/A	$9.96 \pm 0.47 \times 10^5$
Day 508	N/A	N/A

On sample day 362, a second peak was found in the melting temperature profile at 82.5 °C for the comammox *Nitrospira* clade B, indicating the presence of a second qPCR product that can be amplified with the applied primer set. This could lead to an overestimation of the actual concentration of comammox *Nitrospira* clade B. Although, they were mainly available in the first half of operation of the aquaponic system, comammox *Nitrospira* clade B were most abundant in the end of operation (day 472) with approximately 10^6 gene copies µL^{-1}. However, they were not detectable in the months before and after this day.

2.5. **Discussion**

2.5.1. Performance of the aquaponic system

Ammonia concentration is one of the most important parameters in aquaculture since it is toxic to fish species in relatively low concentrations (0.94 mmol L^{-1} for acute intoxication and 0.11 mmol L^{-1} for chronic intoxication at pH 7 and 20 °C) (USEPA, 2013). In an aquaponic system, ammonia nitrogen is released into the fish tank and taken up by the plants in the grow beds either as ammonium or after oxidation to nitrate (Xu *et al.*, 2012). The nitrifying microbial community in the sediments converts the residual ammonium that is not taken up by plants to nitrate, which is less harmful to fish species than ammonia (Stormer *et al.*, 1996, Alonso & Camargo, 2003). The crucial concentration of ammonium is at the end of the hydroponic part at the influent to the aquaculture fish tank. In our aquaponic system, a nitrifying community was efficiently established reducing the ammonium concentration effectively below 23 µM.

Nitrification in aquaculture biofilters is most efficient at slightly alkaline pH of 7.5 to 9.0 (Hochheimer & Wheaton, 1998, Kim *et al.*, 2007). However, hydroponic plants grow best at slightly acidic conditions such as pH 5.5 for romaine lettuce crops (Pantanella *et al.*, 2012) and 5.5 to 6.0 for greenhouse cucumber (Hochmuth, 2001). Compromising the efficiencies of nitrification, fish cultivation and plant growth, neutral pH 7 is commonly accepted as the optimal pH for aquaponic systems (Rakocy *et al.*, 2006). Our aquaponic system was continuously running at pH 6.8-7.0 without adjustment providing an efficiently self-regulated system with optimal nitrogen removal.

2.5.2. Microbial community composition

Since the focus was on microbial nitrification processes, we installed our test sediments in the pump sump located between the grow beds and the fish tank. Until now, microbial diversity in aquaculture and aquaponic systems was mainly studied on biofilters (Sugita *et al.*, 2005, Itoi *et al.*, 2006, Brown *et al.*, 2012, Bartelme *et al.*, 2017, Schmautz *et al.*, 2017). In aquaponic systems, however, the biofilter function is replaced by the grow beds.

In our test sediments the most abundant OTUs were member of *Proteobacteria*, *Bacteroidetes*, *Verrucomicrobia*, *Acidobacteria* and *Actinobacteria*. The same phyla were also among the most dominant ones of an aquaponics biofilter community (Schmautz *et al.*, 2017). In contrast, Bartelme *et al.* (2017) identified *Actinobacteria*, *Gammaproteobacteria*, *Planctomycetes*, and *Sphingobacteria* as the most dominant phyla in freshwater recirculating aquaculture systems (RAS). Sugita *et al.* (2005) found *Alphaproteobacteria*, *Betaproteobacteria*, *Nitrospira*, *Actinobacteria*, *Bacilli*, *Gammaproteobacteria*, *Planctomycetacia*, and *Sphingobacteria* as predominant phyla in similar systems.

Surprisingly, in our aquaponic system the microbial community compositions in the aquaponic system changed continuously over 508 days. Since the parameters determined for the aquaponic system were relatively constant, the change of microbial community compositions only correlated with the factor time. There was no correlation between the nitrifying community and the nitrate concentrations detectable. Since the ammonium concentration was always very little, the removal of the nitrogen compounds by the plants was in equilibrium with the ammonia production by the fish and the microbial nitrification keeping all nitrogen species at low steady state concentrations.

Oxygen concentrations have a strong influence on the microbial communities since ammonia oxidation depends on the oxygen availability in the system. However, the fish biomass and, thus, the fish food increased continuously over time, which certainly led to a continuous increase of the ammonia release rate by the fish. Although, this did obviously not influence the steady state concentrations of the nitrogen species, it will have influenced the compound fluxes.

2.5.3. Two-step nitrification or comammox?

The microbial community composition on the sediments revealed *Nitrospira* as the only organisms potentially involved in nitrification. The classically known members of the genus *Nitrospira* perform the second part of the two-step nitrification, the oxidation of nitrite to nitrate. For a complete nitrification process, a second organism such as *Nitrosomonas* would be essential to oxidise ammonia to nitrite. However,

ammonia-oxidising bacteria like *Nitrosomonas* were at negligible abundance in our aquaponic sediments. *Nitrospira* belonged to the most abundant organisms in the aquaponic system and is most likely the organism performing the complete ammonia oxidation to nitrate. Similar results were reported by Schmautz *et al.* (2017), who found *Nitrospira* to be one of the most abundant species in the aquaponic system. Since other ammonia-oxidising bacteria were only found at very low abundance, the authors assumed that the detected *Nitrospira* were comammox organisms.

Ammonia is first oxidised to hydroxylamine by ammonia monooxygenase, which consists of at least three subunits (*amoA*, *amoB*, and *amoC*). Hydroxylamine is then oxidised to nitrite catalysed by the hydroxylamine reductase. These genes can, therefore, be taken as indicators for ammonia oxidation. Detection of both genes for ammonia and nitrite oxidation in one genome are strongly indicative of comammox (Daims *et al.*, 2015). In our aquaponic system, the scaffolds of genes for the ammonia-oxidising enzymes were only found on scaffolds classified as *Nitrospira*. *Nitrosomonas* und *Nitrobacter*, which have been regarded as the main nitrifying bacteria so far, do probably not play a pivotal role in nitrification in our well-performing freshwater aquaponic systems. Hence, the interpretation of the community analysis was strongly supported by the metagenomic analysis and the detection of genes coding for enzymes involved in nitrification.

Comammox *Nitrospira* were predicted to survive in environments with low ammonium concentrations (Costa *et al.*, 2006). This assumption was recently underlined, when comammox *Nitrospira* were detected in groundwater (Fowler *et al.*, 2018), drinking water systems (Pinto *et al.*, 2016, Wang *et al.*, 2017) as well as recirculating aquaculture systems with low ammonium loading (Bartelme *et al.*, 2017). Due to the high similarities of the genes involved in complete ammonia oxidation between known comammox *Nitrospira* and those obtained in this study, it is concluded that in the aquaponic system ammonia was completely oxidised by comammox *Nitrospira*.

2.5.4. Abundances of comammox *Nitrospira* in the aquaponic system

The quantification of comammox *Nitrospira* via qPCR reveals measurable abundances throughout the operation of the aquaponic system and that comammox *Nitrospira* clade B are more abundant than those of clade B. As the efficiencies are extremely low, comammox *Nitrospira* may remain undetected in many samples. Despite the first sampling day (day 9), PCR products are amplified on sampling days that reveal a distinct melting temperature from the standard sequences. In consent with the metagenomic analysis showing clear presence of comammox *Nitrospira* in all samples, it is assumed, that those PCR products with different melting temperatures might indeed originate from comammox *Nitrospira* but are undetectable due to the inadequate efficiencies. Efficiencies in real-time qPCR decrease significantly with the amplicon lengths, which usually range between 100 to 250 bp (Wang & Seed, 2006). Manufacturers of qPCR system even recommend lower amplicon sizes of 75 to 200 bp (Bio-Rad Laboratories Inc., 2006) or below 150 bp (QIAGEN, 2010) to ensure successful amplification of the target DNA. The specific primer sets for comammox *Nitrospira* clade A and clade B used in this study target sequences with an amplicon length of 415 bp (Pjevac *et al.*, 2017) and do not seem to be applicable for the detection and clade differentiation of comammox *Nitrospira* in this aquaponic system.

2.6. **Appendix**

Table 2.5.4-1 | Genes annotated as ammonia monooxygenase and hydroxylamine reductase.

Ammonia monooxygenase												
NODE_8879 length_2199 cov_2.755131_1	UniRef100_A0A0S4LM25	98.4	246	247	282	4E-142	512.7	UniRef100_A0A0S4LM25 Ammonia monooxygenase, subunit A n=1 Tax=*Candidatus* Nitrospira nitrificans TaxID=1742973 RepID=A0A0S4LM25_9BACT	Taxonomy=Bacteria; Nitrospirae; *Nitrospirales; Nitrospiraceae; Nitrospira*			
NODE_8879 length_2199 cov_2.755131_2	UniRef100_A0A0S4LUC5	92.8	419	420	419	2E-232	813.5	UniRef100_A0A0S4LUC5 Ammonia monooxygenase, subunit B n=1 Tax=*Candidatus* Nitrospira nitrificans TaxID=1742973 RepID=A0A0S4LUC5_9BACT	Taxonomy=Bacteria; Nitrospirae; *Nitrospirales; Nitrospiraceae; Nitrospira*			
NODE_10762 length_1994 cov_3.495616_1	UniRef100_A0A177QD36	92.4	262	265	266	5E-147	529.3	UniRef100_A0A177QD36 Methane monooxygenase/ammonia monooxygenase subunit C n=1 Tax=*Nitrospira* sp. SCGC AG-212-E16 TaxID=1799664 RepID=A0A177QD36_9BACT	Taxonomy=Bacteria; Nitrospirae; *Nitrospirales; Nitrospiraceae; Nitrospira*			
NODE_11067 length_1964 cov_3.334730_4	UniRef100_A0A0S4LD97	85.9	71	72	272	2.7E-31	142.9	UniRef100_A0A0S4LD97 Ammonia monooxygenase, subunit C n=1 Tax=*Candidatus* Nitrospira nitrosa TaxID=1742972 RepID=A0A0S4LD97_9BACT	Taxonomy=Bacteria; Nitrospirae; *Nitrospirales; Nitrospiraceae; Nitrospira*			
NODE_24566 length_1301 cov_9.516854_1	UniRef100_A0A0S4LPG4	98.2	217	217	280	4E-124	453	UniRef100_A0A0S4LPG4 Ammonia monooxygenase, subunit A n=2 Tax=Bacteria TaxID=2 RepID=A0A0S4LPG4_9BACT	Taxonomy=			
NODE_24566 length_1301 cov_9.516854_2	UniRef100_A0A0S4LEU9	97.7	174	175	245	2.3E-97	363.6	UniRef100_A0A0S4LEU9 Ammonia monooxygenase, subunit C n=1 Tax=*Candidatus* Nitrospira nitrificans TaxID=1742973 RepID=A0A0S4LEU9_9BACT	Taxonomy=Bacteria; Nitrospirae; *Nitrospirales; Nitrospiraceae; Nitrospira*			
Hydroxylamine reductase												
NODE_7910 length_2329 cov_2.131047_1	UniRef100_A0A099KDI2	80.3	76	108	541	1.3E-29	137.9	UniRef100_A0A099KDI2 Hydroxylamine reductase n=1 Tax=*Thalassotalea* sp. ND16A TaxID=1535422 RepID=A0A099KDI2_9GAMM	Taxonomy=Bacteria; Proteobacteria; *Gammaproteobacteria; Alteromonadales; Colwelliaceae; Thalassotalea*			
NODE_19566 length_1462 cov_1.855011_2	UniRef100_A0A177QNG2	66.7	66	115	569	1.3E-19	104.8	UniRef100_A0A177QNG2 Hydroxylamine reductase n=1 Tax=*Nitrospira* sp. SCGC AG-212-E16 TaxID=1799664 RepID=A0A177QNG2_9BACT	Taxonomy=Bacteria; Nitrospirae; *Nitrospirales; Nitrospiraceae; Nitrospira*			
NODE_19566 length_1462 cov_1.855011_3	UniRef100_A0A177QNG2	85.6	90	90	569	3.3E-39	169.5	UniRef100_A0A177QNG2 Hydroxylamine reductase n=1 Tax=*Nitrospira* sp. SCGC AG-212-E16 TaxID=1799664 RepID=A0A177QNG2_9BACT	Taxonomy=Bacteria; Nitrospirae; *Nitrospirales; Nitrospiraceae; Nitrospira*			
NODE_30472 length_1165 cov_3.902703_1	UniRef100_A0A177QNG2	86	387	388	569	3E-206	726.5	UniRef100_A0A177QNG2 Hydroxylamine reductase n=1 Tax=*Nitrospira* sp. SCGC AG-212-E16 TaxID=1799664 RepID=A0A177QNG2_9BACT	Taxonomy=Bacteria; Nitrospirae; *Nitrospirales; Nitrospiraceae; Nitrospira*			

Table 2.5.4-2 | Predicted amino acid sequences of genes annotated as ammonia monooxygenase and hydroxylamine reductase.

Ammonia monooxygenase subunit A	
>NODE_8879 length_2199 cov_2.755131_1 # 2 # 742 # 1 # ID=667_1	IVGTFHMHTALLCGDWDFWLDWKDRQWWPIVTPVTLITFCAALQYYNWVNYRQPFGATLCILALGAGKWIAVYTSWWWWSN YPPNFVMPATAIPGALVLDITLLLTRNWTLTAVIGAWMFAALFYPSNWPIFAYSHTPLVVDGALLSWADYMGFMYVRTGTPEYI RMIEVGSLRTFGGHSTMISAFFSAFASSLTYILWWQFGKFFCTSYFYMTDDRQRTTKVYDVFAFATLGPQGDKAKLSGGKA
>NODE_24566 length_1301 cov_9.516854_1 # 1 # 651 # -1 # ID=4036_1	MFRTDEIIKASKLPPEGVAMSRHLDHIYFIPILFITIVGTFHMHTALLCGDWDFWIDWKDRQWWPIVTPVTTITFCAALQYYNWVN YRQPFGATITILALAFGKWIAVYTSWWWWSNYPPNFVMPATLLPSALVLDITLLLTRNWTLTAVIGAWMYAILFYPSNWPIFGYS HTPIVVDGSLLSWADYMGFMYVRTGTPEYIRMIEVGSLRTFGGHST
Ammonia monooxygenase subunit B	
>NODE_8879 length_2199 cov_2.755131_2 # 739 # 1998 # 1 # ID=667_2	MTAKHVFKLWMIRLCGVVTLAATPALDITPAFAHGERSQEPFLRMRTVNWYDTEWVGKSTKVNDVTELKGKFHLSEDWPRAV VKPTRTFINVGSPSSVFVRLSSKVNGTPMFVSGPMEIGRDYEYIVKLKARLPGHHHIHPMFAVKEAGPIAGPGGWMDITGRYE DFTNPIKTLTNETFDSETMGSMTGIGWHIWWIALGIFWVGFFAIRPMYLIRARVLAAYGDEILLDPIDRKVGVAVLVLTLTVVAGY MAAEAKHPISVPLQAGEAKIKPMPIKPNPLTVDVIHAEYDVPGRALRMVLHATNNGTSPITIGEFTTAGIRFTNKFGAARVDPNYP AELVASAGLTMDNEAPIQPGQTVDIKVESKDVLWEVQRLVDILHDPDQRFAGLFLSWTDSGERLINPVWAPVLPVFTRMGA
Ammonia monooxygenase subunit C	
>NODE_10762 length_1994 cov_3.495616_1 # 991 # 1785 # 1 # ID=2550_1	MATTWGGADRGYDMSLWYDSKPLKIGWFAMLAAVGSEVIFQRVFGYSHGLDSMTPEFENVWMGLWRFNVISNIIFSAATLG WIWSTRDRNVANVDPKTELKRYFYWMMWLAIYVFGVYWAGSYTLEQDASWHQVIIRDTSFTASHIIAFYFTFPLYITCGVASYL YAMTRLPQFSKAVSFPLVGAIVGPMMILPNVGLNEWGHAFWFVDELFAAPLHWGFVTLGWCGLFGGTGGVAAQIVARMSNL CDVVWNNESKDCLHVIPY
>NODE_24566 length_1301 cov_9.516854_2 # 775 # 1299 # -1 # ID=4036_2	KRYFYWMGWLVCYIWGVYYAGSYTLEQDAAWHQVIIRDTSFTASHIVAFYGTFPLYITCGVSSYLYAQTRLPLYSQATSFPLVA AVVGPMFILPNVGLNEWGHAFWFVDELFAAPLHWGFVTLGWCGLFGAAGGVAAQIVSRMSNLADVIWNNAPKSILDPFASQI GPGAKSVY
Hydroxylamine reductase	
>NODE_19566 length_1462 cov_1.855011_2 # 908 # 1252 # 1 # ID=3142_2	MVKHVAKYAMVLCGLLLAAPAHAQYSSIPKETFEALNIQRSATPKEFHEALTKRYKDPGKGAGKGQYGQYWEPIPXXXXAVCE VPHRRIAWLGGHVEAKHPCQSGPDPQAHAER
>NODE_19566 length_1462 cov_1.855011_3 # 1191 # 1460 # 1 # ID=3142_3	MWKRSTHANLDQIRKLTPKDDTFYKKAKLEEIEGNLRSLGKLGPKENLKEVSCIDCHVDINAKKAADHRVDLKMPTSDTCGSCH LMEYAE
>NODE_30472 length_1165 cov_3.902703_1 # 2 # 1165 # -1 # ID=1730_1	IDCHVDINAKKAADHRVDLKMPTADVCGNCHLMEYAERESERDTILWPKNQWPRGRPSHVLDWRANVETDIWAGMSQREIAE GCSMCHTNQNKCDNCHTRHEFSVADSRKPEACGTCHSGADHINWEAYNGSQHGLGYQASKNRWNWNLQLKDMVVKGGQK FPTCQSCHMEYQGKFSHNTVRKVRWANYPFVPGIREAVFDNWGMQRYEAWVKTCTTCHSETFARAYLEFIDNGTSHGLDKY DEAHNVVHKQFEARLLTGQRTNRPAPPAPAKALFDQFWQIYWSKNNSPTAIELKLFEMAEDHLVQLHVALAHQYPGFTYTVG WAAMNRAYVEIMDEDTKLKDRMLLMDRVTKLEEKTKTSSLLDFDSTDGKLTIGSLGGGMLLTGT

Table 2.5.4-3 | Raw qPCR data for the samples from the aquaponic system (AP) using the primer set for the amplification of comammox *Nitrospira* clade A (comaA).

Well	Fluor	Content	Sample	Cq	Starting Quantity (SQ)	Melt Temperature	Peak Height
A01	SYBR	Std-1		26.86	1.000E+06	85.00	1735.61
A02	SYBR	Std-1		27.40	1.000E+06	85.00	1773.51
A03	SYBR	Std-1		27.46	1.000E+06	84.50	1789.23
A04	SYBR	Unkn	AP2	39.36	6.549E+03	None	None
A05	SYBR	Unkn	AP2	39.10	7.351E+03	None	None
A06	SYBR	Unkn	AP10	29.26	5.338E+05	None	None
A07	SYBR	Unkn	AP10	28.74	6.687E+05	None	None
B01	SYBR	Std-2		33.64	1.000E+05	85.00	1340.67
B02	SYBR	Std-2		32.56	1.000E+05	84.50	1471.59
B03	SYBR	Std-2		32.99	1.000E+05	84.50	1484.06
B04	SYBR	Unkn	AP3	34.34	5.826E+04	None	None
B05	SYBR	Unkn	AP3	34.30	5.950E+04	None	None
B06	SYBR	Unkn	AP11	33.37	8.896E+04	None	None
B07	SYBR	Unkn	AP11	32.82	1.134E+05	None	None
C01	SYBR	Std-3		39.91	1.000E+04	None	None
C02	SYBR	Std-3		40.34	1.000E+04	None	None
C03	SYBR	Std-3		40.36	1.000E+04	None	None
C04	SYBR	Unkn	AP4	36.53	2.248E+04	None	None
C05	SYBR	Unkn	AP4	35.67	3.275E+04	None	None
C06	SYBR	Unkn	AP12	30.22	3.510E+05	None	None
C07	SYBR	Unkn	AP12	29.97	3.916E+05	None	None
D01	SYBR	Std-4		41.72	1.000E+03	None	None
D02	SYBR	Std-4		41.63	1.000E+03	None	None
D03	SYBR	Std-4		44.09	1.000E+03	None	None
D04	SYBR	Unkn	AP5	35.87	3.001E+04	None	None
D05	SYBR	Unkn	AP5	35.66	3.279E+04	None	None
D06	SYBR	Unkn	AP13	39.41	6.423E+03	None	None
D07	SYBR	Unkn	AP13	39.01	7.630E+03	None	None
E01	SYBR	Std-5		N/A	1.000E+02	None	None
E02	SYBR	Std-5		N/A	1.000E+02	None	None
E03	SYBR	Std-5		N/A	1.000E+02	None	None
E04	SYBR	Unkn	AP6	31.99	1.621E+05	None	None
E05	SYBR	Unkn	AP6	31.52	1.995E+05	None	None
F01	SYBR	Std-6		N/A	1.000E+01	None	None
F02	SYBR	Std-6		N/A	1.000E+01	None	None
F03	SYBR	Std-6		N/A	1.000E+01	None	None
F04	SYBR	Unkn	AP7	35.69	3.243E+04	None	None
F05	SYBR	Unkn	AP7	33.60	8.046E+04	None	None
G01	SYBR	Std		N/A	1.000E+00	None	None
G02	SYBR	Std		N/A	1.000E+00	None	None
G03	SYBR	Std		N/A	1.000E+00	None	None
G04	SYBR	Unkn	AP8	34.16	6.322E+04	None	None
G05	SYBR	Unkn	AP8	34.32	5.887E+04	None	None
H01	SYBR	NTC		N/A	N/A	None	None
H02	SYBR	NTC		N/A	N/A	None	None
H03	SYBR	NTC		N/A	N/A	None	None
H04	SYBR	Unkn	AP9	29.81	4.195E+05	84.00	960.71
H05	SYBR	Unkn	AP9	30.42	3.214E+05	84.00	924.42

Table 2.5.4-4 | Raw qPCR data for the samples from the aquaponic system (AP) using the primer set for the amplification of comammox *Nitrospira* clade B (comaB).

Well	Fluor	Content	Sample	Cq	Starting Quantity (SQ)	Melt Temperature	Peak Height
A08	SYBR	Unkn	AP6	36.34	2.894E+05	None	None
A09	SYBR	Unkn	AP6	35.81	3.576E+05	None	None
A10	SYBR	Std		32.44	1.000E+06	86.00	1556.34
A11	SYBR	Std		34.31	1.000E+06	86.50	1314.84
A12	SYBR	Std		32.08	1.000E+06	86.50	1562.99
B08	SYBR	Unkn	AP7	42.01	3.043E+04	None	None
B09	SYBR	Unkn	AP7	42.23	2.787E+04	None	None
B10	SYBR	Std		39.69	1.000E+05	None	None
B11	SYBR	Std		40.07	1.000E+05	None	None
B12	SYBR	Std		38.99	1.000E+05	None	None
C08	SYBR	Unkn	AP8	42.90	2.133E+04	None	None
C09	SYBR	Unkn	AP8	43.02	2.037E+04	None	None
C10	SYBR	Std		N/A	1.000E+04	None	None
C11	SYBR	Std		N/A	1.000E+04	None	None
C12	SYBR	Std		43.96	1.000E+04	None	None
D08	SYBR	Unkn	AP9	37.00	2.226E+05	None	None
D09	SYBR	Unkn	AP9	36.50	2.720E+05	None	None
D10	SYBR	Std-4		N/A	1.000E+03	None	None
D11	SYBR	Std-4		N/A	1.000E+03	None	None
D12	SYBR	Std-4		N/A	1.000E+03	None	None
E06	SYBR	Unkn	AP2	41.50	3.724E+04	None	None
E07	SYBR	Unkn	AP2	42.02	3.031E+04	None	None
E08	SYBR	Unkn	AP10	31.86	1.723E+06	83.00	1320.29
E09	SYBR	Unkn	AP10	31.89	1.703E+06	83.00	1356.95
E10	SYBR	Std-5		N/A	1.000E+02	None	None
E11	SYBR	Std-5		N/A	1.000E+02	None	None
E12	SYBR	Std-5		N/A	1.000E+02	None	None
F06	SYBR	Unkn	AP3	38.87	1.061E+05	None	None
F07	SYBR	Unkn	AP3	38.69	1.140E+05	None	None
F08	SYBR	Unkn	AP11	36.15	3.133E+05	None	None
F09	SYBR	Unkn	AP11	36.40	2.826E+05	None	None
F10	SYBR	Std-6		N/A	1.000E+01	None	None
F11	SYBR	Std-6		N/A	1.000E+01	None	None
F12	SYBR	Std-6		N/A	1.000E+01	None	None
G06	SYBR	Unkn	AP4	38.18	1.395E+05	None	None
G07	SYBR	Unkn	AP4	38.03	1.482E+05	None	None
G08	SYBR	Unkn	AP12	33.31	9.666E+05	86.00	962.86
G09	SYBR	Unkn	AP12	33.18	1.018E+06	86.00	957.69
G10	SYBR	Unkn	wasted	40.58	5.380E+04	None	None
G11	SYBR	Std		N/A	1.000E+00	None	None
G12	SYBR	Std		N/A	1.000E+00	None	None
H06	SYBR	Unkn	AP5	39.07	9.810E+04	None	None
H07	SYBR	Unkn	AP5	38.52	1.221E+05	None	None
H08	SYBR	Unkn	AP13	41.74	3.384E+04	None	None
H09	SYBR	Unkn	AP13	N/A	N/A	None	None
H10	SYBR	Std		N/A	1.000E+00	None	None
H11	SYBR	NTC		N/A	N/A	None	None
H12	SYBR	NTC		N/A	N/A	None	None

3. Denitrification in bioelectrochemical systems for the treatment of nitrate contaminated groundwater

3.1. **Abstract**

Groundwater reservoirs are the major source for drinking water production in Germany. Intensive agricultural land use applying nitrogen containing fertilizers and animal manure from livestock farming resulted in nitrate contaminations exceeding the World's Health Organisation's guideline value of 50 mg NO_3^- L^{-1}. In this study the nitrate removal was investigated in bioelectrochemical batch systems using intermittent and continuous potential settings and the microbial community compositions were studied over time. Complete nitrate removal was efficiently achieved with both potential settings, though it was faster in the reactors running with continuous potential. The electrochemically active community compositions were different in both systems. Amplicon sequencing variations assigned to the genera *Geobacter* and *Thauera* became predominant on the carbon felt cathode and in the medium with applied continuous potential. Using intermittent potential settings, amplicon sequencing variations belonging to the genera *Candidatus* Nitrotoga and *Thiobacillus* were most abundant on the cathode and amplicon sequencing variations assigned to the genera *Anaerobacillus*, *Azoarcus* and *Delftia* became dominant members in the medium, respectively. The intermittent potential conditions stimulate the denitrification process in the system. These intermittent running bioelectrochemical systems can be implemented into the drinking water production process to efficiently remove nitrate from groundwater without consistent energy supply.

3.2. **Introduction**

The neutral (non-contaminated) level of nitrate in groundwater reservoirs are usually less than 10 mg NO_3^- L^{-1} (2 mg NO_3^--N L^{-1}) (Mueller *et al.*, 1995). Higher concentrations of nitrate in groundwater are implicated to anthropogenic influences that are mainly intensive livestock farming and leaching of nutrients from synthetic fertilizers containing nitrate and animal manure in agricultural land use (Smith *et al.*, 2015, European Commission, 2018). However, in an *in-situ* tracer experiment in France it could be shown that only 61% to 65% of the nitrate applied to the agricultural areas can be taken up by plants for metabolism (Sebilo *et al.*, 2013). The surplus of nitrate leaches with (rain-)water through the soil systems with an overall negative charge reaching the groundwater after 5 to 30 years or later (Sebilo *et al.*, 2013, Keeler & Polasky, 2014), as the negatively charged nitrate is a soluble and a very mobile compound in soils (Maier *et al.*, 2009, Smith *et al.*, 2015). Due to possible health risks a guideline value of 50 mg NO_3^- L^{-1} (10 mg NO_3^--N L^{-1}) in groundwater and drinking water was introduced by the World's Health Organization (WHO) in 1958.

Data from 2012 to 2015 reveal that 13.2% of all sampling sites in Europe exceeded the guideline value of 50 mg NO_3^- L^{-1} (European Commission, 2018). In Germany, even 28% of sampled groundwater wells exceeded 50 mg NO_3^- L^{-1} and 22.8% have elevated concentrations of nitrate between 25 mg and 50 mg NO_3^- L^{-1} (European Commission, 2018). More than 70% of the water used for drinking water production is taken from groundwater reservoirs (Wricke, 2014, Smith *et al.*, 2015). Agricultural intensification over the last 60 years has led to contaminations (>25 mg NO_3 L^{-1}) of about 50% of groundwater wells in Germany (European Commission, 2018). 2.5 kg ha^{-1} $year^{-1}$ of pesticides and growth control chemicals are applied in average onto agricultural areas (Wricke, 2014), resulting in expensive processing techniques to provide safe drinking water.

Since the rediscovery of bioelectrochemical systems (BES) in the 1970's, BES have been being investigated for various applications, including nitrate removal on both bioanodes and biocathodes. A BES is an electrochemical cell, in which electrochemically active microorganisms form biofilms on either one of the electrodes or both and catalyse oxidation and/or reduction reactions (Larminie *et al.*, 2003).

Electrons are extracellularly transferred by microorganisms through the biofilms either directly between microorganism and electrodes via membrane associated redox proteins (Afkar *et al.*, 2005, Mehta *et al.*, 2005, Pous *et al.*, 2014) and conductive pili structures (Reguera *et al.*, 2005) or indirectly via autochthonous redox shuttles, such as pyocyanin from *Pseudomonas aeruginosa* (Rabaey *et al.*, 2004, Rabaey *et al.*, 2005) and allochthonous redox shuttles such as hydrogen (Rabaey *et al.*, 2008) as well as artificial ones such as neutral red (Park & Zeikus, 2000).

Several studies have been conducted addressing autotrophic denitrification in groundwater revealing various removal efficiencies. In BES, nitrate reduction from 28.32 ± 6.15 mg NO_3-N L^{-1} to 12.14 ± 3.59 mg NO_3-N L^{-1} were obtained for low conductive (955 ± 121 µS cm^{-1}) groundwater (Pous *et al.*, 2013). 78% of the applied nitrate were removed from the influent, when using a bioanode (Nguyen *et al.*, 2015). A nitrate removal efficiency of more than 90% were achieved at −0.303 V (Molognoni *et al.*, 2017). However, in these studies, acetate oxidation was required at the bioanode to guarantee a flow of electrons and protons. Maximum nitrate removal rates of 43% (Nguyen *et al.*, 2015) and 62.15 ± 3.04 g NO_3-N m^{-3} d^{-1} (Cecconet *et al.*, 2018) were achieved at biocathodes with abiotic anodes. In one of the first approaches of *in situ* nitrate removal using bioelectrical systems in groundwater, 90.5% of nitrate was removed (Zhang & Angelidaki, 2013). The groundwater was not directly applied to the system, but nitrate could penetrate the membrane into the cathodic chamber. In a sand-filled reactor buried fully in an aquifer a nitrate removal rate of 322.6 mg m^{-2} d^{-1} was obtained at a potential of -0.7 V (Nguyen *et al.*, 2016).

The enhancing potential of intermittent conditions was studied at anodes before (Hsu *et al.*, 2017, Wang *et al.*, 2018). It was suggested that some materials are capable of storing energy (Wang *et al.*, 2018). A study on intermittently applied current at cathodes was only recently reported, where the production of methane from carbon dioxide as renewable electricity conversion was improved using granular carbon-based biocathodes (Liu *et al.*, 2018). Another study reports that intermittent potential conditions enhanced hydrogen production up to 41% in microbial electrolysis cells (Cho *et al.*, 2019). The hydrogen then can be used as electron shuttles by electrochemically active bacteria (Rabaey *et al.*, 2008).

In this study, a cathodic BES was operated with intermittently and continuously applied potential, respectively, for complete nitrate removal. It is the first report investigating the microbial community compositions on the cathodes and in the medium using 16S rRNA gene sequencing.

3.3. **Experimental procedure**

3.3.1. Growth medium for denitrifying bacteria in BES

The growth medium used in these experiments was adapted from Kamp *et al.* (2006). All solutions (Table 3.3.1-1) were prepared using ultra-pure water and were autoclaved for 20 min at 120 °C. The vitamin solution was filter sterilised (2 µm pore size). As the nitrate and the carbonate solution were added under anoxic conditions, both solutions were sparged with N_2/CO_2 (80:20 (v/v)) gas [Air Liquide, Düsseldorf, Germany] prior to autoclaving. The 0.5 mol L^{-1} nitrate solution was sparged for 20 min. The 1 mol L^{-1} carbonate solution was prepared with anoxic hot water and the headspace was exchange for 5 min with N_2/CO_2 (80:20 (v/v)) gas. Basal medium, $MgSO_4$ solution, $CaCl_2$ solution and carbonate were stored at room temperature. Other solutions were stored at 4 °C.

Table 3.3.1-1 | Solutions used as growth medium for denitrifying bacteria.

		Final concentrations	
	Compound	**[g L^{-1}]**	**[mmol L^{-1}]**
Basal medium, pH 7.0	EDTA	0.01	0.03
	NaCl	0.02	0.27
	$Na_2HPO_4 \cdot 2\ H_2O$	0.22	1.24
	$NaH_2PO_4 \cdot 2\ H_2O$	0.16	1.15
$MgSO_4$ solution	$MgSO_4 \cdot 7\ H_2O$	0.20	0.81
$CaCl_2$ solution	$CaCl_2 \cdot 2\ H_2O$	0.26	1.80
$FeCl_3$ solution	$FeCl_3$ (anhydrous)	0.58	3.58
Nitrate solution	$NaNO_3$	0.09	1.00
Carbonate solution	$NaHCO_3$	2.52	30.00
Micronutrient solution	Cf. Table 3.3.1-2	1X	1X
Vitamin solution	Cf. Table 3.3.1-3	1X	1X

Table 3.3.1-2 | Micronutrient solution used for the growth medium of denitrifying bacteria. The solution was prepared as 1000X.

		Final concentrations	
	Compound	**[mg L^{-1}]**	**[µmol L^{-1}]**
Micronutrient solution	H_2SO_4	0.5 µL L^{-1}	9.380
	$MnSO_4 \cdot H_2O$	2.280	13.490
	$ZnSO_4 \cdot 7\ H_2O$	0.500	1.739
	H_3BO_3	0.500	8.087
	$CuSO_4 \cdot 5\ H_2O$	0.025	0.100
	$Na_2MoO_4 \cdot 2\ H_2O$	0.025	0.103
	$CoCl_2 \cdot 6\ H_2O$	0.045	0.190

Table 3.3.1-3 | Vitamin solution used for the growth medium of denitrifying bacteria. Each vitamin was separately dissolved in 10 mL ultra-pure water and filter sterilised. For the final stock solution 1 mL of each stock solution were combined in 100 mL ultra-pure water (50X).

		Concentrations of separate stock solutions [g L^{-1}]	**Final concentrations**	
	Compound		**[mg L^{-1}]**	**[µmol L^{-1}]**
Vitamin solution	Cyanocobalamin (B12)	0.1	0.019	0.014
	Inositol	0.1	0.019	0.104
	Biotin	0.1	0.019	0.077
	Folic acid	0.1	0.019	0.042
	p-Aminobenzoic acid	1.0	0.188	1.367
	Nicotinic acid	10.0	1.875	15.230
	D-Pantothenate	10.0	1.875	7.869
	Thiamine-HCl (B1)	20.0	3.750	11.119

3.3.2. Inoculum for denitrification

A sediment sample was taken from a freshwater tideland of the river Elbe near Fährmannssand, Schleswig-Holstein, Germany, as inoculum. For the first enrichment of denitrifying bacteria and for the depletion of organic substances by organotrophic bacteria, 100 mL of growth medium (cf. section 3.3.1) with 0.5 mmol L^{-1} Na_2S was inoculated with 10% (v/v) with the sediment sample in a serum bottle and sparged with N_2/CO_2 (80:20 (v/v)) gas [Air Liquide, Düsseldorf, Germany]. The bottle was sealed

with a butyl rubber and it was incubated at 30 °C in the dark until nitrate was almost completely consumed.

3.3.3. Setup of the cathodic bioelectrochemical system

For the experiments on denitrification at the cathode a batch reactor was built from a 5-necked glass flask and a hungate tube designed in the glass blowing workshop as previously described in (Patil *et al.*, 2015). The main materials used for the setup are given in Table 3.3.3-1. An image of the reactor is shown below in Figure 3.3.3-1.

Table 3.3.3-1 | Materials used for assembling a bioelectrochemical system used for denitrification processes at the cathode.

	Material	Specification	Manufacturers
Cathode	Carbon felt	1.0x5.0 cm	Alfa Aeser (Thermo Fisher GmbH), Karlsruhe, Germany
Anode	Stainless steel felt	1.5x5.0 cm	Alfa Aeser (Thermo Fisher GmbH), Karlsruhe, Germany
Reference electrode	RE-1B (Ag/AgCl)		ALS Co., Ltd., Tokyo, Japan
Membrane	Fumasep FKB-PK-130	2.0x2.0 cm	Fumatech BWT GmbH, Bietigheim-Bissingen, Germany
Wirings	Titan, WirePurity 99.6%+	10 cm, 5 cm. Ø 1 mm	Advent Research Materials Ltd., England, Great Britain
Rubber stopper	Butyl	N20 and GL45	Glasgerätebau Ochs GmbH, Bovenden, Germany

All materials were thoroughly cleaned with ultra-pure water before usage. The carbon felt cathodes (1x5x0.1 cm) [Alfa Aeser, Karlsruhe, Germany] were pre-treated by cleaning the material for 24 h in 1 M HCl and 1 M NaOH, respectively. After each step the felts were rinsed with ultra-pure water. Pieces of 2x2 cm of the cation exchange membrane (Fumasep FKB-PK-130) [Fumatech BWT GmbH, Bietigheim-Bissingen, Germany] were pre-treated by up-swelling in a 4% NaCl solution for 24 h.

The 5-necked glass flask was used as cathode chamber including the carbon felt cathode, an Ag/AgCl reference electrode (RE-1B) [ALS Co., Ltd., Tokyo, Japan] and sampling needles [B. Braun, Melsungen, Germany]. As experiments were conducted

under anoxic conditions, all holes were sealed with N20 butyl rubbers [Glasgerätebau Ochs GmbH, Bovenden, Germany]. The electrodes were connected to the 1000C potentiostat [CH Instruments, Ltd., Austin, USA] via titan wirings (Ø 1 mm, WirePurity 99.6%+) [Advent Research Materials Ltd., England, Great Britain]. Needles were used for sampling the medium as well as the gas phase and were sealed with 3-way valves [B. Braun, Melsungen, Germany]. A hungate tube [Glasgerätebau Ochs GmbH, Bovenden, Germany] was used as anode chamber cutting the bottom. The membrane was placed onto a N20 butyl rubber with a hole and both was fixed with aluminium caps to the N20 opening of the hungate tube. The anode chamber was placed upside-down into the cathode chamber. The stainless steel felt anode was placed into the hungate tube by cutting the bottom of the tube.

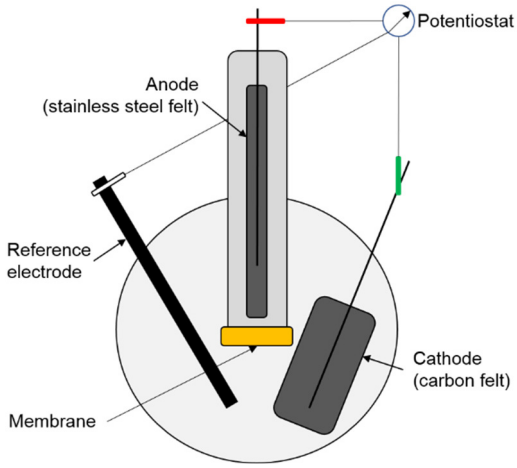

Figure 3.3.3-1 | Schematic view of the cathodic BES.

The cathode chamber was filled with growth medium (Table 3.3.1-1) to a final volume of 220 mL after adding nitrate, carbonate, and the inoculum between the cyclic voltammetry procedures (cf. section 3.3.4). The medium in the cathode chamber was sparged with N_2/CO_2 (80:20 (v/v)) gas [Air Liquide, Düsseldorf, Germany] and was continuously stirred during the experiments using a stirring bar. The anodic chamber was filled with 22 mL of growth medium lacking nitrate, carbonate and the inoculum.

3.3.4. Stability test using chronoamperiometry and investigation of redox active compounds using cyclic voltammetry in a cathodic BES

Before starting the denitrification experiments, a stability test was performed at a potential of -0.5 V vs. Ag/AgCl for 24 hours to examine leakages and connection issues. The reactors were used for the experiments, when the current stayed constant within this time.

Cyclic voltammetry was done before and after the addition of nitrate and carbonate as well as the inoculation. The applied potential ranged from 0.2 V vs. Ag/AgCl to -0.8 V Ag/AgCl and 5 cycles were used.

3.3.5. Run of the experiment

For the main experiments, two sets of reactors were prepared. The first set (three reactors) was run under continuous application of a potential of -0.5 V Ag/AgCl. The second set (three reactors) was running under intermittent conditions using alternating on- and off-phases of 6 h each. During the on-phases a potential of -0.5 V Ag/AgCl was applied. Abiotic controls missing the inoculum were additionally built for each set. A biotic control was established by running a reactor without application of potential.

Reactors were run until complete nitrate turnover measured via ion chromatography (cf. section 2.3.3). One reactor of each set was taken for microbial community analyses on the cathode (cf. section 3.3.7). Again, 1 mol L^{-1} nitrate and 30 mol L^{-1} carbonate were added to the remaining reactors and the main run was continued. They were analysed after the second and the third cycles of complete nitrate depletion, respectively.

Current densities were obtained by averaging the current densities over 6 hours. The nitrate removal rates were calculated for each cycle of complete nitrate turnover using the first three to five concentrations measured after nitrate addition to get the highest nitrate removal rate. Gas overpressure in the reactors were weekly released through the gas outlet. Raw data of currents measured in the reactors are shown in the appendix (Table 3.5.4-1 and Table 3.5.4-2).

3.3.6. Analysis of nitrogen species via ion chromatography

Samples of 500 µL were taken twice a week from the catholyte for measuring concentrations of nitrate, nitrite, and ammonium. All samples were prepared and measured via ion chromatography as described in section 2.3.3. The summarized raw data of the ion concentrations are shown in the appendix (Table 3.5.4-3 to Table 3.5.4-7).

3.3.7. DNA extraction and 16S rRNA amplicon library preparation

Samples for DNA extraction were taken from the cathode material by cutting the carbon felt in pieces of 60-70 mg as duplicates. DNA extraction was performed using the FastDNA^{TM} SPIN Kit for Soil [MP Biomedicals, Heidelberg, Germany] and applying the bead-beating settings as previously described in section 2.3.5. The samples were stored at -20 °C until further usage.

The 16S rRNA amplicon library was prepared according to the Illumina 16S sequencing library preparation guide (part no. 15044223 Rev. B) as stated above (cf. section 2.3.6) using the primers, indices and material as mentioned. The samples were stored at -20 °C until shipping for analysis to GATC Biotech AG [Konstanz, Germany].

3.3.8. Analysis of 16S rRNA gene sequencing data

Analysis of the 16S rRNA gene sequences was done in the R environment (R Core Team, 2018). The DADA2 pipeline tutorial 1.8 (Callahan *et al.*, 2016) was applied using the phyloseq R package (McMurdie & Holmes, 2013). Graphs were obtained with the ggplot2 package (Wickham, 2017). Since reverse amplicons had been trimmed, overlapping of the forward and reverse amplicons were expected to be insufficient during merging. Therefore, forward and reverse amplicons were analysed separately and abundances of amplicon sequence variants (asv) were summarised based on genus level using the forward primers. 16S gene sequencing data for the most abundant species are shown in the appendix in Table 3.5.4-8.

3.4. **Results**

3.4.1. Nitrate turnover in BES using intermittent and continuous potential

The nitrate removal was usually slower in batch BES running with intermittently applied potential than with continuously applied potential (Figure 3.4.1-1), which accordingly resulted in higher nitrate removal rates at continuous potential settings (Table 3.4.1-1). Three cycles of complete nitrate turnover were achieved in 82 days at intermittent potential and 60 days at continuous potential settings. Independent on the potential settings, the first cycles lasted about 5 days longer than the following cycles due to adaption of microorganisms to the cathode material, resulting in smaller nitrate removal rates during the first cycle. However, a very low rate (28.1 µmol L^{-1} d-1) was obtained in the reactor running continuously for two turnover cycles and in the reactor running intermittently for three cycles indicating the presence of potential inhibitors. Initial high concentrations of nitrate above 1 mmol L^{-1} in the reactors arose from addition of nitrate to residual nitrate in the inoculum. High concentrations of nitrite that might inhibit denitrification were not measured.

Table 3.4.1-1 | Nitrate removal rates after each cycle of complete nitrate turnover obtained in batch BES running with intermittent and continuous potential, respectively.

	Cycles of N-turnover	Nitrate removal rate intermittent conditions	Nitrate removal rate continuous conditions
Reactor 1	1	98.0 µmol L^{-1} d^{-1}	53.5 µmol L^{-1} d^{-1}
Reactor 2	1	57.4 µmol L^{-1} d^{-1}	77.4 µmol L^{-1} d^{-1}
	2	90.5 µmol L^{-1} d^{-1}	28.1 µmol L^{-1} d^{-1}
Reactor 3	1	60.7 µmol L^{-1} d^{-1}	191.7 µmol L^{-1} d^{-1}
	2	80.3 µmol L^{-1} d^{-1}	185.4 µmol L^{-1} d^{-1}
	3	63.6 µmol L^{-1} d^{-1}	205.6 µmol L^{-1} d^{-1}
Abiotic control		3.9 µmol L^{-1} d^{-1}	12.1 µmol L^{-1} d^{-1}
		Nitrate removal rate without potential	
Biotic control			2.6 µmol L^{-1} d^{-1}

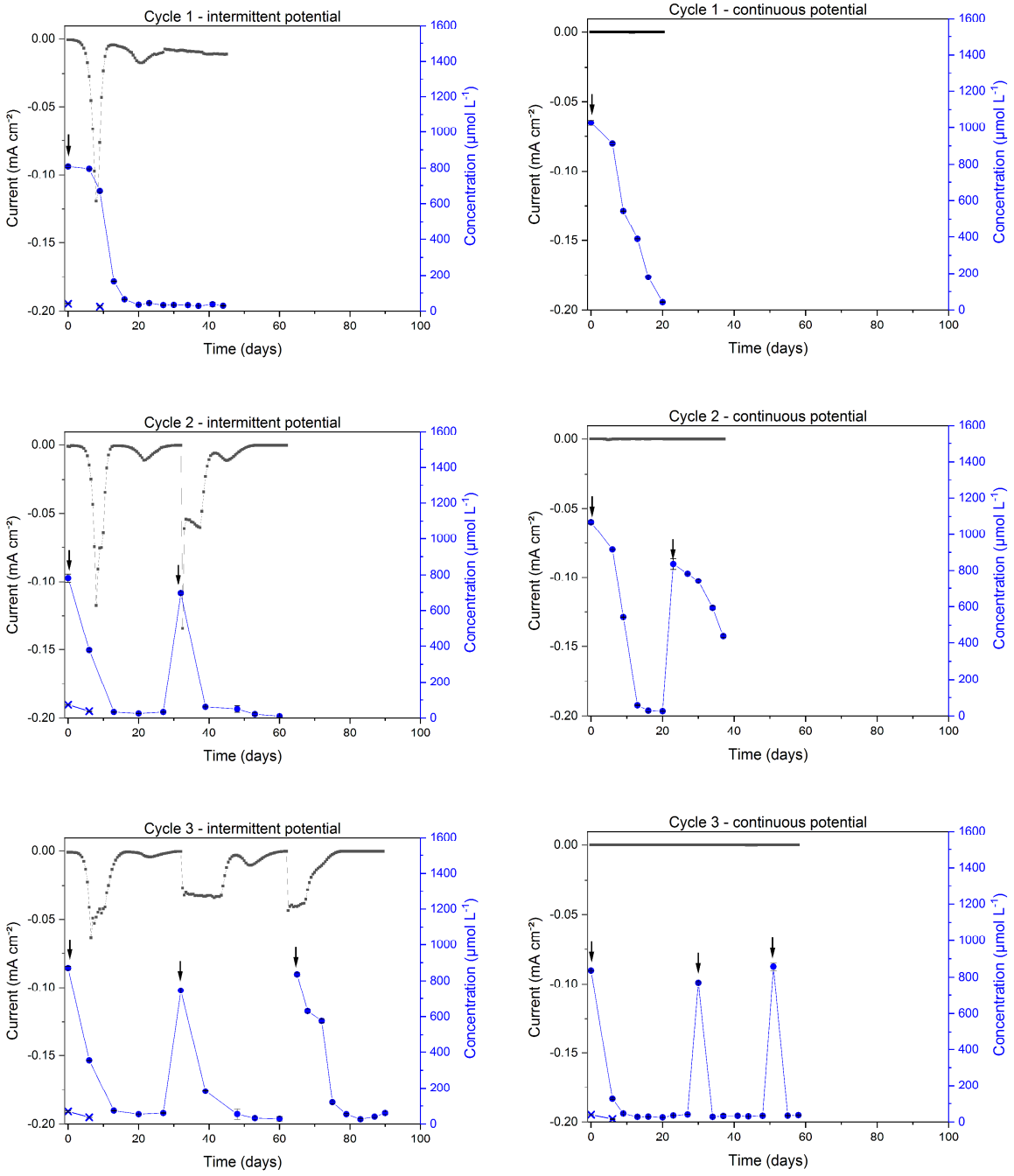

Figure 3.4.1-1 | Current densities (–▪–) and concentrations of nitrate (–●–), nitrite (–×–), and ammonium (–○–) in batch BES during the cycles of complete nitrogen turnover running with intermittent (left site) and continuous (right site) potential, respectively. The black arrows mark the addition of nitrate.

While current densities were constantly very low at continuously applied potential in the range of 10^{-4} to 10^{-7} mA cm^{-2}, peaks of current densities visibly marked the denitrification process with up to 0.13 mA cm^{-2}. Large peaks were obtained for the first denitrification step from nitrate to nitrite followed by smaller peaks presenting further

downstream reactions. The enhanced current consumption indicated that the denitrification process is stimulated in these reactors. The peaks correlated with the measured nitrate concentrations. Nitrite was only detectable in small concentrations around 19 µmol L^{-1}. Ammonia was not measurable in quantifiable concentrations.

Current densities were very low in the abiotic controls as shown in Figure 3.4.1-2. Nitrate concentrations decreased only slightly with removal rates of 3.9 µmol L^{-1} d^{-1} and 12.1 µmol L^{-1} d^{-1} at intermittent and continuous potential, respectively.

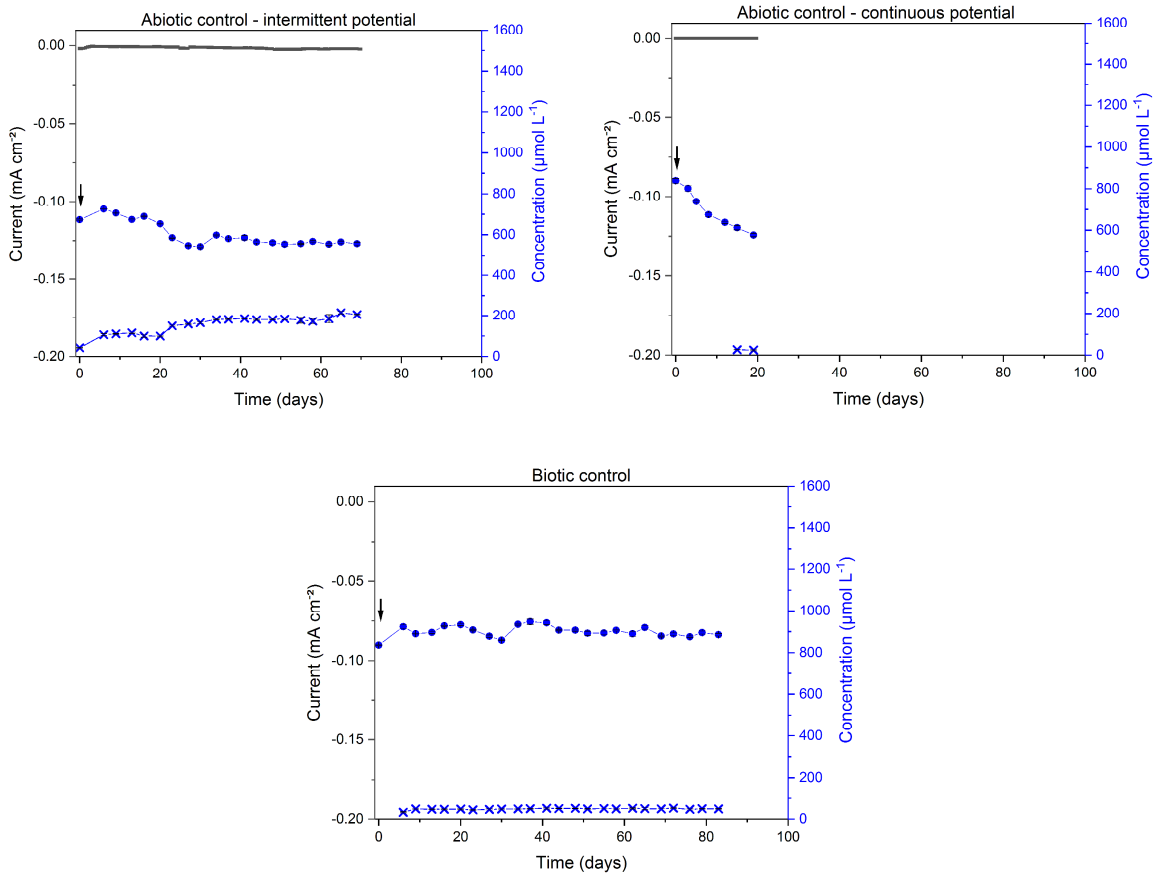

Figure 3.4.1-2 | Current densities (–▪–) and concentrations of nitrate (–●–), nitrite (–×–), and ammonium (–○–) in batch BES controls running with intermittent (abiotic control, left site) and continuous (abiotic control, right site) potential, respectively. The concentrations of nitrogen species in the biotic control is shown below.

The findings indicated abiotic reactions at the cathode or biotic reduction by organisms that did not originate from the sediment preculture but were introduced into the system during the reactor assembling because the reactor materials were not

autoclaved. The nitrite concentration increased in the abiotic control running at intermittent potential to 200 µM L^{-1} at the end of operation. The biotic control showed the smallest nitrate removal rate with 2.6 µmol L^{-1} d^{-1}.

Gas overpressure was observed in the batch reactors running with intermittent potential indicating the formation of either nitrogen gas or nitrous oxide. However, the accumulation of nitrous oxide was not measurable using gas chromatography in previously conducted experiments using carbon cloth as cathode material (data not shown).

Since sulphate was additionally available for microorganisms as electron acceptor in concentrations of approximately 1 mmol L^{-1}, the concentrations were compared between the intermittent and continuous potential settings (Figure 3.4.1-3).

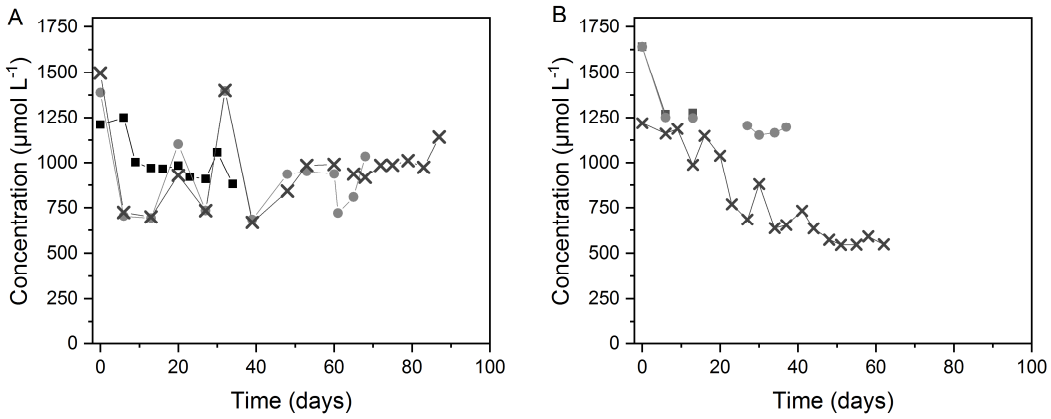

Figure 3.4.1-3 | Sulphate concentrations in the batch BES at intermittently (A) and at continuously (B) applied potential during 1 (–▪–), 2 (–●–) and 3 (–×–) cycles of complete nitrate turnover.

Varying sulphate concentrations indicated sulphur cycling in all reactors. At continuously applied potential, the sulphate concentrations slightly decreased showing that the reduction rate seemed to be higher than the sulphide oxidation rate.

3.4.2. Analyses of microbial biofilm community compositions on the cathode

Different microbial community compositions were obtained at the cathode and in the medium when using intermittent and continuous potential settings (Figure 3.4.2-1).

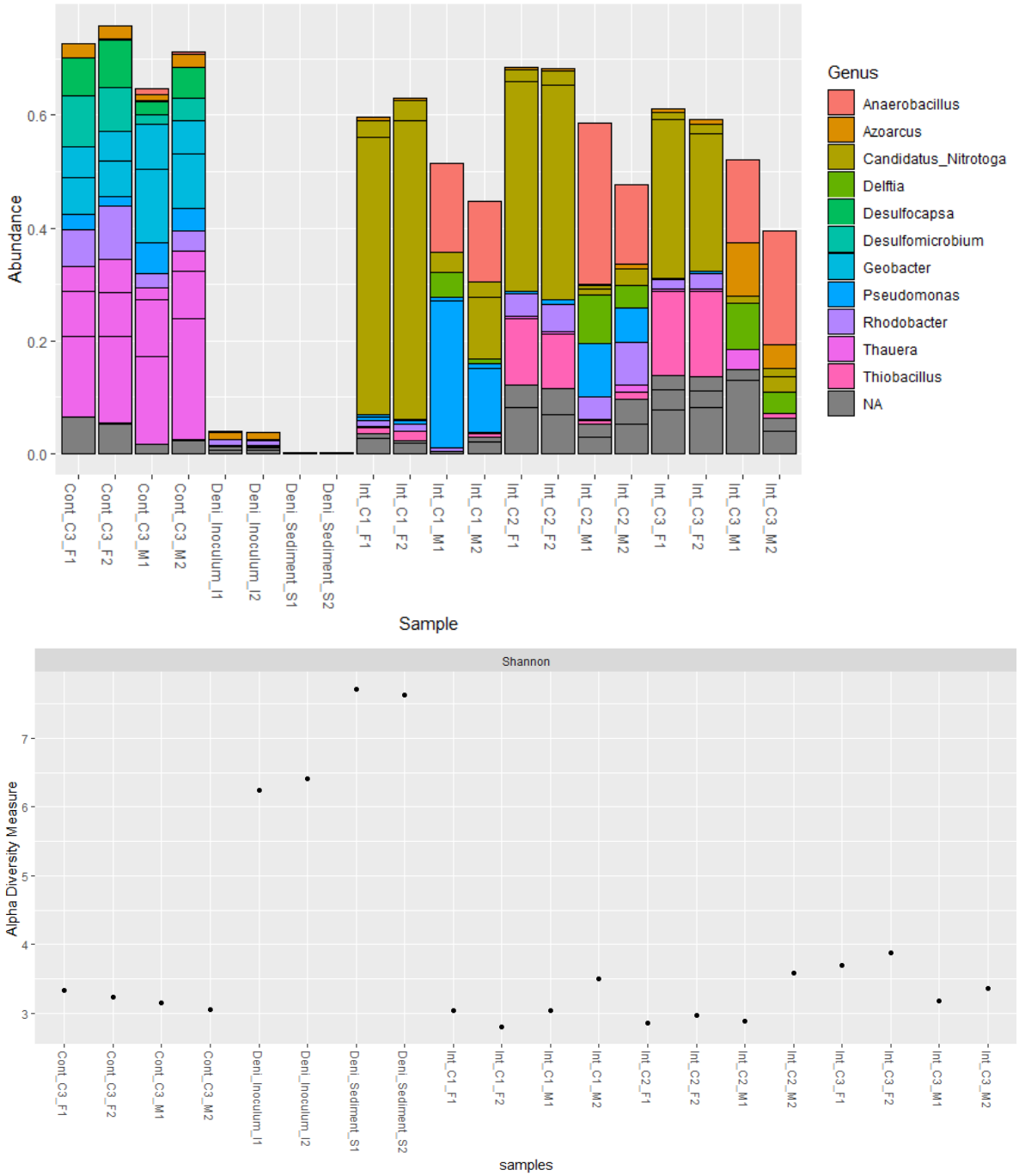

Figure 3.4.2-1 | Microbial community compositions by means of the 20 most abundant asv (above) and the alpha diversity indices (below) on the cathode material (carbon felt = F) and in the medium (M) obtained in batch BES running at intermittent (Int) and continuous (Cont) potential for one (C1), two (C2), and three (C3) cycles of complete nitrate turnover. Additionally, the freshwater sediment and the pre-cultivated inoculum are shown.

The 20 most abundant amplicon sequence variants (asv) of all samples represented in average 70% in the batch reactors running at continuous potential. With intermittent conditions they represent 65% on the cathode and 50% in the medium, respectively. At intermittent applied potential the 20 most abundant asv accounted for 40% to 60% of the total microbial community. The most abundant asv belonged to the genus *Candidatus* Nitrotoga and were found on the cathode material after the first cycle of complete nitrate turnover but decreased during the second and third cycle. On the contrary, asv that were assigned to the genus *Thiobacillus*, increased in the biofilm community on the cathode. In the medium, however, asv belonging to *Pseudomonas* and *Anaerobacillus* were most abundant. While asv of *Pseudomonas* decreased again and were not present in the medium of the reactor running for three cycles, asv of *Anaerobacillus* were still present. Additionally, the asv assigned to the genera *Delftia* and *Azoarcus* established themselves in the medium.

In the reactors running with continuously applied potential the microbial community composition on the cathode did not differ from the one in the medium. The 20 most abundant asv made up approximately 70% of the total community composition. Asv assigned to *Thauera* and *Geobacter* were most abundant in the medium. On the cathode felt, asv belonging to *Thauera*, *Rhodobacter*, *Geobacter*, *Desulfocapsa*, and *Desulfomicrobium* were the dominant ones.

The highly diverse freshwater sediment comprised more than 5000 genera making up 80% of the total community composition showing the need of clustering the asv based on the relative abundances of genera. The 20 most abundant genera, then, accounted for approximately 45% of the total community composition in this sample (Figure 3.4.2-2, right). In the pre-cultured inoculum, the 20 most abundant genera in this sample accounted for almost 70% of the total community composition after clustering asv (Figure 3.4.2-2, left). Approximately 5% of the present asv became members of the electrochemically denitrifying communities in the reactors. The alpha diversity indices (Figure 3.4.2-1, below) underlined the high diversity of these two samples with values of approximately 7.7 in the freshwater sediment and 6.3 in the pre-cultured inoculum.

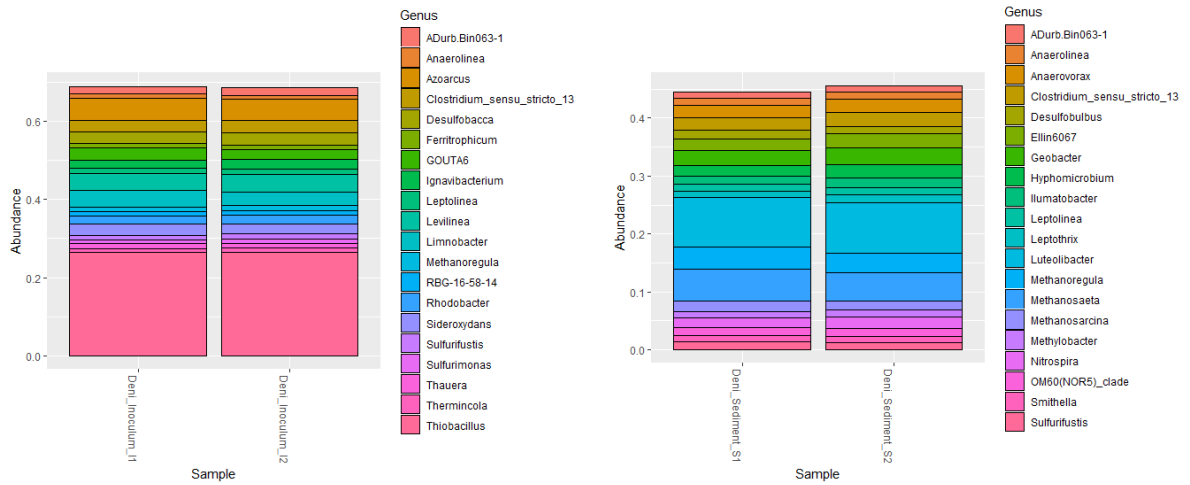

Figure 3.4.2-2 | Microbial community compositions in the pre-cultured inoculum (left) and in the sediment sample (right) by means of the 20 most abundant genera after clustering asv based on genera abundances.

In summary, denitrifying community compositions were established in both systems with intermittent and continuous potential, respectively. *Beggiatoa* and other vacuolated bacteria seemed not to be present in the sediment sampled from the freshwater tideland on the river Elbe, Germany.

Since the genus *Geobacter* was often described in literature as electrochemically active species and *Candidatus* Nitrotoga was the most dominant genus found on the electrode material, the 10 most abundant asv assigned to these genera were analysed separately (Figure 3.4.2-3). In the batch BES running at continuous potential, the 10 most dominant asv belonging to the genus *Geobacter* accounted for 13% and 20% of the total microbial community composition on the electrode and in the medium, respectively. *Geobacter* asv were also available in the sediment and decreased in the pre-cultured inoculum. They were scarcely present in the reactors running under intermittent potential conditions.

In contrast, in the reactors running under intermittent potential conditions, asv assigned to the genus *Candidatus* Nitrotoga were found to be highly abundant. They accounted for almost 60%, 40% and 30% during the three cycles of complete nitrate turnover, respectively, on the carbon felt electrode showing a continuous decrease of abundance. *Candidatus* Nitrotoga asv did not play a pivotal role in the reactors under

continuous potential and were also very minor abundant in the freshwater sediment and in the pre-cultured inoculum.

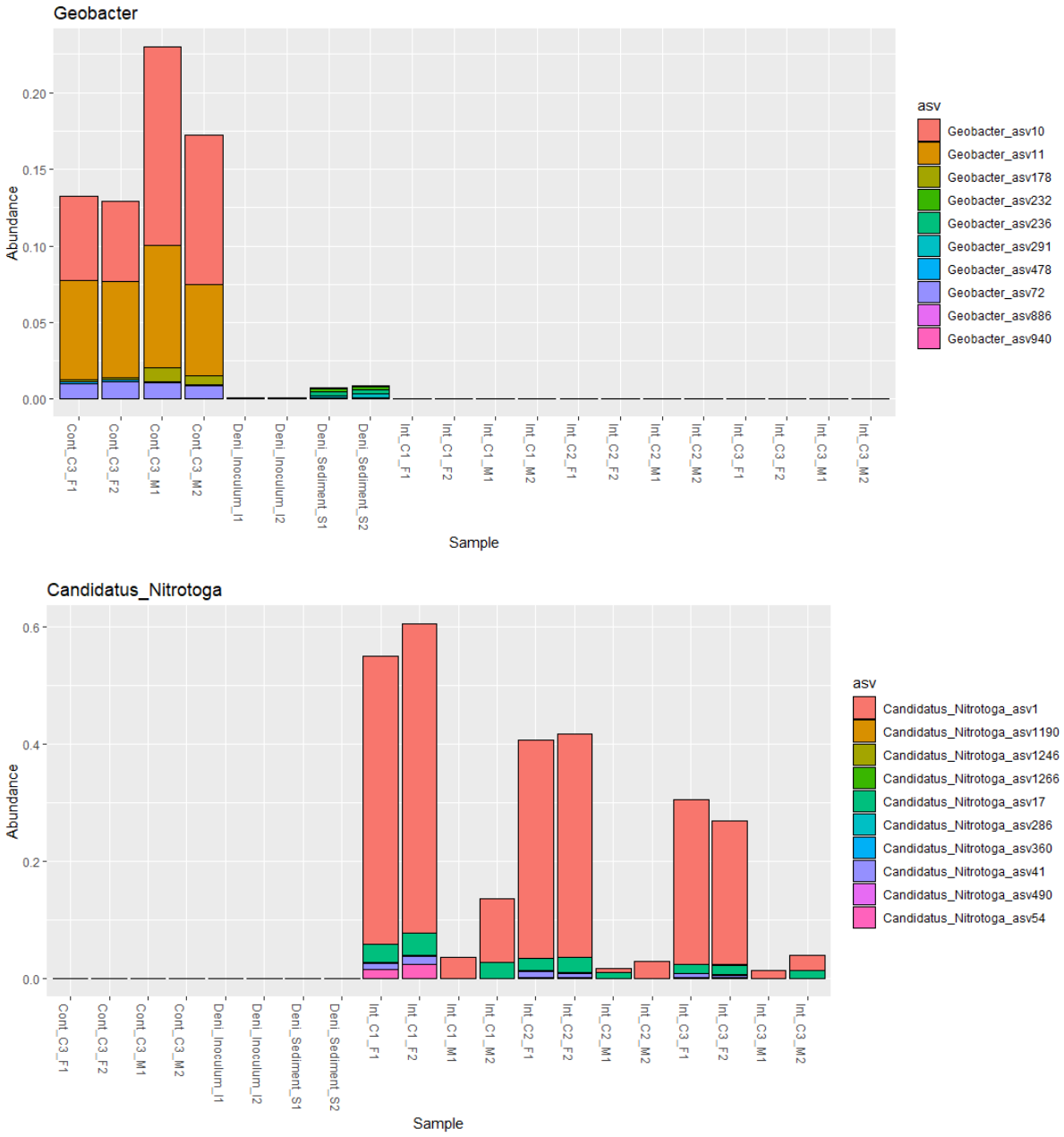

Figure 3.4.2-3 | The 10 most abundant asv of *Geobacter* (above) and *Candidatus* Nitrotoga (below) on the cathode material (carbon felt = F) and in the medium (M) obtained in batch BES running at intermittent (Int) and continuous (Cont) potential for one (C1), two (C2), and three (C3) cycles of complete nitrate turnover as well as in the freshwater sediment and in the pre-cultured inoculum.

The relationship between the microbial community compositions under different potential settings and in both sampling sources (electrode and medium) was visualized

using a heat map (Figure 3.4.2-4). Clear distinct microbial community compositions were revealed on the cathode and in the medium in the reactors with applied intermittent potential.

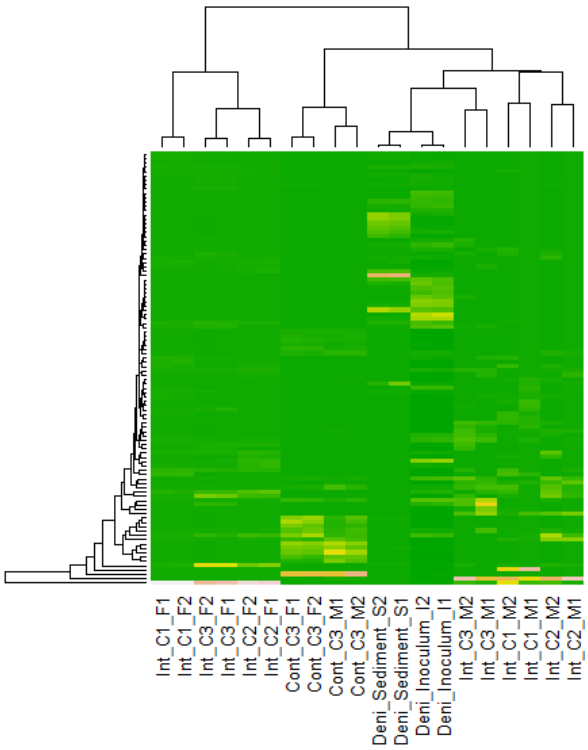

Figure 3.4.2-4 | Heatmap for the visualization of relationships between reactor samples from the cathode material (carbon felt = F) and from the medium (M) obtained in batch BES running at intermittent (Int) and continuous (Cont) potential for one (C1), two (C2), and three (C3) cycles of complete nitrate turnover as well as from the freshwater sediment and in the pre-cultured inoculum.

The microbial community compositions on the cathode significantly changed over time in the reactors with intermittent potential. These compositions had the least in common with the inoculum and the freshwater sediment as well as with the community compositions in the medium of the same reactor. Interestingly, the community compositions on the cathodes and those in the medium in the batch BES running at continuous potential resembled more than the compositions on the cathode and in the medium at intermittent potential.

3.5. **Discussion**

3.5.1. Bioelectrochemical systems for nitrate removal

The present study is the first one investigating denitrification in BES with intermittent potential conditions. However, it focused on the development of microbial community compositions on the cathodes rather than optimal BES performance. Complete nitrate removal was achieved in both systems running with continuously and intermittently applied potential settings. The consistently applied potential guarantees a constant electron flow utilized by the electrochemically active bacteria for nitrate reduction resulting in shorter time frames of complete nitrate turnover. In the reactors running with intermittent potential, on the contrary, nitrate reduction is stimulated. Enhanced hydrogen production by intermittently applied potential (Cho *et al.*, 2019) might have occurred accelerating the electron transport between electrochemically active microorganisms and the hydrogen (Rabaey *et al.*, 2008). During the starvation period, when the intermittently applied potential is paused, nitrate could also be stored in vacuoles within the bacterial cells as in the case of *Beggiatoa* species (Teske & Salman, 2014). When the potential is switched on again, the nitrate would be rapidly available for reduction. The enhancement of energy consumption during denitrification at the cathode can be seen in the current peaks, while current consumption at continuously applied potential stays constantly low. If the enhancement of energy consumption provides a pivotal advantage in BES performance was not observed here and should be investigated in further studies.

Most studies on denitrification use organic carbon (e. g. acetate) favouring heterotrophic denitrification at the cathode or acetate oxidation at the anode providing the electrons (Nguyen *et al.*, 2015, Pous *et al.*, 2015, Molognoni *et al.*, 2017). Here, addition of organic substrates was relinquished to lower costs and to avoid the use of organic substrates in a drinking water treatment plant. Groundwater naturally constitutes of low concentrations of dissolved organic and inorganic compounds depending on the travelling time through soils (Appelo & Postma, 2004) serving as substrates for microorganisms. In drinking water production, the denitrification process on the cathode may be implemented as the first step, taking advantage of the presence

of substrates such as carbonate and minerals in the natural groundwater to ensure denitrification. The growth medium was used here due to the focus on the enrichment of microorganisms and must be replaced by natural or synthetic groundwater in further studies of denitrification in BES.

The time for complete nitrate turnover in the reactors running with continuously applied potential takes two third the time interval than that of the reactors running intermittently. However, the intermittent potential was applied only half the time. Therefore, energy can be saved, and the denitrification process may accelerate, when time intervals are optimized.

3.5.2. Microbial community compositions

Completely different denitrifying community compositions are established in both systems with intermittent and continuous potential settings, respectively. It was assumed that vacuolated bacterial species would be enriched during intermittent potential settings that have advantage over other denitrifying bacteria by storage of nitrate within their cells (Teske & Salman, 2014) during the off-phases of applied potential. The stored nitrate would be immediately available for nitrate reduction at the cathode as soon as the potential is switched on. However, vacuolated bacteria such as *Beggiatoa* are not present. The results show that the presence of vacuolated bacteria is not necessary for stimulated nitrate reduction with intermittent potential condition for efficient groundwater treatment. It might be the case that other bacteria are present in the community possessing vacuoles, which are so far unknown and which would need further investigation.

Amplicon sequencing variants (asv) assigned to the genera *Geobacter* and *Thauera* are predominant in the reactors when potential is applied continuously. *Geobacter* species have been intensively studied as electrochemically active species in BES, for instance in Nevin *et al.* (2008), Strycharz *et al.* (2011), Rotaru *et al.* (2014), Kashima & Regan (2015), Wan *et al.* (2018). Both genera exhibit facultative nitrate reducers such as *Geobacter metallireducens* (Kashima & Regan, 2015), *Thauera aromatica* (Anders *et al.*, 1995), and *Thauera mechernichensis* (Scholten *et al.*, 1999). Additionally, it was recently reported that syntrophic growth of denitrifying bacteria and

the non-denitrifying *Geobacter sulfurreducens* enhances denitrification by direct interspecies electron transfer (Wan *et al.*, 2018). Direct interspecies electron transfer describes the electron transfer between species under syntrophic growth conditions (Summers *et al.*, 2010). This was also shown for methanogens, where the direct electron transfer between *Methanosarcina barkeri* and *Geobacter metallireducens* was investigated (Rotaru *et al.*, 2014). The asv of *Geobacter* are not further analysed in this study allowing both assumptions that the enriched *Geobacter* species are either denitrifying species or they accelerate denitrification by direct interspecies electron transfer between the cathode and the denitrifiers through *Geobacter* species.

In the reactors running with intermittently applied potential the bacterial denitrifying community shifts over time from the medium onto the cathode indicating the conversion of nitrate by microorganisms using residual electron donors in the medium. Afterwards, a rapid adaptation to the cathode takes place, where electrons are provided. The most dominant species found on the cathodes of these reactors belonged to the genus *Candidatus* Nitrotoga. This is the first report of *Candidatus* Nitrotoga playing a major part as an electrochemically active microorganism in a BES. The finding indicates that nitrite might have been produced but was rapidly consumed by nitrite oxidation back to nitrate since *Candidatus* Nitrotoga is known as nitrite-oxidising genus (Kitzinger *et al.*, 2018). The produced nitrate is further cycled via denitrification as nitrite was always measured in low concentrations in the medium.

As sulphide plays a major role in nitrate conversion in the environment especially regarding nitrate storing bacteria (Nelson *et al.*, 1986, McHatton *et al.*, 1996, Otte *et al.*, 1999), the sulphate concentrations in the medium were analysed. The sulphate concentration in the reactors running with intermittent potential does not change significantly. It can be assumed that biological reduction of sulphate to sulphide or elemental sulphur takes place under consumption of electrons from the cathode. Then, the reaction back to sulphate must also take place. This is indicated by the presence of asv assigned to sulphur oxidising *Thiobacillus* species (Madigan & Martinko, 2006). The sulphur oxidation to sulphate results in the release of electrons, which could flow into the nitrate reduction by detour. This way of electron usage could moreover explain the longer timeframe needed for nitrate reduction besides the intermittent potential settings. Sulphide could also be chemically oxidised back to sulphate by Fe^{2+} ions

(Preisler *et al.*, 2007). Fe^{3+} ions are present in the medium with a concentration of 3.58 mmol L^{-1} and could also be cycled to Fe^{2+} ions to a certain extend. Nevertheless, the complete nitrate reduction around 15 days shows that most of the electrons are flowing into the nitrogen cycle.

While the sulphur cycle seems to be a complete cycle under intermittent potential settings, in the reactor running continuously with the same potential the sulphate is consumed. This is indicated by the presence of asv related to species such as *Desulfomicrobium* species that can use sulphate as electron acceptor (Kuever & Galushko, 2014). In this case, electrons are also flowing into the sulphur cycle making the electrons unavailable for nitrate reduction. The shorter timeframe for complete nitrate reduction within approximately ten days is due to the continuously poised cathode. Whether sulphur cycling contributes to the conversion of nitrate and to what extend it does so is not clear and should further be studied.

3.5.3. Nitrate reduction via denitrification or DNRA?

While denitrification occurs under carbon-limited and terminal electron-acceptor rich environments, DNRA is favoured in carbon-rich and terminal electron acceptor poor environments (Maier *et al.*, 2009). Nevertheless, ammonium was not detectable in all reactors except in the beginning, which may be residual ammonium from the pre-cultures. Instead, gas pressure rose in the reactors. It can be assumed that elemental nitrogen was formed during operation, which had to be released from time to time. Thus, this study indicates that nitrate reduction in BES running with intermittently applied potential is carried out via the denitrification pathway.

The production of nitrous oxide is always a crucial step in the denitrification process, since it is a greenhouse gas and approximately 300 times stronger than carbon dioxide (IPCC Climate Change, 2007). Nitrous oxide generation might occur in the batch systems running intermittently if the time frame of applied potential is too short. The reaction would stop because of missing electrons from the cathode. Prolonging the time frame in the intermittent settings can solve this issue. The accumulation of nitrous oxide in BES has been observed before (Pous *et al.*, 2013,

Van Doan *et al.*, 2013). However, nitrous oxide does not seem to accumulate in the reactors used in this study but should be further investigated in future studies.

3.5.4. BES performance for denitrification in batch reactors

Until now, biofilm communities have not been studied in cathodic BES running with intermittent potential since the focus usually lies on the efficient bioremediation of wastes with no regard to specific microorganisms. This is the first report on the comparison of community structures in intermittently and continuously running cathodic BES so far. It is shown, that they are completely different from each other resulting in different additional reactions. The knowledge of microbial community compositions may enhance BES performance for instance by improving optimal growth conditions, application of specific microorganisms for a special purpose. New insights into the communities could also reveal another possible usage in bioremediation due to an electrochemically active but previously unknown microorganism. However, it remains unclear why exactly the community compositions differ significantly between the intermittent und continuous potential setting.

The BES performance greatly depends on its setup. Especially in the small batch systems on has to consider several issues. For instance, a close proximity between the electrodes is essential because H^+ ions travel better in the medium without getting lost the nearer the electrodes are located together (Logan *et al.*, 2006). In the batch BES, it is difficult to always match the same distances between the electrodes causing rather long travelling times of H^+ ions. This explains the varying performances of the reactors as there were different nitrate removal rates obtained for the cycles. Another point to mention is the kind of membrane and its size of the surface. Here, a cation exchange membrane was applied but also bipolar membranes are commercially available. The latter can help to maintain a more stable pH in the system (Ter Heijne *et al.*, 2006). The medium in the experiments in this study became rather acidic over time due to the prolonged travelling time of H^+ ions. The size of the membrane surface is quite small with a diameter of 1 cm that can be used effectively. The small size again limits the diffusion of H^+ ions into the counter chamber.

Nevertheless, the small batch reactors used in this study perfectly suit basic research questions as there are easy to build, low in cost and they allow the accumulation of microorganisms in the medium in contrast to flow cells. In large scale, however, different reactor settings have to be investigated.

3.6. **Appendix**

Table 3.5.4-1 | Current averaged over 6 hours in batch BES running at intermittent potential settings.

Time	Time	Current	Current	Current	Current
hours	days	mA/cm²	mA/cm²	mA/cm²	mA/cm²
		Cycle 1	Cycle 2	Cycle 3	Abiotic control
0	0	-7.32E-04	-1.09E-03	-1.04E-03	-2.02E-03
12	0.5	-6.87E-04	-1.31E-03	-1.05E-03	-2.07E-03
24	1	-7.11E-04	-5.97E-04	-1.07E-03	-1.89E-03
36	1.5	-7.99E-04	-6.55E-04	-1.17E-03	-1.59E-03
48	2	-1.17E-03	-6.83E-04	-1.28E-03	-1.05E-03
60	2.5	-1.38E-03	-7.48E-04	-1.43E-03	-8.07E-04
72	3	-2.00E-03	-9.30E-04	-2.03E-03	-6.11E-04
84	3.5	-2.94E-03	-1.29E-03	-3.07E-03	-6.45E-04
96	4	-4.41E-03	-1.69E-03	-4.52E-03	-6.87E-04
108	4.5	-6.77E-03	-2.61E-03	-7.65E-03	-6.84E-04
120	5	-1.06E-02	-4.48E-03	-1.33E-02	-6.91E-04
132	5.5	-1.72E-02	-7.99E-03	-2.25E-02	-7.01E-04
144	6	-2.72E-02	-1.46E-02	-4.13E-02	-6.98E-04
156	6.5	-4.55E-02	-2.48E-02	-6.32E-02	-7.21E-04
168	7	-6.66E-02	-4.35E-02	-4.91E-02	-7.17E-04
180	7.5	-9.72E-02	-7.47E-02	-5.29E-02	-8.19E-04
192	8	-1.20E-01	-1.18E-01	-4.84E-02	-8.37E-04
204	8.5	-1.12E-01	-9.08E-02	-4.48E-02	-8.43E-04
216	9	-7.66E-02	-7.56E-02	-4.27E-02	-8.31E-04
228	9.5	-4.31E-02	-7.53E-02	-4.56E-02	-8.03E-04
240	10	-2.32E-02	-6.40E-02	-4.24E-02	-7.64E-04
252	10.5	-1.28E-02	-3.50E-02	-4.11E-02	-8.27E-04
264	11	-7.34E-03	-1.68E-02	-3.09E-02	-8.20E-04
276	11.5	-5.35E-03	-7.32E-03	-2.50E-02	-8.15E-04
288	12	-4.62E-03	-3.26E-03	-1.87E-02	-8.22E-04
300	12.5	-4.38E-03	-1.31E-03	-1.34E-02	-8.06E-04
312	13	-4.41E-03	-7.65E-04	-9.73E-03	-7.98E-04
324	13.5	-4.56E-03	-6.96E-04	-6.74E-03	-7.83E-04
336	14	-5.11E-03	-6.90E-04	-4.76E-03	-8.02E-04
348	14.5	-5.45E-03	-7.11E-04	-3.45E-03	-8.19E-04
360	15	-5.67E-03	-7.61E-04	-2.25E-03	-9.02E-04
372	15.5	-6.06E-03	-8.68E-04	-1.52E-03	-9.37E-04
384	16	-6.53E-03	-9.97E-04	-1.04E-03	-9.40E-04
396	16.5	-7.13E-03	-1.20E-03	-8.29E-04	-9.39E-04
408	17	-8.12E-03	-1.49E-03	-8.26E-04	-9.42E-04
420	17.5	-9.30E-03	-1.85E-03	-8.57E-04	-9.32E-04
432	18	-9.92E-03	-2.31E-03	-9.20E-04	-9.10E-04
444	18.5	-1.18E-02	-2.96E-03	-1.03E-03	-8.88E-04
456	19	-1.38E-02	-3.79E-03	-1.17E-03	-8.70E-04
468	19.5	-1.57E-02	-4.83E-03	-1.35E-03	-8.86E-04
480	20	-1.69E-02	-6.13E-03	-1.60E-03	-8.51E-04
492	20.5	-1.74E-02	-7.68E-03	-1.95E-03	-9.23E-04
504	21	-1.73E-02	-9.29E-03	-2.38E-03	-9.67E-04
516	21.5	-1.68E-02	-1.12E-02	-3.34E-03	-1.02E-03
528	22	-1.56E-02	-1.09E-02	-3.86E-03	-1.04E-03
540	22.5	-1.45E-02	-9.97E-03	-4.16E-03	-1.05E-03
552	23	-1.34E-02	-9.09E-03	-4.40E-03	-1.04E-03
564	23.5	-1.26E-02	-7.92E-03	-4.37E-03	-1.06E-03
576	24	-1.17E-02	-6.73E-03	-4.23E-03	-1.09E-03
588	24.5	-1.09E-02	-5.75E-03	-3.95E-03	-1.11E-03
600	25	-1.14E-02	-4.82E-03	-3.59E-03	-1.83E-03
612	25.5	-1.10E-02	-4.10E-03	-3.26E-03	-1.83E-03
624	26	-1.04E-02	-3.11E-03	-2.88E-03	-1.83E-03
636	26.5	-1.02E-02	-2.05E-03	-2.50E-03	-1.86E-03

Time	Time	Current	Current	Current	Current
hours	days	mA/cm²	mA/cm²	mA/cm²	mA/cm²
		Cycle 1	Cycle 2	Cycle 3	Abiotic control
648	27	-9.79E-03	-1.71E-03	-2.17E-03	-1.90E-03
660	27.5	-7.34E-03	-1.40E-03	-1.93E-03	-1.11E-03
672	28	-7.68E-03	-1.12E-03	-1.63E-03	-1.10E-03
684	28.5	-7.76E-03	-8.83E-04	-1.40E-03	-1.12E-03
696	29	-7.97E-03	-6.88E-04	-1.14E-03	-1.15E-03
708	29.5	-8.10E-03	-5.34E-04	-9.53E-04	-1.17E-03
720	30	-8.12E-03	-4.37E-04	-7.64E-04	-1.18E-03
732	30.5	-8.55E-03	-4.16E-04	-6.16E-04	-1.18E-03
744	31	-8.67E-03	-4.03E-04	-4.91E-04	-1.18E-03
756	31.5	-8.41E-03	-4.06E-04	-4.40E-04	-1.15E-03
768	32	-8.22E-03	-4.02E-04	-4.20E-04	-1.26E-03
780	32.5	-8.15E-03	-1.34E-01	-2.68E-02	-1.31E-03
792	33	-8.48E-03	-6.10E-02	-3.26E-02	-1.36E-03
804	33.5	-8.70E-03	-5.43E-02	-3.05E-02	-1.40E-03
816	34	-9.09E-03	-5.46E-02	-3.16E-02	-1.42E-03
828	34.5	-8.87E-03	-5.48E-02	-3.21E-02	-1.39E-03
840	35	-9.13E-03	-5.62E-02	-3.20E-02	-1.44E-03
852	35.5	-8.99E-03	-5.65E-02	-3.19E-02	-1.46E-03
864	36	-9.29E-03	-5.78E-02	-3.29E-02	-1.51E-03
876	36.5	-9.39E-03	-5.90E-02	-3.28E-02	-1.53E-03
888	37	-9.42E-03	-5.98E-02	-3.31E-02	-1.55E-03
900	37.5	-9.52E-03	-6.04E-02	-3.29E-02	-1.60E-03
912	38	-9.58E-03	-4.86E-02	-3.29E-02	-1.62E-03
924	38.5	-1.06E-02	-3.46E-02	-3.35E-02	-1.63E-03
936	39	-1.09E-02	-2.28E-02	-3.34E-02	-1.64E-03
948	39.5	-1.11E-02	-1.54E-02	-3.29E-02	-1.65E-03
960	40	-1.11E-02	-1.07E-02	-3.27E-02	-1.64E-03
972	40.5	-1.10E-02	-7.79E-03	-3.27E-02	-1.64E-03
984	41	-1.10E-02	-6.67E-03	-3.35E-02	-1.61E-03
996	41.5	-1.06E-02	-6.01E-03	-3.44E-02	-1.59E-03
1008	42	-1.09E-02	-5.98E-03	-3.37E-02	-1.63E-03
1020	42.5	-1.09E-02	-6.45E-03	-3.35E-02	-1.59E-03
1032	43	-1.12E-02	-7.50E-03	-3.36E-02	-1.64E-03
1044	43.5	-1.10E-02	-8.57E-03	-3.27E-02	-1.70E-03
1056	44	-1.10E-02	-9.76E-03	-2.54E-02	-1.74E-03
1068	44.5	-1.13E-02	-1.09E-02	-1.79E-02	-1.76E-03
1080	45	-1.11E-02	-1.13E-02	-1.21E-02	-1.76E-03
1092	45.5		-1.11E-02	-8.16E-03	-1.82E-03
1104	46		-1.04E-02	-5.77E-03	-1.85E-03
1116	46.5		-9.49E-03	-4.30E-03	-2.05E-03
1128	47		-8.48E-03	-3.50E-03	-2.13E-03
1140	47.5		-7.20E-03	-3.22E-03	-2.16E-03
1152	48		-6.14E-03	-3.22E-03	-2.19E-03
1164	48.5		-5.10E-03	-3.63E-03	-2.65E-03
1176	49		-4.13E-03	-4.41E-03	-2.55E-03
1188	49.5		-3.28E-03	-5.52E-03	-2.55E-03
1200	50		-2.56E-03	-7.14E-03	-2.54E-03
1212	50.5		-1.94E-03	-8.78E-03	-2.53E-03
1224	51		-1.43E-03	-9.95E-03	-2.50E-03
1236	51.5		-1.04E-03	-1.04E-02	-2.48E-03
1248	52		-7.44E-04	-1.03E-02	-2.49E-03
1260	52.5		-5.48E-04	-9.99E-03	-2.49E-03
1272	53		-4.00E-04	-9.25E-03	-2.48E-03
1284	53.5		-3.62E-04	-8.36E-03	-2.51E-03
1296	54		-3.47E-04	-7.39E-03	-2.46E-03
1308	54.5		-3.50E-04	-6.51E-03	-2.47E-03
1320	55		-3.48E-04	-5.59E-03	-2.47E-03
1332	55.5		-3.30E-04	-4.71E-03	-2.26E-03
1344	56		-3.36E-04	-4.04E-03	-2.22E-03
1356	56.5		-3.29E-04	-3.37E-03	-2.18E-03

Time	Time	Current	Current	Current	Current
hours	days	mA/cm²	mA/cm²	mA/cm²	mA/cm²
		Cycle 1	Cycle 2	Cycle 3	Abiotic control
1368	57		-3.34E-04	-2.82E-03	-2.15E-03
1380	57.5		-3.27E-04	-2.31E-03	-2.18E-03
1392	58		-3.31E-04	-1.89E-03	-2.16E-03
1404	58.5		-3.30E-04	-1.50E-03	-2.13E-03
1416	59		-3.30E-04	-1.18E-03	-2.19E-03
1428	59.5		-3.25E-04	-9.26E-04	-2.29E-03
1440	60		-3.27E-04	-7.34E-04	-2.37E-03
1452	60.5		-3.29E-04	-5.82E-04	-2.34E-03
1464	61		-3.30E-04	-4.73E-04	-2.31E-03
1476	61.5		-3.25E-04	-3.86E-04	-2.28E-03
1488	62		-3.24E-04	-3.63E-04	-2.33E-03
1500	62.5			-4.37E-02	-2.16E-03
1512	63			-4.07E-02	-2.15E-03
1524	63.5			-3.96E-02	-2.17E-03
1536	64			-4.11E-02	-2.13E-03
1548	64.5			-4.07E-02	-2.16E-03
1560	65			-4.08E-02	-2.17E-03
1572	65.5			-4.02E-02	-2.18E-03
1584	66			-3.91E-02	-2.18E-03
1596	66.5			-3.88E-02	-2.15E-03
1608	67			-3.85E-02	-2.16E-03
1620	67.5			-3.55E-02	-2.13E-03
1632	68			-2.83E-02	-2.13E-03
1644	68.5			-2.29E-02	-2.13E-03
1656	69			-1.92E-02	-2.13E-03
1668	69.5			-1.69E-02	-2.39E-03
1680	70			-1.55E-02	-2.40E-03
1692	70.5			-1.38E-02	-2.46E-03
1704	71			-1.26E-02	-2.50E-03
1716	71.5			-1.17E-02	-2.53E-03
1728	72			-1.06E-02	-2.54E-03
1740	72.5			-9.32E-03	-2.55E-03
1752	73			-7.89E-03	-2.60E-03
1764	73.5			-6.29E-03	-2.45E-03
1776	74			-4.92E-03	-2.47E-03
1788	74.5			-3.73E-03	-2.45E-03
1800	75			-2.77E-03	-2.43E-03
1812	75.5			-1.98E-03	-2.47E-03
1824	76			-1.36E-03	-2.49E-03
1836	76.5			-8.94E-04	
1848	77			-5.47E-04	
1860	77.5			-3.86E-04	
1872	78			-3.83E-04	
1884	78.5			-3.73E-04	
1896	79			-3.65E-04	
1908	79.5			-3.70E-04	
1920	80			-3.79E-04	
1932	80.5			-3.69E-04	
1944	81			-3.80E-04	
1956	81.5			-3.82E-04	
1968	82			-3.85E-04	
1980	82.5			-3.75E-04	
1992	83			-3.75E-04	
2004	83.5			-3.76E-04	
2016	84			-3.91E-04	
2028	84.5			-3.93E-04	
2040	85			-3.91E-04	
2052	85.5			-3.77E-04	
2064	86			-3.78E-04	
2076	86.5			-3.82E-04	

Time	Time	Current	Current	Current	Current
hours	days	mA/cm²	mA/cm²	mA/cm²	mA/cm²
		Cycle 1	Cycle 2	Cycle 3	Abiotic control
2088	87			-3.91E-04	
2100	87.5			-3.85E-04	
2112	88			-3.75E-04	
2124	88.5			-3.78E-04	
2136	89			-3.78E-04	
2148	89.5			-3.78E-04	

Table 3.5.4-2 | Current averaged over 6 hours in batch BES running at continuous potential settings.

Time	Time	Current	Current	Current	Current
hours	days	mA/cm²	mA/cm²	mA/cm²	mA/cm²
		Cycle 1	Cycle 2	Cycle 3	Abiotic control
0	0	-8.19E-06	-2.63E-06	-2.85E-06	-6.52E-07
6	0.25	-4.74E-06	-1.51E-06	-2.47E-06	-6.36E-07
12	0.5	-2.55E-06	-1.11E-06	-2.11E-06	-6.28E-07
18	0.75	-2.77E-06	-1.06E-06	-1.86E-06	-6.19E-07
24	1	-2.64E-06	-1.06E-06	-1.71E-06	-6.10E-07
30	1.25	-2.32E-06	-1.12E-06	-1.56E-06	-6.05E-07
36	1.5	-1.97E-06	-1.19E-06	-1.39E-06	-6.05E-07
42	1.75	-1.65E-06	-1.30E-06	-1.23E-06	-5.99E-07
48	2	-1.47E-06	-1.52E-06	-8.97E-07	-5.94E-07
54	2.25	-1.28E-06	-2.10E-06	-8.43E-07	-5.90E-07
60	2.5	-1.13E-06	-3.69E-06	-1.04E-06	-5.86E-07
66	2.75	-1.03E-06	-6.91E-06	-1.18E-06	-5.90E-07
72	3	-9.24E-07	-1.28E-05	-5.37E-07	-5.77E-07
78	3.25	-8.63E-07	-2.42E-05	-5.09E-07	-5.75E-07
84	3.5	-8.27E-07	-4.65E-05	-5.00E-07	-5.74E-07
90	3.75	-7.98E-07	-8.97E-05	-5.06E-07	-5.85E-07
96	4	-7.63E-07	-1.70E-04	-5.05E-07	-5.79E-07
102	4.25	-7.47E-07	-3.01E-04	-4.88E-07	-5.85E-07
108	4.5	-7.46E-07	-4.54E-04	-4.89E-07	-5.88E-07
114	4.75	-7.42E-07	-5.45E-04	-4.85E-07	-5.96E-07
120	5	-7.42E-07	-5.42E-04	-4.84E-07	-5.88E-07
126	5.25	-7.34E-07	-4.69E-04	-4.84E-07	-5.82E-07
132	5.5	-7.32E-07	-3.79E-04	-4.77E-07	-5.85E-07
138	5.75	-7.10E-07	-2.87E-04	-4.79E-07	-5.89E-07
144	6	-6.59E-07	-2.08E-04	-4.69E-07	-5.91E-07
150	6.25	-6.34E-07	-1.60E-04	-4.67E-07	-5.94E-07
156	6.5	-6.30E-07	-1.35E-04	-4.54E-07	-6.00E-07
162	6.75	-6.80E-07	-1.08E-04	-4.33E-07	-6.08E-07
168	7	-6.52E-07	-8.29E-05	-4.16E-07	-6.08E-07
174	7.25	-6.36E-07	-7.09E-05	-4.21E-07	-6.22E-07
180	7.5	-6.28E-07	-6.59E-05	-4.23E-07	-6.28E-07
186	7.75	-6.19E-07	-5.83E-05	-4.25E-07	-6.30E-07
192	8	-6.10E-07	-5.44E-05	-4.19E-07	-6.28E-07
198	8.25	-6.05E-07	-5.59E-05	-4.19E-07	-6.27E-07
204	8.5	-6.05E-07	-6.18E-05	-4.16E-07	-6.31E-07
210	8.75	-5.99E-07	-6.86E-05	-4.10E-07	-6.32E-07
216	9	-5.94E-07	-7.93E-05	-4.08E-07	-6.32E-07
222	9.25	-5.90E-07	-9.11E-05	-4.11E-07	-6.36E-07
228	9.5	-5.86E-07	-9.62E-05	-4.05E-07	-6.35E-07
234	9.75	-5.90E-07	-9.29E-05	-4.01E-07	-6.44E-07
240	10	-5.77E-07	-8.31E-05	-4.05E-07	-6.42E-07
246	10.25	-5.75E-07	-7.55E-05	-4.38E-07	-6.43E-07
252	10.5	-5.74E-07	-7.73E-05	-4.46E-07	-6.46E-07
258	10.75	-5.85E-07	-8.00E-05	-4.55E-07	-6.52E-07
264	11	-8.49E-05	-4.96E-05	-4.58E-07	-2.92E-06

Time	Time	Current	Current	Current	Current
hours	days	mA/cm²	mA/cm²	mA/cm²	mA/cm²
		Cycle 1	Cycle 2	Cycle 3	Abiotic control
270	11.25	-7.62E-05	-5.94E-05	-4.70E-07	-2.80E-06
276	11.5	-7.74E-05	-6.22E-05	-4.63E-07	-2.90E-06
282	11.75	-6.94E-05	-6.21E-05	-4.56E-07	-3.36E-06
288	12	-6.58E-05	-5.55E-05	-4.50E-07	-3.54E-06
294	12.25	-6.31E-05	-4.50E-05	-4.60E-07	-3.62E-06
300	12.5	-5.82E-05	-6.25E-05	-4.58E-07	-3.65E-06
306	12.75	-5.41E-05	-6.97E-05	-4.60E-07	-3.68E-06
312	13	-5.21E-05	-6.72E-05	-4.65E-07	-4.77E-06
318	13.25	-5.01E-05	-6.64E-05	-4.84E-07	-4.79E-06
324	13.5	-4.68E-05	-6.52E-05	-4.77E-07	-4.73E-06
330	13.75	-4.48E-05	-6.37E-05	-4.72E-07	-4.62E-06
336	14	-4.33E-05	-5.96E-05	-4.75E-07	-4.58E-06
342	14.25	-4.21E-05	-5.84E-05	-4.92E-07	-4.47E-06
348	14.5	-3.94E-05	-5.53E-05	-5.16E-07	-4.49E-06
354	14.75	-3.97E-05	-5.31E-05	-5.18E-07	-4.49E-06
360	15	-3.87E-05	-5.77E-05	-5.16E-07	-4.50E-06
366	15.25	-3.68E-05	-7.62E-05	-5.29E-07	-4.58E-06
372	15.5	-3.53E-05	-7.00E-05	-5.37E-07	-4.51E-06
378	15.75	-3.34E-05	-6.67E-05	-5.25E-07	-4.57E-06
384	16	-3.38E-05	-6.84E-05	-5.19E-07	-4.63E-06
390	16.25	-3.34E-05	-6.96E-05	-5.24E-07	-4.65E-06
396	16.5	-3.31E-05	-6.38E-05	-5.13E-07	-5.36E-06
402	16.75	-3.33E-05	-4.34E-05	-5.18E-07	-4.77E-06
408	17	-3.31E-05	-2.89E-05	-5.22E-07	-4.66E-06
414	17.25	-3.35E-05	-2.18E-05	-5.33E-07	-4.68E-06
420	17.5	-3.34E-05	-1.80E-05	-5.43E-07	-4.83E-06
426	17.75	-3.34E-05	-1.61E-05	-5.46E-07	-4.94E-06
432	18	-3.38E-05	-1.54E-05	-5.33E-07	-4.96E-06
438	18.25	-3.39E-05	-1.55E-05	-5.40E-07	-5.00E-06
444	18.5	-5.13E-05	-1.37E-05	-5.55E-07	-5.05E-06
450	18.75	-5.10E-05	-1.52E-05	-5.58E-07	-5.04E-06
456	19	-5.04E-05	-1.73E-05	-5.58E-07	-5.06E-06
462	19.25	-5.02E-05	-2.06E-05	-5.68E-07	-5.07E-06
468	19.5	-5.06E-05	-2.54E-05	-5.73E-07	-5.09E-06
474	19.75	-4.98E-05	-3.23E-05	-5.69E-07	-5.08E-06
480	20	-4.91E-05	-4.23E-05	-5.55E-07	
486	20.25	-4.86E-05	-5.22E-05	-5.60E-07	
492	20.5		-1.20E-04	-5.64E-07	
498	20.75		-1.23E-04	-5.58E-07	
504	21		-1.21E-04	-5.50E-07	
510	21.25		-1.18E-04	-5.61E-07	
516	21.5		-1.16E-04	-5.75E-07	
522	21.75		-1.12E-04	-5.91E-07	
528	22		-1.09E-04	-5.90E-07	
534	22.25		-1.11E-04	-5.89E-07	
540	22.5		-1.13E-04	-5.84E-07	
546	22.75		-1.11E-04	-5.87E-07	
552	23		-1.10E-04	-5.82E-07	
558	23.25		-1.12E-04	-5.73E-07	
564	23.5		-1.12E-04	-5.60E-07	
570	23.75		-1.12E-04	-6.64E-06	
576	24		-1.43E-04	-5.12E-06	
582	24.25		-1.41E-04	-4.12E-06	
588	24.5		-1.22E-04	-3.63E-06	
594	24.75		-1.17E-04	-3.30E-06	
600	25		-1.13E-04	-3.06E-06	
606	25.25		-1.12E-04	-2.20E-06	
612	25.5		-1.08E-04	-1.71E-06	
618	25.75		-1.06E-04	-1.73E-06	
624	26		-1.05E-04	-1.64E-06	

Time	Time	Current	Current	Current	Current
hours	days	mA/cm²	mA/cm²	mA/cm²	mA/cm²
		Cycle 1	Cycle 2	Cycle 3	Abiotic control
630	26.25		-1.03E-04	-1.57E-06	
636	26.5		-1.01E-04	-1.50E-06	
642	26.75		-9.89E-05	-1.46E-06	
648	27		-9.92E-05	-1.44E-06	
654	27.25		-9.69E-05	-1.34E-06	
660	27.5		-1.17E-04	-1.17E-06	
666	27.75		-1.09E-04	-1.08E-06	
672	28		-1.05E-04	-9.86E-07	
678	28.25		-1.03E-04	-8.88E-07	
684	28.5		-1.01E-04	-8.15E-07	
690	28.75		-1.01E-04	-7.57E-07	
696	29		-9.91E-05	-7.15E-07	
702	29.25		-1.03E-04	-6.57E-07	
708	29.5		-1.01E-04	-6.09E-07	
714	29.75		-1.00E-04	-5.70E-07	
720	30		-9.86E-05	-5.40E-07	
726	30.25		-9.81E-05	-5.28E-07	
732	30.5		-1.20E-04	-5.29E-07	
738	30.75		-1.23E-04	-5.15E-07	
744	31		-1.21E-04	-4.97E-07	
750	31.25		-1.18E-04	-4.94E-07	
756	31.5		-1.16E-04	-4.96E-07	
762	31.75		-1.12E-04	-4.92E-07	
768	32		-1.09E-04	-4.84E-07	
774	32.25		-1.11E-04	-4.78E-07	
780	32.5		-1.13E-04	-4.77E-07	
786	32.75		-1.11E-04	-4.95E-07	
792	33		-1.10E-04	-5.04E-07	
798	33.25		-1.12E-04	-5.01E-07	
804	33.5		-1.12E-04	-5.03E-07	
810	33.75		-1.12E-04	-5.04E-07	
816	34		-1.43E-04	-5.03E-07	
822	34.25		-1.41E-04	-5.08E-07	
828	34.5		-1.22E-04	-5.06E-07	
834	34.75		-1.18E-04	-5.11E-07	
840	35		-1.13E-04	-4.92E-07	
846	35.25		-1.12E-04	-4.76E-07	
852	35.5		-1.08E-04	-4.84E-07	
858	35.75		-1.06E-04	-4.83E-07	
864	36		-1.05E-04	-4.74E-07	
870	36.25		-1.03E-04	-4.76E-07	
876	36.5		-1.01E-04	-4.84E-07	
882	36.75		-9.89E-05	-4.80E-07	
888	37		-9.92E-05	-4.74E-07	
894	37.25		-9.69E-05	-4.89E-07	
900	37.5			-4.94E-07	
906	37.75			-5.11E-07	
912	38			-5.11E-07	
918	38.25			-5.02E-07	
924	38.5			-4.97E-07	
930	38.75			-5.02E-07	
936	39			-4.99E-07	
942	39.25			-5.00E-07	
948	39.5			-4.96E-07	
954	39.75			-4.94E-07	
960	40			-4.93E-07	
966	40.25			-2.13E-06	
972	40.5			-1.69E-06	
978	40.75			-1.53E-06	
984	41			-1.45E-06	

Time	Time	Current	Current	Current	Current
hours	days	mA/cm²	mA/cm²	mA/cm²	mA/cm²
		Cycle 1	Cycle 2	Cycle 3	Abiotic control
990	41.25			-1.58E-06	
996	41.5			-1.83E-06	
1002	41.75			-2.24E-06	
1008	42			-2.74E-06	
1014	42.25			-3.77E-06	
1020	42.5			-5.51E-06	
1026	42.75			-9.29E-06	
1032	43			-1.86E-05	
1038	43.25			-3.75E-05	
1044	43.5			-7.44E-05	
1050	43.75			-1.45E-04	
1056	44			-2.57E-04	
1062	44.25			-2.17E-04	
1068	44.5			-1.79E-04	
1074	44.75			-1.57E-04	
1080	45			-1.43E-04	
1086	45.25			-1.28E-04	
1092	45.5			-1.13E-04	
1098	45.75			-1.02E-04	
1104	46			-9.92E-05	
1110	46.25			-6.99E-05	
1116	46.5			-5.12E-05	
1122	46.75			-4.36E-05	
1128	47			-3.93E-05	
1134	47.25			-3.77E-05	
1140	47.5			-3.96E-05	
1146	47.75			-4.26E-05	
1152	48			-4.37E-05	
1158	48.25			-4.27E-05	
1164	48.5			-4.28E-05	
1170	48.75			-4.54E-05	
1176	49			-4.74E-05	
1182	49.25			-4.67E-05	
1188	49.5			-4.45E-05	
1194	49.75			-4.24E-05	
1200	50			-4.09E-05	
1206	50.25			-3.95E-05	
1212	50.5			-3.83E-05	
1218	50.75			-3.67E-05	
1224	51			-3.69E-05	
1230	51.25			-1.50E-06	
1236	51.5			-1.72E-06	
1242	51.75			-1.24E-06	
1248	52			-1.00E-06	
1254	52.25			-9.90E-07	
1260	52.5			-1.09E-06	
1266	52.75			-1.20E-06	
1272	53			-1.40E-06	
1278	53.25			-1.53E-06	
1284	53.5			-1.61E-06	
1290	53.75			-1.72E-06	
1296	54			-1.94E-06	
1302	54.25			-2.13E-06	
1308	54.5			-2.98E-06	
1314	54.75			-3.00E-06	
1320	55			-3.49E-06	
1326	55.25			-3.21E-06	
1332	55.5			-3.25E-06	
1338	55.75			-5.04E-06	
1344	56			-7.10E-06	

Time	Time	Current	Current	Current	Current
hours	days	mA/cm²	mA/cm²	mA/cm²	mA/cm²
		Cycle 1	Cycle 2	Cycle 3	Abiotic control
1350	56.25			-7.68E-06	
1356	56.5			-8.00E-06	
1362	56.75			-8.07E-06	
1368	57			-8.86E-06	
1374	57.25			-9.42E-06	
1380	57.5			-9.27E-06	
1386	57.75			-8.62E-06	
1392	58			-8.31E-06	

Table 3.5.4-3 | Nitrate and nitrite concentrations in the batch BES running with intermittent potential settings.

C1	Time	S1	S2	S3	Conc1	Conc2	Conc3	Nitrate	Nitrate	S1	S2	S3	Conc1	Conc2	Conc3	Nitrite	Nitrite
#	days	µM	µM	µM	µM	µM	µM	µM	µM	µM	µM	µM	µM	µM	µM	µM	µM
								Mean	Std							Mean	Std
0	0	81.2508	80.1821	81.2458	812.5083	801.8213	812.4584	808.9293	6.1558	4.2561	4.0126	3.8430	42.5612	40.1265	38.4303	40.3727	2.0764
1	6	79.3392	80.0254	79.4390	793.3917	800.2543	794.3896	796.0119	3.7078	n.a.	n.a.	n.a.	n.a.	n.a.	n.a.	n.a.	n.a.
2	9	67.5564	66.8150	66.3962	675.5636	668.1499	663.9621	669.2252	5.8750	2.6230	2.1864	2.7839	26.2301	21.8641	27.8390	25.3111	3.0916
3	13	16.3449	16.5982	16.2421	163.4490	165.9820	162.4210	163.9507	1.8327							n.a.	n.a.
4	16	6.7125	6.3914	6.3128	67.1249	63.9135	63.1278	64.7221	2.1177							n.a.	n.a.
5	20	3.4776	3.5000	3.6467	34.7761	35.0002	36.4671	35.4145	0.9185							n.a.	n.a.
6	23	4.4480	4.6634	4.1915	44.4795	46.6337	41.9147	44.3426	2.3625							n.a.	n.a.
7	27	3.2114	3.4177	3.4737	32.1136	34.1771	34.7369	33.6759	1.3816							n.a.	n.a.
8	30	3.4107	3.6986	3.2586	34.1066	36.9862	32.5865	34.5598	2.2346							n.a.	n.a.
9	34	3.2891	3.3853	3.4251	32.8908	33.8530	34.2513	33.6650	0.6994							n.a.	n.a.
10	37	2.9307	2.8342	2.8371	29.3067	28.3417	28.3710	28.6731	0.5489							n.a.	n.a.
11	41	3.2056	2.9477	5.0828	32.0558	29.4774	50.8277	37.4536	11.6538							n.a.	n.a.
12	44	3.1982	3.0151	2.7945	31.9815	30.1506	27.9445	30.0256	2.0214							n.a.	n.a.
C2	Time	S1	S2	S3	Conc1	Conc2	Conc3	Nitrate	Nitrate	S1	S2	S3	Conc1	Conc2	Conc3	Nitrite	Nitrite
#	days	µM	µM	µM	µM	µM	µM	µM	µM	µM	µM	µM	µM	µM	µM	µM	µM
								Mean	Std							Mean	Std
0	0	38.0040	39.0768	40.2555	760.0801	781.5355	805.1103	782.2420	22.5234	3.5435	3.7228	3.6644	70.8696	74.4556	73.2871	72.8708	1.8289
1	6	38.3494	37.1923	37.9131	383.4941	371.9229	379.1314	378.1828	5.8436	3.8882	3.5496	3.9950	38.8817	35.4956	39.9502	38.1092	2.3256
2	13	3.3665	3.1449	3.3733	33.6646	31.4490	33.7327	32.9488	1.2993							n.a.	n.a.
3	20	2.6069	2.3664	2.6408	26.0690	23.6644	26.4084	25.3806	1.4959							n.a.	n.a.
4	27	3.2288	3.1017	3.5510	32.2882	31.0168	35.5101	32.9384	2.3161							n.a.	n.a.
5	32	35.1886	34.5236	34.5608	703.7728	690.4719	691.2154	695.1534	7.4739							n.a.	n.a.
6	39	6.4961	5.8412	6.0876	64.9611	58.4125	60.8758	61.4165	3.3076							n.a.	n.a.
7	48	5.3887	6.5370	3.0196	53.8870	65.3700	30.1956	49.8175	17.9369							n.a.	n.a.
8	53	2.9836	1.6890	1.6912	29.8358	16.8897	16.9117	21.2124	7.4681							n.a.	n.a.
9	60	1.3837	0.7939	0.6618	13.8369	7.9390	6.6180	9.4646	3.8437							n.a.	n.a.
C3	Time	S1	S2	S3	Conc1	Conc2	Conc3	Nitrate	Nitrate	S1	S2	S3	Conc1	Conc2	Conc3	Nitrite	Nitrite
#	days	µM	µM	µM	µM	µM	µM	µM	µM	µM	µM	µM	µM	µM	µM	µM	µM
								Mean	Std							Mean	Std
0	0	43.8655	43.7713	42.8991	877.3105	875.4268	857.9814	870.2395	10.6576	3.7120	3.4258	3.2501	74.2398	68.5164	65.0024	69.2529	4.6625
1	6	35.4802	35.5802	35.1463	354.8024	355.8024	351.4635	354.0228	2.2721	4.0296	3.4746	3.6640	40.2957	34.7459	36.6405	37.2274	2.8211
2	13	7.4168	7.1840	7.5513	74.1676	71.8404	75.5133	73.8404	1.8582	3.4671	3.3340	n.a.	34.6709	33.3395	#VALUE!	n.a.	n.a.
3	20	5.1910	5.5622	5.5780	51.9098	55.6220	55.7802	54.4373	2.1903							n.a.	n.a.
4	27	6.0199	6.2509	5.9171	60.1986	62.5087	59.1708	60.6260	1.7095							n.a.	n.a.
5	32	37.3098	37.2580	37.1973	746.1964	745.1609	743.9469	745.1014	1.1259							n.a.	n.a.
6	39	18.3495	18.3778	18.1611	183.4952	183.7779	181.6113	182.9615	1.1778							n.a.	n.a.
7	48	4.4510	3.2153	8.7649	44.5103	32.1527	87.6494	54.7708	29.1364							n.a.	n.a.
8	53	3.1358	3.8654	2.6037	31.3575	38.6536	26.0366	32.0159	6.3342							n.a.	n.a.
9	60	1.5155	3.4188	3.6989	15.1547	34.1881	36.9887	28.7772	11.8802							n.a.	n.a.
10	61	n.a.	n.a.	n.a.	n.a.	n.a.	n.a.	#DIV/0!	#DIV/0!							n.a.	n.a.
11	65	84.5021	83.2889	82.8377	845.0210	832.8894	828.3765	835.4290	8.6080							n.a.	n.a.
12	68	62.3212	64.2089	62.6387	623.2123	642.0893	626.3869	630.5628	10.1076							n.a.	n.a.
13	72	28.5950	28.4161	29.3504	571.9003	568.3224	587.0074	575.7434	9.9176							n.a.	n.a.
14	75	11.2377	12.3281	12.4580	112.3772	123.2812	124.5801	120.0795	6.7019							n.a.	n.a.
15	79	5.6069	4.9286	5.7538	56.0693	49.2862	57.5379	54.2978	4.4019							n.a.	n.a.
16	83	3.0019	2.5430	2.2688	30.0188	25.4302	22.6880	26.0456	3.7039							n.a.	n.a.
17	87	4.5736	4.0713	3.5293	45.7357	40.7126	35.2932	40.5805	5.2225							n.a.	n.a.
18	90	6.7773	5.3277	5.9581	67.7731	53.2770	59.5814	60.2105	7.2685							n.a.	n.a.

Table 3.5.4-4 |Nitrate and nitrite concentrations in the abiotic control running with intermittent potential settings.

AC #	Time days	S1 µM	S2 µM	S3 µM	Conc1 µM	Conc2 µM	Conc3 µM	Nitrate µM Mean	Nitrate µM Std	S1 µM	S2 µM	S3 µM	Conc1 µM	Conc2 µM	Conc3 µM	Nitrite µM Mean	Nitrite µM Std
0	0	67.1523	67.6014	67.0552	671.5225	676.0138	670.5520	**672.6961**	**2.9139**	4.2782	3.9592	4.4070	42.7824	39.5921	44.0702	**42.1482**	**2.3054**
1	6	72.3498	72.6420	72.7024	723.4975	726.4205	727.0237	**725.6472**	**1.8860**	10.2141	11.2266	10.3644	102.1410	112.2662	103.6438	**106.0170**	**5.4639**
2	9	70.5648	70.5024	70.4753	705.6476	705.0243	704.7532	**705.1417**	**0.4586**	10.8230	11.1716	11.0033	108.2300	111.7157	110.0332	**109.9930**	**1.7432**
3	13	67.4794	67.6076	67.1165	674.7945	676.0764	671.1646	**674.0118**	**2.5477**	11.4178	11.7691	11.1548	114.1779	117.6914	111.5478	**114.4723**	**3.0824**
4	16	68.8936	69.1118	68.6858	688.9361	691.1183	686.8580	**688.9708**	**2.1304**	9.2399	10.4065	10.1447	92.3994	104.0654	101.4471	**99.3040**	**6.1212**
5	20	65.2984	65.2687	65.3887	652.9844	652.6868	653.8870	**653.1861**	**0.6250**	10.4218	9.6705	9.6808	104.2180	96.7051	96.8081	**99.2437**	**4.3081**
6	23	58.8091	58.1567	58.4948	588.0906	581.5668	584.9478	**584.8684**	**3.2626**	14.7836	14.7259	15.2282	147.8361	147.2589	152.2821	**149.1257**	**2.7487**
7	27	54.6830	54.7396	54.5654	546.8300	547.3957	545.6540	**546.6266**	**0.8885**	15.8128	16.0290	15.5817	158.1279	160.2903	155.8173	**158.0785**	**2.2369**
8	30	53.8302	54.7103	53.9076	538.3019	547.1026	539.0760	**541.4935**	**4.8730**	16.7265	16.6667	15.9179	167.2652	166.6666	159.1790	**164.3703**	**4.5057**
9	34	60.0491	59.4309	59.7618	600.4914	594.3093	597.6179	**597.4729**	**3.0936**	17.8464	18.2270	18.1311	178.4635	182.2696	181.3112	**180.6814**	**1.9796**
10	37	58.4953	57.8184	57.9619	584.9528	578.1837	579.6191	**580.9186**	**3.5668**	17.9611	18.2131	18.3865	179.6113	182.1311	183.8650	**181.8691**	**2.1389**
11	41	57.3155	59.4547	58.8318	573.1550	594.5472	588.3181	**585.3401**	**11.0026**	18.4565	18.4567	18.6295	184.5653	184.5674	186.2946	**185.1424**	**0.9978**
12	44	56.8556	56.6759	55.8468	568.5559	566.7589	558.4684	**564.5944**	**5.3808**	18.4018	18.1833	17.5762	184.0178	181.8326	175.7621	**180.5375**	**4.2775**
13	48	56.9181	55.3010	55.9360	569.1808	553.0104	559.3600	**560.5171**	**8.1470**	18.0310	17.8484	18.2745	180.3102	178.4845	182.7447	**180.5131**	**2.1374**
14	51	54.4202	55.5007	56.0110	544.2024	555.0075	560.1105	**553.1068**	**8.1226**	18.0501	18.2960	18.6611	180.5005	182.9603	186.6111	**183.3573**	**3.0746**
15	55	55.9225	55.3884	55.5078	559.2253	553.8837	555.0781	**556.0624**	**2.8035**	18.7040	16.0335	18.4954	187.0398	160.3354	184.9539	**177.4430**	**14.8523**
16	58	56.3680	56.5238	57.1264	563.6799	565.2376	571.2639	**566.7271**	**4.0054**	18.8079	16.6146	16.1368	188.0792	166.1460	161.3676	**171.8643**	**14.2443**
17	62	54.6794	55.9188	55.4111	546.7943	559.1875	554.1112	**553.3643**	**6.2303**	18.6335	20.4029	16.2213	186.3348	204.0287	162.2132	**184.1923**	**20.9899**
18	65	56.5118	55.9323	56.9259	565.1176	559.3232	569.2592	**564.5666**	**4.9909**	20.8289	21.7865	21.8408	208.2891	217.8652	218.4082	**214.8542**	**5.6920**
19	69	56.0170	56.0844	54.7257	560.1702	560.8436	547.2575	**556.0905**	**7.6570**	20.4174	20.3631	20.7341	204.1743	203.6305	207.3413	**205.0487**	**2.0040**
20	72	55.7883	53.1524	54.2900	557.8832	531.5236	542.9003	**544.1023**	**13.2209**	20.9969	19.3056	20.0768	209.9693	193.0559	200.7678	**201.2643**	**8.4676**
21	76	56.4600	55.7262	55.4177	564.5999	557.2617	554.1775	**558.6797**	**5.3539**	19.8146	20.9936	20.7881	198.1459	209.9357	207.8808	**205.3208**	**6.2980**
22	79	54.9632	54.6580	55.0563	549.6322	546.5800	550.5632	**548.9251**	**2.0836**	19.0107	19.5782	19.5399	190.1072	195.7825	195.3990	**193.7629**	**3.1717**
23	83	56.0421	54.3542	54.6327	560.4213	543.5419	546.3272	**550.0968**	**9.0491**	20.9350	20.1261	19.1892	209.3505	201.2606	191.8916	**200.8342**	**8.7373**

Table 3.5.4-5 | Nitrate and nitrite concentrations in the biotic control without potential settings.

BC #	Time days	S1 µM	S2 µM	S3 µM	Conc1 µM	Conc2 µM	Conc3 µM	Nitrate µM Mean	Nitrate µM Std	S1 µM	S2 µM	S3 µM	Conc1 µM	Conc2 µM	Conc3 µM	Nitrite µM Mean	Nitrite µM Std
0	0	83.5180	83.3888	83.8363	835.1798	833.8885	838.3627	**835.8103**	**2.3028**	3.9717	n.a.	3.6634	39.7172	#VALUE!	36.6342	**#VALUE!**	**#VALUE!**
1	6	93.1213	92.4865	91.4955	931.2132	924.8648	914.9547	**923.6775**	**8.1940**	3.5719	3.1387	3.0506	35.7186	31.3871	30.5059	**32.5372**	**2.7902**
2	9	88.9141	88.8865	89.0857	889.1414	888.8653	890.8574	**889.6214**	**1.0793**	4.7913	4.7753	4.9555	47.9130	47.7534	49.5549	**48.4071**	**0.9972**
3	13	89.9620	89.1065	89.9016	899.6204	891.0650	899.0159	**896.5671**	**4.7746**	4.5879	4.6272	4.8779	45.8789	46.2722	48.7788	**46.9766**	**1.5731**
4	16	92.7435	93.0558	92.5866	927.4351	930.5577	925.8663	**927.9530**	**2.3882**	4.4251	4.8259	4.8603	44.2514	48.2591	48.6033	**47.0379**	**2.4193**
5	20	92.9465	93.3603	93.7158	929.4648	933.6027	937.1575	**933.4083**	**3.8500**	4.5045	4.7507	5.1524	45.0446	47.5068	51.5237	**48.0250**	**3.2705**
6	23	91.0315	90.3732	90.9552	910.3149	903.7315	909.5519	**907.8661**	**3.6009**	4.5078	4.3623	4.3001	45.0782	43.6227	43.0005	**43.9005**	**1.0663**
7	27	87.2294	88.2463	88.0698	872.2937	882.4635	880.6977	**878.4850**	**5.4340**	4.3607	4.5846	4.8869	43.6074	45.8455	48.8685	**46.1072**	**2.6403**
8	30	85.7941	86.0195	85.9526	857.9408	860.1949	859.5264	**859.2207**	**1.1577**	4.8490	4.8533	4.5466	48.4903	48.5335	45.4655	**47.4964**	**1.7590**
9	34	93.3977	93.9432	93.1442	933.9769	939.4322	931.4415	**934.9502**	**4.0833**	4.9608	4.7062	4.8047	49.6081	47.0624	48.0470	**48.2392**	**1.2837**
10	37	95.5253	93.2836	95.4605	955.2532	932.8359	954.6051	**947.5647**	**12.7597**	5.0660	4.7710	5.0568	50.6605	47.7095	50.5675	**49.6458**	**1.6776**
11	41	93.5624	93.8161	95.3300	935.6244	938.1613	953.3002	**942.3619**	**9.5573**	4.9340	5.5298	5.0644	49.3398	55.2984	50.6440	**51.7607**	**3.1323**
12	44	90.4280	91.1602	90.6758	904.2797	911.6019	906.7582	**907.5466**	**3.7242**	5.1103	4.9646	5.1031	51.1028	49.6464	51.0314	**50.5935**	**0.8210**
13	48	90.3664	90.5703	91.3300	903.6637	905.7027	913.2997	**907.5554**	**5.0782**	5.2557	5.0105	5.1480	52.5570	50.1045	51.4800	**51.3805**	**1.2292**
14	51	88.2191	89.2388	90.2591	882.1905	892.3878	902.5907	**892.3897**	**10.2001**	4.7259	4.9672	4.9708	47.2591	49.6722	49.7083	**48.8799**	**1.4037**
15	55	88.3952	90.2329	89.5835	883.9517	902.3289	895.8347	**894.0384**	**9.3194**	5.0488	5.0752	5.0622	50.4877	50.7523	50.6220	**50.6207**	**0.1323**
16	58	90.2962	91.0547	90.6306	902.9621	910.5470	906.3064	**906.6052**	**3.8013**	4.8485	4.9518	4.8429	48.4852	49.5180	48.4285	**48.8106**	**0.6133**
17	62	90.3580	88.2534	88.2864	903.5802	882.5336	882.8640	**889.6593**	**12.0570**	5.3378	5.2240	4.7933	53.3783	52.2404	47.9325	**51.1838**	**2.8726**
18	65	91.2216	92.8764	91.9871	912.2158	928.7639	919.8711	**920.2836**	**8.2818**	4.3872	5.2101	5.3360	43.8721	52.1013	53.3605	**49.7779**	**5.1532**
19	69	87.7382	87.6976	88.4056	877.3823	876.9758	884.0559	**879.4713**	**3.9755**	4.8659	4.9281	4.9258	48.6593	49.2811	49.2577	**49.0660**	**0.3524**
20	72	89.0872	89.3159	88.2771	890.8720	893.1588	882.7714	**888.9341**	**5.4582**	5.1900	5.1716	5.3819	51.8996	51.7163	53.8194	**52.4784**	**1.1649**
21	76	88.0164	87.3799	87.3266	880.1640	873.7995	873.2659	**875.7431**	**3.8379**	4.5657	4.9350	4.4436	45.6568	49.3501	44.4361	**46.4810**	**2.5586**
22	79	90.0425	89.9059	88.7792	900.4254	899.0592	887.7921	**895.7589**	**6.9332**	4.7745	4.9740	4.9792	47.7445	49.7397	49.7920	**49.0921**	**1.1673**
23	83	89.1626	88.4270	88.0578	891.6257	884.2699	880.5782	**885.4913**	**5.6241**	4.8976	4.6742	4.9774	48.9757	46.7420	49.7739	**48.4972**	**1.5716**

Table 3.5.4-6 | Nitrate and nitrite concentrations in the batch BES running with continuous potential settings.

C3	Time	S1	S2	S3	Conc1	Conc2	Conc3	Nitrate	Nitrate	S1	S2	S3	Conc1	Conc2	Conc3	Nitrite	Nitrite
#	days	μM	μM	μM	μM	μM	μM	μM	μM	μM	μM	μM	μM	μM	μM	μM	μM
								Mean	Std							Mean	Std
0	0	83.3591	83.5690	83.8157	833.5908	835.6896	838.1566	835.8123	2.2854	3.7743	4.1388	4.0721	37.7428	41.3881	40.7210	39.9507	1.9409
1	6	12.3575	12.9901	12.3710	123.5750	129.9013	123.7100	125.7288	3.6141	1.7154	1.4131	1.5840	17.1538	14.1310	15.8403	15.7084	1.5157
2	9	4.7610	4.8198	4.1303	47.6104	48.1980	41.3034	45.7039	3.8223							n.a.	n.a.
3	13	2.5752	3.2172	2.5149	25.7521	32.1718	25.1494	27.6911	3.8921							n.a.	n.a.
4	16	2.7801	2.8160	2.9134	27.8015	28.1599	29.1339	28.3651	0.6895							n.a.	n.a.
5	20	2.5713	2.4733	2.4507	25.7130	24.7330	24.5073	24.9845	0.6410							n.a.	n.a.
6	23	3.5218	3.5146	3.4239	35.2185	35.1455	34.2390	34.8677	0.5457							n.a.	n.a.
7	27	4.0363	4.0208	4.1286	40.3628	40.2076	41.2863	40.6189	0.5832							n.a.	n.a.
8	30	38.5083	38.1836	38.7789	770.1657	763.6717	775.5780	769.8051	5.9613							n.a.	n.a.
9	34	2.4233	3.5341	2.4852	24.2331	35.3408	24.8521	28.1420	6.2420							n.a.	n.a.
10	37	3.5009	2.2838	3.9082	35.0087	22.8375	39.0817	32.3093	8.4518							n.a.	n.a.
11	41	3.7962	2.6636	3.4152	37.9622	26.6356	34.1520	32.9166	5.7635							n.a.	n.a.
12	44	3.1441	3.0170	3.0774	31.4414	30.1699	30.7745	30.7953	0.6360							n.a.	n.a.
13	48	3.2517	3.5814	3.1811	32.5171	35.8145	31.8109	33.3808	2.1370							n.a.	n.a.
14	51	85.9524	87.6463	83.5085	859.5240	876.4629	835.0853	857.0240	20.8018							n.a.	n.a.
15	55	3.5944	3.3119	3.4296	35.9440	33.1193	34.2965	34.4533	1.4189							n.a.	n.a.
16	58	3.9469	3.4720	3.5130	39.4688	34.7195	35.1298	36.4394	2.6315							n.a.	n.a.
17	62	3.1846	2.0144	3.1584	31.8458	20.1445	31.5839	27.8581	6.6815							n.a.	n.a.
C1	Time	S1	S2	S3	Conc1	Conc2	Conc3	Nitrate	Nitrate	S1	S2	S3	Conc1	Conc2	Conc3	Nitrite	Nitrite
#	days	μM	μM	μM	μM	μM	μM	μM	μM	μM	μM	μM	μM	μM	μM	μM	μM
								Mean	Std							Mean	Std
0	0	50.4744	51.7740	51.7753	1009.4873	1035.4800	1035.5056	1026.8243	15.0143							n.a.	n.a.
1	6	90.4991	91.8324	91.5328	904.9915	918.3237	915.3276	912.8809	6.9948							n.a.	n.a.
2	9	54.4711	54.2439	54.4169	544.7110	542.4390	544.1690	543.7730	1.1866							n.a.	n.a.
3	13	39.1939	38.8846	38.6074	391.9390	388.8459	386.0743	388.9531	2.9338							n.a.	n.a.
4	16	17.6387	17.7449	18.3132	176.3866	177.4493	183.1321	178.9893	3.6269							n.a.	n.a.
5	20	4.1396	4.4453	4.1244	41.3956	44.4526	41.2437	42.3640	1.8104							n.a.	n.a.
C2	Time	S1	S2	S3	Conc1	Conc2	Conc3	Nitrate	Nitrate	S1	S2	S3	Conc1	Conc2	Conc3	Nitrite	Nitrite
#	days	μM	μM	μM	μM	μM	μM	μM	μM	μM	μM	μM	μM	μM	μM	μM	μM
								Mean	Std							Mean	Std
0	0	54.0244	53.1960	53.2080	1080.4877	1063.9208	1064.1602	1069.5229	9.4965							n.a.	n.a.
1	6	91.9199	91.4119	91.6298	919.1991	914.1195	916.2977	916.5388	2.5484							n.a.	n.a.
2	9	54.4711	54.2439	54.4169	544.7111	542.4394	544.1692	543.7732	1.1865							n.a.	n.a.
3	13	6.0881	5.6251	5.7086	60.8806	56.2513	57.0862	58.0727	2.4673							n.a.	n.a.
4	16	2.2348	3.1722	3.2286	22.3484	31.7220	32.2856	28.7853	5.5816							n.a.	n.a.
5	20	2.6754	2.7508	2.3841	26.7535	27.5083	23.8414	26.0344	1.9363							n.a.	n.a.
6	23	42.5339	42.7949	40.0734	850.6777	855.8985	801.4675	836.0145	30.0323							n.a.	n.a.
7	27	78.1685	77.8106	78.6099	781.6853	778.1057	786.0991	781.9634	4.0039							n.a.	n.a.
8	30	74.3606	73.1843	74.6427	743.6061	731.8428	746.4273	740.6254	7.7356							n.a.	n.a.
9	34	58.8947	60.4964	58.5185	588.9474	604.9639	585.1845	593.0319	10.5032							n.a.	n.a.
10	37	43.9071	43.8713	42.9075	439.0707	438.7132	429.0753	435.6197	5.6705							n.a.	n.a.
AC	Time	S1	S2	S3	Conc1	Conc2	Conc3	Nitrate	Nitrate	S1	S2	S3	Conc1	Conc2	Conc3	Nitrite	Nitrite
#	days	μM	μM	μM	μM	μM	μM	μM	μM	μM	μM	μM	μM	μM	μM	μM	μM
								Mean	Std							Mean	Std
0	0	42.1149	42.3642	41.2949	842.2980	847.2846	825.8985	838.4937	11.1891							n.a.	n.a.
1	6	79.1162	79.5152	81.6808	791.1620	795.1522	816.8085	801.0409	13.8001							n.a.	n.a.
2	9	73.2577	73.9840	74.0326	732.5768	739.8399	740.3265	737.5811	4.3407							n.a.	n.a.
3	13	67.2969	66.7332	68.4975	672.9686	667.3318	684.9752	675.0919	9.0113							n.a.	n.a.
4	16	63.9502	64.1676	63.2417	639.5022	641.6761	632.4173	637.8652	4.8416							n.a.	n.a.
5	20	62.3459	60.5411	60.6861	623.4592	605.4106	606.8605	611.9101	10.0280	2.5989	2.5039	2.5864	25.9889	25.0388	25.8636	25.6304	0.5162
6	23	58.6460	57.1797	57.3522	586.4601	571.7968	573.5219	577.2596	8.0144	2.2350	2.7803	2.2997	22.3497	27.8033	22.9966	24.3832	2.9795

Table 3.5.4-7 | Sulphate concentrations in the batch BES running with intermittent (int) and with continuous (cont) potential settings.

Cycle	Reactor	Time	Area 1	Area 2	Area 3	MEAN	Conc. IC	Conc.	Cycle	Reactor	Time	Area 1	Area 2	Area 3	MEAN	Conc. IC	Conc.
Int C1	D9 R2	T0	2.6802	2.7519	2.7389	2.7237	121.1483	1211.4831	Con C1	D10 R1	T0	1.8071	1.8546	1.8468	1.8362	82.0514	1641.0279
		T1	2.7918	2.8292	2.8174	2.8128	125.0749	1250.7489			T1	2.8047	2.8389	2.9286	2.8574	127.0396	1270.3965
		T2	2.3025	2.2207	2.2252	2.2495	100.2584	1002.5844			T2	failed	failed	failed	#DIV/0!	#DIV/0!	#DIV/0!
		T3	2.2263	2.1106	2.1851	2.1740	96.9339	969.3392			T3	2.8809	2.8995	2.8379	2.8728	127.7166	1277.1659
		T4	failed	2.2013	2.1299	2.1656	96.5639	965.6388			T4	failed	failed	failed	#DIV/0!	#DIV/0!	
		T5	2.2391	2.1849	2.1938	2.2059	98.3407	983.4068			T5	failed	failed	failed	#DIV/0!	#DIV/0!	
		T6	2.0734	2.0757	2.0443	2.0645	92.1087	921.0866									
		T7	2.0796	1.9842	2.0429	2.0356	90.8355	908.3554									
		T8	2.5193	2.5412	2.0646	2.3750	105.7900	1057.9001									
Cycle	Reactor	Time	Area 1	Area 2	Area 3	MEAN	Conc. IC	Conc.	Cycle	Reactor	Time	Area 1	Area 2	Area 3	MEAN	Conc. IC	Conc.
Int C2	D8 R5	T0	1.5397	1.5523	1.5572	1.5497	69.4332	1388.6637	Con C1	D10 R2	T0	1.8427	1.8246	1.838	1.8351	82.0044053	1640.08811
		T1	1.5463	1.6027	1.5615	1.5702	70.3333	703.3333			T1	2.7882	2.8227	2.8318	2.8142	125.138032	1251.38032
		T2	1.5737	1.501	1.5615	1.5454	69.2423	692.4229			T2	failed	failed	failed	#DIV/0!	#DIV/0!	#DIV/0!
		T3	2.3822	2.4965	2.5488	2.4758	110.2305	1102.3054			T3	2.8368	2.8821	2.7028	2.8072	124.829662	1248.29662
		T4	1.6383	1.6462	1.6379	1.6408	73.4449	734.4493			T4	failed	failed	failed	#DIV/0!	#DIV/0!	#DIV/0!
		T5	1.5149	1.5859	1.5774	1.5594	69.8590	1397.1806			T5	failed	failed	failed	#DIV/0!	#DIV/0!	#DIV/0!
		T6	1.5434	1.528	1.5098	1.5271	68.4347	684.3465			T6	failed	failed	failed	#DIV/0!	#DIV/0!	#DIV/0!
		T7	2.069	2.1214	2.1033	2.0979	93.5815	935.8150			T7	2.7741	2.7312	2.6248	2.7100	120.5477	1205.4772
		T8	2.1049	2.1555	2.1341	2.1315	95.0617	950.6167			T8	2.5734	2.6103	2.587	2.5902	115.2702	1152.7019
		T9	2.1028	2.1014	2.097	2.1004	93.6916	936.9163			T9	2.6622	2.6467	2.547	2.6186	116.5213	1165.2129
		T10	1.6225	1.6078	1.6	1.6101	72.0925	720.9251			T10	2.7218	2.6633	2.685	2.6900	119.6667	1196.6667
		T11	1.811	1.8089	1.8135	1.8111	80.9486	809.4860									
		T12	2.3223	2.3149	2.3284	2.3219	103.4479	1034.4787									
Cycle	Reactor	Time	Area 1	Area 2	Area 3	MEAN	Conc. IC	Conc.	Cycle	Reactor	Time	Area 1	Area 2	Area 3	MEAN	Conc. IC	Conc.
Int C3	D8 R6	T0	1.6676	1.6749	1.6755	1.6727	74.8488	1496.9750	Con C3	D9 R1	T0	2.7308	2.771	2.7225	2.7414	121.9310	1219.3098
		T1	1.6079	1.6198	1.6206	1.6161	72.3568	723.5683			T1	2.5653	2.6212	2.6431	2.6099	116.1351	1161.3510
		T2	1.5613	1.5618	1.5543	1.5591	69.8473	698.4728			T2	2.6477	2.6749	2.6825	2.6684	118.7122	1187.1219
		T3	2.1118	2.0806	2.0603	2.0842	92.9794	929.7944			T3	2.2125	2.2106	2.2253	2.2161	98.7900	987.9001
		T4	1.6406	1.6267	1.6495	1.6389	73.3627	733.6270			T4	2.5418	2.6169	2.5826	2.5804	114.8385	1148.3847
		T5	1.5987	1.5272	1.5620	1.5626	70.0015	1400.0294			T5	2.2805	2.3677	2.3412	2.3298	103.7974	1037.9736
		T6	1.5290	1.5291	1.4175	1.4919	66.8840	668.8399			T6	1.6426	1.7524	1.7667	1.7206	76.9589	769.5888
		T7	1.3694	2.1691	2.1119	1.8835	84.1351	841.3510			T7	1.4315	1.5887	1.5571	1.5258	68.3774	683.7739
		T8	2.2096	2.2344	2.1842	2.2094	98.4934	984.9339			T8	0.9641	0.9384	1.0145	0.9723	43.9971	879.9413
		T9	2.2462	2.2226	2.2019	2.2236	99.1175	991.1747			T9	1.3582	1.4381	1.4592	1.4185	63.6520	636.5198
		~~T10~~				#DIV/0!	#DIV/0!	#DIV/0!			T10	1.3707	1.545	1.4546	1.4568	65.3377	653.3774
		T11	2.1194	2.0885	2.0924	2.1001	93.6784	936.7841			T11	1.5384	1.6327	1.7417	1.6376	73.3040	733.0396
		T12	2.0595	2.0872	2.0297	2.0588	91.8590	918.5903			T12	1.3605	1.4465	1.4413	1.4161	63.5463	635.4626
		T13	2.2191	2.2253	2.1822	2.2089	98.4699	984.6990			T13	1.1598	1.3308	1.3368	1.2758	57.3656	573.6564
		T14	2.1982	2.1901	2.2488	2.2124	98.6241	986.2408			T14	1.1619	1.2607	1.2169	1.2132	54.6065	546.0646
		T15	2.2211	2.2668	2.3239	2.2706	101.1894	1011.8943			T15	1.1733	1.2482	1.2192	1.2136	54.6241	546.2408
		T16	2.1916	2.1879	2.1736	2.1844	97.3906	973.9060			T16	1.2247	1.3633	1.3573	1.3151	59.0969	590.9692
		T17	2.5655	2.6217	2.5111	2.5661	114.2070	1142.0705			T17	1.1172	1.2247	1.3088	1.2169	54.7709	547.7093
dilution 1:20			failed: co-elution with an unknown species, no clear peak separation possible														

Table 3.5.4-8 | The most abundant 16S gene sequencing data (count of sequence ≥ 10) of all samples obtained from the batch reactors used for nitrate removal from synthetic groundwater. Asv were summarised on genus level and shown on the lowest classified level.

Row Labels	Count of Sequence
Archaea	**649**
Crenarchaeota	**87**
Bathyarchaeia	77
NA	10
Euryarchaeota	**92**
Methanomicrobia	46
Methanomicrobiales	**23**
Methanoregulaceae	23
Methanoregula	23
Methanosarcinales	**23**
Methanoperedenaceae	10
Candidatus_Methanoperedens	10
Methanosaetaceae	13
Methanosaeta	13
Thermoplasmata	46
Methanomassiliicoccales	**31**
Methanomassiliicoccaceae	14
NA	17
NA	**15**
NA	**95**
Nanoarchaeaeota	**375**
NA	12
Woesearchaeia	363
Bacteria	**11523**
Acidobacteria	**597**
Acidobacteriia	52
Solibacterales	**52**
Solibacteraceae_(Subgroup_3)	52
Bryobacter	15
Candidatus_Solibacter	10
NA	14
Paludibaculum	13
Aminicenantia	40
Aminicenantales	**40**
AT-s3-28	13
Holophagae	55
Holophagales	**23**
Holophagaceae	23
Subgroup_7	**32**
NA	23
Subgroup_17	60
Subgroup_18	26
Subgroup_22	61
Subgroup_6	186
Thermoanaerobaculia	81
Thermoanaerobaculales	**81**
Thermoanaerobaculaceae	81
Subgroup_10	42
Subgroup_23	11
Thermoanaerobaculum	13
TPD-58	15
Actinobacteria	**455**
Acidimicrobiia	123
Actinomarinales	**33**
IMCC26256	**20**
Microtrichales	**70**
Ilumatobacteraceae	28
CL500-29_marine_group	13
Ilumatobacter	15
Microtrichaceae	22
NA	10
Sva0996_marine_group	12
NA	20
Actinobacteria	65
NA	**52**
Propionibacteriales	**13**
Nocardioidaceae	13
Nocardioides	13
Coriobacteriia	68
NA	**12**
OPB41	**56**
MB-A2-108	26
NA	50
Thermoleophilia	107
Gaiellales	**68**
Gaiellaceae	14
Gaiella	14
NA	54
Solirubrobacterales	**39**
67-14	29
Solirubrobacteraceae	10
WCHB1-81	16
Armatimonadetes	**73**
Chthonomonadetes	10
Chthonomonadales	**10**
Fimbriimonadia	15
Fimbriimonadales	**15**
Fimbriimonadaceae	15
NA	48
Atribacteria	**11**
JS1	11
Bacteroidetes	**1063**
Bacteroidia	802
Bacteroidales	**336**
Bacteroidetes_BD2-2	28
Bacteroidetes_vadinHA17	155
NA	39
Prolixibacteraceae	75
BSV13	17
NA	45
WCHB1-32	13
Rikenellaceae	15
Blvii28_wastewater-sludge_group	15
SB-5	24
Chitinophagales	**177**
37-13	11
Chitinophagaceae	33
NA	20
Terrimonas	13
NA	18
Saprospiraceae	115
NA	104
Phaeodactylibacter	11
Cytophagales	**18**
Microscillaceae	18
Flavobacteriales	**31**
Flavobacteriaceae	31
Flavobacterium	19
NA	12
NA	**83**
Sphingobacteriales	**157**
AKYH767	33
env.OPS_17	14
Lentimicrobiaceae	47

- NA 53
- NS11-12_marine_group 10
- Ignavibacteria 251
- **Ignavibacteriales 86**
- Ignavibacteriaceae 26
- Ignavibacterium 26
- NA 15
- PHOS-HE36 17
- SR-FBR-L83 28
- **Kryptoniales 111**
- BSV26 96
- MSB-3C8 15
- **OPB56 17**
- **SJA-28 37**
- Rhodothermia 10
- **Rhodothermales 10**
- Rhodothermaceae 10

BRC1 70

Calditrichaeota 11
- Calditrichia 11
- **Calditrichales 11**
- Calditrichaceae 11

Chlamydiae 64
- Chlamydiae 64
- **Chlamydiales 64**
- NA 24
- Parachlamydiaceae 40
- NA 17
- Neochlamydia 23

Chloroflexi 1361
- Anaerolineae 1074
- **ADurb.Bin180 26**
- **Anaerolineales 476**
- Anaerolineaceae 476
- Anaerolinea 51
- GWD2-49-16 18
- Leptolinea 32
- Levilinea 19
- NA 299
- Pelolinea 10
- RBG-16-58-14 24
- UTCFX1 23
- **Ardenticatenales 18**
- **Caldilineales 193**
- Caldilineaceae 193
- Litorilinea 14
- NA 179
- **NA 106**
- **RBG-13-54-9 54**
- **SBR1031 91**
- A4b 32
- NA 59
- **SJA-15 98**
- **01/01/2020 12**
- Chloroflexia 23
- **Thermomicrobiales 23**
- JG30-KF-CM45 23
- Dehalococcoidia 92
- **GIF9 23**
- **MSBL5 11**
- **NA 41**
- **S085 17**
- JG30-KF-CM66 22
- KD4-96 53
- NA 58
- OLB14 25
- TK10 14

Cyanobacteria 191
- Melainabacteria 10
- **Gastranaerophilales 10**
- Oxyphotobacteria 168
- **Chloroplast 93**
- **NA 48**
- **Nostocales 16**
- **Synechococcales 11**
- Cyanobiaceae 11
- Cyanobium_PCC-6307 11
- Sericytochromatia 13

Dependentiae 200
- Babeliae 200
- **Babeliales 200**
- Babeliaceae 21
- NA 98
- UBA12409 14
- Vermiphilaceae 67

Elusimicrobia 74
- Elusimicrobia 32
- **Lineage_IV 19**
- **MVP-88 13**
- Lineage_IIb 21
- Lineage_IIc 11
- NA 10

FCPU426 12

Fibrobacteres 13
- Fibrobacteria 13
- **Fibrobacterales 13**

Firmicutes 465
- Bacilli 73
- **Bacillales 73**
- Bacillaceae 58
- Anaerobacillus 16
- Bacillus 24
- NA 18
- Paenibacillaceae 15
- Paenibacillus 15
- Clostridia 350
- **Clostridiales 336**
- Christensenellaceae 13
- Christensenellaceae_R-7_group 13
- Clostridiaceae_1 63
- Clostridium_sensu_stricto_1 13
- Clostridium_sensu_stricto_13 14
- NA 36
- Family_XII 26
- Acidaminobacter 16
- NA 10
- Family_XIII 31
- Anaerovorax 21
- NA 10
- Heliobacteriaceae 12
- Hydrogenispora 12
- Lachnospiraceae 17
- NA 66
- Peptococcaceae 38
- Desulfosporosinus 22
- NA 16
- Ruminococcaceae 58
- NA 40
- Ruminiclostridium_1 18
- Syntrophomonadaceae 12
- Syntrophomonas 12
- **NA 14**

- NA 27
- Negativicutes 15
- **Selenomonadales 15**
- Veillonellaceae 15

Gemmatimonadetes 80
- BD2-11_terrestrial_group 20
- Gemmatimonadetes 60
- **Gemmatimonadales 60**
- Gemmatimonadaceae 60

Hydrogenedentes 98
- Hydrogenedentia 98
- **Hydrogenedentiales 98**
- Hydrogenedensaceae 98

Kiritimatiellaeota 47
- Kiritimatiellae 47
- **WCHB1-41 47**

Latescibacteria 142
- Latescibacteria 33
- **Latescibacterales 33**
- Latescibacteraceae 33
- Candidatus_Latescibacter 12
- NA 21
- NA 109

LCP-89 10

Margulisbacteria 17

NA 929

Nitrospinae 30
- P9X2b3D02 30

Nitrospirae 91
- 4-29-1 13
- Nitrospira 18
- **Nitrospirales 18**
- Nitrospiraceae 18
- Nitrospira 18
- Thermodesulfovibrionia 60

Omnitrophicaeota 47
- NA 30
- Omnitrophia 17
- **Omnitrophales 17**
- Omnitrophaceae 17
- Candidatus_Omnitrophus 17

Patescibacteria 713
- ABY1 82
- **Candidatus_Falkowbacteria 15**
- **Candidatus_Kerfeldbacteria 31**
- **Candidatus_Magasanikbacteria 23**
- **NA 13**
- Berkelbacteria 23
- CPR2 25
- Gracilibacteria 89
- **Absconditabacteriales_(SR1) 20**
- **Candidatus_Peregrinibacteria 21**
- **Candidatus_Peribacteria 10**
- **NA 38**
- Microgenomatia 169
- **Candidatus_Levybacteria 10**
- **Candidatus_Pacebacteria 38**
- **Candidatus_Roizmanbacteria 17**
- **Candidatus_Woesebacteria 83**
- **NA 21**
- NA 44
- Parcubacteria 136
- **Candidatus_Kaiserbacteria 20**
- **Candidatus_Moranbacteria 32**
- **Candidatus_Nomurabacteria 16**
- **Candidatus_Yanofskybacteria 11**
- **NA 57**
- Saccharimonadia 66
- **Saccharimonadales 66**
- WS6_(Dojkabacteria) 30
- WWE3 49

Planctomycetes 598
- OM190 39
- Phycisphaerae 128
- **CCM11a 14**
- **Phycisphaerales 47**
- AKAU3564_sediment_group 13
- Phycisphaeraceae 34
- NA 16
- SM1A02 18
- **Pla1_lineage 31**
- **Tepidisphaerales 36**
- WD2101_soil_group 36
- Pla4_lineage 15
- Planctomycetacia 416
- **Gemmatales 52**
- Gemmataceae 52
- Gemmata 16
- NA 36
- **Pirellulales 313**
- Pirellulaceae 313
- Blastopirellula 35
- Candidatus_Anammoximicrobium 17
- NA 148
- Pir4_lineage 41
- Pirellula 50
- Rhodopirellula 22
- **Planctomycetales 51**
- Gimesiaceae 10
- NA 41

Proteobacteria 3145
- Alphaproteobacteria 373
- **NA 109**
- **Rhizobiales 116**
- Hyphomicrobiaceae 32
- Hyphomicrobium 22
- Pedomicrobium 10
- NA 42
- Rhizobiaceae 20
- Rhizobiales_Incertae_Sedis 11
- Xanthobacteraceae 11
- **Rhodobacterales 137**
- Rhodobacteraceae 137
- Frigidibacter 11
- NA 111
- Rhodobacter 15
- **Sphingomonadales 11**
- Sphingomonadaceae 11
- Deltaproteobacteria 1346
- **Bdellovibrionales 89**
- Bacteriovoracaceae 25
- NA 11
- Peredibacter 14
- Bdellovibrionaceae 64
- Bdellovibrio 38
- OM27_clade 26
- **Deltaproteobacteria_Incertae_Sedis 27**
- Syntrophorhabdaceae 27
- Syntrophorhabdus 27
- **Desulfarculales 75**
- Desulfarculaceae 75
- Desulfatiglans 43

- NA 32
- **Desulfobacterales 146**
  - Desulfobacteraceae 76
    - NA 44
    - Sva0081_sediment_group 32
  - Desulfobulbaceae 70
    - Desulfobulbus 20
    - NA 50
- **Desulfuromonadales 119**
  - Desulfuromonadaceae 14
    - Desulfuromonas 14
  - Geobacteraceae 82
    - Geobacter 72
    - Geothermobacter 10
  - NA 23
- **MBNT15 35**
- **Myxococcales 233**
  - Archangiaceae 25
    - Anaeromyxobacter 25
  - BIrii41 18
  - Blfdi19 14
  - Haliangiaceae 44
    - Haliangium 44
  - MidBa8 12
  - NA 50
  - P3OB-42 16
  - Phaselicystidaceae 15
    - Phaselicystis 15
  - Sandaracinaceae 39
    - NA 28
    - Sandaracinus 11
- **NA 185**
- **NB1-j 45**
- **Oligoflexales 64**
  - 0319-6G20 37
  - Oligoflexaceae 27
- **RCP2-54 10**
- **Sva0485 49**
- **Syntrophobacterales 269**
  - Syntrophaceae 210
    - Desulfobacca 96
    - Desulfomonile 19
    - NA 25
    - Smithella 23
    - Syntrophus 47
  - Syntrophobacteraceae 59
    - Desulfovirga 13
    - NA 30
    - Syntrophobacter 16
- Gammaproteobacteria 1325
  - **1013-28-CG33 10**
  - **Acidiferrobacterales 27**
    - Acidiferrobacteraceae 27
      - Sulfurifustis 27
  - **Betaproteobacteriales 791**
    - Burkholderiaceae 172
      - Lautropia 14
      - Leptothrix 10
      - Limnobacter 12
      - NA 136
    - Gallionellaceae 99
      - Candidatus_Nitrotoga 60
      - Gallionella 13
      - NA 26
    - Hydrogenophilaceae 101
      - NA 11
      - Thiobacillus 90
    - NA 110
    - Nitrosomonadaceae 87
      - Ellin6067 31
      - mle1-7 10
      - MND1 24
      - NA 10
      - Nitrosomonas 12
    - Rhodocyclaceae 132
      - Azoarcus 18
      - Denitratisoma 11
      - NA 45
      - Sulfurisoma 11
      - Sulfuritalea 23
      - Thauera 24
    - SC-I-84 52
    - Sulfuricellaceae 13
      - Ferritrophicum 13
    - TRA3-20 25
  - **Cellvibrionales 46**
    - Halieaceae 31
      - Halioglobus 12
      - OM60(NOR5)_clade 19
    - Spongiibacteraceae 15
      - BD1-7_clade 15
  - **Competibacterales 14**
    - Competibacteraceae 14
      - Candidatus_Competibacter 14
  - **Coxiellales 28**
    - Coxiellaceae 28
      - Coxiella 28
  - **Diplorickettsiales 23**
    - Diplorickettsiaceae 23
      - Aquicella 23
  - **Gammaproteobacteria_Incertae_Sedis 32**
    - Unknown_Family 32
  - **Legionellales 19**
    - Legionellaceae 19
      - Legionella 19
  - **Methylococcales 41**
    - Methylomonaceae 41
      - Crenothrix 14
      - Methylobacter 10
      - NA 17
  - **NA 197**
  - **PLTA13 24**
  - **Pseudomonadales 11**
    - Pseudomonadaceae 11
      - Pseudomonas 11
  - **Steroidobacterales 52**
    - Steroidobacteraceae 29
    - Woeseiaceae 23
      - Woeseia 23
  - **Xanthomonadales 10**
    - Xanthomonadaceae 10
      - Stenotrophomonas 10
- NA 101
- **Rokubacteria 12**
  - NC10 12
    - **Methylomirabilales 12**
      - Methylomirabilaceae 12
        - Sh765B-TzT-35 12
- **Spirochaetes 196**
  - Leptospirae 47
    - **Leptospirales 47**
      - Leptospiraceae 47

RBG-16-49-21	47
MVP-15	18
Spirochaetia	131
Spirochaetales	**131**
Spirochaetaceae	131
NA	70
Spirochaeta_2	61
Tenericutes	**22**
Mollicutes	22
Izimaplasmatales	**22**
Verrucomicrobia	**598**
Verrucomicrobiae	598
Chthoniobacterales	**24**
Chthoniobacteraceae	24
Chthoniobacter	24
NA	**12**
Pedosphaerales	**340**
Pedosphaeraceae	340
ADurb.Bin063-1	51
NA	289
S-BQ2-57_soil_group	**20**
Verrucomicrobiales	**202**
DEV007	60
NA	18
Rubritaleaceae	95
Luteolibacter	82
NA	13
Verrucomicrobiaceae	29
WS2	**12**
WS4	**29**
Zixibacteria	**47**
Eukaryota	**526**
NA	**133**
Grand Total	**12831**

4. Ammonia removal from wastewater using partial nitrification and the anammox process

Studies in the batch reactors regarding the ammonium removal and the microbial community compositions were conducted by B. Sc. Constantin Soffner. The investigation of oxygen evolution rates in the upflow BES was done by Julia Heise.

4.1. **Abstract**

The intention to save drinking water by reduced usage in households leads to high concentrations of ammonium in the sewage systems. The ammonium removal of the wastewater streams is a huge challenge for the wastewater treatment plants. In this study bioelectrochemical systems have been applied to remove ammonium from synthetic wastewater via nitrification and the anammox process. In a first step nitrifying bacteria are enriched on the anode as a preliminary biofilm. Anammox bacteria are added in a second step joining the anaerobic outer layer of the biofilm.

Oxygen evolution rates at an abiotic anode revealed that adjustment of oxygen concentrations was best achieved in upflow BES due to lower activation and ohmic losses. Ammonium removal and microbial community studies were done in batch reactors revealing constant ammonium removal. The predominant asv assigned to the genera *Hyphobmicrobium*, *Dechloromonas*, *Pseusoxanthomonas*, *Pseudomonas*, and *Anaerobacillus* and *Azonexus* were found on the anode and asv assigned to the genera *Pedobacter* and *Candidatus* Kuenenia were found in the synthetic wastewater medium.

This is the first report of a bioelectrochemical system to continuously apply a constant oxygen concentration for optimization of ammonium removal from wastewater using nitrifying and anammox bacteria. The efficiency of the process shows great potential for application in a wastewater treatment plant.

4.2. **Introduction**

Wastewater treatment plants (WWTPs) must deal with highly ammonia concentrated municipal wastewater streams. The complete removal of ammonium is a crucial step in municipal wastewater treatment as residual ammonia in the effluent is discharged into the environment leading to contaminations of open water bodies. Subsequent depletion of dissolved oxygen due to ammonium oxidation results in killing of fishes and invertebrates due to almost anoxic conditions in the freshwater systems (Camargo & Alonso, 2006). Therefore, the statutory requirement set a limit value of 10 mg NH_4^+-N L^{-1} for ammonium in the waste water discharge (Deutsche Bundesregierung, 2004).

In WWTPs, the combination of nitrification (oxidation of ammonium to nitrate) and denitrification (reduction of nitrate to nitrogen gas) in activated sludge have usually been widely used for ammonia removal. Mainly due to the required aeration for the nitrification reaction, the process is rather expensive. In contrast to this process, however, ammonia can also be removed anoxically by anaerobic ammonium oxidation (anammox), a process discovered for the first time in a denitrifying fluidised bed reactor (Mulder *et al.*, 1995). Bacteria that are capable of anaerobic ammonia oxidation convert ammonium together with nitrite to nitrogen gas (Jetten *et al.*, 1998) and belong to the *Planctomycetes*. So far, five genera have been studied: *Brocadia*, *Kuenenia*, *Scalindua*, *Jettenia* and *Anammoxoglobus* (van Niftrik & Jetten, 2012).

Since 2002, several pilot plants have been implementing the anammox process, also known as the completely autotrophic nitrogen removal over nitrite (CANON) process (Sliekers *et al.*, 2003), or the single reactor system for high-rate ammonia removal over nitrite (SHARON) process (Van Dongen *et al.*, 2001). The nitrite essential for the reaction is gained from partial nitrification (nitritation) of ammonium to nitrite. Although, anammox bacteria are very susceptible to dissolved oxygen concentrations of more than 2.3 mg L^{-1} in granular anammox enrichment cultures (Carvajal-Arroyo *et al.*, 2013), the co-existence of both aerobic and anaerobic bacteria in one reactor is possible in systems kept under oxygen limitations (Sliekers *et al.*, 2003). The co-existence of aerobic and anaerobic microorganisms in aquatic systems has been shown before. Microorganisms form microbial communities in flocs,

granules, and biofilms (Flemming & Wingender, 2010), where anoxic regions occur in the inner parts due to oxygen diffusion limitations (De Beer *et al.*, 1994). Using the anammox process, 90% of the ammonium present in a wastewater stream can be converted to elemental nitrogen (Kumar & Lin, 2010). The residual 10% is nitrate, which is a side product in the anammox process (Kumar & Lin, 2010). The anammox process provides the advantage that addition of organic carbon and aeration is not necessary (Kartal *et al.*, 2010).

Besides the CANON- and the SHARON-Processes, also bioelectrochemical systems (BES) can be applied. In a BES, electrochemically active microorganisms form biofilms on the electrodes and catalyse oxidation and/or reduction reactions (Larminie *et al.*, 2003). Ammonia removal by nitrification reactions in BES have already been reported in literature. For instance, in a reactor consisting of two celite biocarrier filled columns, the removal of nitrate nitrogen and ammonia nitrogen have been investigated at room temperature (Goel & Flora, 2005). At a current density of 0.5 mA cm^{-2} an ammonia nitrogen removal up to 56% was measured. The simultaneous removal of carbon at the anode and nitrogen (nitrate and ammonia nitrogen) at the cathode was studied in a microbial fuel cell using a loop configuration (Virdis *et al.*, 2010). Up to 94.1 % of nitrogen could be eliminated at -0.146 V.

The idea of using the nitritation-anammox process in BES is rather new. The advantage of such a system is the simultaneous generation of energy from the microbial reactions (Rabaey & Verstraete, 2005). Recently, such a system was built using a membrane-aerated cathode and anaerobic sludge at the anode to drive the reaction (Yang *et al.*, 2017). A nitrogen removal efficiency of 94.8 ± 7.7% was achieved at a current density of 72.3 ± 1.9 A m^{-3}.

In the present study an anodic BES using the nitritation-anammox process is constructed. The anode is preconditioned with a preliminary biofilm of nitrifying bacteria using the oxygen generated at the anode as electron acceptor for nitritation. In a second step the, anammox bacteria added to the system can inhabit the outer anoxic zones of the established biofilm converting ammonium and nitrite to nitrogen gas. Aeration of the system and addition of organic carbon is not required.

4.3. **Experimental procedure**

4.3.1. Growth medium for ammonium oxidising bacteria in BES

The growth medium used in these experiments was adapted from Ke (2014). All solutions were prepared using ultra-pure water and were autoclaved for 20 min at 120 °C. As the ammonium and the carbonate solution were added under anoxic conditions, both solutions were sparged with N_2/CO_2 (80:20 (v/v)) gas [Air Liquide, Düsseldorf, Germany] prior to autoclaving. The ammonium solution was sparged for 20 min. A 1 mol L^{-1} carbonate solution was prepared with anoxic hot water and the headspace was exchange for 5 min with N_2/CO_2 (80:20 (v/v)) gas prior to autoclaving. K_2HPO_4 solution, $MgSO_4$ solution, $CaCl_2$ solution and carbonate were stored at room temperature. Other solutions were stored at 4 °C.

Table 4.3.1-1 | Solutions used as growth medium for ammonia oxidising bacteria.

		Final concentrations	
	Compound	**[g L^{-1}]**	**[mmol L^{-1}]**
K_2HPO_4 solution	K_2HPO_4	0.03	0.20
$MgSO_4$ solution	$MgSO_4 \cdot 7\ H_2O$	0.30	1.22
$CaCl_2$ solution	$CaCl_2 \cdot 2\ H_2O$	0.18	1.22
Ammonium solution	NH_4Cl	0.05	1.00
Carbonate solution	$NaHCO_3$	0.42	5.00
Trace elements solution A	Cf. Table 4.3.1-2	1X	1X
Trace elements solution B	Cf. Table 4.3.1-3	1X	1X

Table 4.3.1-2 | Trace elements solution A used for the growth medium of ammonia oxidising bacteria. The solution was prepared as 1000X.

		Final concentrations	
	Compound	**[mg L^{-1}]**	**[µmol L^{-1}]**
Trace elements solution A	Na_2EDTA	6.37	17.11
	$FeSO_4 \cdot 7\ H_2O$	9.15	32.91

Table 4.3.1-3 | Trace elements solution B used for the growth medium of ammonia oxidising bacteria. The solution was prepared as 1000X.

		Final concentrations	
	Compound	**[mg L^{-1}]**	**[µmol L^{-1}]**
Trace elements solution B	Na_4EDTA	21.37	51.35
	$ZnCl_2$	0.204	1.50
	$CoCl_2 \cdot 6\ H_2O$	0.24	1.01
	$MnCl_2 \cdot 4\ H_2O$	0.99	5.00
	$CuSO_4 \cdot 5\ H_2O$	0.25	1.00
	$Na_2MoO_4 \cdot 2\ H_2O$	0.22	0.91
	$NiCl_2 \cdot 6\ H_2O$	0.19	0.80
	$Na_2SeO_3 \cdot 5\ H_2O$	0.22	0.84
	H_3BO_3	0.014	0.23

4.3.2. Inoculum for partial nitrification and anammox in BES

For the partial nitrification, activated granular sludge was taken from a running reactor of the Department of Municipal Water and Waste Water Management, University of Duisburg-Essen, Germany, maintained by Dr. Leon Steuernagel. The anammox inoculum derived from a reactor of the Department of Environmental Biotechnology, University of Delft, Netherlands, maintained by Dr. Michele Laureni. As the anammox sample was introduced under anoxic conditions during the experiments, the flask was sparged with N_2/CO_2 (80:20 (v/v)) gas [Air Liquide, Düsseldorf, Germany] beforehand.

4.3.3. Setup of the anodic batch bioelectrochemical system

For the experiments on ammonia oxidation at the anode, batch reactors were built as described previously in section 3.3.3 except for the electrode material. The main materials used for the setup are given in Table 4.3.3-1. Iridium oxide (IrOx) coated titanium anodes were chosen for oxygen evolution on the anode. Additionally, a sensor spot was glued with silicon glue on the inside of the anode chamber for non-invasive measurement of oxygen concentration in the medium. All materials used were

cleaned thoroughly with ultra-pure water. The membrane was pre-treated by up-swelling in a 4% NaCl solution for 24 h.

Table 4.3.3-1 | Materials used for assembling an anodic batch bioelectrochemical system for ammonium oxidation at the anode.

	Material	Specification	Manufacturers
Anode	IrOx coated titanium	1.0x5.0 cm	Magneto Special Anodes B.V., Schiedam, Netherlands
Cathode	Carbon felt	1.5x5.0 cm	Alfa Aeser (Thermo Fisher GmbH), Karlsruhe, Germany
Reference electrode	RE-1B (Ag/AgCl)		ALS Co., Ltd., Tokyo, Japan
Membrane	Fumasep FKB-PK-130	2.0x2.0 cm	Fumatech BWT GmbH, Bietigheim-Bissingen, Germany
Wirings	Titan, WirePurity 99.6%+	10 cm, 5 cm. Ø 1 mm	Advent Research Materials Ltd., England, Great Britain
Rubber stopper	Butyl	N20 and GL45	Glasgerätebau Ochs GmbH, Bovenden, Germany
Sensor spot	SP-PSt6-NAU-D5-YOP		PreSens GmbH, Regensburg, Germany

The anode chamber was filled with growth medium (Table 4.3.1-1) to a final volume of 220 mL after adding ammonium, carbonate, and one or both inoculums between the cyclic voltammetry procedures (cf. section 4.3.5). The medium was sparged with N_2/CO_2 (80:20 (v/v)) gas [Air Liquide, Düsseldorf, Germany] for 45 min. Continuous stirring during the experiments was achieved using a stirring bar. The cathode chamber was filled with 22 mL of growth medium lacking ammonium, carbonate and the inoculum.

4.3.4. Setup of the anodic upflow bioelectrochemical system

An upflow BES was built of Perspex as described previously (Gildemyn *et al.*, 2015). The chambers were built from two identical frames with dimensions of 20.0x5.0x2.0 cm covered with two Perspex plates at the outsides. All Perspex parts were merged using rubber sheets between all parts to prevent leaking. To collect electrons from the carbon felt cathode, a current made of stainless steel was used that was connected to the potentiostat. The main materials used are given in Table 4.3.4-1.

A setup scheme is shown in Figure 4.3.4-1. A sensor spot for oxygen measurement was glued with silicon glue onto the Perspex at the inside of the anode chamber. The pre-treatment of materials was done as described in the previous section 4.3.3.

Table 4.3.4-1 | Materials used for assembling an anodic upflow bioelectrochemical system for ammonium oxidation at the anode.

	Material	Specification	Manufacturers
Anode	IrOx coated titanium	20.0x5.0 cm, diamond shaped	Magneto Special Anodes B.V., Schiedam, Netherlands
Cathode	Carbon felt	22.0x8.0 cm	Alfa Aeser (Thermo Fisher GmbH), Karlsruhe, Germany
Reference electrode	RE-1B (Ag/AgCl)		ALS Co., Ltd., Tokyo, Japan
Membrane	Fumasep FKB-PK-130	2.0x2.0 cm	Fumatech BWT GmbH, Bietigheim-Bissingen, Germany
Wirings	Titan, WirePurity 99.6%+	10 cm, 5 cm. Ø 1 mm	Advent Research Materials Ltd., England, Great Britain
Rubber stopper	Butyl	N20 and GL45	Glasgerätebau Ochs GmbH, Bovenden, Germany
Sensor spot	SP-PSt6-NAU-D5-YOP		PreSens GmbH, Regensburg, Germany

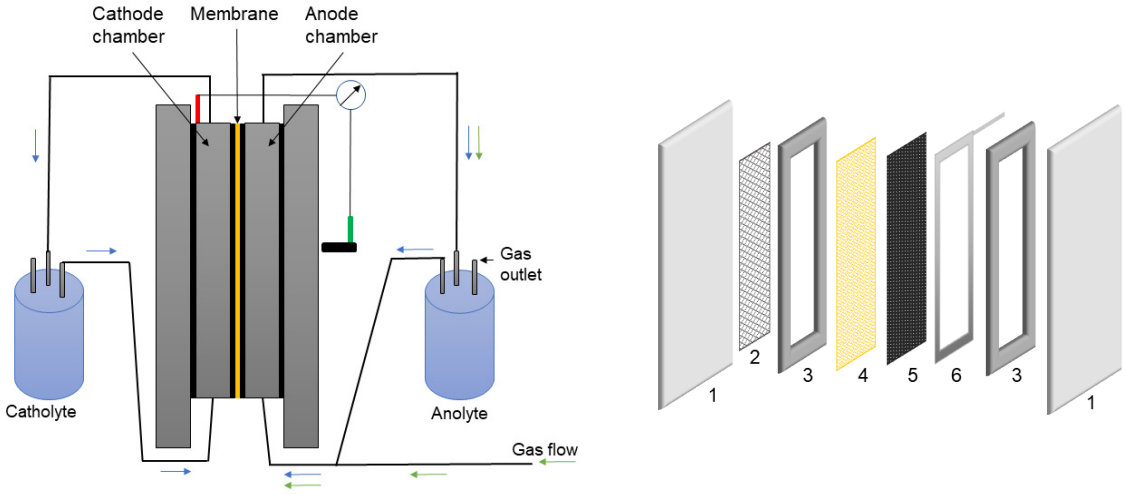

Figure 4.3.4-1 | Schematic view of the upflow BES from the side (left) and its single parts (right). The medium is pumped from the below into the cell compartments (Perspex frames). 1: Perspex plate, 2: Ir-coated Ti-oxide anode, 3: Perspex frame used as anode/cathode chamber, 4: membrane, 5: carbon felt cathode, 6: current collector.

1 L growth medium (Table 4.3.1-1) was pumped continuously through the anodic chamber with 10 mL min^{-1} and sparged steadily with N_2/CO_2 (80:20 (v/v)) gas [Air Liquide, Düsseldorf, Germany]. Ammonium and carbonate were added between the cyclic voltammetry procedures (cf. section 4.3.5). Medium without ammonium and carbonate was pumped through the cathode chamber.

4.3.5. Stability test using chronoamperiometry and investigation of redox active compounds using cyclic voltammetry in an anodic BES

A stability test was performed at a potential of 0.7 V vs. Ag/AgCl for 24 hours to examine leakages and connection issues before starting the main experiments. When the current stayed constant within this time, the reactor was regarded as stable.

Cyclic voltammetry was done before and after the addition of ammonium, carbonate and the inoculation. The applied potential ranged from 0.0 V vs. Ag/AgCl to 1.0 V Ag/AgCl and 5 cycles were used.

4.3.6. Investigation of oxygen evolution rates

To study the oxygen evolution on the anode the batch reactors were run abiotically with potentials ranging from 0.7 V to 0.9 V vs. Ag/AgCl for 8 h. Oxygen concentrations in the medium were measured every hour non-invasively through the sensor spot via an optical fibre and the Fibox 4 trace oxygen meter [PreSens GmbH, Regensburg, Germany]. Oxygen evolution rates were calculated from the slope of the oxygen concentrations over time. The upflow system was run with potentials ranging from 0.6 V to 0.8 V vs. Ag/AgCl. Oxygen concentrations were measured every 3 s over 24 h. The summarized raw data are shown in the appendix in Table 4.5.2-1.

4.3.7. Setup of batch reactors for microbial community investigations

Studies regarding the changes of the microbial communities on the anode were conducted in two sets of batch reactors by B.Sc. Constantin Soffner. Nitrifying bacteria were enriched first in order to establish a preliminary biofilm on the anode. In a second step, anammox bacteria were added.

The AerAOB were enriched for seven days with constantly poised anodes at 0.95 V vs. Ag/AgCl. This potential was also kept after adding anammox bacteria for the main run. Current densities were obtained by averaging the current densities over 6 hours. The averaged current densities are shown in the appendix in Table 4.5.2-2 (Reactor 1), Table 4.5.2-3 (Reactor 2), and Table 4.5.2-4 (Reactor 3).

4.3.8. Analysis of nitrogen species via ion chromatography

The preparation of samples for ion chromatography was performed as previously described in section 2.3.3 and was conducted by B. Sc. Constantin Soffner. Also, the further mentioned specifications for the measurement were the same. The summarized raw data of ion concentrations are shown in the appendix (Table 4.5.2-5 (ammonium), Table 4.5.2-6 (nitrate), and Table 4.5.2-7 (nitrite)).

4.3.9. DNA extraction, 16S rRNA amplicon library preparation and analysis

Samples for DNA extraction were taken from the anode by scrapping the biofilm from the material as duplicates using cell scrapers [Sarstedt, Nümbrecht, Germany]. DNA extraction was performed using the FastDNA™ SPIN Kit for Soil [MP Biomedicals, Heidelberg, Germany] and applying the bead-beating settings as previously described in section 2.3.4. The 16S rRNA amplicon library was prepared as stated above (cf. section 2.3.6). The samples were stored at -20 °C until shipping for analysis to GATC Biotech AG [Konstanz, Germany]. Analysis of the 16S rRNA gene sequences was done in the R environment using the DADA2 pipeline as previously described in section 3.3.8. 16S gene sequencing data are shown in the appendix in Table 4.5.2-8.

4.4. **Results**

4.4.1. Oxygen evolution rates in batch and upflow anodic BES

The oxygen evolution at the anode was investigated in both batch and upflow BES and are shown below in Figure 4.4.1-1. In the upflow BES, oxygen concentrations measured in the medium were not as high as in the batch systems. The oxygen evolution rate increased from 0.04 µg L^{-1} h^{-1} to 0.63 µg L^{-1} h^{-1} between 0.7 V to 0.8 V vs. Ag/AgCl in the upflow BES. In the batch systems, the rate increased from 0.67 µg L^{-1} h^{-1} to 22.17 µg L^{-1} h^{-1} within the potential range of only 0.85 V to 0.90 V vs. Ag/AgCl. Standard deviations of oxygen evolution rates measured in the upflow BES (±0.35 µg L^{-1} h^{-1} the highest) were significantly smaller than those obtained in the batch systems (±21.44 µg L^{-1} h^{-1} the highest), where the medium was constantly stirred but not flushed.

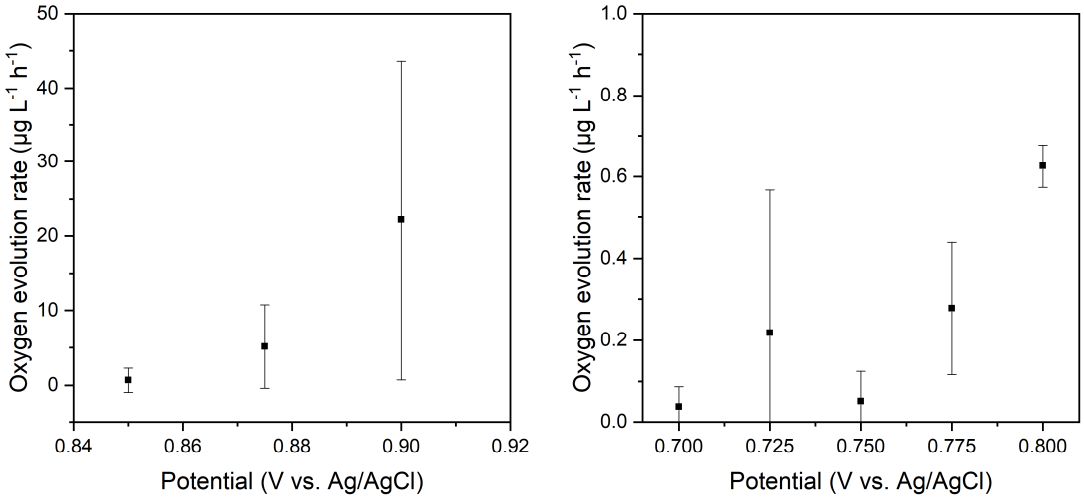

Figure 4.4.1-1 | Oxygen evolution rates (n=3) obtained in bioelectrochemical batch systems (left) and in upflow cells (right). Mind the scales.

Oxygen concentrations were more straightforward to adjust in the upflow systems than in the batch reactors. However, the exact oxygen concentrations at the anode could not be measured in both systems since the sensor spots were located at the inner side of the batch flask and on the frame of the upflow reactor, respectively.

4.4.2. Ammonium removal in batch systems

For the removal of ammonium in batch BES, AerAOB were cultivated for seven days to ensure the establishment of a biofilm on the anodes. Figure 4.4.2-1 shows the current densities and the concentration of nitrogen species during the cultivation of AerAOB and the subsequent additional cultivation of anammox bacteria.

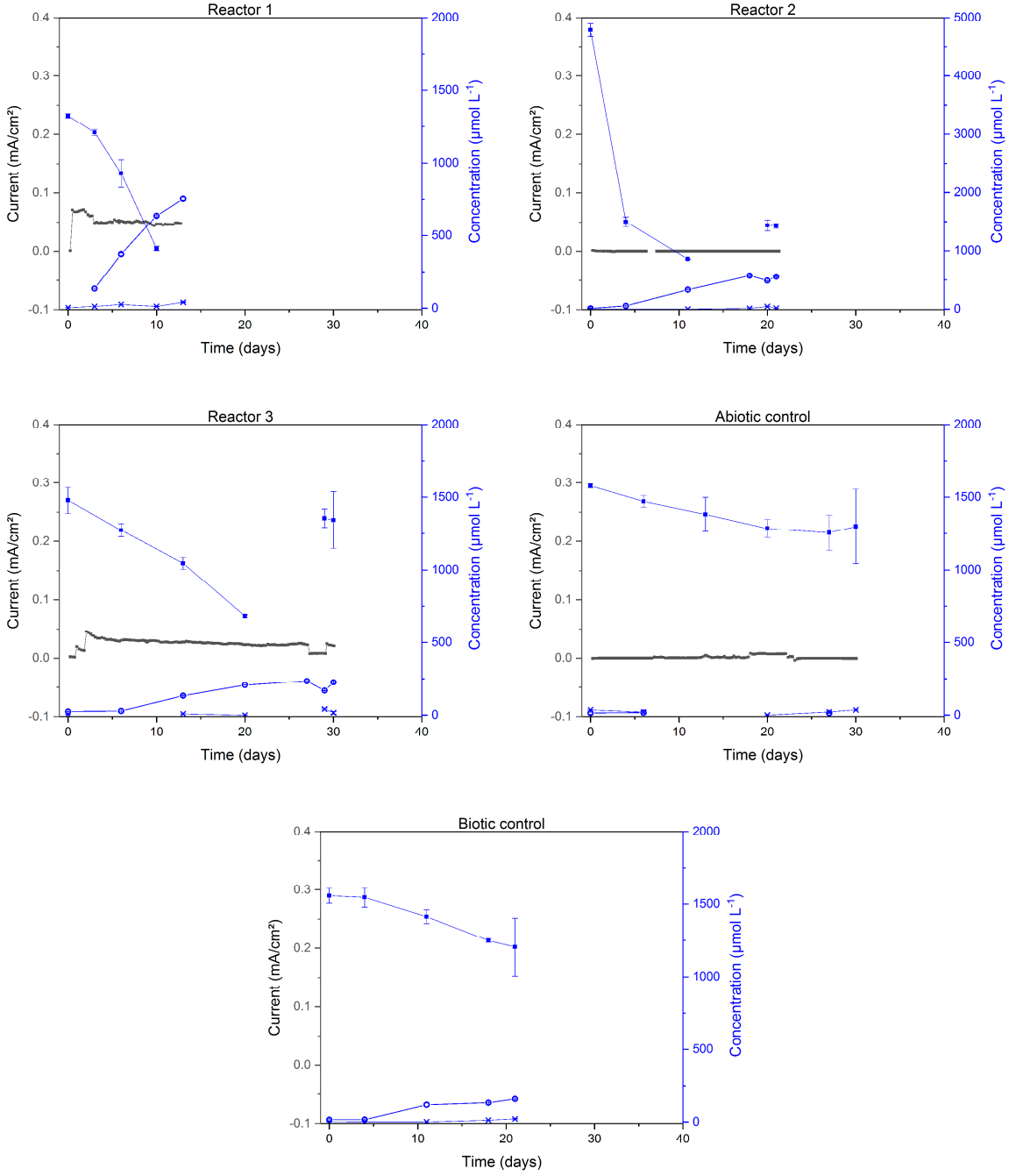

Figure 4.4.2-1 | Current densities (–▪–) and concentrations of ammonium (–▪–), nitrate (–○–), and nitrite (–×–) in batch BES. The anammox bacteria were added on day 5 and were cultivated for one, two, and three weeks, respectively. Mind the scale for reactor 2.

The ammonium was depleted after 13 days, 18 days and 27 days in reactor 1, 2 and 3, respectively. In reactors 2 and 3, ammonium was, therefore, added again to ensure continuous growth of the microbial community for further molecular studies.

However, nitrate was produced during the operation of the reactors reaching 753.9 µmol L^{-1}, 556.9 µmol L^{-1} and 225.6 µmol L^{-1} in reactors 1, 2 and 3, respectively, indicating active ammonium oxidation by AerAOB. The highest nitrite concentrations measured were 41.4 µmol L^{-1}, 45.0 µmol L^{-1} and 41.8 µmol L^{-1} in reactors 1, 2 and 3, respectively. Nevertheless, the sum of the nitrate and nitrite concentrations did not reach the initial ammonium concentration. This finding indicated that ammonia oxidation to elemental nitrogen was possibly carried out by AerAOB and anammox bacteria.

Ammonium oxidation took also place in the controls most likely due to the presence of low oxygen concentrations, though it was slower than in the main reactors. In the abiotic control 279.2 µmol ammonium L^{-1} were converted within 30 days and 352.1 µmol ammonium L^{-1} within 21 days were consumed in the biotic control. In the latter nitrate was also produced up to 175.5 µmol L^{-1}.

Current was measured in reactor 1 with about 0.05 mA cm^{-2} and between 0.00 mA cm^{-2} and 0.05 mA cm^{-2} in reactor 3, which were lower than in the currents measured in the reactor set 1. In reactor 2 and in the abiotic control, currents were measured only in µA cm^{-2} range.

4.4.3. Microbial community compositions for ammonium oxidation

As inoculums for the ammonium removal in batch BES, AerAOB and anammox bacteria were taken from currently running reactors treating wastewater. In Figure 4.4.3-1 the 50 most abundant genera are shown for both inoculums. The dominant asv in the AerAOB community belonged to the genera *Nitrospira* and *Candidatus* Nitrocosmicus. In the anammox inoculum, the most dominant asv were assigned to the genus *Candidatus* Kuenenia. Other main asv belonged to members of the genera *Ignavibacterium* and *Denitratisoma*.

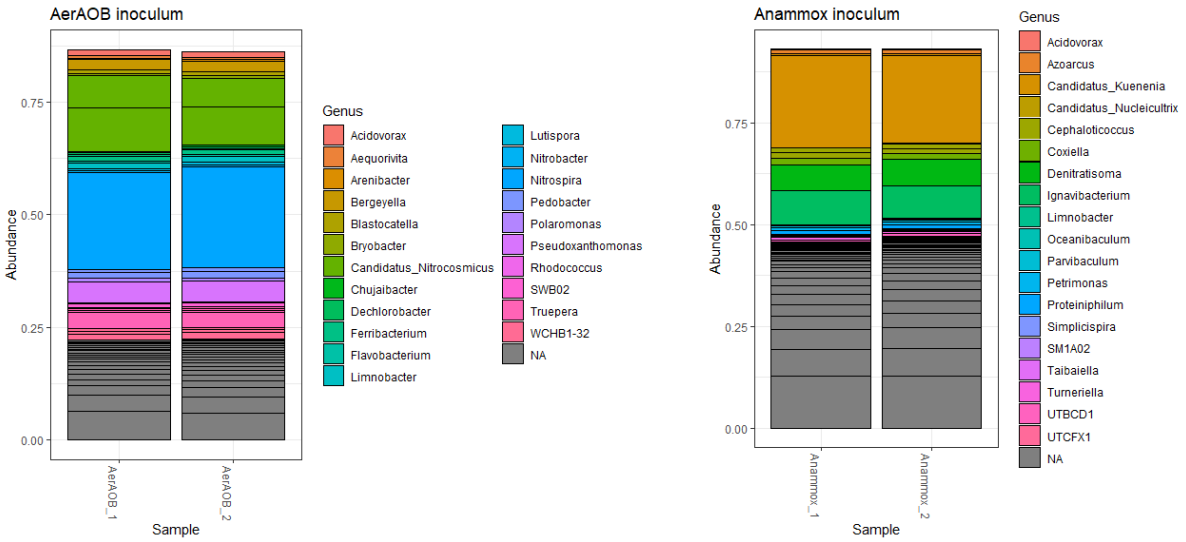

Figure 4.4.3-1 | Microbial community compositions of the enriched inoculums taken from currently running reactors for wastewater treatment. The 50 most abundant asv are visualized.

The 50 most abundant asv of all samples were analysed for ammonium oxidation in batch BES covering in average 60% to 70% of the total community compositions in each sample. Though, only 30% of the community composition was displayed in the medium of the biotic control.

In the batch reactors, the microbial community compositions showed different structures (Figure 4.4.3-2). While differences were expected between the community compositions on the anode and in the medium, there was no clear shift in compositions over time of incubation (from reactor 1 to reactor 3). In general, the community compositions were composed of several abundant genera. The predominant asv in reactor 1 belonged to the three genera *Hyphobmicrobium*, *Dechloromonas*, and *Azonexus*. In the medium, the most abundant asv were assigned to the genera *Pedobacter* and *Candidatus* Kuenenia. In reactor 2, the anode was colonized with asv belonging to *Dechloromonas*. Other asv assigned to the genera *Pseusoxanthomonas*, *Pseudomonas*, and *Anaerobacillus* became established as well, although, their abundances were lower than that of the genera *Dechloromonas*. In the medium of reactor 2, the predominant asv belonged to the genera *Nitrospira*, *Candidatus* Nitrocosmicus, and *Ferribacterium*. On the anode of reactor 3, asv assigned to the genus *Pseudomonas* became dominant. The community composition in the medium

did not show dominant asv but several asv that became established, for instance belonging to the genera *Pseudomonas*, Candidatus *Kuenenia*, and *Bergeyella*.

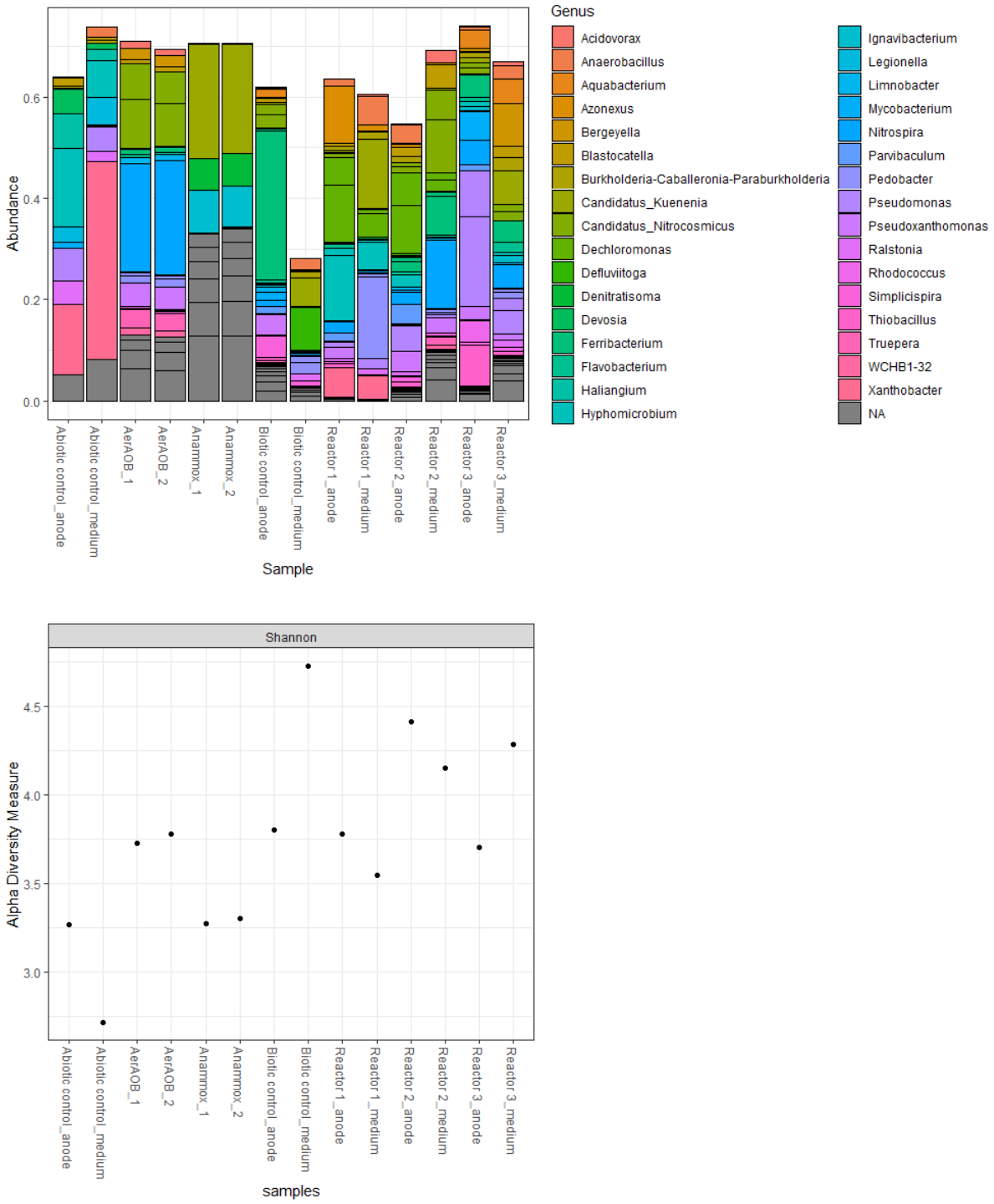

Figure 4.4.3-2 | Microbial community compositions (above) at the anode and in the medium of the reactors and the inoculum samples (AerAOB and anammox bacteria) and the alpha diversity shown as Shannon indices (below). The 50 most abundant genera of all samples are visualized for the community structures.

In the biotic control, asv assigned to the genus *Flavobacterium* became the most dominant member of the community on the anode. In the medium, however, the community composition seemed to be more diverse and the low coverage of the total community composition with only 30% did not allow adequate conclusions. Unfortunately, growth was also observed in the abiotic control. In the medium, asv assigned to the genus *Xanthobacter* were most dominant. On the anode, the community composition was made of several abundant genera, among them were *Xanthobacter* and *Hyphomicrobium*.

The diversity analysis showed Shannon indices (Figure 4.4.3-2) approximately between 2.7 (in the medium of the abiotic control) and 4.75 (in the medium of the biotic control). Enrichments of specific microorganisms on the anode or in the medium over time that would be indicated by decreasing indices from reactor 1 to reactor 3 were not observed.

To investigate the relationships between the community compositions a heatmap based on 100 asv was generated (Figure 4.4.3-3). Two clusters could be determined: First, the community compositions in the media of reactor 1, reactor 3, and the biotic control showed similar structures but the community in the medium of reactor 2 differed. The latter resembled the community composition in the inoculum of anammox bacteria. The second cluster could be made up by the community compositions on the anodes with applied voltage (all but the anode in the biotic control).

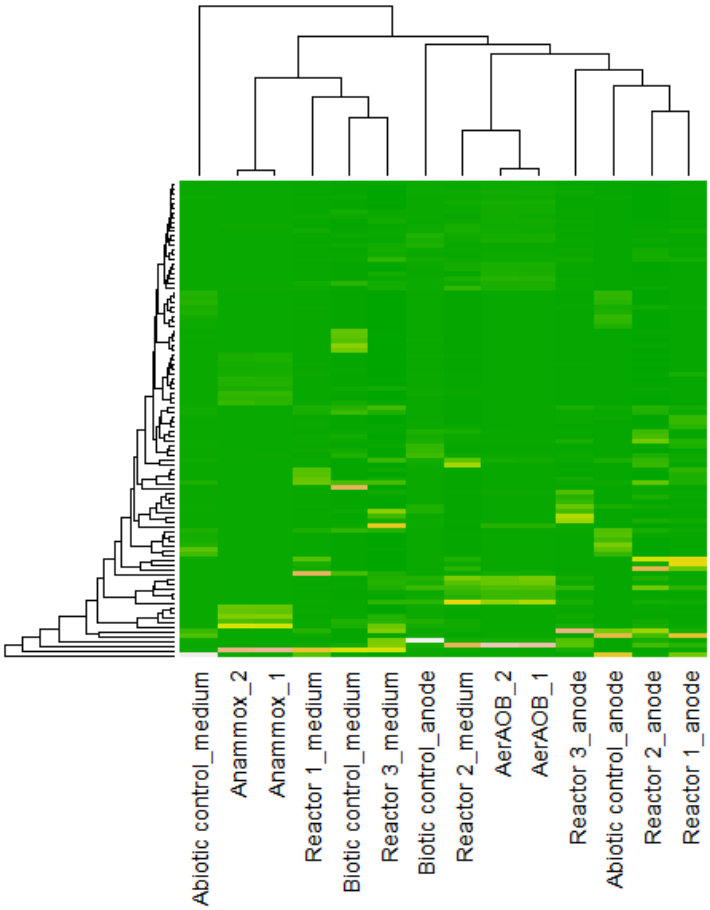

Figure 4.4.3-3 | Heatmap for the visualization of relationships between reactor samples from the anode material and from the medium obtained in batch BES for ammonium oxidation and the inoculum samples (AerAOB and anammox bacteria).

Furthermore, samples were investigated regarding the anammox bacteria (Figure 4.4.3-4). In the inoculum, only asv assigned to *Candidatus* Brocadia and *Candidatus* Kuenenia were detectable. While the presence of *Candidatus* Brocadia was almost neglectable (about 0.03% of the total community composition), *Candidatus* Kuenenia made up approximately 25% of the total community composition in the inoculum. The major asv of *Candidatus* Kuenenia (asv2) in the inoculum was also found in all reactor samples and the biotic control. The abundances were generally higher in the medium than on the related anode. The asv accounted for approximately 13%, 1%, 7%, and 6% of the total microbial community composition in the media of reactor 1, reactor 2, reactor 3, and the biotic control, respectively. The major asv of *Candidatus* Brocadia (asv697) was not detectable in the reactor samples or the controls. Another asv (*Candidatus* Brocadia asv1848), however, was detectable in the medium of reactor 2.

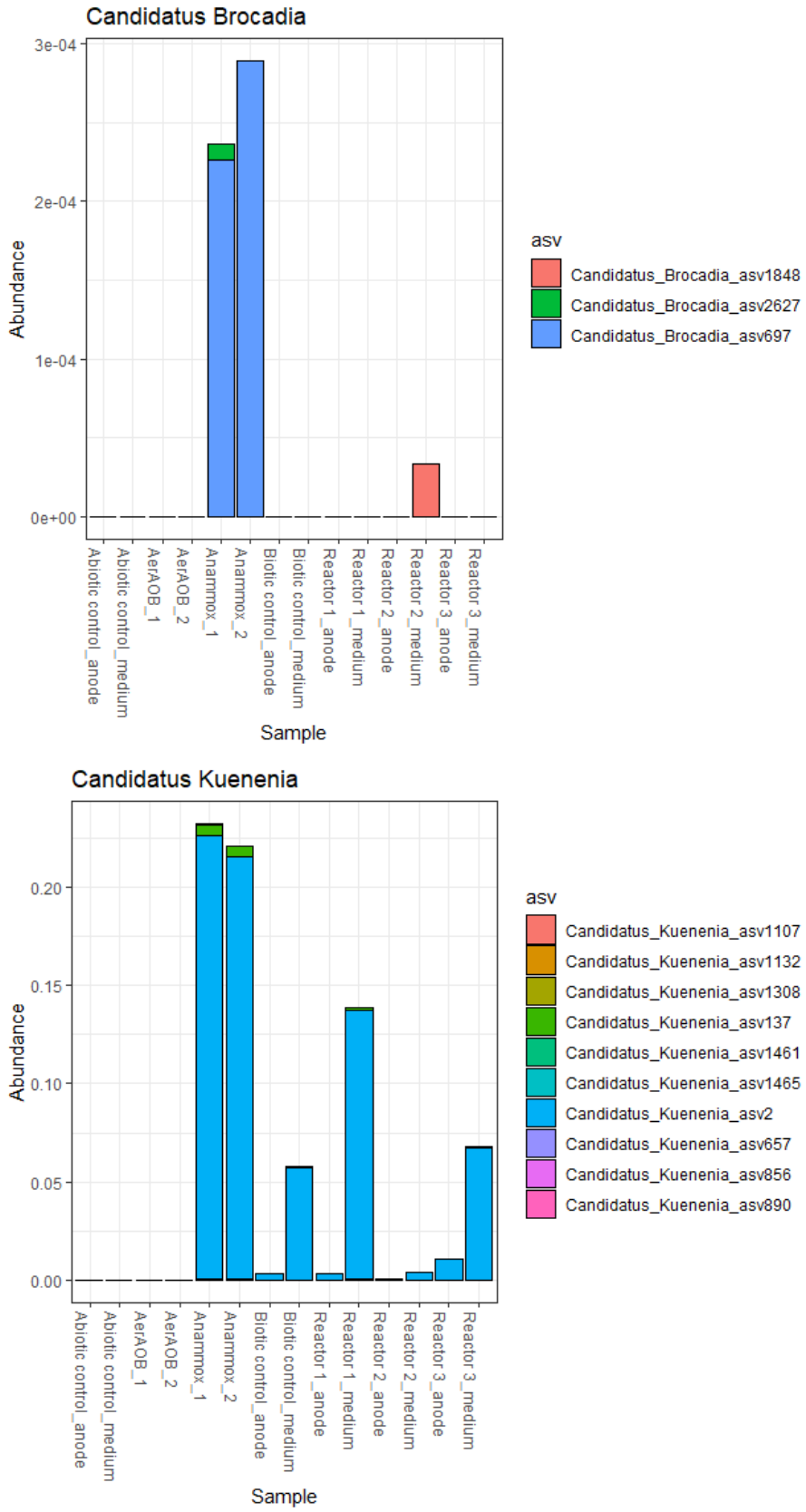

Figure 4.4.3-4 | The ten major asv assigned to the genera *Candidatus* Brocadia (above) and to *Candidatus* Kuenenia (below) in the batch BES for ammonium removal. Mind the scale.

4.5. Discussion

4.5.1. Oxygen evolution rates and the performance of BES systems

A low oxygen concentration is inevitable for ammonia removal when using nitrification and the anammox process in a BES. While the anammox process is inhibited by oxygen, the nitrification depends on its availability. In a BES, the oxygen evolution can be adjusted at the anode to a specified concentration by the applied potential to keep both reactions, nitrification and anammox, running.

The adjustment of oxygen evolution was easier to achieve in the upflow BES. Although, the system was continuously sparged with nitrogen/CO_2 gas resulting in oxygen losses with the gas outflow, the oxygen evolution rates obtained in the upflow BES showed low standard deviations. The reason why the upflow BES revealed a better performance than the batch system is the overall setup. In the upflow BES, the electrode surfaces as well as the membrane are approximately 9 times and 100 times larger, respectively, than in the batch BES. With increasing electrode surface area, the activation losses can be decreased, which arise from the electron transfer directly or indirectly from the bacterial cell to the electrode due to kinetic slowness of reactions (Logan *et al.*, 2006). Additionally, the energy used for biological catalysed reactions has to be considered, which are determined by the amount of catalysing microorganisms relative to the available electrode surface area, the electron transfer rate as well as the biological activity of the microbial community (Clauwaert *et al.*, 2008). The activation losses are the main overpotentials present in the system in low current densities ranges (Freguia *et al.*, 2008). Low current densities were also measured in all batch reactors in this study. A higher potential of approximately 0.875 V vs. Ag/AgCl was set to the batch reactors in contrast to the upflow system (about 0.725 V vs. Ag/AgCl) to generate oxygen. This overvoltage that had to be applied to the batch reactors indicates the presence of those losses.

Moreover, the electrodes and the membrane are put together in close spatial proximity. The spatial distances between the electrodes and the membrane in the upflow BES are very narrow with 1 mm due to the rubber sheets used for sealing the system. In the batch systems, the spatial distances of the electrodes and the

membrane can be several centimetres and vary from reactor to reactor. The spacing between the electrodes is responsible for ohmic losses in a system because of the long travel distance of electrons through the electrolytes (Logan *et al.*, 2006). The ohmic losses can also be reduced, when electrolytes with increased conductivity are applied. Since waste waters show high conductivities and the spacing between the electrodes were narrow, we can assume that ohmic losses do not play a pivotal role in the upflow BES. However, in the batch BES the ohmic losses have to be further investigated, when they are used for microbial enrichment studies.

Oxygen was not measured directly at the anode but at the glass frame. This means that the oxygen originally production cannot be determined and has to be considered as the residual oxygen concentration, which dissolved from the anode into the medium. The oxygen concentration was measured in the medium because the concentration was most crucial there due to the oxygen sensitivity of the anammox bacteria.

The findings show that the upflow BES is a suitable application for ammonium removal via nitrification and the anammox process. The oxygen concentrations can be adjusted relative precisely. Future studies should also focus on the activation losses and the ohmic losses in the systems since they will determine the overall activity of the BES.

4.5.2. Ammonium removal in batch reactors

Ammonium was constantly converted in all three reactors. However, nitrate was also produced indicating that the anammox process was not successful. This can be explained by the enrichment procedure. To establish a preliminary biofilm on the anode, AerAOB were enriched before adding the anammox bacteria. The time frame of seven days might have been too long. It seems that a microbial community was formed, which converted the ammonium to elemental nitrogen with nitrate as accumulating side product in the absence of anammox bacteria. This assumption can be underlined with the diversity of the samples. The Shannon index of the AerAOB inoculum was approximately 3.75 indicating that the inoculum was already enriched to a competent ammonium oxidising microbial community.

The diversities of the samples taken from the BES were slightly higher (between 3.5 and 4.5) than in the inoculums. This was expected due to the fact that two microbial communities, the AerAOB and the anammox community were combined. However, the Shannon indices seem to increase over time (from reactor 1 to reactor 3). This leads to the assumption that a competent microbial community composition consisting of AerAOB and anammox bacteria could not have been established in these few weeks. The precondition of the anode with a single strain or several nitrifying strains for the oxidation of ammonium to nitrite might overcome this problem. The precondition then might take less than a week.

In the community compositions obtained in this study, one main genus capable of ammonium oxidation, namely *Nitrospira*, was detected. This genus was also reported to be capable of complete ammonium oxidation to elemental nitrogen (Daims *et al.*, 2015). This finding additionally supports the assumption stated above that ammonium and nitrite are converted by this genus instead of anammox bacteria. Several genera, however, were found as predominant members that were capable of using nitrate as electron acceptor such as *Pseudomonas* (Palleroni, 2015), *Dechloromonas* (Coates *et al.*, 2001, Horn *et al.*, 2005), *Azonexus* (Quan *et al.*, 2006), and *Pseudoxanthomonas* (Yang *et al.*, 2005). Therefore, the produced nitrite or nitrate can also be converted to elemental nitrogen or ammonium by denitrification or dissimilatory nitrate reduction. Interestingly, nitrate accumulated in the reactors over time. This finding indicates that the relative abundance of a strain might not necessarily correspond with its activity in bioelectrochemical systems.

As anammox bacterium, *Candidatus* Kuenenia has been found in the medium (approximately 13% and 7% of the total community composition in reactor 1 and reactor 3, respectively) showing that ammonium is also anaerobically oxidised. The presence of *Candidatus* Kuenenia in the medium indicates that the oxygen concentration at the anode might have been too high for acceptable accumulation in the biofilm. Nevertheless, asv assigned to this genus were detected in the anode communities in low abundances as well. The results show that preconditioning of the anode with AerAOB for a preliminary biofilm and the subsequent accumulation of anammox bacteria are achievable. Future studies may address the optimization of

several parameters such as oxygen evolution rates at the anode. The studies should especially focus on the pre-conditioning of the anode.

Slow ammonium removal was additionally observed in the controls. While ammonium might have consumed by AerAOB and anammox bacteria using residual dissolved oxygen in the biotic control, in the abiotic control ammonium oxidation might have happened also abiotically. However, the presence of bacterial asv in the abiotic control indicates additional biotic ammonium conversion. Interestingly, asv assigned to the genus *Xanthobacter*, a nitrogen-fixing genus was the dominant genus in the medium of the abiotic control. The genus also comprises bacteria described as hydrogen oxidiser (Knallgas bacteria), which produce water from elemental hydrogen and oxygen (Wiegel, 2006). This means that hydrogen is not only present as H^+ deriving from the electrolysis reaction but also as H_2, which is produced due to the high applied potential of 0.95 V vs. Ag/AgCl (Larminie *et al.*, 2003).

Despite the drawbacks concerning the enrichment of nitrifying and anammox bacteria in an oxygen generating BES, this study reveals the potential of such a system in contrast to currently systems in use. In the BES, the nitrification can be steered by adjusting the oxygen evolution rate at the anode leading to an optimized ammonium removal from wastewater.

4.6. **Appendix**

Table 4.5.2-1 | Oxygen concentrations measured in batch BES (A, B and C; manually once per half an hour) and oxygen concentrations calculated in upflow BES (D; concentrations measured continuously once per ten seconds and averaged per hour).

A

850 mV				
Time hours	c [O2] µg L^{-1} h^{-1} Reactor 1	c [O2] µg L^{-1} h^{-1} Reactor 2	c [O2] µg L^{-1} h^{-1} Reactor 3	c [O2] µg L^{-1} h^{-1} Reactor 4
0	10	7	9	5
0.5	11	6	10	6
1				
1.5				
2				
2.5	19	6	10	6
3	19	6	10	6
3.5				
4	20	6	10	6
4.5	19	6	9	6
5	19	6	9	6
5.5	17	6	9	6
6				
6.5				
7				
7.5				
8				

B

875 mV				
Time hours	c [O2] µg L^{-1} h^{-1} Reactor 1	c [O2] µg L^{-1} h^{-1} Reactor 2	c [O2] µg L^{-1} h^{-1} Reactor 3	c [O2] µg L^{-1} h^{-1} Reactor 4
0	10	6	9	6
0.5				
1				
1.6	36	7	22	6
2	43	6	23	6
2.5	47	6	28	6
3	51	6	28	6
3.5	63	6	25	6
4	60	6	25	6
4.5	69	6	23	6
5	72	6	21	6
5.5	70	6	23	6
6	66	7	17	6
6.5	68	7	15	6
7	57	7	14	6
7.5	58	6	13	6
8	55	7	12	6

C

900 mV				
Time hours	c [O2] µg L^{-1} h^{-1} Reactor 1	c [O2] µg L^{-1} h^{-1} Reactor 2	c [O2] µg L^{-1} h^{-1} Reactor 3	c [O2] µg L^{-1} h^{-1} Reactor 4
0	10	6	9	6
0.5	14	11	10	6
1	34	16	12	6
1.5	58	18	18	6
2	78	19	34	6
2.5	92	18	43	6
3	110	17	51	6
3.5	119	16	58	6
4	130	14	58	6
4.5	134	11	58	6
5	135	11	54	6
5.5	140	8	52	6
6	144	8	46	6
6.5	144	7	47	6
7	146	7	45	6
7.5	154	7	43	6
8	145	7	35	6

D

Potential V vs. Ag/Ag	Oxygen concentrations µg L^{-1} h^{-1} Run 1	µg L^{-1} h^{-1} Run 2	µg L^{-1} h^{-1} Run 3
0.700	0.01404		0
0.725	0.0091	0.02332	
0.750	0.01283	0	0.1364
0.775	0.1132	0.43534	0.2846
0.800	0.66623	0.64336	0.56719
0.825			1.02639

Table 4.5.2-2 | Raw data of currents of Reactor 1 and the abiotic control measured in batch BES.

Time s	Current A Reactor 1	Current A Abiotic control	Time h	Time days	Current mA/cm² Reactor 1	Current mA/cm² Abiotic control
21600	1.09E-05	-3.18E-06	6.00E+00	2.50E-01	2.19E-03	-6.36E-04
21600	8.85E-06	-2.61E-06	1.20E+01	5.00E-01	1.77E-03	-5.22E-04
21600	8.18E-06	-1.98E-06	1.80E+01	7.50E-01	1.64E-03	-3.96E-04
21600	9.70E-05	-3.21E-07	2.40E+01	1.00E+00	1.94E-02	-6.41E-05
21600	7.77E-05	-7.45E-07	3.00E+01	1.25E+00	1.55E-02	-1.49E-04
21600	6.90E-05	-7.26E-07	3.60E+01	1.50E+00	1.38E-02	-1.45E-04
21600	6.52E-05	-6.34E-07	4.20E+01	1.75E+00	1.30E-02	-1.27E-04
7200	6.34E-05	-6.29E-07	4.40E+01	1.83E+00	1.27E-02	-1.26E-04
21600	2.28E-04	-3.20E-07	5.00E+01	2.08E+00	4.55E-02	-6.40E-05
21600	2.17E-04	-5.55E-07	5.60E+01	2.33E+00	4.34E-02	-1.11E-04
21600	2.03E-04	-5.99E-07	6.20E+01	2.58E+00	4.06E-02	-1.20E-04
21600	1.90E-04	-6.07E-07	6.80E+01	2.83E+00	3.80E-02	-1.21E-04
21600	1.77E-04	-6.05E-07	7.40E+01	3.08E+00	3.54E-02	-1.21E-04
21600	1.69E-04	-6.25E-07	8.00E+01	3.33E+00	3.37E-02	-1.25E-04
21600	1.68E-04	-6.13E-07	8.60E+01	3.58E+00	3.35E-02	-1.23E-04
21600	1.73E-04	-5.66E-07	9.20E+01	3.83E+00	3.46E-02	-1.13E-04
21600	1.68E-04	-5.98E-07	9.80E+01	4.08E+00	3.35E-02	-1.20E-04
21600	1.58E-04	-6.04E-07	1.04E+02	4.33E+00	3.16E-02	-1.21E-04
21600	1.56E-04	-5.97E-07	1.10E+02	4.58E+00	3.12E-02	-1.19E-04
21600	1.57E-04	-5.89E-07	1.16E+02	4.83E+00	3.14E-02	-1.18E-04
21600	1.54E-04	-5.90E-07	1.22E+02	5.08E+00	3.08E-02	-1.18E-04
21600	1.50E-04	-5.98E-07	1.28E+02	5.33E+00	2.99E-02	-1.20E-04
21600	1.45E-04	-5.75E-07	1.34E+02	5.58E+00	2.90E-02	-1.15E-04
14400	1.43E-04	-5.90E-07	1.38E+02	5.75E+00	2.85E-02	-1.18E-04
7200	1.44E-04	-5.74E-07	1.40E+02	5.83E+00	2.88E-02	-1.15E-04
21600	1.51E-04	-5.38E-07	1.46E+02	6.08E+00	3.02E-02	-1.08E-04
21600	1.54E-04	-5.26E-07	1.52E+02	6.33E+00	3.09E-02	-1.05E-04
21600	1.56E-04	-5.61E-07	1.58E+02	6.58E+00	3.11E-02	-1.12E-04
21600	1.53E-04	-3.64E-07	1.64E+02	6.83E+00	3.06E-02	-7.27E-05
12600	1.52E-04	1.41E-06	1.68E+02	6.98E+00	3.04E-02	2.82E-04
21600	1.50E-04	8.16E-06	1.74E+02	7.23E+00	3.00E-02	1.63E-03
21600	1.50E-04	5.77E-06	1.80E+02	7.48E+00	3.01E-02	1.15E-03
21600	1.48E-04	6.69E-06	1.86E+02	7.73E+00	2.97E-02	1.34E-03
21600	1.46E-04	8.24E-06	1.92E+02	7.98E+00	2.93E-02	1.65E-03
21600	1.48E-04	6.71E-06	1.98E+02	8.23E+00	2.96E-02	1.34E-03
21600	1.49E-04	8.03E-07	2.04E+02	8.48E+00	2.97E-02	1.61E-04
21600	1.46E-04	1.19E-06	2.10E+02	8.73E+00	2.91E-02	2.39E-04
9000	1.43E-04	1.38E-06	2.12E+02	8.83E+00	2.86E-02	2.76E-04
7200	1.33E-04	1.66E-06	2.14E+02	8.92E+00	2.66E-02	3.32E-04
7200	1.41E-04	1.63E-06	2.16E+02	9.00E+00	2.82E-02	3.26E-04
21600	1.47E-04	1.97E-06	2.22E+02	9.25E+00	2.93E-02	3.95E-04
21600	1.48E-04	2.69E-06	2.28E+02	9.50E+00	2.96E-02	5.38E-04
21600	1.47E-04	2.32E-06	2.34E+02	9.75E+00	2.95E-02	4.65E-04
21600	1.45E-04	2.19E-06	2.40E+02	1.00E+01	2.90E-02	4.38E-04
21600	1.42E-04	8.70E-07	2.46E+02	1.03E+01	2.83E-02	1.74E-04
21600	1.33E-04	1.56E-06	2.52E+02	1.05E+01	2.66E-02	3.12E-04
21600	1.34E-04	8.41E-07	2.58E+02	1.08E+01	2.68E-02	1.68E-04
21600	1.37E-04	1.54E-06	2.64E+02	1.10E+01	2.74E-02	3.08E-04
21600	1.34E-04	2.15E-06	2.70E+02	1.13E+01	2.69E-02	4.30E-04
21600	1.31E-04	2.78E-06	2.76E+02	1.15E+01	2.62E-02	5.56E-04
21600	1.31E-04	2.78E-06	2.82E+02	1.18E+01	2.62E-02	5.56E-04
21600	1.34E-04	2.55E-06	2.88E+02	1.20E+01	2.68E-02	5.11E-04
21600	1.36E-04	3.43E-06	2.94E+02	1.23E+01	2.72E-02	6.85E-04
21600	1.32E-04	4.33E-06	3.00E+02	1.25E+01	2.63E-02	8.66E-04
21600	1.32E-04	1.24E-05	3.06E+02	1.28E+01	2.63E-02	2.47E-03
21600	1.34E-04	2.39E-05	3.12E+02	1.30E+01	2.69E-02	4.77E-03
12600	1.34E-04	1.93E-05	3.16E+02	1.31E+01	2.69E-02	3.85E-03
21600	1.41E-04	1.16E-05	3.22E+02	1.34E+01	2.82E-02	2.32E-03

Table 4.6-3 | continued

Time s	Current A Reactor 1	Current A Abiotic control	Time h	Time days	Current mA/cm² Reactor 1	Current mA/cm² Abiotic control
21600	1.38E-04	5.32E-06	3.28E+02	1.36E+01	2.76E-02	1.06E-03
21600	1.36E-04	4.04E-06	3.34E+02	1.39E+01	2.72E-02	8.08E-04
21600	1.32E-04	6.39E-06	3.40E+02	1.41E+01	2.64E-02	1.28E-03
21600	1.32E-04	7.23E-06	3.46E+02	1.44E+01	2.63E-02	1.45E-03
21600	1.30E-04	5.30E-06	3.52E+02	1.46E+01	2.60E-02	1.06E-03
21600	1.32E-04	6.40E-06	3.58E+02	1.49E+01	2.63E-02	1.28E-03
21600	1.29E-04	1.38E-05	3.64E+02	1.51E+01	2.58E-02	2.76E-03
14400	1.27E-04	3.27E-06	3.68E+02	1.53E+01	2.55E-02	6.55E-04
21600	1.26E-04	1.70E-06	3.74E+02	1.56E+01	2.52E-02	3.39E-04
21600	1.29E-04	2.62E-06	3.80E+02	1.58E+01	2.59E-02	5.24E-04
21600	1.29E-04	5.14E-06	3.86E+02	1.61E+01	2.57E-02	1.03E-03
14400	1.27E-04	1.65E-05	3.90E+02	1.62E+01	2.54E-02	3.30E-03
21600	1.24E-04	4.55E-06	3.96E+02	1.65E+01	2.48E-02	9.09E-04
21600	1.25E-04	9.43E-06	4.02E+02	1.67E+01	2.50E-02	1.89E-03
21600	1.25E-04	3.52E-06	4.08E+02	1.70E+01	2.50E-02	7.03E-04
21600	1.23E-04	1.45E-06	4.14E+02	1.72E+01	2.46E-02	2.90E-04
10800	1.19E-04	1.57E-06	4.17E+02	1.74E+01	2.39E-02	3.13E-04
21600	1.16E-04	2.95E-06	4.23E+02	1.76E+01	2.32E-02	5.90E-04
21600	1.16E-04	9.59E-06	4.29E+02	1.79E+01	2.32E-02	1.92E-03
21600	1.20E-04	4.07E-05	4.35E+02	1.81E+01	2.41E-02	8.15E-03
21600	1.23E-04	3.38E-05	4.41E+02	1.84E+01	2.47E-02	6.77E-03
21600	1.22E-04	3.40E-05	4.47E+02	1.86E+01	2.44E-02	6.79E-03
21600	1.21E-04	3.76E-05	4.53E+02	1.89E+01	2.43E-02	7.52E-03
21600	1.22E-04	3.85E-05	4.59E+02	1.91E+01	2.44E-02	7.69E-03
21600	1.21E-04	3.95E-05	4.65E+02	1.94E+01	2.42E-02	7.91E-03
21600	1.17E-04	3.96E-05	4.71E+02	1.96E+01	2.35E-02	7.92E-03
21600	1.13E-04	3.71E-05	4.77E+02	1.99E+01	2.25E-02	7.43E-03
21600	1.12E-04	3.43E-05	4.83E+02	2.01E+01	2.24E-02	6.85E-03
21600	1.13E-04	3.51E-05	4.89E+02	2.04E+01	2.27E-02	7.02E-03
21600	1.10E-04	3.44E-05	4.95E+02	2.06E+01	2.21E-02	6.89E-03
21600	1.07E-04	3.41E-05	5.01E+02	2.09E+01	2.14E-02	6.82E-03
21600	1.08E-04	3.68E-05	5.07E+02	2.11E+01	2.17E-02	7.35E-03
21600	1.06E-04	3.63E-05	5.13E+02	2.14E+01	2.11E-02	7.26E-03
21600	1.06E-04	3.54E-05	5.19E+02	2.16E+01	2.12E-02	7.09E-03
21600	1.04E-04	3.59E-05	5.25E+02	2.19E+01	2.08E-02	7.17E-03
21600	1.07E-04	3.82E-05	5.31E+02	2.21E+01	2.15E-02	7.64E-03
21600	1.06E-04	6.42E-06	5.37E+02	2.24E+01	2.12E-02	1.28E-03
21600	1.15E-04	1.35E-05	5.43E+02	2.26E+01	2.30E-02	2.70E-03
21600	1.11E-04	1.01E-05	5.49E+02	2.29E+01	2.22E-02	2.01E-03
21600	1.13E-04	-1.87E-05	5.55E+02	2.31E+01	2.25E-02	-3.74E-03
3600	1.13E-04	-1.92E-05	5.56E+02	2.31E+01	2.26E-02	-3.84E-03
21600	1.12E-04	-5.68E-06	5.62E+02	2.34E+01	2.24E-02	-1.14E-03
21600	1.09E-04	-3.02E-06	5.68E+02	2.36E+01	2.17E-02	-6.05E-04
21600	1.09E-04	-2.20E-06	5.74E+02	2.39E+01	2.17E-02	-4.41E-04
21600	1.10E-04	-1.95E-06	5.80E+02	2.41E+01	2.20E-02	-3.90E-04
21600	1.10E-04	-1.87E-06	5.86E+02	2.44E+01	2.20E-02	-3.75E-04
21600	1.08E-04	-1.79E-06	5.92E+02	2.46E+01	2.16E-02	-3.58E-04
21600	1.12E-04	-1.80E-06	5.98E+02	2.49E+01	2.24E-02	-3.60E-04
21600	1.17E-04	-1.70E-06	6.04E+02	2.51E+01	2.34E-02	-3.39E-04
21600	1.18E-04	-1.69E-06	6.10E+02	2.54E+01	2.36E-02	-3.39E-04
21600	1.18E-04	-1.94E-06	6.16E+02	2.56E+01	2.36E-02	-3.88E-04
21600	1.20E-04	-1.79E-06	6.22E+02	2.59E+01	2.40E-02	-3.58E-04
21600	1.24E-04	-1.82E-06	6.28E+02	2.61E+01	2.48E-02	-3.65E-04
21600	1.23E-04	-2.06E-06	6.34E+02	2.64E+01	2.46E-02	-4.12E-04
21600	1.18E-04	-2.19E-06	6.40E+02	2.66E+01	2.35E-02	-4.39E-04
21600	1.13E-04	-2.41E-06	6.46E+02	2.69E+01	2.26E-02	-4.82E-04
18000	1.12E-04	-2.40E-06	6.51E+02	2.71E+01	2.23E-02	-4.80E-04
21600	3.77E-05	-2.57E-06	6.57E+02	2.74E+01	7.54E-03	-5.15E-04
21600	3.89E-05	-2.58E-06	6.63E+02	2.76E+01	7.79E-03	-5.16E-04

Table 4.6-3 | continued

Time s	Current A Reactor 1	Current A Abiotic control	Time h	Time days	Current mA/cm² Reactor 1	Current mA/cm² Abiotic control
21600	3.97E-05	-2.66E-06	6.69E+02	2.79E+01	7.95E-03	-5.32E-04
21600	3.88E-05	-2.71E-06	6.75E+02	2.81E+01	7.76E-03	-5.43E-04
21600	3.99E-05	-2.60E-06	6.81E+02	2.84E+01	7.98E-03	-5.19E-04
21600	3.97E-05	-2.91E-06	6.87E+02	2.86E+01	7.94E-03	-5.81E-04
21600	3.98E-05	-2.96E-06	6.93E+02	2.89E+01	7.97E-03	-5.91E-04
21600	3.91E-05	-3.00E-06	6.99E+02	2.91E+01	7.81E-03	-6.00E-04
14400	1.21E-04	-3.14E-06	7.03E+02	2.93E+01	2.43E-02	-6.29E-04
21600	1.10E-04	-3.17E-06	7.09E+02	2.95E+01	2.21E-02	-6.33E-04
21600	1.08E-04	-3.14E-06	7.15E+02	2.98E+01	2.15E-02	-6.28E-04
21600	1.03E-04	-3.28E-06	7.21E+02	3.00E+01	2.06E-02	-6.56E-04
5400	1.02E-04	-3.54E-06	7.22E+02	3.01E+01	2.05E-02	-7.08E-04

Table 4.5.2-3 | Raw data of currents of Reactor 2 measured in batch BES.

Time s	Current A Reactor 2	Time h	Time days	Current mA/cm² Reactor 2
21600	6.35E-06	6.00E+00	2.50E-01	1.27E-03
21600	3.16E-06	1.20E+01	5.00E-01	6.32E-04
21600	1.30E-06	1.80E+01	7.50E-01	2.60E-04
21600	1.10E-06	2.40E+01	1.00E+00	2.21E-04
21600	4.38E-07	3.00E+01	1.25E+00	8.76E-05
21600	-1.26E-07	3.60E+01	1.50E+00	-2.52E-05
21600	2.43E-07	4.20E+01	1.75E+00	4.86E-05
21600	-4.03E-08	4.80E+01	2.00E+00	-8.07E-06
21600	-3.21E-07	5.40E+01	2.25E+00	-6.42E-05
21600	-2.80E-06	6.00E+01	2.50E+00	-5.60E-04
21600	-2.80E-06	6.60E+01	2.75E+00	-5.60E-04
21600	-7.60E-07	7.20E+01	3.00E+00	-1.52E-04
21600	-5.51E-07	7.80E+01	3.25E+00	-1.10E-04
21600	-7.85E-07	8.40E+01	3.50E+00	-1.57E-04
21600	-8.71E-07	9.00E+01	3.75E+00	-1.74E-04
21600	-1.28E-06	9.60E+01	4.00E+00	-2.55E-04
12600	-5.97E-07	9.95E+01	4.15E+00	-1.19E-04
21600	-5.41E-07	1.06E+02	4.40E+00	-1.08E-04
21600	-5.44E-07	1.12E+02	4.65E+00	-1.09E-04
21600	-5.40E-07	1.18E+02	4.90E+00	-1.08E-04
21600	-5.07E-07	1.24E+02	5.15E+00	-1.01E-04
21600	-5.26E-07	1.30E+02	5.40E+00	-1.05E-04
21600	-5.28E-07	1.36E+02	5.65E+00	-1.06E-04
21600	-5.54E-07	1.42E+02	5.90E+00	-1.11E-04
21600	-5.12E-07	1.48E+02	6.15E+00	-1.02E-04
14400	-5.74E-07	1.52E+02	6.31E+00	-1.15E-04
86400		1.76E+02	7.31E+00	
14400	-5.82E-07	1.80E+02	7.48E+00	-1.16E-04
21600	-5.48E-07	1.86E+02	7.73E+00	-1.10E-04
21600	-5.46E-07	1.92E+02	7.98E+00	-1.09E-04
21600	-5.53E-07	1.98E+02	8.23E+00	-1.11E-04
21600	-5.78E-07	2.04E+02	8.48E+00	-1.16E-04
10800	-6.01E-07	2.07E+02	8.60E+00	-1.20E-04
21600	-5.30E-07	2.13E+02	8.85E+00	-1.06E-04
21600	-4.90E-07	2.19E+02	9.10E+00	-9.81E-05
21600	-5.09E-07	2.25E+02	9.35E+00	-1.02E-04
21600	-4.86E-07	2.31E+02	9.60E+00	-9.73E-05
21600	-5.51E-07	2.37E+02	9.85E+00	-1.10E-04
21600	-5.04E-07	2.43E+02	1.01E+01	-1.01E-04
21600	-5.06E-07	2.49E+02	1.04E+01	-1.01E-04
21600	-5.10E-07	2.55E+02	1.06E+01	-1.02E-04

Table 4.6-4 | continued

Time s	Current A Reactor 2	Time h	Time days	Current mA/cm² Reactor 2
21600	-5.48E-07	2.61E+02	1.09E+01	-1.10E-04
21600	-5.25E-07	2.67E+02	1.11E+01	-1.05E-04
21600	-5.06E-07	2.73E+02	1.14E+01	-1.01E-04
21600	-5.82E-07	2.79E+02	1.16E+01	-1.16E-04
21600	-4.26E-07	2.85E+02	1.19E+01	-8.51E-05
21600	-5.56E-07	2.91E+02	1.21E+01	-1.11E-04
21600	-5.19E-07	2.97E+02	1.24E+01	-1.04E-04
21600	-5.57E-07	3.03E+02	1.26E+01	-1.11E-04
21600	-3.36E-07	3.09E+02	1.29E+01	-6.72E-05
21600	-4.69E-07	3.15E+02	1.31E+01	-9.39E-05
21600	-4.92E-07	3.21E+02	1.34E+01	-9.83E-05
21600	-6.94E-07	3.27E+02	1.36E+01	-1.39E-04
21600	-5.21E-07	3.33E+02	1.39E+01	-1.04E-04
21600	-5.10E-07	3.39E+02	1.41E+01	-1.02E-04
21600	-4.60E-07	3.45E+02	1.44E+01	-9.19E-05
3600	-4.44E-07	3.46E+02	1.44E+01	-8.88E-05
21600	-5.67E-07	3.52E+02	1.46E+01	-1.13E-04
21600	-5.22E-07	3.58E+02	1.49E+01	-1.04E-04
21600	-5.47E-07	3.64E+02	1.51E+01	-1.09E-04
21600	-5.46E-07	3.70E+02	1.54E+01	-1.09E-04
21600	-5.82E-07	3.76E+02	1.56E+01	-1.16E-04
21600	-5.16E-07	3.82E+02	1.59E+01	-1.03E-04
21600	-5.18E-07	3.88E+02	1.61E+01	-1.04E-04
21600	-5.07E-07	3.94E+02	1.64E+01	-1.01E-04
21600	-5.57E-07	4.00E+02	1.66E+01	-1.11E-04
21600	-5.59E-07	4.06E+02	1.69E+01	-1.12E-04
21600	-5.34E-07	4.12E+02	1.71E+01	-1.07E-04
21600	-6.89E-07	4.18E+02	1.74E+01	-1.38E-04
21600	-8.24E-07	4.24E+02	1.76E+01	-1.65E-04
21600	-8.99E-07	4.30E+02	1.79E+01	-1.80E-04
21600	-9.98E-07	4.36E+02	1.81E+01	-2.00E-04
18000	-1.01E-06	4.41E+02	1.84E+01	-2.02E-04
21600	-9.99E-07	4.47E+02	1.86E+01	-2.00E-04
21600	-9.79E-07	4.53E+02	1.89E+01	-1.96E-04
21600	-1.02E-06	4.59E+02	1.91E+01	-2.04E-04
21600	-1.07E-06	4.65E+02	1.94E+01	-2.14E-04
21600	-1.08E-06	4.71E+02	1.96E+01	-2.15E-04
21600	-1.12E-06	4.77E+02	1.99E+01	-2.24E-04
21600	-1.18E-06	4.83E+02	2.01E+01	-2.36E-04
21600	-1.25E-06	4.89E+02	2.04E+01	-2.50E-04
14400	-1.27E-06	4.93E+02	2.05E+01	-2.54E-04
21600	-9.81E-07	4.99E+02	2.08E+01	-1.96E-04
21600	-7.97E-07	5.05E+02	2.10E+01	-1.59E-04
21600	-7.62E-07	5.11E+02	2.13E+01	-1.52E-04
5400	-7.38E-07	5.12E+02	2.13E+01	-1.48E-04

Table 4.5.2-4 | Raw data of currents of Reactor 3 measured in batch BES.

Time s	Current A Reactor 3	Time h	Time days	Current mA/cm² Reactor 2
21600	2.95E-06	6.00E+00	2.50E-01	5.90E-04
21600	3.55E-04	1.20E+01	5.00E-01	7.09E-02
21600	3.38E-04	1.80E+01	7.50E-01	6.76E-02
21600	3.37E-04	2.40E+01	1.00E+00	6.74E-02
21600	3.45E-04	3.00E+01	1.25E+00	6.89E-02
21600	3.52E-04	3.60E+01	1.50E+00	7.04E-02
21600	3.56E-04	4.20E+01	1.75E+00	7.12E-02
21600	3.37E-04	4.80E+01	2.00E+00	6.74E-02
21600	3.13E-04	5.40E+01	2.25E+00	6.26E-02
21600	3.02E-04	6.00E+01	2.50E+00	6.04E-02
21600	3.03E-04	6.60E+01	2.75E+00	6.06E-02
21600	2.42E-04	7.20E+01	3.00E+00	4.83E-02
21600	2.49E-04	7.80E+01	3.25E+00	4.97E-02
21600	2.42E-04	8.40E+01	3.50E+00	4.83E-02
21600	2.45E-04	9.00E+01	3.75E+00	4.90E-02
21600	2.41E-04	9.60E+01	4.00E+00	4.82E-02
21600	2.40E-04	1.02E+02	4.25E+00	4.80E-02
21600	2.47E-04	1.08E+02	4.50E+00	4.94E-02
21600	2.52E-04	1.14E+02	4.75E+00	5.03E-02
21600	2.48E-04	1.20E+02	5.00E+00	4.97E-02
21600	2.70E-04	1.26E+02	5.25E+00	5.40E-02
21600	2.59E-04	1.32E+02	5.50E+00	5.17E-02
21600	2.63E-04	1.38E+02	5.75E+00	5.26E-02
3600	2.48E-04	1.39E+02	5.79E+00	4.95E-02
21600	2.58E-04	1.45E+02	6.04E+00	5.16E-02
21600	2.51E-04	1.51E+02	6.29E+00	5.01E-02
21600	2.49E-04	1.57E+02	6.54E+00	4.98E-02
21600	2.52E-04	1.63E+02	6.79E+00	5.04E-02
21600	2.49E-04	1.69E+02	7.04E+00	4.98E-02
21600	2.44E-04	1.75E+02	7.29E+00	4.87E-02
21600	2.53E-04	1.81E+02	7.54E+00	5.05E-02
21600	2.60E-04	1.87E+02	7.79E+00	5.19E-02
21600	2.54E-04	1.93E+02	8.04E+00	5.09E-02
21600	2.47E-04	1.99E+02	8.29E+00	4.93E-02
21600	2.49E-04	2.05E+02	8.54E+00	4.98E-02
21600	2.55E-04	2.11E+02	8.79E+00	5.10E-02
21600	2.47E-04	2.17E+02	9.04E+00	4.94E-02
21600	2.34E-04	2.23E+02	9.29E+00	4.67E-02
21600	2.24E-04	2.29E+02	9.54E+00	4.47E-02
18000	2.18E-04	2.34E+02	9.75E+00	4.37E-02
21600	2.31E-04	2.40E+02	1.00E+01	4.61E-02
21600	2.33E-04	2.46E+02	1.03E+01	4.66E-02
21600	2.32E-04	2.52E+02	1.05E+01	4.63E-02
21600	2.24E-04	2.58E+02	1.08E+01	4.48E-02
21600	2.31E-04	2.64E+02	1.10E+01	4.63E-02
21600	2.29E-04	2.70E+02	1.13E+01	4.58E-02
21600	2.29E-04	2.76E+02	1.15E+01	4.59E-02
21600	2.28E-04	2.82E+02	1.18E+01	4.55E-02
14400	2.30E-04	2.86E+02	1.19E+01	4.60E-02
21600	2.43E-04	2.92E+02	1.22E+01	4.87E-02
21600	2.42E-04	2.98E+02	1.24E+01	4.84E-02
21600	2.36E-04	3.04E+02	1.27E+01	4.72E-02
5400	2.37E-04	3.06E+02	1.27E+01	4.73E-02

Table 4.5.2-5 | Raw data of ammonium concentrations measured in batch BES.

R18	R1	Ammonium							
#	days	1	2	3	C 1	C 2	C 3	Mean	Std.
0	**0**	70.339	78.937	72.456	1.407	1.579	1.449	**1.478**	**0.090**
1	**6**	61.257	65.625	63.968	1.225	1.313	1.279	**1.272**	**0.044**
2	**13**	50.228	52.267	54.285	1.005	1.045	1.086	**1.045**	**0.041**
3	**20**	34.182	34.541	33.563	0.684	0.691	0.671	**0.682**	**0.010**
4	**27**	n.a.	n.a.	n.a.	#VALUE!	#VALUE!	#VALUE!	**#VALUE!**	**#VALUE!**
5	**29**	71.414	66.344	65.569	1.428	1.327	1.311	**1.356**	**0.063**
6	**30**	61.456	61.525	78.385	1.229	1.231	1.568	**1.342**	**0.195**
R19	**AC**	**Ammonium**							
#	days	1	2	3	C 1	C 2	C 3	Mean	Std.
0	**0**	78.611	79.727	78.398	1.572	1.595	1.568	**1.578**	**0.014**
1	**6**	74.239	75.087	71.193	1.485	1.502	1.424	**1.470**	**0.041**
2	**13**	62.712	74.188	70.369	1.254	1.484	1.407	**1.382**	**0.117**
3	**20**	67.682	63.508	61.521	1.354	1.270	1.230	**1.285**	**0.063**
4	**27**	69.219	57.159	61.844	1.384	1.143	1.237	**1.255**	**0.122**
5	**30**	50.216	72.086	72.547	1.004	1.442	1.451	**1.299**	**0.255**
R21	**BC**	**Ammonium**							
#	days	1	2	3	C 1	C 2	C 3	Mean	Std.
0	**0**	80.614	75.478	77.415	1.612	1.510	1.548	**1.557**	**0.052**
1	**4**	75.095	81.049	75.551	1.502	1.621	1.511	**1.545**	**0.066**
2	**11**	69.360	69.302	73.372	1.387	1.386	1.467	**1.414**	**0.047**
3	**18**	63.144	62.269	61.934	1.263	1.245	1.239	**1.249**	**0.012**
4	**21**	62.441	68.873	49.368	1.249	1.377	0.987	**1.205**	**0.199**
R22	**R2**	**Ammonium**							
#	days	1	2	3	C 1	C 2	C 3	Mean	Std.
0	**0**	243.474	232.907	241.127	4.869	4.658	4.823	**4.783**	**0.111**
1	**4**	70.392	78.629	75.526	1.408	1.573	1.511	**1.497**	**0.083**
2	**11**	43.155	42.899	42.851	0.863	0.858	0.857	**0.859**	**0.003**
3	**18**	n.a.	n.a.	n.a.	#VALUE!	#VALUE!	#VALUE!	**#VALUE!**	**#VALUE!**
4	**20**	66.391	74.047	74.868	1.328	1.481	1.497	**1.435**	**0.094**
5	**21**	73.812	69.721	70.650	1.476	1.394	1.413	**1.428**	**0.043**
R23	**R3**	**Ammonium**							
#	days	1	2	3	C 1	C 2	C 3	Mean	Std.
0	**0**	65.641	67.136	65.987	1.313	1.343	1.320	**1.325**	**0.016**
1	**3**	61.485	60.531	59.250	1.230	1.211	1.185	**1.208**	**0.022**
2	**6**	41.004	47.983	50.157	0.820	0.960	1.003	**0.928**	**0.096**
3	**10**	21.268	20.507	19.822	0.425	0.410	0.396	**0.411**	**0.014**
4	**13**	n.a.	n.a.	n.a.	#VALUE!	#VALUE!	#VALUE!	**#VALUE!**	**#VALUE!**

Table 4.5.2-6 | Raw data of nitrate concentrations measured in batch BES.

R18	R1	Nitrate							
#	days	1	2	3	C 1	C 2	C 3	Mean	Std.
0	**0**	4.930	4.926	5.185	0.025	0.025	0.026	**0.025**	**0.001**
1	**6**	5.769	5.524	5.779	0.029	0.028	0.029	**0.028**	**0.001**
2	**13**	26.829	26.667	26.124	0.134	0.133	0.131	**0.133**	**0.002**
3	**20**	41.305	41.338	41.610	0.207	0.207	0.208	**0.207**	**0.001**
4	**27**	46.996	46.707	46.680	0.235	0.234	0.233	**0.234**	**0.001**
5	**29**	33.320	33.818	33.889	0.167	0.169	0.169	**0.168**	**0.002**
6	**30**	45.517	44.230	45.620	0.228	0.221	0.228	**0.226**	**0.004**
R19	**AC**	**Nitrate**							
#	days	1	2	3	C 1	C 2	C 3	Mean	Std.
0	**0**	2.342	2.244	4.425	0.012	0.011	0.022	**0.015**	**0.006**
1	**6**	3.537	3.565	3.295	0.018	0.018	0.016	**0.017**	**0.001**
2	**13**	n.a.	n.a.	n.a.	#VALUE!	#VALUE!	#VALUE!	**#VALUE!**	**#VALUE!**
3	**20**	n.a.	n.a.	n.a.	#VALUE!	#VALUE!	#VALUE!	**#VALUE!**	**#VALUE!**
4	**27**	2.063	3.065	2.954	0.010	0.015	0.015	**0.013**	**0.003**
5	**30**	n.a.	n.a.	n.a.	#VALUE!	#VALUE!	#VALUE!	**#VALUE!**	**#VALUE!**
R21	**BC**	**Nitrate**							
#	days	1	2	3	C 1	C 2	C 3	Mean	Std.
0	**0**	3.740	2.086	3.827	0.019	0.010	0.019	**0.016**	**0.005**
1	**4**	3.312	3.428	3.130	0.017	0.017	0.016	**0.016**	**0.001**
2	**11**	26.380	22.402	22.104	0.132	0.112	0.111	**0.118**	**0.012**
3	**18**	26.302	26.388	26.602	0.132	0.132	0.133	**0.132**	**0.001**
4	**21**	31.461	31.458	31.607	0.157	0.157	0.158	**0.158**	**0.000**
R22	**R2**	**Nitrate**							
#	days	1	2	3	C 1	C 2	C 3	Mean	Std.
0	**0**	2.847	2.369	2.553	0.014	0.012	0.013	**0.013**	**0.001**
1	**4**	11.208	11.615	10.394	0.056	0.058	0.052	**0.055**	**0.003**
2	**11**	67.461	64.704	66.554	0.337	0.324	0.333	**0.331**	**0.007**
3	**18**	114.256	115.850	113.094	0.571	0.579	0.565	**0.572**	**0.007**
4	**20**	96.556	99.118	96.532	0.483	0.496	0.483	**0.487**	**0.007**
5	**21**	113.354	111.108	109.675	0.567	0.556	0.548	**0.557**	**0.009**
R23	**R3**	**Nitrate**							
#	days	1	2	3	C 1	C 2	C 3	Mean	Std.
0	**0**	n.a.	n.a.	n.a.	#VALUE!	#VALUE!	#VALUE!	**#VALUE!**	**#VALUE!**
1	**3**	26.956	26.910	26.628	0.135	0.135	0.133	**0.134**	**0.001**
2	**6**	73.446	73.970	76.135	0.367	0.370	0.381	**0.373**	**0.007**
3	**10**	127.617	126.414	127.821	0.638	0.632	0.639	**0.636**	**0.004**
4	**13**	151.521	152.422	148.405	0.758	0.762	0.742	**0.754**	**0.011**

Table 4.5.2-7 | Raw data of nitrite concentrations measured in batch BES.

R18	R1	Nitrite							
#	days	1	2	3	C 1	C 2	C 3	Mean	Std.
0	**0**	1.004	1.257	1.204	0.005	0.006	0.006	**0.006**	**0.001**
1	**6**	n.a.	n.a.	n.a.	#VALUE!	#VALUE!	#VALUE!	**#VALUE!**	**#VALUE!**
2	**13**	1.991	1.714	2.031	0.010	0.009	0.010	**0.010**	**0.001**
3	**20**	0.020	0.030	n.a.	0.000	0.000	#VALUE!	**#VALUE!**	**#VALUE!**
4	**27**	n.a.	n.a.	n.a.	#VALUE!	#VALUE!	#VALUE!	**#VALUE!**	**#VALUE!**
5	**29**	7.705	8.073	9.318	0.039	0.040	0.047	**0.042**	**0.004**
6	**30**	5.405	2.435	2.184	0.027	0.012	0.011	**0.017**	**0.009**
R19	**AC**	**Nitrite**							
#	**days**	**1**	**2**	**3**	**C 1**	**C 2**	**C 3**	**Mean**	**Std.**
0	**0**	7.177	7.487	7.106	0.036	0.037	0.036	**0.036**	**0.001**
1	**6**	2.998	6.095	3.827	0.015	0.030	0.019	**0.022**	**0.008**
2	**13**	n.a.	n.a.	n.a.	#VALUE!	#VALUE!	#VALUE!	**#VALUE!**	**#VALUE!**
3	**20**	0.100	0.150	0.120	0.001	0.001	0.001	**0.00**	**0.000**
4	**27**	4.242	5.372	3.921	0.021	0.027	0.020	**0.02**	**0.004**
5	**30**	7.027	7.428	7.318	0.035	0.037	0.037	**0.04**	**0.001**
R21	**BC**	**Nitrite**							
#	**days**	**1**	**2**	**3**	**C 1**	**C 2**	**C 3**	**Mean**	**Std.**
0	**0**	0.300	0.020	0.340	0.002	0.000	0.002	**0.001**	**0.001**
1	**4**	0.040	0.030	0.040	0.000	0.000	0.000	**0.000**	**0.000**
2	**11**	0.170	0.140	0.150	0.001	0.001	0.001	**0.001**	**0.000**
3	**18**	2.631	2.493	2.464	0.013	0.012	0.012	**0.013**	**0.000**
4	**21**	4.331	4.617	4.029	0.022	0.023	0.020	**0.022**	**0.001**
R22	**R2**	**Nitrite**							
#	**days**	**1**	**2**	**3**	**C 1**	**C 2**	**C 3**	**Mean**	**Std.**
0	**0**	0.060	0.080	0.100	0.000	0.000	0.001	**0.000**	**0.000**
1	**4**	0.080	0.090	0.080	0.000	0.000	0.000	**0.000**	**0.000**
2	**11**	0.110	0.120	0.120	0.001	0.001	0.001	**0.001**	**0.000**
3	**18**	2.905	4.371	1.676	0.015	0.022	0.008	**0.015**	**0.007**
4	**20**	8.852	8.895	9.221	0.044	0.044	0.046	**0.045**	**0.001**
5	**21**	3.526	3.470	2.955	0.018	0.017	0.015	**0.017**	**0.002**
R23	**R3**	**Nitrite**							
#	**days**	**1**	**2**	**3**	**C 1**	**C 2**	**C 3**	**Mean**	**Std.**
0	**0**	7.602	0.98	1.005	0.038	0.005	0.005	**0.005**	**0.000**
1	**3**	2.523	2.648	2.535	0.013	0.013	0.013	**0.013**	**0.000**
2	**6**	5.188	5.213	5.124	0.026	0.026	0.026	**0.026**	**0.000**
3	**10**	2.368	2.509	2.767	0.012	0.013	0.014	**0.013**	**0.001**
4	**13**	8.410	8.576	7.826	0.042	0.043	0.039	**0.041**	**0.002**

Table 4.5.2-8 | The most abundant 16S gene sequencing data (count of sequence ≥ 10) of all samples obtained from the batch reactors used for ammonium removal from wastewater. Asv were summarised on genus level and shown on the lowest classified level.

Row Labels	Count of Sequence
Archaea	**60**
Euryarchaeota	**12**
Methanomicrobia	12
Methanosarcinales	**12**
Methanosaetaceae	12
Methanosaeta	12
Thaumarchaeota	**48**
Nitrososphaeria	48
Nitrososphaerales	**48**
Nitrososphaeraceae	48
Candidatus_Nitrocosmicus	48
Bacteria	**1179**
Acidobacteria	**11**
Blastocatellia_(Subgroup_4)	11
Blastocatellales	**11**
Blastocatellaceae	11
Actinobacteria	**70**
Acidimicrobiia	11
Actinomarinales	**11**
Actinobacteria	36
Corynebacteriales	**11**
Mycobacteriaceae	11
Mycobacterium	11
Micrococcales	**14**
Microbacteriaceae	14
NA	**11**
NA	11
Thermoleophilia	12
Gaiellales	**12**
Armatimonadetes	**21**
Fimbriimonadia	21
Fimbriimonadales	**21**
Bacteroidetes	**94**
Bacteroidia	94
Bacteroidales	**26**
Dysgonomonadaceae	14
Proteiniphilum	14
Prolixibacteraceae	12
WCHB1-32	12
Chitinophagales	**23**
Chitinophagaceae	23
NA	**35**
Sphingobacteriales	**10**
Chloroflexi	**202**
Anaerolineae	124
Anaerolineales	**27**
Anaerolineaceae	27
Ardenticatenales	**10**
Caldilineales	**25**
Caldilineaceae	25
RBG-13-54-9	**26**
SBR1031	**36**
A4b	23
NA	13
Chloroflexia	36
Thermomicrobiales	**36**
AKYG1722	14
JG30-KF-CM45	22
Gitt-GS-136	18
NA	10
OLB14	14
Deferribacteres	**10**
Deferribacteres	10
Deferribacterales	**10**
Deferribacteraceae	10
Deinococcus-Thermus	**22**
Deinococci	22
Deinococcales	**22**
Trueperaceae	22
Truepera	22
Firmicutes	**56**
Bacilli	34
Bacillales	**34**
Bacillaceae	34
Anaerobacillus	12
Bacillus	12
NA	10
Clostridia	22
Clostridiales	**22**
Family_XI	10
Soehngenia	10
Peptococcaceae	12
Desulfosporosinus	12
Hydrogenedentes	**11**
Hydrogenedentia	11
Hydrogenedentiales	**11**
Hydrogenedensaceae	11
NA	**131**
Nitrospirae	**24**
Nitrospira	24
Nitrospirales	**24**
Nitrospiraceae	24
Nitrospira	24
Patescibacteria	**11**
Parcubacteria	11
Planctomycetes	**35**
Brocadiae	35
Brocadiales	**35**
Brocadiaceae	35
Candidatus_Kuenenia	35
Proteobacteria	**437**
Alphaproteobacteria	155
NA	**75**
Parvibaculales	**11**
Parvibaculaceae	11
Parvibaculum	11
Rhizobiales	**69**
NA	34
Rhizobiaceae	18
Xanthobacteraceae	17
Deltaproteobacteria	13
Oligoflexales	**13**
0319-6G20	13
Gammaproteobacteria	241
Betaproteobacteriales	**158**
Burkholderiaceae	61
Limnobacter	14
NA	47
NA	20
Rhodocyclaceae	77
Dechloromonas	11
Denitratisoma	13
Ferribacterium	36
NA	17

Legionellales	**10**
Legionellaceae	10
Legionella	10
NA	**33**
Pseudomonadales	**14**
Pseudomonadaceae	14
Pseudomonas	14
Xanthomonadales	**26**
Xanthomonadaceae	26
NA	11
Thermomonas	15
NA	28
Spirochaetes	**10**
Leptospirae	10
Leptospirales	**10**
Leptospiraceae	10
Turneriella	10
Synergistetes	**14**
Synergistia	14
Synergistales	**14**
Synergistaceae	14
Thermovirga	14
Thermotogae	**20**
Thermotogae	20
Petrotogales	**20**
Petrotogaceae	20
Defluviitoga	20
Eukaryota	**218**
NA	**21**
Grand Total	**1478**

5. Establishment of the restriction fragment length polymorphism (RFLP) technique as an easy and rapid analysis of low diverse bacterial community compositions

5.1. **Abstract**

In this study the restriction fragment length polymorphism (RFLP) technique has been investigated for implementation to monitor enriched community compositions in laboratory systems and to verify pre-defined cultures used in the laboratory. The DNA is amplified with non-labelled primers and the amplicons restricted with two restriction enzymes simultaneously. The restriction patterns of the applied strains are visualized using a fragment analyser.

The six test strains almost matched the *in silico* determined restriction lengths *in situ*. Although, the lengths varied slightly over time. The highest calculated standard deviations were 11.2 bp (*Pseudomonas fluorescens*) and 6.9 bp (*Escherichia coli*). The standard deviations of all other restriction fragments were below 2.4 bp. The single strains also revealed clear peaks with acceptable intensities up to 5000 RFU. When mixed together and normalised to a certain concentration, the strains were still detectable but peak intensities were very low for some strains or two slightly distinct restrictions fragments reveal the same peak.

The RFLP technique is suitable for the identification of pure cultures but still needs to be improved for mixed cultures with low diversities concerning the restriction enzymes as well as the procedures. However, it is an easy, rapid and cost-effective technique and shows great potential for in-house investigation of microbial community compositions with low diversity.

5.2. **Introduction**

To apprehend microbial processes in technical systems, it is important to understand the dynamics in the microbial communities. Therefore, such communities are investigated concerning their species richness, referring to the number of species in a community, and their species evenness, meaning the sizes of species populations within a community. As it is not possible to cultivate most of the bacteria found in the environment in the laboratory, culture-independent methods are necessary to study biodiversity by fingerprinting communities. Techniques such as denaturing gradient gel electrophoresis (DGGE) (Muyzer *et al.*, 1993) or temperature gradient gel electrophoresis (TGGE) (Rosenbaum & Riesner, 1987), single-strand conformation polymorphism (SSCP) (Schwieger & Tebbe, 1998), and terminal restriction fragment length polymorphism (T-RFLP) (Liu *et al.*, 1997) have been the methods of choice.

In T-RFLP the 16S rRNA gene target region is first amplified via PCR (Avaniss-Aghajani *et al.*, 1994, Liu *et al.*, 1997). Universal primers have been developed covering a broad range of bacteria. They can be tagged with a fluorophore on the forward primer allowing to compress the analysis to one single fragment per species. The obtained amplicons of all bacteria present in a sample show almost the same lengths. Subsequent digestion of the amplicons by specified restrictions endonucleases lead to specific restriction fragment (RF) lengths (Liu *et al.*, 1997). These enzymes typically have recognition sites of 4 to 6 bp in lengths. Many restrictions endonucleases are now commercially available facilitating the applications regarding different recognition sites and incubation temperatures. This also allows the simultaneous usage of two or more restriction enzymes in one digestion step. The restriction patterns are then visualized computer-assisted using gel or capillary electrophoresis and the digitally received profiles can be directly compared with constantly growing 16S rRNA gene databanks (Liu *et al.*, 1997). In DGGE, TGGE, and SSCP, however, visualization is done on polyacrylamide gels revealing generally lower resolution (Marsh, 1999).

Since its development, T-RFLP was used to describe microbial communities in various environments such as clinical specimens (Avaniss-Aghajani *et al.*, 1996, Hayashi *et al.*, 2003, Layer *et al.*, 2006), soils (Lukow *et al.*, 2000, Fierer & Jackson,

2006, Smalla *et al.*, 2007), sediments (Scala & Kerkhof, 2000, Konstantinidis *et al.*, 2003, Edlund *et al.*, 2006), wastewater (Kelly *et al.*, 2005, Siripong & Rittmann, 2007, Kraigher *et al.*, 2008) as well as bioelectrochemical systems (Lefebvre *et al.*, 2010, Harnisch *et al.*, 2011, Patil *et al.*, 2011).

For T-RFLP, however, a sequencer is essential for the analysis of the restriction profiles that is usually not available in each institution as they are very expensive. In contrast to sequencer, capillary electrophoresis systems are more reasonable. In this study an in-house fragment analyser will be applied for the implementation of RFLP without labelled primers as an easy and rapid technique to monitor and verify pre-defined community compositions used in our laboratory rather than complex environmental samples. Non-labelled primers are used as most of the cultures are enriched and will reveal distinct RF profiles. What seems to be a step backwards in history, could be a step forward to an easy and cost-effective technique for the rapid in-house monitoring of enrichment cultures applied in the laboratory.

5.3. **Experimental procedure**

5.3.1. Bacterial strains and cultivation

The bacterial strains shown in Table 5.3.1-1 were cultivated overnight on nutrient agar [Merck GmbH, Darmstadt, Germany]. The media is composed of 5.00 g L^{-1} peptone, 3.00 g L^{-1} meat extract, and 12.00 g L^{-1} agar-agar. The pH was 7.0.

Table 5.3.1-1 | Bacterial strains used as model strains for RFLP. The strains were cultivated overnight on nutrient agar.

Strain	DSMZ No.	Incubation temperature	Incubation medium
Aeromonas hydrophila	30187	30 °C	Nutrient agar
Pseudomonas aeruginosa	50071	37 °C	Nutrient agar
Pseudomonas fluorescens	50090	30 °C	Nutrient agar
Sphingomonas koreensis	15582	30 °C	Nutrient agar
Flavobacterium johnsoniae	2064	30 °C	Nutrient agar
Escherichia coli	30083	37 °C	Nutrient agar

5.3.2. Extraction of genomic DNA

The DNA of the model strains was extracted using the Blood & Tissue Kit provided by QIAGEN GmbH [Hilden, Germany]. For cell lysing the samples were pre-treated with proteinase K as described for gram-negative cells. The DNA extracts were stored at -20 °C until further usage.

5.3.3. Quantification of DNA yield

The DNA yields in the extractions were quantified using the Invitrogen Qubit™ 4 fluorometer [ThermoFisher Scientific, Dreieich, Germany]. The attendant Invitrogen Qubit™ dsDNA HS Assay Kit [ThermoFisher Scientific, Dreieich, Germany] was applied according to the manufacturers' instructions using 1 µL of sample.

5.3.4. Amplification of 16S rRNA genes

For the amplification of the 16S rRNA genes the primer set Ba27f/Ba907r (Table 5.3.4-1) was applied. The primers were purchased from Eurofins Genomics [Ebersberg, Germany].

Table 5.3.4-1 | Primers used for the amplification of 16S rRNA genes.

	Name	Sequence	Reference
Forward primer	Ba27f	AGAGTTTGATCMTGGCTCAG	Pilloni *et al.* (2011)
Reverse primer	Ba907r	CCGTCAATTCMTTTRAGTTT	Lane *et al.* (1985)

The PCR components were mixed as described in Table 5.3.4-2. All components for the PCR were purchased from ThermoFisher Scientific [Dreieich, Germany], Promega GmbH [Mannheim, Germany] and Sigma-Aldrich Chemie GmbH [Munich, Germany]. The DNA extraction products of all samples used as templates were normalized to 10 ng/µL in nuclease-free water beforehand. The thermal profile used for the PCR is shown in Table 5.3.4-3 and was done in the Mastercycler epgradient S [Eppendorf GmbH, Wesseling-Berzdorf, Germany]. Strains were tested separately and all mixed together. In case of the latter the normalized concentration was 10 ng/µL in total.

Table 5.3.4-2 | PCR reaction mix used for RFLP.

	Stock concentration	Final concentration	Per reaction
DNA template	1-20 ng μL^{-1}	0.02-0.4 ng μL^{-1}	1 µL
Nuclease-free water	-	-	39.25 µL
PCR Buffer	10 X	1 X	5 µL
$MgCl_2$	25 mmol L^{-1}	1.5 mmol L^{-1}	3 µL
BSA	20 µg μL^{-1}	0.2 µg L^{-1}	0.5 µL
dNTPs	10 mmol L^{-1}	0.1 mmol L^{-1}	0.5 µL
Forward primer Ba27f	100 µmol L^{-1}	0.5 µmol L^{-1}	0.25 µL
Reverse primer Ba907r	100 µmol L^{-1}	0.5 µmol L^{-1}	0.25 µL
Taq polymerase	5 U μL^{-1}	0.025 U μL^{-1}	0.25 µL

Table 5.3.4-3 | Thermal profile for PCR amplification for RFLP.

Temperature	Time	
94 °C	5 min	
94 °C	0.5 min	25 cycles
52 °C	0.5 min	
70 °C	1 min	
70 °C	5 min	
4 °C	hold	

5.3.5. Purification of amplicons

After PCR, the amplicons were purified using the NucleoSpin PCR and Gel Clean-Up provided by Macherey-Nagel GmbH und Co. KG [Düren, Germany] following the manufacturers' instructions. The amplicons were eluted in 15 µL buffer NE and stored at -20 °C until further analyses.

5.3.6. Selection of restriction enzymes and in-silico restriction analysis

The 16S rRNA sequences of the strains (Table 5.3.1-1) were derived from NCBI's nr database using the PCR primers (Table 5.3.4-1). *In silico* restriction fragments were obtained using different restriction enzymes in the restriction mapper Version 3 (http://www.restrictionmapper.org). The enzymes Kpn2I and SacI were chosen as they have only one restriction site and they revealed distinct RF lengths for the tested bacterial strains.

5.3.7. Restriction of PCR amplicons

The PCR amplicons used as templates were normalized to the lowest DNA yield measured in the samples beforehand using the Invitrogen Qubit™ 4 fluorometer [ThermoFisher Scientific, Dreieich, Germany] as previously described in section 5.3.3. The enzymes Kpn2I and SacI (Table 5.3.7-1) and the respective buffer were purchased from Invitrogen, Thermo Scientific [Dreieich, Germany]. They were applied simultaneously for the restriction of the amplicons. The restriction mix was prepared as described in the manufacturers' instructions (Table 5.3.7-2). Nuclease-free water

was purchased from Promega GmbH [Mannheim, Germany]. The samples were incubated for 20 min in the Mastercycler epgradient S [Eppendorf GmbH, Wesseling-Berzdorf, Germany].

Table 5.3.7-1 | Restriction enzymes used in RFLP.

Enzyme	Restriction site	Dilution buffer	Incubation temperature
Kpn2I	T|CCGGA	Anza™ 10x Buffer	37 °C
SacI	AGT|ACT	Anza™ 10x Buffer	37 °C

Table 5.3.7-2 | Restriction mix used for RFLP.

	Stock concentration	Final concentration	For 1 reaction
Amplicon template	100 ng μL^{-1}	25 ng μL^{-1}	10.00 µL
Nuclease-free water	-	-	6.50 µL
Buffer (incl. BSA)	10 X	1 X	2.00 µL
SacI	10 U μL^{-1}	0.5 U μL^{-1}	1.00 µL
Kpn2I	20 U μL^{-1}	0.5 U μL^{-1}	0.50 µL

5.3.8. Visualization of restriction fragments on the fragment analyser and analyses of restriction fragments

The restriction fragments (RFs) were visualized using the Fragment Analyzer [Advanced Analytical Technologies GmbH, Heidelberg, Germany]. For the detection of the RFs the DNF-910 dsDNA Reagent Kit for fragments between 35 bp and1500 bp length was used as described in the manufacturers' instructions. As templates, 4 µL of the restriction products were applied. To verify PCR results, amplicons were additionally visualized.

PCR and restriction of single tested strains was conducted eleven times for *A. hydrophila*, ten times for *E.coli*, and nine times for the other strains. Mean values and standard deviations were calculated of the lengths given by the fragment analyser. Raw data obtained from the fragment analyser are shown in the appendix (Table 5.4.2-1 to Table 5.4.2-9).

5.4. **Results**

To implement the RFLP technique for monitoring microbial cultures used in the laboratory, six test strains were evaluated as single strains investigating the differences of *in silico* RFs and experimentally tested RFs. Mixtures of five strains were analysed whether differentiation of those strains was achieved.

5.4.1. Evaluation of test strains: *in silico* and *in situ*

The RFs of each of the six chosen strain was determined *in silico* with both restriction enzymes, SacI and Kpn2I, and investigated experimentally. The analyses revealed that the RFs of *E. coli* and *A. hydrophila* had almost the same length with 848 bp and 851 bp, respectively. They also shared the same restriction fragment at 70 bp. Series of *in situ* experiments, however, showed that both strains could be clearly separated as the RF of *A. hydrophila* was only 825 ± 2.4 bp in length (Table 5.4.1-1, Figure 5.4.1-1). Although, all strains were normalized to the concentration of the strain with the lowest concentration (between 50 and 60 ng μL^{-1}) before restriction, the relative fluorescence varied between each run.

Table 5.4.1-1 | Restriction fragments (RFs) of test strains. Experimentally generated RFs were obtained from test series of n=11 for A. hydrophila, n=10 for E. coli and n=9 for *P. aeruginosa*, *P. fluorescens*, *Sph. koreensis* and *F johnsoniae*.

	Restriction enzyme	*In silico* RF	Tested RF
Aeromonas hydrophila	Kpn2I	70 bp	79.3 ± 0.8 bp
		851 bp	825.0 ± 2.4 bp
Escherichia coli	Kpn2I	70 bp	79.8 ± 0.4 bp
		848 bp	847.5 ± 6.9 bp
Pseudomonas aeruginosa	Kpn2I	143 bp	143 ± 0.0 bp
		770 bp	760.0 ± 2.4 bp
Pseudomonas fluorescens	SacI	77 bp	93.2 ± 0.4 bp
		836 bp	846.5 ± 11.2 bp
Sphingomonas koreensis	SacI	306 bp	298.9 ± 2.7 bp
		556 bp	562.8 ± 1.6 bp
Flavobacterium johnsoniae	Kpn2I	366 bp	379.0 ± 1.1 bp
		536 bp	534.7 ± 0.9 bp

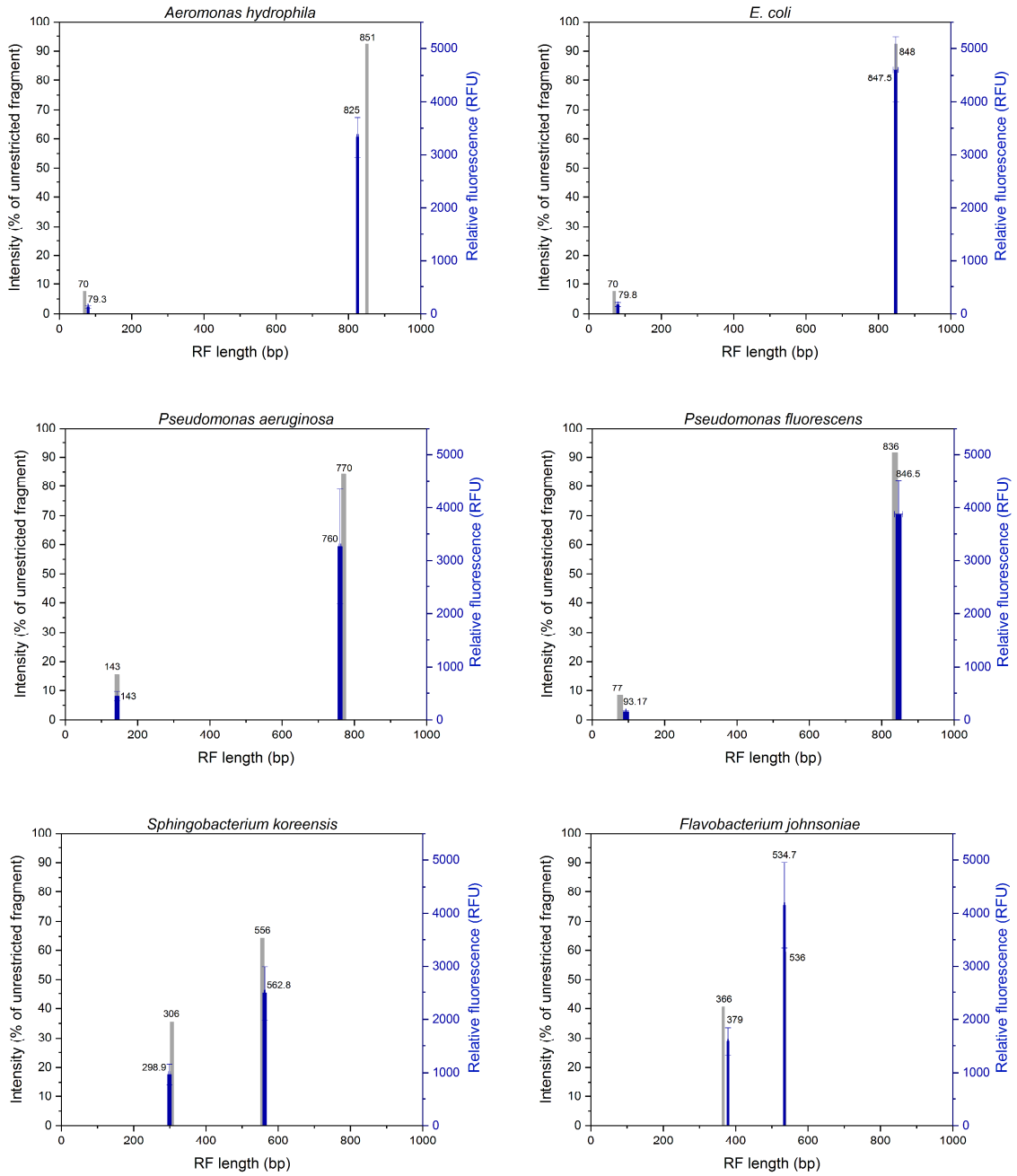

Figure 5.4.1-1 | Relative intensities of *in silico* RFs (grey) and intensities of experimentally tested RFs of test strains (blue; n=11 for A. hydrophila, n=10 for E. coli and n=9 for *P. aeruginosa*, *P. fluorescens*, *Sph. koreensis* and *F johnsoniae*).

The standard deviations of the measured RFs lengths were generally low between ± 0 bp and ± 2.4 bp. Only in the case of *E. coli* and *P. fluorescens* the standard deviations reached ± 6.9 bp and ± 11.2 bp. In summary, the RFLP technique provided good results for the identification of most of the single strains.

5.4.2. Differentiation of test strains in mixtures

The *in silico* analysis resulted in a pattern as shown in Figure 5.4.2-1 with clearly distinct restriction fragments for all test strains except for *E. coli* and *A. hydrophila*. These strains had almost the same length with 848 bp and 851 bp, respectively. As the relative fluorescence would be low in the case of small amounts of input templates, the longest fragments were used for identification, here determined as RF1 in Figure 5.4.2-1.

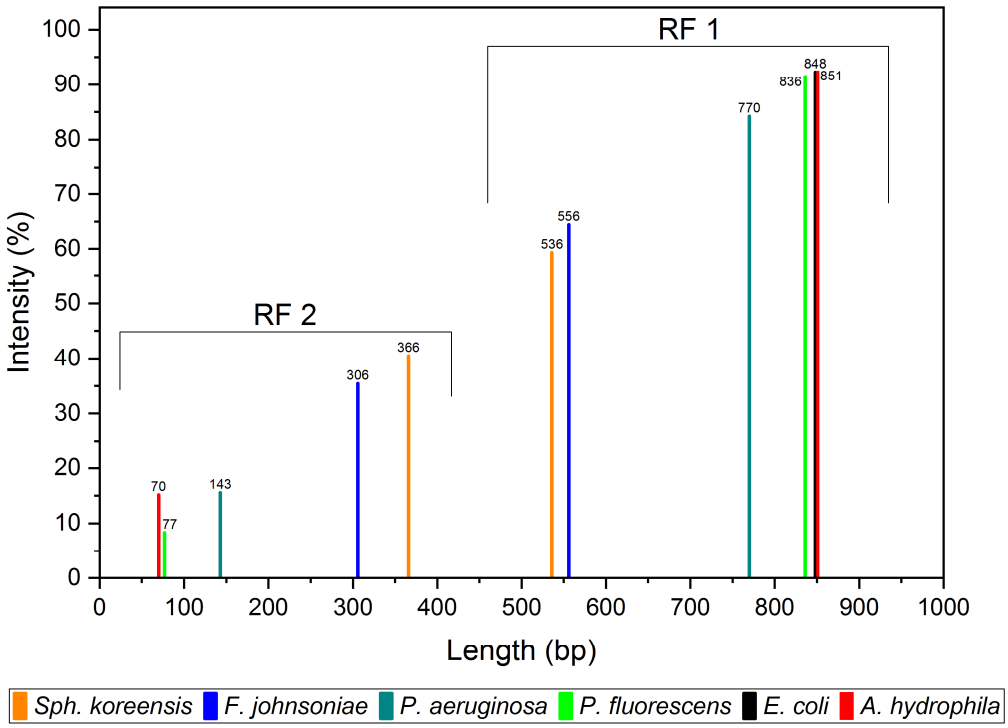

Figure 5.4.2-1 | *In silico* constructed pattern of RFs of test strains.

The experimental series revealed a different pattern of the five strains used in these experiments (Figure 5.4.2-2). The electropherograms showed generally low relative fluorescence of most of the strains compared to the size markers applied in the fragment analyser. Not all peaks could be clearly assigned to the test strains *A. hydrophila*, *P. aeruginosa*, *P. fluorescens*, *Sph. koreensis*, and *F. johnsoniae*. In the first set, for instance, the peak at 843 bp might be identified as *E. coli* (single strain tests: 847.5 ± 6.9 bp). However, this strain was not part of the set. *A. hydrophila* (single strain tests: 825.0 ± 2.4 bp) could not be found in the pattern. In the second pattern the peak showing a RF length of 831 bp could be assigned to *A. hydrophila*,

although, it was 6 bp higher than the calculated average size. *P. aeruginosa* and *P. fluorescens* were only identified by their minor peaks of 143 bp and 91 to 93 bp (single strain tests: 143.0 ± 0.0 bp for *P. aeruginosa* and 93.2 ± 0.4 bp for *P. fluorescens*), respectively, but their major peaks of about 760 bp and 852 bp could not be found in the first set of experiments. In the second set a minor peak with 766 bp could be identified as *P. aeruginosa* (single strain tests: 760.0 ± 2.4 bp). *Sph. koreensis* was not detectable in the first set of experiments at all. In the second set it was represented by a very low peak with a RF size of 302 bp (single strain tests: 298.9 ± 2.7 bp). *F. johnsoniae* (single strain tests: 379.0 ± 1.1 bp, however, was clearly detectable in both sets at least by one peak at 374 bp (set 1) and 380 bp (set 2). The second RFs were 4 bp and 7 bp longer than the calculated average size of 534.7 ± 0.9 bp but still identifiable as *F. johnsoniae*.

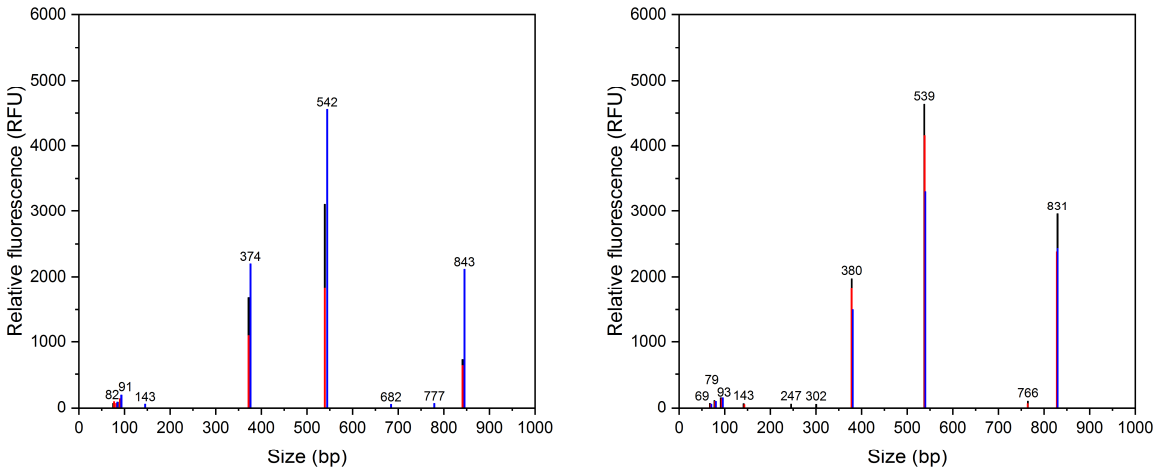

Figure 5.4.2-2 | Experimentally achieved RF patterns of five species (except *E. coli*) of two sets of experiments.

Differences of RF lengths and intensities between the single analysed strains and mixed strains were also obtained, when only two, three or four strains were mixed (data not shown). The obtained RF lengths differed up to 24 bp and 17 bp from the average values for *A. hydrophila* and *P. aeruginosa*, respectively. In conclusion, for identification of strains in mixed samples, the RFLP technique required optimization procedures for accurate applications.

5.5. **Discussion**

In this study, a potential in-house RFLP technique for the analysis of community compositions of samples with low microbial diversity is addressed. The aim is to rapidly investigate the microbial communities within a running system such as a bioelectrochemical system and to verify enriched and pure cultures used in a strain collection. Although, the RFLP technique shows great potential, there were several issues that have to be focused on in further investigations.

The study showed that this in-house RFLP technique can be easily utilised for the verification of pure cultures as the RFs of all single strains are obtained with low standard deviations. Only the RFs for *E. coli* were getting longer over time and it was, therefore, not used for the experiments where strains were mixed. Unfortunately, it cannot be explained why this phenomenon occurred. Amplicons may become degraded over time during storage due to the presence of DNA degrading enzymes resulting from improper DNA extractions, rapid freeze-thawing conditions (QIAGEN Service & Support Centre, 2013-2020), or storage buffer compositions (Röder *et al.*, 2010). DNA degradation, however, was not observed. All strains were efficiently tested as single samples in the same run without observation of DNA degradation processes in the stored DNA extractions. Studies showed that parameters concerning the PCR may have an influence on the resulting T-RFLP profiles (Clement *et al.*, 1998, Osborn *et al.*, 2000). The PCR parameters and products used in this study, however, were not changed. Furthermore, the restriction process can affect the T-RFLP profiles as incomplete digestion may result in additional T-RFs (Bruce, 1997, Clement *et al.*, 1998). This phenomenon can occur in complex environmental communities and, consequently, leads to overestimations of the microbial diversity in the samples (Osborn *et al.*, 2000). In this study, only five known strains make up the microbial community. Incomplete digestion might have been a problem but were identifiable as PCR products with approximately 920 bp, which were seldomly observed.

The main problems of this technique are observed when mixing two or more strains together. The longer the fragments are, the higher is their relative fluorescence intensity because of the staining. These longer fragments, therefore, are regarded as

the major fragments revealing the strains identity. Unfortunately, it seems that RFs of different strains are coeluting leading to false results. A reason for this might be the concentration of the gel solution. In electrophoresis, the gel concentration is justified to the lengths of DNA molecules. The higher the concentration of the gel is, the lower is the ability of resolving the molecules and the fragments may be separated inaccurately (Yılmaz *et al.*, 2012). For the experiments the gel concentration was freshly prepared according to the manufacturers' advices so that evaporation of the water from the gel solution can be excluded. Additionally, the ladder with an upper band of 1,500 bp was efficiently resolved on the gel, while PCR products with approximately 920 bp were additionally adequately resolved, which were applied on the fragment analyser to verify efficient PCR processes.

Interestingly, *P. aeruginosa* is always detectable with its RF at 143 bp with a very low intensity in the mixed samples but not its major RF. The latter could coelute with the major RF of another strain. However, no RF of the other strains has approximately the same size. Here, the aforementioned possibility of DNA degradation may play a role, although it was excluded as mentioned above. Another point to mention are unspecific restrictions that can occur as it was observed to happen in T-RFLP analyses (Egert & Friedrich, 2003). It was shown that these unspecific restrictions may result from single-stranded DNA fragments since endonucleases are only able to cleave double-stranded DNA fragments at their specific recognition sites (Nishigaki *et al.*, 1985). This phenomenon might have indeed occurred as well in this study and has to be further addressed.

Small fragment lengths below 200 bp generally show very little intensities. They might be overcome by using higher amount of loading dye, although, the amount of dye added to the samples according to the manuals is usually more than sufficient to stain all fragments completely. The initial concentration of the sample must be known if one prefers to efficiently adapt the concentration of the loading dye to prevent depletion of the dye.

Another point to mention is the simultaneous application of two restriction enzymes. Although, they have two completely different restriction sites, the enzymes could interfere with each other. For instance, the recognition site of the first enzyme

might be close to a region that resembles the recognition site of the second enzyme. This second enzyme might be attracted to the possible restriction site without cutting but blocking the entire region for the first enzyme for a certain time. This might lead to incomplete restriction. Indeed, for instance, a recognition site for the enzyme SacI that differs in one base pair is directly located beside the restriction site for Kpn2I in the amplicon of *A. hydrophila*. Nevertheless, unrestricted fragments were not present or only detectable in low concentrations showing that the restriction was in general complete. The restriction in the sample mixtures has to be investigated using only one restriction enzyme at a time. This should allow the restriction of only *P. fluorescens* and *S. koreensis* in one run and *A. hydrophila*, *P. aeruginosa*, *F. johnsoniae* and, *E. coli* in the next run. Nevertheless, the simultaneous application of restriction enzymes would save time and money and, therefore, is the preferred approach.

For each strain tested, the restriction enzymes must be chosen well to avoid enzyme inefficiencies and incomplete restrictions. The same holds true for the concentration of enzymes, the application time as well as temperature. While the application temperature depends on the used enzymes, the concentration and time could be adjusted individually. However, the change of parameters related to the restriction process as well as to PCR does not necessarily solve the problem concerning unspecific restrictions (Egert & Friedrich, 2003).

During the study, the drawbacks of this technique could not be entirely investigated. Although, the technique is very suitable for the verification of pure cultures, further optimization steps have to be tested for the application of RFLP to monitor mixed samples. The implementation of RFLP as a rapid in-house test would save time and money and enhance the efficiency of laboratory experiments.

5.6. **Appendix**

Table 5.4.2-1 | Raw data from electrophoresis on the fragment analyzer (23.11.2017). Aero = *A. hydrophila*, Psae = *P. aeruginosa*, Psfl = *P. fluorescens*, Sphingo = *Sph. koreensis*.

F1	Aero 1						F7	Pafl 1				
Peak ID	Size (bp)	% (Conc.)	nmole/L	ng/ul	RFU		Peak ID	Size (bp)	% (Conc.)	nmole/L	ng/ul	RFU
1	35 (LM)		22.674	0.4856	10583		1	35 (LM)		22.278	0.4771	7172
2	68	2.3	5.567	0.2308	169		2	82	4	3.509	0.1761	100
3	79	4.1	8.389	0.4041	191		3	93	7.2	5.654	0.3197	109
4	735	0.9	0.19	0.0849	75		4	827	88.8	7.815	3.9265	1700
5	829	92.7	18.218	9.1795	4929		5	1500 (UM)		0.549	0.5	11959
6	1500 (UM)		0.549	0.5	17068							
								TIC:	4.4222	ng/uL		
	TIC:	9.8992	ng/uL					TIM:	16.979	nmole/L		
	TIM:	32.365	nmole/L					Total Conc	4.7149	ng/uL		
	Total Conc	10.1513	ng/uL									
							F8	Psfl 2				
F2	Aero 2						Peak ID	Size (bp)	% (Conc.)	nmole/L	ng/ul	RFU
Peak ID	Size (bp)	% (Conc.)	nmole/L	ng/ul	RFU		1	35 (LM)		22.061	0.4725	7332
1	35 (LM)		23.4	0.5012	10601		2	83	0.4	0.721	0.0364	64
2	68	3.1	3.746	0.1553	142		3	93	2.3	3.785	0.2153	86
3	79	4.1	4.161	0.2004	132		4	858	97.3	17.548	9.1434	3166
4	825	92.8	9.137	4.5775	3585		5	1500 (UM)		0.549	0.5	12505
5	1500 (UM)		0.549	0.5	16876							
								TIC:	9.3951	ng/uL		
	TIC:	4.9333	ng/uL					TIM:	22.054	nmole/L		
	TIM:	17.044	nmole/L					Total Conc	9.672	ng/uL		
	Total Conc	5.2568	ng/uL									
							F9	Psfl 3				
F3	Aero 3						Peak ID	Size (bp)	% (Conc.)	nmole/L	ng/ul	RFU
Peak ID	Size (bp)	% (Conc.)	nmole/L	ng/ul	RFU		1	35 (LM)		23.052	0.4937	8887
1	35 (LM)		22.899	0.4904	8962		2	82	2.6	3.995	0.2004	133
2	69	6.9	3.374	0.141	121		3	93	5.4	7.249	0.4099	165
3	79	6.7	2.857	0.1376	102		4	841	90.8	13.519	6.9087	2933
4	822	86.4	3.533	1.7649	1941		5	1169	1.2	0.126	0.0897	58
5	1500 (UM)		0.549	0.5	14841		6	1500 (UM)		0.549	0.5	14409
	TIC:	2.0435	ng/uL					TIC:	7.6087	ng/uL		
	TIM:	9.763	nmole/L					TIM:	24.89	nmole/L		
	Total Conc	2.3212	ng/uL					Total Conc	7.791	ng/uL		
F4	Psae 1						F10	Sphingo 1				
Peak ID	Size (bp)	% (Conc.)	nmole/L	ng/ul	RFU		Peak ID	Size (bp)	% (Conc.)	nmole/L	ng/ul	RFU
1	35 (LM)		21.918	0.4694	10640		1	35 (LM)		22.647	0.485	8881
2	143	4.4	4.286	0.3719	615		2	296	29.2	13.131	2.3631	1192
3	149	7.2	6.69	0.6066	219		3	564	69.7	16.465	5.6384	3159
4	760	88.4	16.126	7.4426	4896		4	865	1.1	0.166	0.0873	119
5	1500 (UM)		0.549	0.5	18078		5	1500 (UM)		0.549	0.5	14698
	TIC:	8.4211	ng/uL					TIC:	8.0888	ng/uL		
	TIM:	27.103	nmole/L					TIM:	29.763	nmole/L		
	Total Conc	8.6317	ng/uL					Total Conc	8.4953	ng/uL		
F5	Psae 2						F11	Sphingo 2				
Peak ID	Size (bp)	% (Conc.)	nmole/L	ng/ul	RFU		Peak ID	Size (bp)	% (Conc.)	nmole/L	ng/ul	RFU
1	35 (LM)		22.272	0.477	9578		1	35 (LM)		22.285	0.4773	10612
2	143	4.1	4.615	0.4004	540		2	296	29.9	9.195	1.6548	1211
3	150	8.4	9.104	0.8282	224		3	561	69	11.215	3.8263	2968
4	760	86.8	18.587	8.5783	4616		4	865	1.1	0.117	0.0615	95
5	1169	0.7	0.102	0.0724	59		5	1500 (UM)		0.549	0.5	17491
6	1500 (UM)		0.549	0.5	15989							
								TIC:	5.5426	ng/uL		
	TIC:	9.8793	ng/uL					TIM:	20.527	nmole/L		
	TIM:	32.407	nmole/L					Total Conc	5.8902	ng/uL		
	Total Conc	10.0716	ng/uL									
							F12	Ladder				
F6	Psae 3						Peak ID	Size (bp)	% (Conc.)	nmole/L	ng/ul	RFU
Peak ID	Size (bp)	% (Conc.)	nmole/L	ng/ul	RFU		1	35 (LM)		22.36	0.4789	11723
1	35 (LM)		23.144	0.4957	8079		2	100	7.4	52.07	3.1709	7624
2	143	12.7	5.667	0.4917	365		3	200	8.2	29.173	3.5485	9886
3	752	85.8	7.252	3.3115	2047		4	300	8.1	19.224	3.5061	10484
4	905	1.4	0.099	0.0546	77		5	400	8.2	14.485	3.5216	10862
5	1500 (UM)		0.549	0.5	13140		6	500	23.2	32.948	10.0116	16460
							7	600	9.3	11.008	4.0133	9553
	TIC:	3.8578	ng/uL				8	700	8.7	8.776	3.733	11557
	TIM:	13.018	nmole/L				9	800	9	7.947	3.8631	11744
	Total Conc	4.1136	ng/uL				10	900	8.7	6.885	3.7646	11460
							11	1000	9.1	6.474	3.9332	11300
							12	1500 (UM)		0.549	0.5	19299
								TIC:	43.066	ng/uL		
								TIM:	188.99	nmole/L		
								Total Conc	43.3411	ng/uL		

Table 5.4.2-2 | Raw data from electrophoresis on the fragment analyzer (23.11.2017). Sphingo = *Sph. koreensis*, Flavo = *F. jonsoniae*, Aero = *A. hydrophila*, Psae = *P. aeruginosa*, Psfl = *P. fluorescens*.

G1	Sphingo 3						G7	Ecoli 3				
Peak ID	Size (bp)	% (Conc.)	nmole/L	ng/ul	RFU		Peak ID	Size (bp)	% (Conc.)	nmole/L	ng/ul	RFU
1	35 (LM)		19.788	0.4238	10583		1	35 (LM)		20.041	0.4292	8207
2	300	34.5	14.066	2.5653	1421		2	69	2.3	5.981	0.2501	144
3	562	64.3	13.972	4.7745	3664		3	80	4	8.782	0.4262	172
4	865	1.2	0.169	0.0886	140		4	853	93.7	19.307	10.0058	5113
5	1500 (UM)		0.549	0.5	19871		5	1500 (UM)		0.549	0.5	15351
	TIC:	7.4284	ng/uL					TIC:	10.6821	ng/uL		
	TIM:	28.206	nmole/L					TIM:	34.07	nmole/L		
	Total Conc	7.7687	ng/uL					Total Conc	10.971	ng/uL		
G2	Flavo 1						G8	NTC PCR				
Peak ID	Size (bp)	% (Conc.)	nmole/L	ng/ul	RFU		Peak ID	Size (bp)	% (Conc.)	nmole/L	ng/ul	RFU
1	35 (LM)		21.758	0.466	10281		1	35 (LM)		19.691	0.4217	8341
2	377	40.4	19.191	4.4026	2077		2	56	63.8	24.116	0.8294	721
3	534	58.7	19.685	6.3924	5456		3	71	15.7	4.722	0.2041	203
4	927	0.8	0.161	0.0905	150		4	912	20.5	0.482	0.2668	322
5	1500 (UM)		0.549	0.5	18302		5	1500 (UM)		0.549	0.5	15890
	TIC:	10.8855	ng/uL					TIC:	1.3004	ng/uL		
	TIM:	39.037	nmole/L					TIM:	29.32	nmole/L		
	Total Conc	11.2416	ng/uL					Total Conc	1.6055	ng/uL		
G3	Flavo 2						G9	Aero 1 PCR				
Peak ID	Size (bp)	% (Conc.)	nmole/L	ng/ul	RFU		Peak ID	Size (bp)	% (Conc.)	nmole/L	ng/ul	RFU
1	35 (LM)		21.643	0.4635	9702		1	35 (LM)		24.399	0.5225	9658
2	378	37	13.705	3.1501	1595		2	60	0.1	2.332	0.086	55
3	429	6.3	2.055	0.5353	169		3	72	0.1	1.659	0.0729	88
4	534	49.9	13.07	4.244	4210		4	257	0.2	0.809	0.1263	216
5	621	6.1	1.377	0.5199	187		5	464	0.1	0.128	0.0362	61
6	927	0.7	0.101	0.0568	89		6	598	0.1	0.134	0.0486	50
7	1500 (UM)		0.549	0.5	16833		7	658	0.1	0.244	0.0977	125
							8	901	99.3	121.771	66.6604	62527
	TIC:	8.506	ng/uL				9	1500 (UM)		0.549	0.5	14625
	TIM:	30.306	nmole/L									
	Total Conc	8.846	ng/uL					TIC:	67.128	ng/uL		
								TIM:	127.078	nmole/L		
G4	Flavo 3							Total Conc	67.6684	ng/uL		
Peak ID	Size (bp)	% (Conc.)	nmole/L	ng/ul	RFU							
1	35 (LM)		19.352	0.4145	11046		G10	Psae 1 PCR				
2	378	40.3	12.032	2.7656	1737		Peak ID	Size (bp)	% (Conc.)	nmole/L	ng/ul	RFU
3	535	58.9	12.432	4.0452	4832		1	35 (LM)		25.05	0.5365	10105
4	927	0.8	0.1	0.0564	115		2	57	0.3	5.408	0.1879	97
5	1500 (UM)		0.549	0.5	21277		3	71	0.2	3.241	0.1412	129
							4	608	0.2	0.361	0.1335	179
	TIC:	6.8672	ng/uL				5	901	99.3	117.12	64.1143	62557
	TIM:	24.564	nmole/L				6	1500 (UM)		0.549	0.5	15074
	Total Conc	7.1601	ng/uL									
								TIC:	64.5769	ng/uL		
G5	Ecoli 1							TIM:	126.13	nmole/L		
Peak ID	Size (bp)	% (Conc.)	nmole/L	ng/ul	RFU			Total Conc	65.168	ng/uL		
1	35 (LM)		20.027	0.4289	9899							
2	72	2.1	5.942	0.2611	175		G11	Psfl 1 PCR				
3	79	3.7	9.456	0.4556	222		Peak ID	Size (bp)	% (Conc.)	nmole/L	ng/ul	RFU
4	860	94.2	22.278	11.6459	6983		1	35 (LM)		22.262	0.4768	11627
5	1500 (UM)		0.549	0.5	18867		2	49	0.1	1.528	0.0455	50
							3	250	0.1	0.446	0.0678	177
	TIC:	12.3625	ng/uL				4	661	0.1	0.172	0.0691	121
	TIM:	37.676	nmole/L				5	916	99.6	89.553	49.8214	62525
	Total Conc	12.6093	ng/uL				6	1500 (UM)		0.549	0.5	19271
G6	Ecoli 2							TIC:	50.0038	ng/uL		
Peak ID	Size (bp)	% (Conc.)	nmole/L	ng/ul	RFU			TIM:	91.7	nmole/L		
1	35 (LM)		21.617	0.463	8640			Total Conc	50.4791	ng/uL		
2	69	2.5	6.349	0.2677	152							
3	79	4	9.045	0.4357	177		G12	Ladder				
4	850	93.5	19.679	10.169	5191		Peak ID	Size (bp)	% (Conc.)	nmole/L	ng/ul	RFU
5	1500 (UM)		0.549	0.5	15099		1	35 (LM)		21.495	0.4604	11837
							2	100	6.7	52.963	3.2254	8093
	TIC:	10.8725	ng/uL				3	200	7.7	30.657	3.729	10756
	TIM:	35.073	nmole/L				4	300	7.8	20.672	3.7701	11773
	Total Conc	11.0893	ng/uL				5	400	8	15.832	3.849	12250
							6	500	23.2	36.844	11.1954	19841
							7	600	9.4	12.42	4.5285	11606
							8	700	9	10.207	4.3416	14491
							9	800	9.1	9.075	4.411	14601
							10	900	9.3	8.188	4.4771	14473
							11	1000	9.8	7.764	4.7169	14814
							12	1500 (UM)		0.549	0.5	20665
								TIC:	48.2439	ng/uL		
								TIM:	204.622	nmole/L		
								Total Conc	48.3635	ng/uL		

Table 5.4.2-3 | Raw data from electrophoresis on the fragment analyzer (11.01.2018). Aero = *A. hydrophila*, Psae = *P. aeruginosa*, Sphingo = *Sph. koreensis*.

A1	Aero 1					A7	Psae 2				
Peak ID	Size (bp)	% (Conc.)	nmole/L	ng/ul	RFU	Peak ID	Size (bp)	% (Conc.)	nmole/L	ng/ul	RFU
1	35 (LM)		21.926	0.4696	9831	1	35 (LM)		22.458	0.481	7983
2	69	2.5	3.785	0.1588	130	2	143	10.7	7.476	0.6506	355
3	80	2.9	3.772	0.1846	121	3	715	2.9	0.4	0.1739	80
4	824	93.6	11.802	5.9089	3258	4	756	86.4	11.439	5.2515	2361
5	1172	0.9	0.083	0.059	62	5	1500 (UM)		0.549	0.5	13303
6	1500 (UM)		0.549	0.5	16842						
							TIC:	6.076	ng/uL		
	TIC:	6.3113	ng/uL				TIM:	19.316	nmole/L		
	TIM:	19.442	nmole/L				Total Conc	6.3299	ng/uL		
	Total Conc	6.5168	ng/uL								
						A8	Psae 3				
A2	Aero 2					Peak ID	Size (bp)	% (Conc.)	nmole/L	ng/ul	RFU
Peak ID	Size (bp)	% (Conc.)	nmole/L	ng/ul	RFU	1	35 (LM)		24.292	0.5203	8527
1	35 (LM)		22.953	0.4916	10913	2	143	3.5	4.454	0.3876	444
2	68	3.9	3.191	0.1328	127	3	149	7.9	9.499	0.8629	178
3	80	4.3	3.019	0.1468	107	4	717	2.3	0.574	0.2501	129
4	822	91.7	6.202	3.0964	2557	5	762	86.3	20.46	9.468	3532
5	1500 (UM)		0.549	0.5	17856	6	1500 (UM)		0.549	0.5	13041
	TIC:	3.376	ng/uL				TIC:	10.9686	ng/uL		
	TIM:	12.412	nmole/L				TIM:	34.987	nmole/L		
	Total Conc	3.6496	ng/uL				Total Conc	11.2888	ng/uL		
A3	Aero 3					A9	Sphingo 1				
Peak ID	Size (bp)	% (Conc.)	nmole/L	ng/ul	RFU	Peak ID	Size (bp)	% (Conc.)	nmole/L	ng/ul	RFU
1	35 (LM)		24.069	0.5155	9992	1	35 (LM)		23.436	0.5019	8196
2	68	1.8	3.104	0.1292	143	2	297	26.9	12.194	2.1991	826
3	80	1.5	2.191	0.1065	98	3	565	72	17.151	5.8841	2302
4	824	96.7	13.934	6.9763	3342	4	863	1.1	0.178	0.0932	112
5	1500 (UM)		0.549	0.5	15759	5	1500 (UM)		0.549	0.5	13131
	TIC:	7.212	ng/uL				TIC:	8.1765	ng/uL		
	TIM:	19.229	nmole/L				TIM:	29.522	nmole/L		
	Total Conc	7.4443	ng/uL				Total Conc	8.508	ng/uL		
A4	Aero 4					A10	Sphingo 2				
Peak ID	Size (bp)	% (Conc.)	nmole/L	ng/ul	RFU	Peak ID	Size (bp)	% (Conc.)	nmole/L	ng/ul	RFU
1	35 (LM)		22.878	0.49	9428	1	35 (LM)		24.086	0.5159	9012
2	68	2.6	4.116	0.1713	130	2	296	25.6	7.275	1.3072	776
3	80	3.1	4.208	0.2045	123	3	562	73.3	10.953	3.7439	2002
4	824	94.2	12.241	6.1287	3141	4	861	1.2	0.113	0.059	79
5	1500 (UM)		0.549	0.5	15871	5	1500 (UM)		0.549	0.5	13843
	TIC:	6.5046	ng/uL				TIC:	5.1101	ng/uL		
	TIM:	20.565	nmole/L				TIM:	18.341	nmole/L		
	Total Conc	6.7799	ng/uL				Total Conc	5.4343	ng/uL		
A5	Aero 5					A11	Sphingo 3				
Peak ID	Size (bp)	% (Conc.)	nmole/L	ng/ul	RFU	Peak ID	Size (bp)	% (Conc.)	nmole/L	ng/ul	RFU
1	35 (LM)		22.71	0.4864	9714	1	35 (LM)		24.27	0.5198	10053
2	69	2.2	4.548	0.1908	134	2	297	6.3	3.451	0.6224	1023
3	80	3.3	5.762	0.28	137	3	303	23.3	12.432	2.2903	1061
4	727	0.9	0.167	0.0737	57	4	566	69.4	19.856	6.8247	2803
5	826	93.6	15.831	7.9484	3523	5	863	1	0.191	0.1002	149
6	1500 (UM)		0.549	0.5	16120	6	1500 (UM)		0.549	0.5	15735
	TIC:	8.4929	ng/uL				TIC:	9.8375	ng/uL		
	TIM:	26.308	nmole/L				TIM:	35.93	nmole/L		
	Total Conc	8.6865	ng/uL				Total Conc	10.1337	ng/uL		
A6	Psae 1					A12	Ladder				
Peak ID	Size (bp)	% (Conc.)	nmole/L	ng/ul	RFU	Peak ID	Size (bp)	% (Conc.)	nmole/L	ng/ul	RFU
1	35 (LM)		21.804	0.467	8842	1	35 (LM)		23.445	0.5021	10980
2	143	11.6	5.256	0.4574	336	2	100	7.4	56.051	3.4134	7483
3	717	2.5	0.229	0.0997	60	3	200	8.3	31.417	3.8215	9579
4	756	85.8	7.352	3.3749	1876	4	300	8.3	21.007	3.8312	10277
5	1500 (UM)		0.549	0.5	15211	5	400	8.1	15.312	3.7227	10545
						6	500	23.1	34.925	10.6122	15830
	TIC:	3.932	ng/uL			7	600	9.1	11.46	4.1781	9012
	TIM:	12.836	nmole/L			8	700	8.8	9.494	4.0381	11564
	Total Conc	4.2136	ng/uL			9	800	8.9	8.401	4.0836	11572
						10	900	8.7	7.275	3.978	11074
						11	1000	9.2	6.974	4.2373	11053
						12	1500 (UM)		0.549	0.5	17532
							TIC:	45.9161	ng/uL		
							TIM:	202.316	nmole/L		
							Total Conc	46.2745	ng/uL		

Table 5.4.2-4 | Raw data from electrophoresis on the fragment analyzer (11.01.2018). Flavo = F. jonsoniae, NTC = no template control

B1	Flavo 1						B7	Ecoli 4				
Peak ID	Size (bp)	% (Conc.)	nmole/L	ng/ul	RFU		Peak ID	Size (bp)	% (Conc.)	nmole/L	ng/ul	RFU
1	35 (LM)		21.719	0.4652	10693		1	35 (LM)		22.366	0.479	8458
2	380	39.9	13.373	3.0914	1459		2	69	3.1	4.233	0.1769	110
3	536	59	14.051	4.5747	3975		3	80	4.4	5.182	0.252	121
4	919	1.1	0.146	0.0815	113		4	834	89.5	10.104	5.1201	2591
5	1500 (UM)		0.549	0.5	19004		5	1172	3	0.239	0.17	93
							6	1500 (UM)		0.549	0.5	14500
	TIC:	7.7476	ng/uL									
	TIM:	27.57	nmole/L					TIC:	5.719	ng/uL		
	Total Conc	8.0321	ng/uL					TIM:	19.758	nmole/L		
								Total Conc	5.8951	ng/uL		
B2	Flavo 2											
Peak ID	Size (bp)	% (Conc.)	nmole/L	ng/ul	RFU		B8	Ecoli 5				
1	35 (LM)		20.705	0.4434	11800		Peak ID	Size (bp)	% (Conc.)	nmole/L	ng/ul	RFU
2	361	0.4	0.15	0.0328	60		1	35 (LM)		22.704	0.4862	8845
3	380	40.4	14.26	3.2905	1621		2	69	1.1	2.681	0.1121	103
4	534	58.4	14.657	4.7533	4343		3	80	1.2	2.577	0.1253	85
5	923	0.9	0.124	0.0694	135		4	843	97.7	19.444	9.964	4045
6	1500 (UM)		0.549	0.5	22119		5	1500 (UM)		0.549	0.5	14808
	TIC:	8.146	ng/uL					TIC:	10.2014	ng/uL		
	TIM:	29.191	nmole/L					TIM:	24.701	nmole/L		
	Total Conc	8.4246	ng/uL					Total Conc	10.4475	ng/uL		
B3	Flavo 3						B9	PCR NTC				
Peak ID	Size (bp)	% (Conc.)	nmole/L	ng/ul	RFU		Peak ID	Size (bp)	% (Conc.)	nmole/L	ng/ul	RFU
1	35 (LM)		25.072	0.537	9709		1	35 (LM)		21.936	0.4698	8958
2	380	38.2	21.293	4.9134	1687		2	46	3.7	2.986	0.0831	58
3	478	1	0.432	0.1256	66		3	57	81.5	52.965	1.8528	1415
4	494	0.4	0.186	0.056	52		4	72	14.8	7.685	0.337	290
5	534	55.9	22.168	7.1889	4507		5	1500 (UM)		0.549	0.5	15877
6	687	3.7	1.144	0.4777	163							
7	919	0.8	0.195	0.1088	135			TIC:	2.2729	ng/uL		
8	1500 (UM)		0.549	0.5	14983			TIM:	63.636	nmole/L		
								Total Conc	2.503	ng/uL		
	TIC:	12.8704	ng/uL									
	TIM:	45.418	nmole/L				B12	Ladder				
	Total Conc	13.3005	ng/uL				Peak ID	Size (bp)	% (Conc.)	nmole/L	ng/ul	RFU
							1	35 (LM)		22.923	0.4909	11040
B4	Ecoli 1						2	100	7.2	53.653	3.2674	7288
Peak ID	Size (bp)	% (Conc.)	nmole/L	ng/ul	RFU		3	200	8.1	30.422	3.7005	9358
1	35 (LM)		20.902	0.4476	9751		4	300	8.1	20.138	3.6727	10139
2	69	1.8	4.513	0.1887	137		5	400	8.1	15.092	3.6692	10733
3	80	3.3	7.158	0.3481	164		6	500	23.3	34.949	10.6195	16494
4	855	95	19.513	10.1392	4483		7	600	9.5	11.873	4.329	9494
5	1500 (UM)		0.549	0.5	17772		8	700	8.8	9.432	4.0116	11946
							9	800	9	8.429	4.0972	12161
	TIC:	10.6759	ng/uL				10	900	8.8	7.332	4.0094	11725
	TIM:	31.185	nmole/L				11	1000	9.1	6.858	4.1665	11482
	Total Conc	10.8844	ng/uL				12	1500 (UM)		0.549	0.5	18373
B5	Ecoli 2							TIC:	45.5429	ng/uL		
Peak ID	Size (bp)	% (Conc.)	nmole/L	ng/ul	RFU			TIM:	198.178	nmole/L		
1	35 (LM)		21.449	0.4594	10745			Total Conc	45.8435	ng/uL		
2	69	0.8	1.942	0.0818	138							
3	80	5.2	10.26	0.5024	173							
4	846	94	17.668	9.0795	4390							
5	1500 (UM)		0.549	0.5	19444							
	TIC:	9.6637	ng/uL									
	TIM:	29.87	nmole/L									
	Total Conc	9.8415	ng/uL									
B6	Ecoli 3											
Peak ID	Size (bp)	% (Conc.)	nmole/L	ng/ul	RFU							
1	35 (LM)		22.096	0.4732	9174							
2	69	2.5	5.219	0.2199	136							
3	80	4.2	7.663	0.3752	160							
4	843	93.3	16.23	8.3172	3829							
5	1500 (UM)		0.549	0.5	16399							
	TIC:	8.9123	ng/uL									
	TIM:	29.112	nmole/L									
	Total Conc	9.1299	ng/uL									

Table 5.4.2-5 | Raw data from electrophoresis on the fragment analyzer (16.01.2017). Aero = *A. hydrophila*, Psae = *P. aeruginosa*, Sphingo = *Sph. koreensis*.

C1	Aero 1					C7	Sphingo 1				
Peak ID	Size (bp)	% (Conc.)	nmole/L	ng/ul	RFU	Peak ID	Size (bp)	% (Conc.)	nmole/L	ng/ul	RFU
1	35 (LM)		22.823	0.4888	9410	1	35 (LM)		24.318	0.5208	7496
2	68	2.1	3.418	0.1423	104	2	300	32.8	3.662	0.6678	387
3	78	4.5	6.345	0.3028	158	3	562	67.2	4.002	1.3679	1080
4	829	93.4	12.557	6.3219	3880	4	1500 (UM)		0.549	0.5	8478
5	1500 (UM)		0.549	0.5	11335						
							TIC:	2.0357	ng/uL		
	TIC:	6.767	ng/uL				TIM:	7.664	nmole/L		
	TIM:	22.32	nmole/L				Total Conc	2.3207	ng/uL		
	Total Conc	7.0377	ng/uL								
						C8	Sphingo 2				
C2	Aero 2					Peak ID	Size (bp)	% (Conc.)	nmole/L	ng/ul	RFU
Peak ID	Size (bp)	% (Conc.)	nmole/L	ng/ul	RFU	1	35 (LM)		25.21	0.5399	8076
1	35 (LM)		22.933	0.4911	10617	2	297	7.5	3.097	0.5584	682
2	68	2.5	3.098	0.1279	103	3	302	26.1	10.551	1.9351	959
3	78	4.8	5.148	0.2456	153	4	564	65.7	14.205	4.8643	2380
4	826	92.7	9.464	4.7516	3591	5	872	0.7	0.093	0.0495	51
5	1500 (UM)		0.549	0.5	12624	6	1500 (UM)		0.549	0.5	8887
	TIC:	5.1252	ng/uL				TIC:	7.4074	ng/uL		
	TIM:	17.71	nmole/L				TIM:	27.946	nmole/L		
	Total Conc	5.3923	ng/uL				Total Conc	7.7183	ng/uL		
C3	Aero 3					C9	Sphingo 3				
Peak ID	Size (bp)	% (Conc.)	nmole/L	ng/ul	RFU	Peak ID	Size (bp)	% (Conc.)	nmole/L	ng/ul	RFU
1	35 (LM)		26.392	0.5652	9680	1	35 (LM)		24.556	0.5259	7669
2	68	2.8	3.55	0.1478	116	2	295	8	2.36	0.4231	546
3	79	4.6	5.179	0.2489	169	3	300	28.4	8.25	1.5047	764
4	824	92.6	9.918	4.9657	3094	4	562	63.6	9.875	3.3754	1812
5	1500 (UM)		0.549	0.5	10133	5	1500 (UM)		0.549	0.5	8633
	TIC:	5.3623	ng/uL				TIC:	5.3032	ng/uL		
	TIM:	18.647	nmole/L				TIM:	20.486	nmole/L		
	Total Conc	5.656	ng/uL				Total Conc	5.5984	ng/uL		
C4	Psae 1					C10	Flavo 1				
Peak ID	Size (bp)	% (Conc.)	nmole/L	ng/ul	RFU	Peak ID	Size (bp)	% (Conc.)	nmole/L	ng/ul	RFU
1	35 (LM)		23.417	0.5015	8741	1	35 (LM)		24.358	0.5217	8648
2	143	11.1	9.302	0.8094	451	2	379	41.7	16.2	3.7327	1395
3	762	88.9	14.01	6.4832	3534	3	535	57.8	15.912	5.1769	3408
4	1500 (UM)		0.549	0.5	10330	4	929	0.5	0.087	0.0489	51
						5	1500 (UM)		0.549	0.5	9792
	TIC:	7.2927	ng/uL								
	TIM:	23.312	nmole/L				TIC:	8.9585	ng/uL		
	Total Conc	7.602	ng/uL				TIM:	32.198	nmole/L		
							Total Conc	9.2673	ng/uL		
C5	Psae 2										
Peak ID	Size (bp)	% (Conc.)	nmole/L	ng/ul	RFU	C11	Flavo 2				
1	35 (LM)		23.366	0.5004	9290	Peak ID	Size (bp)	% (Conc.)	nmole/L	ng/ul	RFU
2	143	12.7	10.22	0.8893	481	1	35 (LM)		24.037	0.5148	9292
3	762	83.1	12.585	5.8241	3721	2	379	40.4	9.25	2.1312	1124
4	863	4.2	0.568	0.2978	202	3	534	59.6	9.699	3.1494	2662
5	1500 (UM)		0.549	0.5	11059	4	1500 (UM)		0.549	0.5	10651
	TIC:	7.0112	ng/uL				TIC:	5.2807	ng/uL		
	TIM:	23.374	nmole/L				TIM:	18.948	nmole/L		
	Total Conc	7.3477	ng/uL				Total Conc	5.5957	ng/uL		
C6	Psae 3					C12	Ladder				
Peak ID	Size (bp)	% (Conc.)	nmole/L	ng/ul	RFU	Peak ID	Size (bp)	% (Conc.)	nmole/L	ng/ul	RFU
1	35 (LM)		23.53	0.5039	8220	1	35 (LM)		24.766	0.5304	9869
2	143	13.7	8.866	0.7715	419	2	100	7.7	61.326	3.7346	6727
3	762	81.1	9.849	4.5578	2780	3	200	8.4	33.552	4.0812	8064
4	865	5.1	0.549	0.2886	146	4	300	8.3	21.973	4.0074	8277
5	1500 (UM)		0.549	0.5	9752	5	400	8.1	16.194	3.937	8002
						6	500	23.6	37.553	11.4109	12363
	TIC:	5.6179	ng/uL			7	600	8.8	11.654	4.2491	6883
	TIM:	19.264	nmole/L			8	700	8.5	9.667	4.1116	7813
	Total Conc	5.8825	ng/uL			9	800	8.8	8.768	4.2619	7841
						10	900	8.7	7.656	4.1862	7570
						11	1000	9.1	7.245	4.4017	7671
						12	1500 (UM)		0.549	0.5	10914
							TIC:	48.3816	ng/uL		
							TIM:	215.587	nmole/L		
							Total Conc	48.7333	ng/uL		

Table 5.4.2-6 | Raw data from electrophoresis on the fragment analyzer (16.01.2018). Flavo = *F. jonsoniae*.

D1	Flavo 3						D12	Ladder				
Peak ID	Size (bp)	% (Conc.)	nmole/L	ng/ul	RFU		Peak ID	Size (bp)	% (Conc.)	nmole/L	ng/ul	RFU
1	35 (LM)		21.296	0.4561	10481		1	35 (LM)		22.79	0.4881	9412
2	380	41.8	10.246	2.365	1567		2	100	7.5	57.333	3.4914	6474
3	536	57.6	10.014	3.2627	3946		3	200	8.3	31.813	3.8696	8333
4	930	0.6	0.064	0.036	53		4	300	8	20.427	3.7255	8753
5	1500 (UM)		0.549	0.5	18060		5	400	8.1	15.488	3.7654	8997
							6	500	23.5	35.938	10.92	14076
	TIC:	5.6637	ng/uL				7	600	9	11.491	4.1896	7948
	TIM:	20.324	nmole/L				8	700	8.6	9.396	3.9966	9675
	Total Conc	5.9293	ng/uL				9	800	9	8.576	4.1685	9842
							10	900	8.7	7.415	4.0544	9346
D2	Ecoli 1						11	1000	9.3	7.154	4.3464	9241
Peak ID	Size (bp)	% (Conc.)	nmole/L	ng/ul	RFU		12	1500 (UM)		0.549	0.5	14766
1	35 (LM)		22.172	0.4748	11165							
2	69	2.1	4.249	0.1777	138			TIC:	46.5274	ng/uL		
3	80	5.1	8.648	0.4197	228			TIM:	205.03	nmole/L		
4	844	92.8	15.003	7.6979	5693			Total Conc	47.5559	ng/uL		
5	1500 (UM)		0.549	0.5	18653							
	TIC:	8.2952	ng/uL									
	TIM:	27.9	nmole/L									
	Total Conc	8.6807	ng/uL									
D3	Ecoli 2											
Peak ID	Size (bp)	% (Conc.)	nmole/L	ng/ul	RFU							
1	35 (LM)		30.532	0.6539	8374							
2	69	2.7	6.118	0.258	129							
3	80	5.6	11.062	0.5368	200							
4	837	91.7	17.316	8.8085	4149							
5	1500 (UM)		0.549	0.5	10269							
	TIC:	9.6033	ng/uL									
	TIM:	34.496	nmole/L									
	Total Conc	9.9528	ng/uL									
D4	Ecoli 3											
Peak ID	Size (bp)	% (Conc.)	nmole/L	ng/ul	RFU							
1	35 (LM)		22.799	0.4883	8756							
2	69	2.2	4.415	0.1862	115							
3	79	4.9	8.756	0.4218	186							
4	844	92.9	15.561	7.984	4549							
5	1500 (UM)		0.549	0.5	14451							
	TIC:	8.592	ng/uL									
	TIM:	28.732	nmole/L									
	Total Conc	8.8776	ng/uL									

Table 5.4.2-7 | Raw data from electrophoresis on the fragment analyzer (09.05.2018).

Well	Sample ID	Peak ID	Size (bp)	% (Conc.) (ng/uL)	nmole/L	ng/ul	RFU	TIC (ng/ul)	TIM (nmole/L)	Total Conc. (ng/ul)
H8	P. fluorescens 1	1	35		20.2741	0.4342	8031	13.795	43.6147	14.1026
H8	P. fluorescens 1	2	84	0.9	2.4887	0.1259	169	13.795	43.6147	14.1026
H8	P. fluorescens 1	3	94	7.1	16.8626	0.9859	335	13.795	43.6147	14.1026
H8	P. fluorescens 1	4	855	83.5	22.3037	11.5187	8164	13.795	43.6147	14.1026
H8	P. fluorescens 1	5	931	8.4	1.9597	1.1644	955	13.795	43.6147	14.1026
H8	P. fluorescens 1	6	1500		0.5498	0.5	15027	13.795	43.6147	14.1026
H9	P. fluorescens 2	1	35		20.7529	0.4445	8645	12.8399	38.5644	13.1382
H9	P. fluorescens 2	2	87	1.9	4.6669	0.2417	170	12.8399	38.5644	13.1382
H9	P. fluorescens 2	3	93	4.9	10.7445	0.6282	301	12.8399	38.5644	13.1382
H9	P. fluorescens 2	4	744	1.6	0.4695	0.2051	119	12.8399	38.5644	13.1382
H9	P. fluorescens 2	5	850	91.1	22.5908	11.6944	8714	12.8399	38.5644	13.1382
H9	P. fluorescens 2	6	1181	0.5	0.0925	0.0704	53	12.8399	38.5644	13.1382
H9	P. fluorescens 2	7	1500		0.5509	0.5	15950	12.8399	38.5644	13.1382
H10	P. fluorescens 3	1	35		20.4042	0.437	9466	12.2937	36.2117	12.5584
H10	P. fluorescens 3	2	87	1.9	4.4892	0.2325	179	12.2937	36.2117	12.5584
H10	P. fluorescens 3	3	93	4.7	9.7839	0.572	310	12.2937	36.2117	12.5584
H10	P. fluorescens 3	4	740	1.7	0.4688	0.2048	113	12.2937	36.2117	12.5584
H10	P. fluorescens 3	5	848	71.1	16.9785	8.7376	7837	12.2937	36.2117	12.5584
H10	P. fluorescens 3	6	931	20.3	4.4278	2.4992	4103	12.2937	36.2117	12.5584
H10	P. fluorescens 3	7	1188	0.4	0.0635	0.0476	51	12.2937	36.2117	12.5584
H10	P. fluorescens 3	8	1500		0.5513	0.5	17981	12.2937	36.2117	12.5584

Table 5.4.2-8 | Raw data from electrophoresis on the fragment analyzer (29.05.2018) for mixed samples of strains.

Well	Sample ID	Peak ID	Size (bp)	% (Conc.) (ng/uL)	nmole/L	ng/ul	RFU	TIC (ng/ul)	TIM (nmole/L)	Total Conc. (ng/ul)
B1	all 5-1	1	35		20.0156	0.4165	10568	8.9276	34.0664	9.174
B1	all 5-1	2	69	0.9	1.8551	0.0792	69	8.9276	34.0664	9.174
B1	all 5-1	3	79	1.9	3.3209	0.1659	111	8.9276	34.0664	9.174
B1	all 5-1	4	93	1.9	2.9697	0.1736	150	8.9276	34.0664	9.174
B1	all 5-1	5	143	0.4	0.4043	0.0352	63	8.9276	34.0664	9.174
B1	all 5-1	6	247	0.5	0.3042	0.0466	56	8.9276	34.0664	9.174
B1	all 5-1	7	302	0.4	0.2127	0.0389	55	8.9276	34.0664	9.174
B1	all 5-1	8	380	26	9.9763	2.3224	1971	8.9276	34.0664	9.174
B1	all 5-1	9	539	34.4	9.3365	3.0751	4632	8.9276	34.0664	9.174
B1	all 5-1	10	766	1.1	0.2236	0.1016	101	8.9276	34.0664	9.174
B1	all 5-1	11	831	23.5	4.1321	2.1014	2955	8.9276	34.0664	9.174
B1	all 5-1	12	930	8.8	1.3309	0.7876	588	8.9276	34.0664	9.174
B1	all 5-1	13	1500		0.5498	0.5	19572	8.9276	34.0664	9.174
B2	all 5-2	1	35		21.5696	0.462	11287	7.3762	28.4375	7.6545
B2	all 5-2	2	69	0.7	1.1599	0.0495	55	7.3762	28.4375	7.6545
B2	all 5-2	3	79	1.8	2.5993	0.1299	96	7.3762	28.4375	7.6545
B2	all 5-2	4	93	2.4	2.9594	0.1784	136	7.3762	28.4375	7.6545
B2	all 5-2	5	143	0.4	0.2984	0.026	52	7.3762	28.4375	7.6545
B2	all 5-2	6	378	28.5	9.041	2.0992	1830	7.3762	28.4375	7.6545
B2	all 5-2	7	538	36.6	8.2078	2.6984	4148	7.3762	28.4375	7.6545
B2	all 5-2	8	764	0.7	0.1061	0.0487	63	7.3762	28.4375	7.6545
B2	all 5-2	9	828	20.7	3.0095	1.525	2367	7.3762	28.4375	7.6545
B2	all 5-2	10	927	8.4	1.0561	0.6211	431	7.3762	28.4375	7.6545
B2	all 5-2	11	1500		0.5516	0.5	19518	7.3762	28.4375	7.6545
B3	all 5-3	1	35		21.2432	0.455	10707	6.5427	25.7861	6.8472
B3	all 5-3	2	69	1	1.4855	0.0634	59	6.5427	25.7861	6.8472
B3	all 5-3	3	79	2.4	3.1197	0.1578	98	6.5427	25.7861	6.8472
B3	all 5-3	4	94	2.8	3.0776	0.1799	150	6.5427	25.7861	6.8472
B3	all 5-3	5	379	25.6	7.2398	1.6766	1499	6.5427	25.7861	6.8472
B3	all 5-3	6	538	31.7	6.3092	2.0742	3301	6.5427	25.7861	6.8472
B3	all 5-3	7	828	26.9	3.4817	1.7621	2417	6.5427	25.7861	6.8472
B3	all 5-3	8	927	6.5	0.7557	0.4251	410	6.5427	25.7861	6.8472
B3	all 5-3	9	993	3.1	0.3169	0.2035	150	6.5427	25.7861	6.8472
B3	all 5-3	10	1500		0.5505	0.5	18306	6.5427	25.7861	6.8472
B4	all 4-1	1	35		19.7262	0.4105	11093	7.9926	29.3296	8.2419
B4	all 4-1	2	69	0.6	1.1819	0.0512	60	7.9926	29.3296	8.2419
B4	all 4-1	3	78	1.5	2.4976	0.1233	112	7.9926	29.3296	8.2419
B4	all 4-1	4	92	0.9	1.2603	0.0729	86	7.9926	29.3296	8.2419
B4	all 4-1	5	143	0.5	0.474	0.0418	75	7.9926	29.3296	8.2419
B4	all 4-1	6	379	29.7	10.2217	2.3733	2064	7.9926	29.3296	8.2419
B4	all 4-1	7	537	39.3	9.5443	3.1378	4938	7.9926	29.3296	8.2419
B4	all 4-1	8	762	0.8	0.1394	0.0641	99	7.9926	29.3296	8.2419
B4	all 4-1	9	828	18.7	2.941	1.4921	2463	7.9926	29.3296	8.2419
B4	all 4-1	10	927	8	1.0694	0.6361	512	7.9926	29.3296	8.2419
B4	all 4-1	11	1500		0.5505	0.5	20734	7.9926	29.3296	8.2419
B5	all 4-2	1	35		20.1189	0.4309	11206	8.3319	30.6454	8.5097
B5	all 4-2	2	69	0.7	1.4321	0.0611	62	8.3319	30.6454	8.5097
B5	all 4-2	3	79	1.6	2.6772	0.1338	120	8.3319	30.6454	8.5097
B5	all 4-2	4	93	0.9	1.3185	0.0763	95	8.3319	30.6454	8.5097
B5	all 4-2	5	143	0.6	0.5732	0.0502	83	8.3319	30.6454	8.5097
B5	all 4-2	6	379	28.9	10.336	2.4061	2074	8.3319	30.6454	8.5097
B5	all 4-2	7	517	0.4	0.1052	0.0329	50	8.3319	30.6454	8.5097
B5	all 4-2	8	539	37.9	9.6024	3.1569	4900	8.3319	30.6454	8.5097
B5	all 4-2	9	764	1.5	0.2754	0.1246	122	8.3319	30.6454	8.5097
B5	all 4-2	10	828	19.2	3.1629	1.6027	2625	8.3319	30.6454	8.5097
B5	all 4-2	11	927	8.2	1.1626	0.6873	495	8.3319	30.6454	8.5097
B5	all 4-2	12	1500		0.5516	0.5	20205	8.3319	30.6454	8.5097
B6	all 3-1	1	35		20.4631	0.4258	9529	11.1376	40.5057	11.3993
B6	all 3-1	2	69	0.6	1.5551	0.0664	60	11.1376	40.5057	11.3993
B6	all 3-1	3	79	1.5	3.2578	0.1628	111	11.1376	40.5057	11.3993
B6	all 3-1	4	93	1	1.9847	0.116	103	11.1376	40.5057	11.3993
B6	all 3-1	5	247	0.2	0.1682	0.0252	52	11.1376	40.5057	11.3993
B6	all 3-1	6	379	29.7	14.1943	3.3129	2149	11.1376	40.5057	11.3993
B6	all 3-1	7	517	0.4	0.139	0.0434	56	11.1376	40.5057	11.3993
B6	all 3-1	8	539	40.2	13.6036	4.4806	5209	11.1376	40.5057	11.3993
B6	all 3-1	9	831	20.6	4.5176	2.292	2969	11.1376	40.5057	11.3993
B6	all 3-1	10	927	5.7	1.0854	0.6384	423	11.1376	40.5057	11.3993
B6	all 3-1	11	1500		0.5513	0.5	17313	11.1376	40.5057	11.3993
B7	all 3-2	1	35		20.5765	0.4282	7300	8.7552	31.5795	9.1091
B7	all 3-2	2	78	1.5	2.6386	0.1318	65	8.7552	31.5795	9.1091
B7	all 3-2	3	92	1.6	2.4117	0.141	84	8.7552	31.5795	9.1091
B7	all 3-2	4	379	30.5	11.4626	2.6684	1414	8.7552	31.5795	9.1091
B7	all 3-2	5	538	40.4	10.7315	3.5346	3440	8.7552	31.5795	9.1091
B7	all 3-2	6	831	19.6	3.3749	1.7122	1817	8.7552	31.5795	9.1091
B7	all 3-2	7	930	6.5	0.9603	0.5671	285	8.7552	31.5795	9.1091
B7	all 3-2	8	1500		0.5498	0.5	13558	8.7552	31.5795	9.1091

Table 5.4.2-9 | Raw data from electrophoresis on the fragment analyzer (26.09.2018) for mixed samples of strains.

Well	Sample ID	Peak ID	Size (bp)	% (Conc.) (ng/uL)	nmole/L	ng/ul	RFU	TIC (ng/ul)	TIM (nmole/L)	Total Conc. (ng/ul)
H1	all 5 I	1	35		22.7729	0.4877	7347	5.4816	21.3663	5.9855
H1	all 5 I	2	77	1.8	2.03	0.0965	69	5.4816	21.3663	5.9855
H1	all 5 I	3	91	1.5	1.5282	0.0847	87	5.4816	21.3663	5.9855
H1	all 5 I	4	374	36.4	8.7869	1.9975	1678	5.4816	21.3663	5.9855
H1	all 5 I	5	541	44.1	7.3369	2.4165	3112	5.4816	21.3663	5.9855
H1	all 5 I	6	843	12.9	1.3708	0.7046	730	5.4816	21.3663	5.9855
H1	all 5 I	7	940	3.3	0.3135	0.1817	122	5.4816	21.3663	5.9855
H1	all 5 I	8	1500		0.5505	0.5	9959	5.4816	21.3663	5.9855
H2	all 4 I	1	35		22.3843	0.4794	7742	4.1289	15.476	4.6065
H2	all 4 I	2	77	1.2	1.0865	0.0503	64	4.1289	15.476	4.6065
H2	all 4 I	3	91	1.5	1.1355	0.0623	76	4.1289	15.476	4.6065
H2	all 4 I	4	372	35.3	6.4256	1.4568	1291	4.1289	15.476	4.6065
H2	all 4 I	5	540	42	5.2839	1.7339	2577	4.1289	15.476	4.6065
H2	all 4 I	6	843	13.9	1.1228	0.5758	643	4.1289	15.476	4.6065
H2	all 4 I	7	940	6.1	0.4218	0.2498	120	4.1289	15.476	4.6065
H2	all 4 I	8	1500		0.5513	0.5	10702	4.1289	15.476	4.6065
H3	all 3 I	1	35		30.2228	0.6289	5417	5.2873	23.7622	5.9813
H3	all 3 I	2	77	2	2.3092	0.107	74	5.2873	23.7622	5.9813
H3	all 3 I	3	82	2.5	2.5782	0.1304	61	5.2873	23.7622	5.9813
H3	all 3 I	4	90	3.8	3.6508	0.2024	117	5.2873	23.7622	5.9813
H3	all 3 I	5	372	30.5	7.1324	1.6127	817	5.2873	23.7622	5.9813
H3	all 3 I	6	540	33.1	5.329	1.752	1422	5.2873	23.7622	5.9813
H3	all 3 I	7	841	18.5	1.9089	0.9777	598	5.2873	23.7622	5.9813
H3	all 3 I	8	940	9.6	0.8537	0.5052	109	5.2873	23.7622	5.9813
H3	all 3 I	9	1500		0.5494	0.5	5835	5.2873	23.7622	5.9813
H4	all 5 II	1	35		24.4308	0.5084	6596	4.1753	19.497	4.6875
H4	all 5 II	2	77	2.3	2.0969	0.0971	95	4.1753	19.497	4.6875
H4	all 5 II	3	82	2.2	1.8553	0.0938	69	4.1753	19.497	4.6875
H4	all 5 II	4	90	4	3.0121	0.167	136	4.1753	19.497	4.6875
H4	all 5 II	5	372	33.8	6.2494	1.4093	1091	4.1753	19.497	4.6875
H4	all 5 II	6	539	35.3	4.5052	1.4729	1834	4.1753	19.497	4.6875
H4	all 5 II	7	841	17.7	1.4386	0.7386	642	4.1753	19.497	4.6875
H4	all 5 II	8	940	4.7	0.3396	0.1966	100	4.1753	19.497	4.6875
H4	all 5 II	9	1500		0.5509	0.5	9096	4.1753	19.497	4.6875
H5	all 4 II	1	35		22.5319	0.4826	8410	8.1512	33.4275	8.5251
H5	all 4 II	2	68	1	1.9898	0.0825	73	8.1512	33.4275	8.5251
H5	all 4 II	3	77	2.5	4.1029	0.2	124	8.1512	33.4275	8.5251
H5	all 4 II	4	91	2.2	3.2017	0.1794	180	8.1512	33.4275	8.5251
H5	all 4 II	5	374	30.9	11.0587	2.5206	2230	8.1512	33.4275	8.5251
H5	all 4 II	6	543	36.5	9.0096	2.9784	4333	8.1512	33.4275	8.5251
H5	all 4 II	7	846	18.9	2.9915	1.5413	1701	8.1512	33.4275	8.5251
H5	all 4 II	8	943	8	1.0733	0.6489	331	8.1512	33.4275	8.5251
H5	all 4 II	9	1500		0.5494	0.5	11503	8.1512	33.4275	8.5251
H6	all 5 III	1	35		22.0735	0.4593	6124	12.0206	44.5164	12.3904
H6	all 5 III	2	82	1.2	2.8193	0.1409	86	12.0206	44.5164	12.3904
H6	all 5 III	3	91	2.5	5.3561	0.3001	191	12.0206	44.5164	12.3904
H6	all 5 III	4	143	0.4	0.5465	0.0472	57	12.0206	44.5164	12.3904
H6	all 5 III	5	374	29.5	15.5565	3.5458	2192	12.0206	44.5164	12.3904
H6	all 5 III	6	542	37.3	13.5904	4.4845	4553	12.0206	44.5164	12.3904
H6	all 5 III	7	682	0.3	0.0999	0.0414	53	12.0206	44.5164	12.3904
H6	all 5 III	8	777	0.7	0.1873	0.0877	66	12.0206	44.5164	12.3904
H6	all 5 III	9	843	22.4	5.22	2.6958	2111	12.0206	44.5164	12.3904
H6	all 5 III	10	943	4.8	0.9932	0.5775	367	12.0206	44.5164	12.3904
H6	all 5 III	11	1105	0.8	0.1472	0.0996	79	12.0206	44.5164	12.3904
H6	all 5 III	12	1500		0.5498	0.5	8877	12.0206	44.5164	12.3904
H7	all 4 III	1	35		23.0048	0.4787	5353	16.1496	59.8841	16.6375
H7	all 4 III	2	82	0.8	2.5147	0.1272	69	16.1496	59.8841	16.6375
H7	all 4 III	3	91	1.7	4.8726	0.2731	154	16.1496	59.8841	16.6375
H7	all 4 III	4	143	0.5	0.8982	0.0787	54	16.1496	59.8841	16.6375
H7	all 4 III	5	375	34.7	24.5151	5.6027	2656	16.1496	59.8841	16.6375
H7	all 4 III	6	543	43.7	21.3696	7.0515	5644	16.1496	59.8841	16.6375
H7	all 4 III	7	777	0.5	0.183	0.0863	58	16.1496	59.8841	16.6375
H7	all 4 III	8	843	14.2	4.4438	2.2869	1596	16.1496	59.8841	16.6375
H7	all 4 III	9	940	3.4	0.9467	0.547	304	16.1496	59.8841	16.6375
H7	all 4 III	10	1105	0.6	0.1404	0.0963	57	16.1496	59.8841	16.6375
H7	all 4 III	11	1500		0.5509	0.5	7423	16.1496	59.8841	16.6375

6. Summary and outlook

The present study comprises three pathways in the nitrogen cycle, the nitrification, the denitrification and the anammox process in two different technical systems, an aquaponic system for sustainable food production and a bioelectrochemical system for bioremediation processes. Both systems provide great potential for the future, although many basic research questions still have to be addressed.

6.1. **Aquaponic systems for food production**

With the world's population growing the necessity of innovative food production systems increases to meet primary human needs. Moreover, climate changes will restrict agricultural areas additionally in the future. An aquaponic system fulfils the requirements as a system for sustainable fish cultivation and vegetable production. The efficiency of an aquaponic system relies on the productivity of the microorganisms that adapted to the system. They cycle the nitrogen species to avoid intoxication of the fish and to provide nutrients for the vegetables and fruits. In this study, it was shown that ammonium produced by fish can be converted by one single organism in the comammox process in an aquaponic system.

The results obtained in this study provide additional information, which were not further investigated. Sequencing data, for instance, revealed high abundances of *Verrucomicrobia*. *Verrucomicrobia* were described as aerobic mixotrophs using methane and hydrogen as electron donors (Carere *et al.*, 2017). Their role in the aquaponic system, however, remains rather unclear. The presence of methanotrophs indicate an influence of the carbon cycle on the efficiency of the system due to the degradation of organic matters. The question is to what extent other nutrient cycles affect the whole aquaponic system in general and the nitrogen turnover specifically. Studying these research questions could provide deep insights into the system and may lead to optimization of the system to meet the growing human needs in future (Eck *et al.*, 2019).

6.2. **Denitrification in BES for drinking water production**

The need for high crop yields for food production elucidated the usage of high amounts of (ammonium) nitrate on agricultural areas. The surplus of nitrate that contaminated the groundwaters turned out to be a major problem in the drinking water production. In this study, fundamental research was carried out to investigate nitrate in batch BES. It was shown that different potential settings, intermittently and continuously runs of BES, revealed different bacterial community compositions in the cathode biofilm. The findings support the assumption that the applied settings for the BES determine the community composition on the electrode (Rabaey *et al.*, 2007, Wrighton *et al.*, 2010). Understanding the community composition then may help to optimize the BES performance, for instance, identifying unwanted side reactions that occur during operation.

The major question that has to be addressed in future is the up-scaling of BES. Although, such systems work very well in laboratory scale, they fail the performance in large scale systems because in contrast to the material sizes the size of bacterial cells cannot be enlarged. The enrichment of bacteria in the medium to increase their concentration takes time. Nevertheless, large scale BES have been introduced as pilot plants already and showed promising results for bioremediation of waste waters (San-Martín *et al.*, 2018, Enzmann & Holtmann, 2019). In future, they may find application in drinking water production plants for the removal of nitrate and other contaminants. They may also be implemented directly in a groundwater aquifer as it was tested before (Zhang & Angelidaki, 2013, Nguyen *et al.*, 2016).

6.3. **The anammox process in BES for wastewater treatment**

Highly ammonium loaded wastewaters pose a major challenge to the performance of treatment plants. Bioelectrochemical systems can address the challenge due to the possibility of steering the reactions by specific potential or current settings towards an optimized bioremediation such as ammonium removal.

The batch reactor is a suitable system for the analysis of communities in BES because they are usually easier to maintain, and the laminar flow of the medium is

less strong than in the upflow BES supporting the adhesion of microorganisms on the electrodes. However, losses occur in these systems, such as activation and ohmic losses, decreasing the overall performance of the BES.

Future studies may focus on the application of upflow BES, where losses can be reduced more easily. This study also showed that the adjustment of specific oxygen concentrations was best achieved in upflow BES. Large electrode surfaces also provide the possibility of expanded biofilm layers to facilitate electron transfer from the bacterial cells to the anodes. It should also be considered whether stacked systems as investigated, for instance, by Aelterman *et al.* (2006) can be introduced to improve the ammonium removal process.

The enrichment of AerAOB and anammox bacteria in a double-layered biofilm on the anode could not be established adequately in this study. The idea of pre-conditioning the oxygen generating anode before adding oxygen sensitive microorganisms, however, seems to be the most promising approach to keep both processes running in a BES.

6.4. **The RFLP technique for rapid in-house analysis**

Next-generation sequencing methods became quite affordable over the past years. However, it still needs some time until results are available. The complete RFLP technique described in this study needs approximately eight hours depending on the kits used and the number of samples. If a fragment analyser is available, the number of samples is of minor importance. For sequencing, the sample preparation alone can last a whole day. Since many samples are usually comprised to lower costs for shipment to appropriate companies for processing, the samples may be stored for days until shipment. Sequencers are relative expensive and not present in many institutes. Furthermore, the results are not directly readable data which makes their processing inevitable. To simply check enrichment cultures and strains used in the laboratory, the costs of shipment, sample processing and data processing are incommensurate with the outcoming results. With the proposed RFLP technique, results are obtained directly after the electrophoresis. The RF patterns can be analysed quickly for low diverse samples.

In this study, however, some issues concerning the application were observed. To implement the technique as standard method, all technical parameters used in the PCR, in the restriction and for the electrophoresis run such as concentrations, temperatures, and incubation times have to be investigated to optimize the procedure concerning its susceptibility to interferences. The RFLP procedure is a first step to facilitate community analysis of very low diverse samples. Since capillary electrophoresis on a fragment analyser measures fragments based on their fluorescence intensity, one could take a step further to analyses only fluorescently labelled terminal RFs, called T-RFs. In this technique, fluorescently labelled primers are used to mark the last fragment of a restricted PCR amplicon. As a result, the RF patterns are thinned out and only the fluorescent T-RFs are visible in an electropherograms. The combination of the T-RFLP on a fragment analyser, therefore, shows promising potential for rapid in-house community analysis for samples that are slightly more diverse such as enrichment cultures used for instance in bioelectrochemical systems or comparable enrichment reactors.

7. Bibliography

Abraham ZH, Lowe D & Smith BE (1993) Purification and characterization of the dissimilatory nitrite reductase from *Alcaligenes xylosoxidans* subsp. *xylosoxidans* (NCIMB 11015): evidence for the presence of both type 1 and type 2 copper centres. *Biochem J* **295**: 587-593.

Aelterman P, Rabaey K, Pham HT, Boon N & Verstraete W (2006) Continuous electricity generation at high voltages and currents using stacked microbial fuel cells. *Environ Sci Technol* **40**: 3388-3394.

Afkar E, Reguera G, Schiffer M & Lovley DR (2005) A novel *Geobacteraceae*-specific outer membrane protein J (OmpJ) is essential for electron transport to Fe (III) and Mn (IV) oxides in *Geobacter sulfurreducens*. *BMC microbiology* **5**: 41.

Agnelli A, Ascher J, Corti G, Ceccherini MT, Nannipieri P & Pietramellara G (2004) Distribution of microbial communities in a forest soil profile investigated by microbial biomass, soil respiration and DGGE of total and extracellular DNA. *Soil Biol Biochem* **36**: 859-868.

Alonso A & Camargo J (2003) Short-term toxicity of ammonia, nitrite, and nitrate to the aquatic snail *Potamopyrgus antipodarum* (Hydrobiidae, Mollusca). *Bull Environ Contam Toxicol* **70**: 1006-1012.

Anders H-J, Kaetzke A, Kämpfer P, Ludwig W & Fuchs G (1995) Taxonomic position of aromatic-degrading denitrifying pseudomonad strains K 172 and KB 740 and their description as new members of the genera *Thauera*, as *Thauera aromatica* sp. nov., and *Azoarcus*, as *Azoarcus evansii* sp. nov., respectively, members of the beta subclass of the *Proteobacteria*. *Int J Syst Evol Microbiol* **45**: 327-333.

Anderson DM, Glibert PM & Burkholder JM (2002) Harmful algal blooms and eutrophication: nutrient sources, composition, and consequences. *Estuaries* **25**: 704-726.

Appelo CAJ & Postma D (2004) *Geochemistry, groundwater and pollution*. CRC press.

Arai H, Igarashi Y & Kodama T (1995) The structural genes for nitric oxide reductase from *Pseudomonas aeruginosa*. *Biochim Biophys Acta, Gene Struct Expression* **1261**: 279-284.

Arp DJ, Sayavedra-Soto LA & Hommes NG (2002) Molecular biology and biochemistry of ammonia oxidation by *Nitrosomonas europaea*. *Arch Microbiol* **178**: 250-255.

Arp DJ, Chain PS & Klotz MG (2007) The impact of genome analyses on our understanding of ammonia-oxidizing bacteria. *Annu Rev Microbiol* **61**: 503-528.

Arrigo KR (2004) Marine microorganisms and global nutrient cycles. *Nature* **437**: 349.

Avaniss-Aghajani E, Jones K, Chapman D & Brunk C (1994) A molecular technique for identification of bacteria using small subunit ribosomal RNA sequences. *BioTechniques* **17**: 144-146, 148-149.

Avaniss-Aghajani E, Jones K, Holtzman A, Aronson T, Glover N, Boian M, Froman S & Brunk CF (1996) Molecular technique for rapid identification of mycobacteria. *J Clin Microbiol* **34**: 98-102.

Bäckman JS, Hermansson A, Tebbe CC & Lindgren P-E (2003) Liming induces growth of a diverse flora of ammonia-oxidising bacteria in acid spruce forest soil as determined by SSCP and DGGE. *Soil Biol Biochem* **35**: 1337-1347.

Bartelme RP, McLellan SL & Newton RJ (2017) Freshwater recirculating aquaculture system operations drive biofilter bacterial community shifts around a stable nitrifying consortium of ammonia-oxidizing *archaea* and comammox *Nitrospira*. *Front Microbiol* **8**: 101.

Beeckman F, Motte H & Beeckman T (2018) Nitrification in agricultural soils: impact, actors and mitigation. *Curr Opin Biotechnol* **50**: 166-173.

Berks B, Richardson D, Reilly A, Willis A & Ferguson S (1995) The napEDABC gene cluster encoding the periplasmic nitrate reductase system of Thiosphaera pantotropha. *Biochem J* **309**: 983-992.

Bio-Rad Laboratories Inc. (2006) Real-Time PCR - Applications Guide. http://wwwbio-radcom/webroot/web/pdf/lsr/literature/Bulletin_5279pdf Last access: 24-04-2020.

Black EM & Just CL (2018) The genomic potentials of NOB and comammox *Nitrospira* in river sediment are impacted by native freshwater mussels. *Front Microbiol* **9**: 2061.

Blasco F, Dos Santos JP, Magalon A, Frixon C, Guigliarelli B, Santini CL & Giordano G (1998) NarJ is a specific chaperone required for molybdenum cofactor assembly in nitrate reductase A of *Escherichia coli*. *Mol Microbiol* **28**: 435-447.

Bock E, Koops H, Harms H & Ahlers B (1991) The biochemistry of nitrifying organisms. In: *Variations in autotrophic life,*(Shirley JM & Barton LL, eds.), 171-200. Academic Press, Ltd., London.

Boon N, De Windt W, Verstraete W & Top EM (2002) Evaluation of nested PCR–DGGE (denaturing gradient gel electrophoresis) with group-specific 16S rRNA primers for the analysis of bacterial communities from different wastewater treatment plants. *FEMS Microbiol Ecol* **39**: 101-112.

Boyle E (2017) Nitrogen pollution knows no bounds. *Science* **356**: 700-701.

Braker G & Tiedje JM (2003) Nitric oxide reductase (norB) genes from pure cultures and environmental samples. *Appl Environ Microbiol* **69**: 3476-3483.

Braker G, Zhou J, Wu L, Devol AH & Tiedje JM (2000) Nitrite reductase genes (nirK andnirS) as functional markers to investigate diversity of denitrifying bacteria in Pacific Northwest marine sediment communities. *Appl Environ Microbiol* **66**: 2096-2104.

Braker G, Ayala-del-Río HL, Devol AH, Fesefeldt A & Tiedje JM (2001) Community structure of denitrifiers, Bacteria, and Archaea along redox gradients in Pacific Northwest marine sediments by terminal restriction fragment length polymorphism analysis of amplified nitrite reductase (nirS) and 16S rRNA genes. *Appl Environ Microbiol* **67**: 1893-1901.

Breitburg D (2002) Effects of hypoxia, and the balance between hypoxia and enrichment, on coastal fishes and fisheries. *Estuaries* **25**: 767-781.

Brender JD, Olive JM, Felkner M, Suarez L, Marckwardt W & Hendricks KA (2004) Dietary nitrites and nitrates, nitrosatable drugs, and neural tube defects. *Epidemiology* **15**: 330-336.

Bridier A, Briandet R, Thomas V & Dubois-Brissonnet F (2011) Resistance of bacterial biofilms to disinfectants: a review. *Biofouling* **27**: 1017-1032.

Brown K, Tegoni M, Prudêncio M, Pereira AS, Besson S, Moura JJ, Moura I & Cambillau C (2000) A novel type of catalytic copper cluster in nitrous oxide reductase. *Nat Struct Mol Biol* **7**: 191.

Brown MN, Briones A, Diana J & Raskin L (2012) Ammonia-oxidizing archaea and nitrite-oxidizing nitrospiras in the biofilter of a shrimp recirculating aquaculture system. *FEMS Microbiol Ecol* **83**: 17-25.

Bruce KD (1997) Analysis of mer gene subclasses within bacterial communities in soils and sediments resolved by fluorescent-PCR-restriction fragment length polymorphism profiling. *Appl Environ Microbiol* **63**: 4914-4919.

Call D & Logan BE (2008) Hydrogen production in a single chamber microbial electrolysis cell lacking a membrane. *Environ Sci Technol* **42**: 3401-3406.

Callahan BJ, McMurdie PJ, Rosen MJ, Han AW, Johnson AJA & Holmes SP (2016) DADA2: high-resolution sample inference from Illumina amplicon data. *Nat Methods* **13**: 581.

Camargo JA & Alonso Á (2006) Ecological and toxicological effects of inorganic nitrogen pollution in aquatic ecosystems: a global assessment. *Environ Int* **32**: 831-849.

Carere CR, Hards K, Houghton KM, Power JF, McDonald B, Collet C, Gapes DJ, Sparling R, Boyd ES & Cook GM (2017) Mixotrophy drives niche expansion of verrucomicrobial methanotrophs. *ISME J* **11**: 2599-2610.

Carvajal-Arroyo JM, Sun W, Sierra-Alvarez R & Field JA (2013) Inhibition of anaerobic ammonium oxidizing (anammox) enrichment cultures by substrates, metabolites and common wastewater constituents. *Chemosphere* **91**: 22-27.

Cecconet D, Devecseri M, Callegari A & Capodaglio A (2018) Effects of process operating conditions on the autotrophic denitrification of nitrate-contaminated groundwater using bioelectrochemical systems. *Sci Total Environ* **613**: 663-671.

Cho S-K, Lee M-E, Lee W & Ahn Y (2019) Improved hydrogen recovery in microbial electrolysis cells using intermittent energy input. *Int J Hydrogen Energ* **44**: 2253-2257.

Cissé IA & Mao X (2008) Nitrate: Health effect in drinking water and management for water quality. *Environ Res* **2**: 311-316.

Clauwaert P, Aelterman P, De Schamphelaire L, Carballa M, Rabaey K & Verstraete W (2008) Minimizing losses in bio-electrochemical systems: the road to applications. *Appl Microbiol Biotechnol* **79**: 901-913.

Clement BG, Kehl LE, DeBord KL & Kitts CL (1998) Terminal restriction fragment patterns (TRFPs), a rapid, PCR-based method for the comparison of complex bacterial communities. *J Microbiol Methods* **31**: 135-142.

Coates JD, Chakraborty R, Lack JG, O'Connor SM, Cole KA, Bender KS & Achenbach LA (2001) Anaerobic benzene oxidation coupled to nitrate reduction in pure culture by two strains of *Dechloromonas*. *Nature* **411**: 1039-1043.

Conley DJ, Paerl HW, Howarth RW, Boesch DF, Seitzinger SP, Havens KE, Lancelot C & Likens GE (2009) Controlling eutrophication: nitrogen and phosphorus. *Science* **323**: 1014-1015.

Costa E, Pérez J & Kreft J-U (2006) Why is metabolic labour divided in nitrification? *Trends Microbiol* **14**: 213-219.

Curtis TP, Sloan WT & Scannell JW (2002) Estimating prokaryotic diversity and its limits. *PNAS* **99**: 10494-10499.

Daims H, Nielsen JL, Nielsen PH, Schleifer KH & Wagner M (2001) In situ characterization of *Nitrospira*-like nitrite-oxidizing bacteria active in wastewater treatment plants. *Appl Environ Microbiol* **67**: 5273-5284.

Daims H, Lebedeva EV, Pjevac P, Han P, Herbold C, Albertsen M, Jehmlich N, Palatinszky M, Vierheilig J & Bulaev A (2015) Complete nitrification by *Nitrospira* bacteria. *Nature* **528**: 504-509.

Damsté JSS, Rijpstra WIC, Geenevasen JA, Strous M & Jetten MSM (2005) Structural identification of ladderane and other membrane lipids of planctomycetes capable of anaerobic ammonium oxidation (anammox). *FEBS J* **272**: 4270-4283.

Damsté JSS, Strous M, Rijpstra WIC, Hopmans EC, Geenevasen JA, Van Duin AC, Van Niftrik LA & Jetten MS (2002) Linearly concatenated cyclobutane lipids form a dense bacterial membrane. *Nature* **419**: 708.

De Beer D, Stoodley P, Roe F & Lewandowski Z (1994) Effects of biofilm structures on oxygen distribution and mass transport. *Biotechnology and bioengineering* **43**: 1131-1138.

De Boer W, Gunnewiek PK, Veenhuis M, Bock E & Laanbroek H (1991) Nitrification at low pH by aggregated chemolithotrophic bacteria. *Appl Environ Microbiol* **57**: 3600-3604.

Deutsche Bundesregierung (2004) *Verordnung über Anforderungen an das Einleiten von Abwasser in Gewässer, AbwV-Abwasserverordnung, Anhang 22 Chemische Industrie*. BGBl.

Dodds WK, Smith VH & Lohman K (2002) Nitrogen and phosphorus relationships to benthic algal biomass in temperate streams. *Can J Fish Aquat Sci* **59**: 865-874.

Dong X, Kleiner M, Sharp CE, Thorson E, Li C, Liu D & Strous M (2017) Fast and simple analysis of MiSeq amplicon sequencing data with MetaAmp. *Front Microbiol* **8**: 1461.

Du Z, Li H & Gu T (2007) A state of the art review on microbial fuel cells: a promising technology for wastewater treatment and bioenergy. *Biotechnol Adv* **25**: 464-482.

Eck M, Körner O & Jijakli MH (2019) Nutrient cycling in aquaponics systems. In: *Aquaponics Food Production Systems,*(Goddek S, Joyce A, Kotzen B & Burnell GM, eds.), 231-246. Springer Nature, Cham.

Edlund A, Soule T, Sjöling S & Jansson JK (2006) Microbial community structure in polluted Baltic Sea sediments. *Environ Microbiol* **8**: 223-232.

Egert M & Friedrich MW (2003) Formation of pseudo-terminal restriction fragments, a PCR-related bias affecting terminal restriction fragment length polymorphism analysis of microbial community structure. *Appl Environ Microbiol* **69**: 2555-2562.

Egli K, Fanger U, Alvarez PJ, Siegrist H, van der Meer JR & Zehnder AJ (2001) Enrichment and characterization of an anammox bacterium from a rotating biological contactor treating ammonium-rich leachate. *Arch Microbiol* **175**: 198-207.

Enzmann F & Holtmann D (2019) Rational Scale-Up of a methane producing bioelectrochemical reactor to 50 L pilot scale. *Chem Eng Sci* **207**: 1148-1158.

Erisman JW, Galloway JN, Seitzinger S, Bleeker A, Dise NB, Petrescu AR, Leach AM & de Vries W (2013) Consequences of human modification of the global nitrogen cycle. *Phil Trans R Soc B* **368**: 20130116.

Espejo-Herrera N, Gràcia-Lavedan E, Boldo E, Aragonés N, Pérez-Gómez B, Pollán M, Molina AJ, Fernández T, Martín V & La Vecchia C (2016) Colorectal cancer risk and nitrate exposure through drinking water and diet. *Int J Cancer* **139**: 334-346.

Espinal P, Marti S & Vila J (2012) Effect of biofilm formation on the survival of *Acinetobacter baumannii* on dry surfaces. *J Hosp Infect* **80**: 56-60.

European Commission (2018) Report from the Commission to the Council and the European Parliament on the implementation of Council Directive 91/676/EEC concerning the protection of waters against pollution caused by nitrates from agricultural sources based on Member State reports for the period 2012–2015. **COM/2018/257 final**,European Commission Brussels.

Fan AM & Steinberg VE (1996) Health implications of nitrate and nitrite in drinking water: an update on methemoglobinemia occurrence and reproductive and developmental toxicity. *Regul Toxicol Pharmacol* **23**: 35-43.

Fierer N & Jackson RB (2006) The diversity and biogeography of soil bacterial communities. *PNAS* **103**: 626-631.

Flemming H-C & Wingender J (2010) The biofilm matrix. *Nat Rev Microbiol* **8**: 623-633.

Foesel BU, Gieseke A, Schwermer C, Stief P, Koch L, Cytryn E, De La Torré JR, Van Rijn J, Minz D & Drake HL (2007) *Nitrosomonas* Nm143-like ammonia oxidizers and *Nitrospira marina*-like nitrite oxidizers dominate the nitrifier community in a marine aquaculture biofilm. *FEMS Microbiol Ecol* **63**: 192-204.

Fowler SJ, Palomo A, Dechesne A, Mines PD & Smets BF (2018) Comammox *Nitrospira* are abundant ammonia oxidizers in diverse groundwater-fed rapid sand filter communities. *Environ Microbiol* **20**: 1002-1015.

Francis CA, Beman JM & Kuypers MM (2007) New processes and players in the nitrogen cycle: the microbial ecology of anaerobic and archaeal ammonia oxidation. *ISME J* **1**: 19.

Freguia S, Rabaey K, Yuan Z & Keller J (2008) Sequential anode–cathode configuration improves cathodic oxygen reduction and effluent quality of microbial fuel cells. *Water Res* **42**: 1387-1396.

Galloway JN, Aber JD, Erisman JW, Seitzinger SP, Howarth RW, Cowling EB & Cosby BJ (2003) The nitrogen cascade. *Bioscience* **53**: 341-356.

Gildemyn S, Verbeeck K, Slabbinck R, Andersen SJ, Prévoteau A & Rabaey K (2015) Integrated production, extraction, and concentration of acetic acid from CO_2 through microbial electrosynthesis. *Environ Sci Technol Lett* **2**: 325-328.

Goel RK & Flora JR (2005) Sequential nitrification and denitrification in a divided cell attached growth bioelectrochemical reactor. *Environ Eng Sci* **22**: 440-449.

Gonzalez-Martinez A, Rodriguez-Sanchez A, van Loosdrecht MM, Gonzalez-Lopez J & Vahala R (2016) Detection of comammox bacteria in full-scale wastewater treatment bioreactors using tag-454-pyrosequencing. *Environ Sci Pollut Res* **23**: 25501-25511.

Gregory KB, Bond DR & Lovley DR (2004) Graphite electrodes as electron donors for anaerobic respiration. *Environ Microbiol* **6**: 596-604.

Gregory SP, Dyson PJ, Fletcher D, Gatland P & Shields RJ (2012) Nitrogen removal and changes to microbial communities in model flood/drain and submerged biofilters treating aquaculture wastewater. *Aquac Eng* **50**: 37-45.

Gudat JC, Singh J & Wharton DC (1973) Cytochrome oxidase from *Pseudomonas aeruginosa*. I. Purification and some properties. *BBA Bioenergetics* **292**: 376-390.

Guo K, Prévoteau A, Patil SA & Rabaey K (2015) Engineering electrodes for microbial electrocatalysis. *Curr Opin Biotechnol* **33**: 149-156.

Harnisch F & Schröder U (2010) From MFC to MXC: chemical and biological cathodes and their potential for microbial bioelectrochemical systems. *Chem Soc Rev* **39**: 4433-4448.

Harnisch F, Schröder U & Scholz F (2008) The suitability of monopolar and bipolar ion exchange membranes as separators for biological fuel cells. *Environ Sci Technol* **42**: 1740-1746.

Harnisch F, Koch C, Patil SA, Hübschmann T, Müller S & Schröder U (2011) Revealing the electrochemically driven selection in natural community derived microbial biofilms using flow-cytometry. *Energy Environ Sci* **4**: 1265-1267.

Hayashi H, Sakamoto M, Kitahara M & Benno Y (2003) Molecular analysis of fecal microbiota in elderly individuals using 16S rDNA library and T-RFLP. *Microbiol Immunol* **47**: 557-570.

Heylen K, Vanparys B, Gevers D, Wittebolle L, Boon N & De Vos P (2007) Nitric oxide reductase (norB) gene sequence analysis reveals discrepancies with nitrite reductase (nir) gene phylogeny in cultivated denitrifiers. *Environ Microbiol* **9**: 1072-1077.

Hino T, Matsumoto Y, Nagano S, Sugimoto H, Fukumori Y, Murata T, Iwata S & Shiro Y (2010) Structural basis of biological N_2O generation by bacterial nitric oxide reductase. *Science* **330**: 1666-1670.

Hochheimer JN & Wheaton F (1998) Biological filters: Trickling and RBC design. *Proc 2nd Intl Conf Recirculating Aquaculture* 291-318.

Hochmuth G (2001) Fertilizer management for greenhouse vegetables. *Florida Greenhouse Vegetable Production Handbook* **3**: 13-31.

Horn MA, Ihssen J, Matthies C, Schramm A, Acker G & Drake HL (2005) *Dechloromonas denitrificans* sp. nov., *Flavobacterium denitrificans* sp. nov., *Paenibacillus anaericanus* sp. nov. and *Paenibacillus terrae* strain MH72, N_2O-producing bacteria isolated from the gut of the earthworm *Aporrectodea caliginosa*. *Int J Syst Evol Microbiol* **55**: 1255-1265.

Hsu L, Mohamed A, Ha PT, Bloom J, Ewing T, Arias-Thode M, Chadwick B & Beyenal H (2017) The influence of energy harvesting strategies on performance and microbial community for sediment microbial fuel cells. *J Electrochem Soc* **164**: H3109-H3114.

Inoue-Choi M, Ward MH, Cerhan JR, Weyer PJ, Anderson KE & Robien K (2012) Interaction of nitrate and folate on the risk of breast cancer among postmenopausal women. *Nutr Cancer* **64**: 685-694.

International Agency for Research on Cancer (2010) Ingested nitrate and nitrite, and cyanobacterial peptide toxins. *IARC monographs on the evaluation of carcinogenic risks to humans* **94**.

IPCC Climate Change (2007) The physical science basis. *Contribution of working group I to the Fourth Assessment Report of the Intergovernmental Panel on Climate Change* **996**.

Itoi S, Niki A & Sugita H (2006) Changes in microbial communities associated with the conditioning of filter material in recirculating aquaculture systems of the pufferfish *Takifugu rubripes*. *Aquaculture* **256**: 287-295.

Jetten MS, Niftrik Lv, Strous M, Kartal B, Keltjens JT & Op den Camp HJ (2009) Biochemistry and molecular biology of anammox bacteria. *Crit Rev Biochem Mol* **44**: 65-84.

Jetten MS, Strous M, Van de Pas-Schoonen KT, Schalk J, van Dongen UG, van de Graaf AA, Logemann S, Muyzer G, van Loosdrecht MC & Kuenen JG (1998) The anaerobic oxidation of ammonium. *FEMS Microbiol Rev* **22**: 421-437.

Jetten MS, Sliekers O, Kuypers M, Dalsgaard T, van Niftrik L, Cirpus I, van de Pas-Schoonen K, Lavik G, Thamdrup B & Le Paslier D (2003) Anaerobic ammonium oxidation by marine and freshwater planctomycete-like bacteria. *Appl Microbiol Biotechnol* **63**: 107-114.

Jones DT, Taylor WR & Thornton JM (1992) The rapid generation of mutation data matrices from protein sequences. *Bioinformatics* **8**: 275-282.

Jones RR, Weyer PJ, DellaValle CT*, et al.* (2016) Nitrate from drinking water and diet and bladder cancer among postmenopausal women in Iowa. *Environ Health Perspect* **124**: 1751-1758.

Kamp A, Stief P & Schulz-Vogt HN (2006) Anaerobic sulfide oxidation with nitrate by a freshwater *Beggiatoa* enrichment culture. *Appl Environ Microbiol* **72**: 4755-4760.

Kartal B, Kuenen Jv & Van Loosdrecht M (2010) Sewage treatment with anammox. *Science* **328**: 702-703.

Kartal B, Van Niftrik L, Sliekers O, Schmid MC, Schmidt I, Van De Pas-Schoonen K, Cirpus I, Van Der Star W, Van Loosdrecht M & Abma W (2004) Application, eco-physiology and biodiversity of anaerobic ammonium-oxidizing bacteria. *Rev Environ Sci Bio* **3**: 255-264.

Kartal B, Rattray J, van Niftrik LA, van de Vossenberg J, Schmid MC, Webb RI, Schouten S, Fuerst JA, Damsté JS & Jetten MS (2007) *Candidatus* "Anammoxoglobus propionicus" a new propionate oxidizing species of anaerobic ammonium oxidizing bacteria. *Syst Appl Microbiol* **30**: 39-49.

Kartal B, Maalcke WJ, de Almeida NM*, et al.* (2011) Molecular mechanism of anaerobic ammonium oxidation. *Nature* **479**: 127-130.

Kashima H & Regan JM (2015) Facultative nitrate reduction by electrode-respiring *Geobacter metallireducens* biofilms as a competitive reaction to electrode reduction in a bioelectrochemical system. *Enviro Sci Technol* **49**: 3195-3202.

Ke Y (2014) Simultaneous Anammox and Denitrification (SAD) Process with Anammox Granular Sludge. Dissertation Thesis, University of Duisburg-Essen.

Keeler BL & Polasky S (2014) Land-use change and costs to rural households: a case study in groundwater nitrate contamination. *Environ Res Lett* **9**: 074002.

Kelly JJ, Siripong S, McCormack J, Janus LR, Urakawa H, El Fantroussi S, Noble PA, Sappelsa L, Rittmann BE & Stahl DA (2005) DNA microarray detection of nitrifying bacterial 16S rRNA in wastewater treatment plant samples. *Water Res* **39**: 3229-3238.

Kemnitz D, Kolb S & Conrad R (2007) High abundance of *Crenarchaeota* in a temperate acidic forest soil. *FEMS Microbiol Ecol* **60**: 442-448.

Kern M & Simon J (2009) Electron transport chains and bioenergetics of respiratory nitrogen metabolism in *Wolinella succinogenes* and other Epsilonproteobacteria. *BBA Bioenergetics* **1787**: 646-656.

Khramenkov S, Kozlov M, Kevbrina M, Dorofeev A, Kazakova E, Grachev V, Kuznetsov B, Polyakov DY & Nikolaev YA (2013) A novel bacterium carrying out anaerobic ammonium oxidation in a reactor for biological treatment of the filtrate of wastewater fermented sludge. *Microbiology* **82**: 628-636.

Kim JR, Cheng S, Oh S-E & Logan BE (2007) Power generation using different cation, anion, and ultrafiltration membranes in microbial fuel cells. *Environ Sci Technol* **41**: 1004-1009.

Kim YM, Park D, Lee DS & Park JM (2007) Instability of biological nitrogen removal in a cokes wastewater treatment facility during summer. *J Hazard Mater* **141**: 27-32.

Kitzinger K, Koch H, Lücker S, Sedlacek CJ, Herbold C, Schwarz J, Daebeler A, Mueller AJ, Lukumbuzya M & Romano S (2018) Characterization of the first "*Candidatus* Nitrotoga" isolate reveals metabolic versatility and separate evolution of widespread nitrite-oxidizing bacteria. *MBio* **9**.

Klotz MG, Arp DJ, Chain PS, El-Sheikh AF, Hauser LJ, Hommes NG, Larimer FW, Malfatti SA, Norton JM & Poret-Peterson AT (2006) Complete genome sequence of the marine, chemolithoautotrophic, ammonia-oxidizing bacterium *Nitrosococcus oceani* ATCC 19707. *Appl Environ Microbiol* **72**: 6299-6315.

Koch H, Lücker S, Albertsen M, Kitzinger K, Herbold C, Spieck E, Nielsen PH, Wagner M & Daims H (2015) Expanded metabolic versatility of ubiquitous nitrite-oxidizing bacteria from the genus *Nitrospira*. *PNAS* **112**: 11371-11376.

Konstantinidis K, Isaacs N, Fett J, Simpson S, Long D & Marsh T (2003) Microbial diversity and resistance to copper in metal-contaminated lake sediment. *Microb Ecol* **45**: 191-202.

Koops H-P, Purkhold U, Pommerening-Röser A, Timmermann G & Wagner M (2006) The lithoautotrophic ammonia-oxidizing bacteria. *The Prokaryotes: Volume 5: Proteobacteria: Alpha and Beta Subclasses* 778-811.

Koops H, Böttcher B, Möller U, Pommerening-Röser A & Stehr G (1991) Classification of eight new species of ammonia-oxidizing bacteria: *Nitrosomonas communis* sp. nov., *Nitrosomonas ureae* sp. nov., *Nitrosomonas aestuarii* sp. nov., *Nitrosomonas marina* sp. nov., *Nitrosomonas nitrosa* sp. nov., *Nitrosomonas eutropha* sp. nov., *Nitrosomonas oligotropha* sp. nov. and *Nitrosomonas halophila* sp. nov. *Microbiology* **137**: 1689-1699.

Kozich JJ, Westcott SL, Baxter NT, Highlander SK & Schloss PD (2013) Development of a dual-index sequencing strategy and curation pipeline for analyzing amplicon sequence data on the MiSeq Illumina sequencing platform. *Appl Environ Microbiol* **79**: 5112-5120.

Kraigher B, Kosjek T, Heath E, Kompare B & Mandic-Mulec I (2008) Influence of pharmaceutical residues on the structure of activated sludge bacterial communities in wastewater treatment bioreactors. *Water Res* **42**: 4578-4588.

Kuenen JG (2008) Anammox bacteria: from discovery to application. *Nat Rev Microbiol* **6**: 320-326.

Kuever J & Galushko A (2014) The family Desulfomicrobiaceae. In: *The Prokaryotes: Deltaproteobacteria and Epsilonproteobacteria,*(Rosenberg E, DeLong EF, Lory S, Stackebrandt E & Thompson F, eds.), 97-102. Springer Berlin Heidelberg.

Kuhn DD, Drahos DD, Marsh L & Flick Jr GJ (2010) Evaluation of nitrifying bacteria product to improve nitrification efficacy in recirculating aquaculture systems. *Aquacult Eng* **43**: 78-82.

Kumar M & Lin J-G (2010) Co-existence of anammox and denitrification for simultaneous nitrogen and carbon removal—strategies and issues. *J Hazard Mater* **178**: 1-9.

Kuypers MM, Sliekers AO, Lavik G, Schmid M, Jørgensen BB, Kuenen JG, Damsté JSS, Strous M & Jetten MS (2003) Anaerobic ammonium oxidation by anammox bacteria in the Black Sea. *Nature* **422**: 608.

Lane DJ, Pace B, Olsen GJ, Stahl DA, Sogin ML & Pace NR (1985) Rapid determination of 16S ribosomal RNA sequences for phylogenetic analyses. *PNAS* **82**: 6955-6959.

LaPara TM, Nakatsu CH, Pantea LM & Alleman JE (2002) Stability of the bacterial communities supported by a seven-stage biological process treating pharmaceutical wastewater as revealed by PCR-DGGE. *Water Res* **36**: 638-646.

Larminie J, Dicks A & McDonald MS (2003) *Fuel cell systems explained*. J. Wiley Chichester, UK.

Layer F, Ghebremedhin B, Moder K-A, König W & König B (2006) Comparative study using various methods for identification of *Staphylococcus* species in clinical specimens. *J Clin Microbiol* **44**: 2824-2830.

Lefebvre O, Nguyen TH, Al-Mamun A, Chang I & Ng H (2010) T-RFLP reveals high β-Proteobacteria diversity in microbial fuel cells enriched with domestic wastewater. *J Appl Microbiol* **109**: 839-850.

Li Y, Hodak M & Bernholc J (2015) Enzymatic mechanism of copper-containing nitrite reductase. *Biochemistry* **54**: 1233-1242.

Lindsay MR, Webb RI, Strous M, Jetten MS, Butler MK, Forde RJ & Fuerst JA (2001) Cell compartmentalisation in planctomycetes: novel types of structural organisation for the bacterial cell. *Arch Microbiol* **175**: 413-429.

Liu D, Puigros MR, Caizan-Juanarena L, Geppert F, Ayudthaya N, Palakawong S, Buisman C & Ter Heijne A (2018) Granular carbon-based electrodes as cathodes in methane-producing bioelectrochemical systems. *Front Bioeng Biotechnol* **6**: 78.

Liu W-T, Marsh TL, Cheng H & Forney LJ (1997) Characterization of microbial diversity by determining terminal restriction fragment length polymorphisms of genes encoding 16S rRNA. *Appl Environ Microbiol* **63**: 4516-4522.

Logan BE (2010) Scaling up microbial fuel cells and other bioelectrochemical systems. *Appl Microbiol Biotechnol* **85**: 1665-1671.

Logan BE, Hamelers B, Rozendal R, Schröder U, Keller J, Freguia S, Aelterman P, Verstraete W & Rabaey K (2006) Microbial fuel cells: methodology and technology. *Environ Sci Technol* **40**: 5181-5192.

Lücker S, Wagner M, Maixner F, Pelletier E, Koch H, Vacherie B, Rattei T, Damsté JSS, Spieck E & Le Paslier D (2010) A *Nitrospira* metagenome illuminates the physiology and evolution of globally important nitrite-oxidizing bacteria. *PNAS* **107**: 13479-13484.

Lukow T, Dunfield PF & Liesack W (2000) Use of the T-RFLP technique to assess spatial and temporal changes in the bacterial community structure within an agricultural soil planted with transgenic and non-transgenic potato plants. *FEMS Microbiol Ecol* **32**: 241-247.

Madigan M & Martinko J (2006) *Brock. Biology of Microorganisms: Pearson Prentice Hall*. Upper Saddle River, NJ.

Maier RM, Pepper IL & Gerba CP (2009) *Environmental microbiology*. Academic press.

Manassaram DM, Backer LC, Messing R, Fleming LE, Luke B & Monteilh CP (2010) Nitrates in drinking water and methemoglobin levels in pregnancy: a longitudinal study. *Environ Health* **9**: 60.

Mansouri A & Lurie AA (1993) Methemoglobinemia. *Am J Hematol* **42**: 7-12.

Marger MD & Saier Jr MH (1993) A major superfamily of transmembrane facilitators that catalyse uniport, symport and antiport. *Trends Biochem Sci* **18**: 13-20.

Marsh TL (1999) Terminal restriction fragment length polymorphism (T-RFLP): an emerging method for characterizing diversity among homologous populations of amplification products. *Curr Opin Microbiol* **2**: 323-327.

McHatton SC, Barry JP, Jannasch HW & Nelson DC (1996) High nitrate concentrations in vacuolate, autotrophic marine *Beggiatoa* spp. *Appl Environ Microbiol* **62**: 954-958.

McMurdie PJ & Holmes S (2013) phyloseq: an R package for reproducible interactive analysis and graphics of microbiome census data. *PloS one* **8**: e61217.

Mehta T, Coppi MV, Childers SE & Lovley DR (2005) Outer membrane c-type cytochromes required for Fe (III) and Mn (IV) oxide reduction in Geobacter sulfurreducens. *Appl Environ Microbiol* **71**: 8634-8641.

Meincke M, Bock E, Kastrau D & Kroneck PM (1992) Nitrite oxidoreductase from *Nitrobacter hamburgensis*: redox centers and their catalytic role. *Arch Microbiol* **158**: 127-131.

Michaud L, Lo Giudice A, Troussellier M, Smedile F, Bruni V & Blancheton J-P (2009) Phylogenetic characterization of the heterotrophic bacterial communities inhabiting a marine recirculating aquaculture system. *J Appl Microbiol* **107**: 1935-1946.

Mirvish SS (1977) N-Nitroso compounds: their chemical and in vivo formation and possible importance as environmental carcinogens. *J Toxicol Environ* **2**: 1267-1277.

Molin S & Tolker-Nielsen T (2003) Gene transfer occurs with enhanced efficiency in biofilms and induces enhanced stabilisation of the biofilm structure. *Curr Opin Biotechnol* **14**: 255-261.

Molognoni D, Devecseri M, Cecconet D & Capodaglio AG (2017) Cathodic groundwater denitrification with a bioelectrochemical system. *J Water Process Eng* **19**: 67-73.

Morales N, del Río ÁV, Vázquez-Padín JR, Méndez R, Mosquera-Corral A & Campos JL (2015) Integration of the Anammox process to the rejection water and main stream lines of WWTPs. *Chemosphere* **140**: 99-105.

Mueller DK, Hamilton PA, Helsel DR, Hitt KJ & Ruddy BC (1995) Nutrients in ground water and surface water of the United States: an analysis of data through 1992. *Water-Resources investigations report* **95**: 4031.

Mulder A, Van de Graaf AA, Robertson L & Kuenen J (1995) Anaerobic ammonium oxidation discovered in a denitrifying fluidized bed reactor. *FEMS Microbiol Ecol* **16**: 177-183.

Mußmann M, Schulz HN, Strotmann B, Kjær T, Nielsen LP, Rosselló-Mora RA, Amann RI & Jørgensen BB (2003) Phylogeny and distribution of nitrate-storing *Beggiatoa* spp. in coastal marine sediments. *Environ Microbiol* **5**: 523-533.

Muyzer G, De Waal EC & Uitterlinden AG (1993) Profiling of complex microbial populations by denaturing gradient gel electrophoresis analysis of polymerase chain reaction-amplified genes coding for 16S rRNA. *Appl Environ Microbiol* **59**: 695-700.

Nadell CD, Xavier JB, Levin SA & Foster KR (2008) The evolution of quorum sensing in bacterial biofilms. *PLoS biology* **6**: e14.

Nelson DC, Jørgensen BB & Revsbech NP (1986) Growth pattern and yield of a chemoautotrophic *Beggiatoa* sp. in oxygen-sulfide microgradients. *Appl Environ Microbiol* **52**: 225-233.

Nevin KP, Richter H, Covalla S, Johnson J, Woodard T, Orloff A, Jia H, Zhang M & Lovley D (2008) Power output and columbic efficiencies from biofilms of *Geobacter sulfurreducens* comparable to mixed community microbial fuel cells. *Environ Microbiol* **10**: 2505-2514.

Nguyen VK, Park Y, Yu J & Lee T (2016) Bioelectrochemical denitrification on biocathode buried in simulated aquifer saturated with nitrate-contaminated groundwater. *Environ Sci Pollut Res* **23**: 15443-15451.

Nguyen VK, Hong S, Park Y, Jo K & Lee T (2015) Autotrophic denitrification performance and bacterial community at biocathodes of bioelectrochemical systems with either abiotic or biotic anodes. *J Biosci Bioeng* **119**: 180-187.

Nishigaki K, Kaneko Y, Wakuda H, Husimi Y & Tanaka T (1985) Type II restriction endonucleases cleave single-stranded DNAs in general. *Nucleic Acids Res* **13**: 5747-5760.

Noren D & Hoffman M (2005) Clarifying the Butler–Volmer equation and related approximations for calculating activation losses in solid oxide fuel cell models. *J Power Sources* **152**: 175-181.

Norton JM, Alzerreca JJ, Suwa Y & Klotz MG (2002) Diversity of ammonia monooxygenase operon in autotrophic ammonia-oxidizing bacteria. *Arch Microbiol* **177**: 139-149.

Op den Camp H, Kartal B, Guven D, Van Niftrik L, Haaijer S, Van Der Star W, Van de Pas-Schoonen K, Cabezas A, Ying Z & Schmid M (2006) Global impact and application of the anaerobic ammonium-oxidizing (anammox) bacteria. *Biochem Soc Trans* **34**: 174–178.

Op den Camp HJ, Jetten MS & Strous M (2007) Anammox. In: *Biology of the nitrogen cycle,*(Bothe H, Ferguson SJ & Newton WE, eds.), 245-262. Elsevier.

Osborn AM, Moore ER & Timmis KN (2000) An evaluation of terminal-restriction fragment length polymorphism (T-RFLP) analysis for the study of microbial community structure and dynamics. *Environ Microbiol* **2**: 39-50.

Otte S, Kuenen JG, Nielsen LP, Paerl HW, Zopfi J, Schulz HN, Teske A, Strotmann B, Gallardo VA & Jørgensen BB (1999) Nitrogen, carbon, and sulfur metabolism in naturalthioploca samples. *Appl Environ Microbiol* **65**: 3148-3157.

Palleroni NJ (2015) Pseudomonas. In: *Bergey's Manual of Systematics of Archaea and Bacteria,*(Whitman WB, ed.) 323–379. John Wiley & Sons, Baltimore.

Palomo A, Pedersen AG, Fowler SJ, Dechesne A, Sicheritz-Pontén T & Smets BF (2018) Comparative genomics sheds light on niche differentiation and the evolutionary history of comammox *Nitrospira*. *ISME J* **12**: 1779–1793.

Pantanella E, Cardarelli M, Colla G, Rea E & Marcucci A (2012) Aquaponics vs. hydroponics: production and quality of lettuce crop. *ActaHortic* **927**: 887-893.

Park DH & Zeikus JG (2000) Electricity generation in microbial fuel cells using neutral red as an electronophore. *Appl Environ Microbiol* **66**: 1292-1297.

Patil SA, Harnisch F, Kapadnis B & Schröder U (2010) Electroactive mixed culture biofilms in microbial bioelectrochemical systems: the role of temperature for biofilm formation and performance. *Biosens Bioelectron* **26**: 803-808.

Patil SA, Arends JB, Vanwonterghem I, Van Meerbergen J, Guo K, Tyson GW & Rabaey K (2015) Selective enrichment establishes a stable performing community for microbial electrosynthesis of acetate from CO_2. *Environ Sci Technol* **49**: 8833-8843.

Patil SA, Harnisch F, Koch C, Hübschmann T, Fetzer I, Carmona-Martínez AA, Müller S & Schröder U (2011) Electroactive mixed culture derived biofilms in microbial bioelectrochemical systems: the role of pH on biofilm formation, performance and composition. *Bioresour Technol* **102**: 9683-9690.

Pedersen L-F, Pedersen PB, Nielsen JL & Nielsen PH (2009) Peracetic acid degradation and effects on nitrification in recirculating aquaculture systems. *Aquaculture* **296**: 246-254.

Philippot L (2002) Denitrifying genes in bacterial and archaeal genomes. *BBA Gene structure and expression* **1577**: 355-376.

Pilloni G, von Netzer F, Engel M & Lueders T (2011) Electron acceptor-dependent identification of key anaerobic toluene degraders at a tar-oil-contaminated aquifer by Pyro-SIP. *FEMS Microbiol Ecol* **78**: 165-175.

Pinto AJ, Marcus DN, Ijaz UZ, Bautista-de lose Santos QM, Dick GJ & Raskin L (2016) Metagenomic evidence for the presence of comammox nitrospira-like bacteria in a drinking water system. *Msphere* **1**: e00054-00015.

Pjevac P, Schauberger C, Poghosyan L, Herbold CW, van Kessel MA, Daebeler A, Steinberger M, Jetten MS, Lücker S & Wagner M (2017) AmoA-targeted polymerase chain reaction primers for the specific detection and quantification of comammox *Nitrospira* in the environment. *Front Microbiol* **8**: 1508.

Pous N, Puig S, Balaguer MD & Colprim J (2015) Cathode potential and anode electron donor evaluation for a suitable treatment of nitrate-contaminated groundwater in bioelectrochemical systems. *Chem Eng J* **263**: 151-159.

Pous N, Puig S, Coma M, Balaguer MD & Colprim J (2013) Bioremediation of nitrate-polluted groundwater in a microbial fuel cell. *J Chem Technol Biotechnol* **88**: 1690-1696.

Pous N, Koch C, Colprim J, Puig S & Harnisch F (2014) Extracellular electron transfer of biocathodes: Revealing the potentials for nitrate and nitrite reduction of denitrifying microbiomes dominated by *Thiobacillus* sp. *Electrochem Commun* **49**: 93-97.

Preisler A, De Beer D, Lichtschlag A, Lavik G, Boetius A & Jørgensen BB (2007) Biological and chemical sulfide oxidation in a *Beggiatoa* inhabited marine sediment. *ISME J* **1**: 341.

QIAGEN (2010) Critical Factors for Successful Real-Time PCR. *https://wwwgene-quantificationde/qiagen-qpcr-sample-assay-tech-guide-2010pdf* Last access: 24-04-2020.

QIAGEN Service & Support Centre (2013-2020) DNA. *https://wwwqiagencom/us/service-and-support/learning-hub/molecular-biology-methods/dna/* Last access: 22-01-2020.

Quan Z-X, Im W-T & Lee S-T (2006) *Azonexus caeni* sp. nov., a denitrifying bacterium isolated from sludge of a wastewater treatment plant. *Int J Syst Evol Microbiol* **56**: 1043-1046.

Quan ZX, Rhee SK, Zuo JE, Yang Y, Bae JW, Park JR, Lee ST & Park YH (2008) Diversity of ammonium-oxidizing bacteria in a granular sludge anaerobic ammonium-oxidizing (anammox) reactor. *Environ Microbiol* **10**: 3130-3139.

Quast C, Pruesse E, Yilmaz P, Gerken J, Schweer T, Yarza P, Peplies J & Glöckner FO (2012) The SILVA ribosomal RNA gene database project: improved data processing and web-based tools. *Nucleic Acids Res* **41**: D590-D596.

R Core Team (2018) R: A language and environment for statistical computing. R Foundation for Statistical Computing, Vienna, Austria. *URL http://wwwR-projectorg*.

Rabaey K & Verstraete W (2005) Microbial fuel cells: novel biotechnology for energy generation. *Trends Biotechnol* **23**: 291-298.

Rabaey K, Boon N, Höfte M & Verstraete W (2005) Microbial phenazine production enhances electron transfer in biofuel cells. *Environ Sci Technol* **39**: 3401-3408.

Rabaey K, Boon N, Siciliano SD, Verhaege M & Verstraete W (2004) Biofuel cells select for microbial consortia that self-mediate electron transfer. *Appl Environ Microbiol* **70**: 5373-5382.

Rabaey K, Read ST, Clauwaert P, Freguia S, Bond PL, Blackall LL & Keller J (2008) Cathodic oxygen reduction catalyzed by bacteria in microbial fuel cells. *ISME J* **2**: 519-527.

Rabaey K, Rodriguez J, Blackall LL, Keller J, Gross P, Batstone D, Verstraete W & Nealson KH (2007) Microbial ecology meets electrochemistry: electricity-driven and driving communities. *ISME J* **1**: 9-18.

Rakocy JE, Masser MP & Losordo TM (2006) Recirculating aquaculture tank production systems: aquaponics—integrating fish and plant culture. *SRAC Publication* **454**: 1-16.

Reguera G, McCarthy KD, Mehta T, Nicoll JS, Tuominen MT & Lovley DR (2005) Extracellular electron transfer via microbial nanowires. *Nature* **435**: 1098-1101.

Rich J, Heichen R, Bottomley P, Cromack K & Myrold D (2003) Community composition and functioning of denitrifying bacteria from adjacent meadow and forest soils. *Appl Environ Microbiol* **69**: 5974-5982.

Röder B, Frühwirth K, Vogl C, Wagner M & Rossmanith P (2010) Impact of long-term storage on stability of standard DNA for nucleic acid-based methods. *J Clin Microbiol* **48**: 4260-4262.

Rosenbaum M, Aulenta F, Villano M & Angenent LT (2011) Cathodes as electron donors for microbial metabolism: which extracellular electron transfer mechanisms are involved? *Bioresour Technol* **102**: 324-333.

Rosenbaum V & Riesner D (1987) Temperature-gradient gel electrophoresis: thermodynamic analysis of nucleic acids and proteins in purified form and in cellular extracts. *Biophys Chem* **26**: 235-246.

Rotaru A-E, Shrestha PM, Liu F, Markovaite B, Chen S, Nevin KP & Lovley DR (2014) Direct interspecies electron transfer between *Geobacter metallireducens* and *Methanosarcina barkeri*. *Appl Environ Microbiol* **80**: 4599-4605.

Rozendal RA, Hamelers HV & Buisman CJ (2006) Effects of membrane cation transport on pH and microbial fuel cell performance. *Environ Sci Technol* **40**: 5206-5211.

Rozendal RA, Hamelers HV, Rabaey K, Keller J & Buisman CJ (2008) Towards practical implementation of bioelectrochemical wastewater treatment. *Trends Biotechnol* **26**: 450-459.

San-Martín MI, Mateos R, Carracedo B, Escapa A & Morán A (2018) Pilot-scale bioelectrochemical system for simultaneous nitrogen and carbon removal in urban wastewater treatment plants. *J Biosci Bioeng* **126**: 758-763.

Sandaa R-A, Magnesen T, Torkildsen L & Bergh Ø (2003) Characterisation of the bacterial community associated with early stages of great scallop (Pecten maximus), using denaturing gradient gel electrophoresis (DGGE). *Syst Appl Microbiol* **26**: 302-311.

Sayama M, Risgaard-Petersen N, Nielsen LP, Fossing H & Christensen PB (2005) Impact of bacterial NO_3^- transport on sediment biogeochemistry. *Appl Environ Microbiol* **71**: 7575-7577.

Scala DJ & Kerkhof LJ (1999) Diversity of nitrous oxide reductase (nosZ) genes in continental shelf sediments. *Appl Environ Microbiol* **65**: 1681-1687.

Scala DJ & Kerkhof LJ (2000) Horizontal heterogeneity of denitrifying bacterial communities in marine sediments by terminal restriction fragment length polymorphism analysis. *Appl Environ Microbiol* **66**: 1980-1986.

Schauer R, Bienhold C, Ramette A & Harder J (2010) Bacterial diversity and biogeography in deep-sea surface sediments of the South Atlantic Ocean. *The ISME Journal* **4**: 159.

Schmautz Z, Graber A, Jaenicke S, Goesmann A, Junge R & Smits TH (2017) Microbial diversity in different compartments of an aquaponics system. *Arch Microbiol* **199**: 613-620.

Schmid M, Twachtmann U, Klein M, Strous M, Juretschko S, Jetten M, Metzger JW, Schleifer K-H & Wagner M (2000) Molecular evidence for genus level diversity of bacteria capable of catalyzing anaerobic ammonium oxidation. *Syst Appl Microbiol* **23**: 93-106.

Scholten E, Lukow T, Auling G, Kroppenstedt RM, Rainey FA & Diekmann H (1999) *Thauera mechernichensis* sp. nov., an aerobic denitrifier from a leachate treatment plant. *Int J Syst Evol Microbiol* **49**: 1045-1051.

Schouten S, Strous M, Kuypers MM, Rijpstra WIC, Baas M, Schubert CJ, Jetten MS & Damsté JSS (2004) Stable carbon isotopic fractionations associated with inorganic carbon fixation by anaerobic ammonium-oxidizing bacteria. *Appl Environ Microbiol* **70**: 3785-3788.

Schrope M (2001) Which way to energy utopia? *Nature* **414**: 682-684.

Schubert CJ, Durisch-Kaiser E, Wehrli B, Thamdrup B, Lam P & Kuypers MM (2006) Anaerobic ammonium oxidation in a tropical freshwater system (Lake Tanganyika). *Environ Microbiol* **8**: 1857-1863.

Schwieger F & Tebbe CC (1998) A new approach to utilize PCR–single-strand-conformation polymorphism for 16S rRNA gene-based microbial community analysis. *Appl Environ Microbiol* **64**: 4870-4876.

Sebilo M, Mayer B, Nicolardot B, Pinay G & Mariotti A (2013) Long-term fate of nitrate fertilizer in agricultural soils. *PNAS* **110**: 18185-18189.

Shapleigh JP (2013) Denitrifying prokaryotes. In: *The Prokaryotes: Prokaryotic Physiology and Biochemistry,*(Rosenberg E, DeLong EF, Lory S, Stackebrandt E & Thompson F, eds.), 405-425. Springer Berlin Heidelberg.

Shuval HI & Gruener N (2013) Infant methemoglobinemia and other health effects of nitrates in drinking water. *Progr Water Technol* **8**: 183-193.

Simões M, Simões LC, Machado I, Pereira MO & Vieira MJ (2006) Control of flow-generated biofilms with surfactants: evidence of resistance and recovery. *Food Bioprod Process* **84**: 338-345.

Siripong S & Rittmann BE (2007) Diversity study of nitrifying bacteria in full-scale municipal wastewater treatment plants. *Water Res* **41**: 1110-1120.

Sliekers AO, Third K, Abma W, Kuenen J & Jetten M (2003) CANON and Anammox in a gas-lift reactor. *FEMS Microbiol Lett* **218**: 339-344.

Smalla K, Oros-Sichler M, Milling A, Heuer H, Baumgarte S, Becker R, Neuber G, Kropf S, Ulrich A & Tebbe CC (2007) Bacterial diversity of soils assessed by DGGE, T-RFLP and SSCP fingerprints of PCR-amplified 16S rRNA gene fragments: do the different methods provide similar results? *J Microbiol Methods* **69**: 470-479.

Smith L, Benson D & Hiscock K (2015) Groundwater protection programmes in Denmark, Germany and the Netherlands. In: *Catchment and River Basin Management: Integrating Science and Governance,*(Smith L, Porter K, Hiscock K, Porter MJ & Benson D, eds.), 127-156. Routledge, London.

Smith RL, Bohlke J, Song B & Tobias CR (2015) Role of anaerobic ammonium oxidation (anammox) in nitrogen removal from a freshwater aquifer. *Environ Sci Technol* **49**: 12169-12177.

Smith VH (2003) Eutrophication of freshwater and coastal marine ecosystems a global problem. *Environ Sci Pollut Res* **10**: 126-139.

Sogin ML, Morrison HG, Huber JA, Welch DM, Huse SM, Neal PR, Arrieta JM & Herndl GJ (2006) Microbial diversity in the deep sea and the underexplored “rare biosphere”. *PNAS* **103**: 12115-12120.

SooHoo CK & Hollocher T (1991) Purification and characterization of nitrous oxide reductase from *Pseudomonas aeruginosa* strain P2. *J Biol Chem* **266**: 2203-2209.

Spieck E, Aamand J, Bartosch S & Bock E (1996) Immunocytochemical detection and location of the membrane-bound nitrite oxidoreductase in cells of *Nitrobacter* and *Nitrospira*. *FEMS Microbiol Lett* **139**: 71-76.

Spieck E, Ehrich S, Aamand J & Bock E (1998) Isolation and immunocytochemical location of the nitrite-oxidizing system in *Nitrospira moscoviensi*. *Arch Microbiol* **169**: 225-230.

Spiro S (2012) Nitrous oxide production and consumption: regulation of gene expression by gas-sensitive transcription factors. *Philos Trans R Soc Lond B Biol Sci* **367**: 1213-1225.

Starkenburg SR, Chain PS, Sayavedra-Soto LA, Hauser L, Land ML, Larimer FW, Malfatti SA, Klotz MG, Bottomley PJ & Arp DJ (2006) Genome sequence of the chemolithoautotrophic nitrite-oxidizing bacterium *Nitrobacter winogradskyi* Nb-255. *Appl Environ Microbiol* **72**: 2050-2063.

Stayner LT, Almberg K, Jones R, Graber J, Pedersen M & Turyk M (2017) Atrazine and nitrate in drinking water and the risk of preterm delivery and low birth weight in four Midwestern states. *Environ Res* **152**: 294-303.

Stein LY, Arp DJ, Berube PM, Chain PS, Hauser L, Jetten MS, Klotz MG, Larimer FW, Norton JM & Op den Camp HJ (2007) Whole-genome analysis of the ammonia-oxidizing bacterium, *Nitrosomonas eutropha* C91: implications for niche adaptation. *Environ Microbiol* **9**: 2993-3007.

Stormer J, Jensen FB & Rankin JC (1996) Uptake of nitrite, nitrate, and bromide in rainbow trout, (*Oncorhynchus mykiss*): effects on ionic balance. *Can J Fish Aquat Sci* **53**: 1943-1950.

Strous M, Kuenen JG & Jetten MS (1999) Key physiology of anaerobic ammonium oxidation. *Appl Environ Microbiol* **65**: 3248-3250.

Strous M, Van Gerven E, Kuenen JG & Jetten M (1997) Effects of aerobic and microaerobic conditions on anaerobic ammonium-oxidizing (anammox) sludge. *Appl Environ Microbiol* **63**: 2446-2448.

Strous M, Van Gerven E, Zheng P, Kuenen JG & Jetten MS (1997) Ammonium removal from concentrated waste streams with the anaerobic ammonium oxidation (anammox) process in different reactor configurations. *Water Res* **31**: 1955-1962.

Strous M, Fuerst JA, Kramer EH, Logemann S, Muyzer G, van de Pas-Schoonen KT, Webb R, Kuenen JG & Jetten MS (1999) Missing lithotroph identified as new planctomycete. *Nature* **400**: 446.

Strycharz SM, Glaven RH, Coppi MV, Gannon SM, Perpetua LA, Liu A, Nevin KP & Lovley DR (2011) Gene expression and deletion analysis of mechanisms for electron transfer from electrodes to *Geobacter sulfurreducens*. *Bioelectrochemistry* **80**: 142-150.

Sugita H, Nakamura H & Shimada T (2005) Microbial communities associated with filter materials in recirculating aquaculture systems of freshwater fish. *Aquaculture* **243**: 403-409.

Suharti, Strampraad MJ, Schröder I & de Vries S (2001) A novel copper A containing menaquinol NO reductase from *Bacillus azotoformans*. *Biochemistry* **40**: 2632-2639.

Summers ZM, Fogarty HE, Leang C, Franks AE, Malvankar NS & Lovley DR (2010) Direct exchange of electrons within aggregates of an evolved syntrophic coculture of anaerobic bacteria. *Science* **330**: 1413-1415.

Sundermeyer-Klinger H, Meyer W, Warninghoff B & Bock E (1984) Membrane-bound nitrite oxidoreductase of *Nitrobacter*: evidence for a nitrate reductase system. *Arch Microbiol* **140**: 153-158.

Sutherland IW (2001) The biofilm matrix–an immobilized but dynamic microbial environment. *Trends Microbiol* **9**: 222-227.

Sweerts J-PR, De Beer D, Nielsen LP, Verdouw H, Van den Heuvel JC, Cohen Y & Cappenberg TE (1990) Denitrification by sulphur oxidizing *Beggiatoa* spp. mats on freshwater sediments. *Nature* **344**: 762-763.

Takahashi S, Tomita J, Nishioka K, Hisada T & Nishijima M (2014) Development of a prokaryotic universal primer for simultaneous analysis of bacteria and archaea using next-generation sequencing. *PLOS ONE* **9**: e105592.

Ter Heijne A, Hamelers HV, De Wilde V, Rozendal RA & Buisman CJ (2006) A bipolar membrane combined with ferric iron reduction as an efficient cathode system in microbial fuel cells. *Environ Sci Technol* **40**: 5200-5205.

Teske A & Salman V (2014) The family Beggiatoaceae. In: *The Prokaryotes: Gammaproteobacteria,*(Rosenberg E, DeLong EF, Lory S, Stackebrandt E & Thompson F, eds.), 93-134. Springer Berlin Heidelberg.

Thauer RK, Jungermann K & Decker K (1977) Energy conservation in chemotrophic anaerobic bacteria. *Bacteriol Rev* **41**: 100.

Throbäck IN, Enwall K, Jarvis Å & Hallin S (2004) Reassessing PCR primers targeting *nirS*, *nirK* and *nosZ* genes for community surveys of denitrifying bacteria with DGGE. *FEMS Microbiol Ecol* **49**: 401-417.

Tiedje JM (1988) Ecology of denitrification and dissimilatory nitrate reduction to ammonium. *Biology of anaerobic microorganisms* **717**: 179-244.

Tielen P, Strathmann M, Jaeger K-E, Flemming H-C & Wingender J (2005) Alginate acetylation influences initial surface colonization by mucoid *Pseudomonas aeruginosa*. *Microbiol Res* **160**: 165-176.

Tierling J & Kuhlmann H (2018) Emissions of nitrous oxide (N_2O) affected by pH-related nitrite accumulation during nitrification of N fertilizers. *Geoderma* **310**: 12-21.

Tokuyama T, Mine A, Kamiyama K, Yabe R, Satoh K, Matsumoto H, Takahashi R & Itonaga K (2004) *Nitrosomonas communis* strain YNSRA, an ammonia-oxidizing bacterium, isolated from the reed rhizoplane in an aquaponics plant. *J Biosci Bioeng* **98**: 309-312.

TrinkwV (2001) Verordnung über die Qualität von Wasser für den menschlichen Gebrauch (Trinkwasserverordnung) vom 21. *BGBl* **1**: 959-981.

Turner JA (2004) Sustainable hydrogen production. *Science* **305**: 972-974.

Umbreit J (2007) Methemoglobin—it's not just blue: a concise review. *Am J Hematol* **82**: 134-144.

USEPA (2013) Aquatic Life Ambient Water Quality Criteria for Ammonia - Freshwater. *Docket ID No EPA-HQ-OW-2009-0921*.

Van De Graaf AA, De Bruijn P, Robertson LA, Jetten MS & Kuenen JG (1997) Metabolic pathway of anaerobic ammonium oxidation on the basis of ^{15}N studies in a fluidized bed reactor. *Microbiology* **143**: 2415-2421.

Van de Graaf AA, Mulder A, de Bruijn P, Jetten M, Robertson L & Kuenen JG (1995) Anaerobic oxidation of ammonium is a biologically mediated process. *Appl Environ Microbiol* **61**: 1246-1251.

Van der Star WR, Abma WR, Blommers D, Mulder J-W, Tokutomi T, Strous M, Picioreanu C & van Loosdrecht MC (2007) Startup of reactors for anoxic ammonium oxidation: experiences from the first full-scale anammox reactor in Rotterdam. *Water Res* **41**: 4149-4163.

Van Doan T, Lee TK, Shukla SK, Tiedje JM & Park J (2013) Increased nitrous oxide accumulation by bioelectrochemical denitrification under autotrophic conditions: kinetics and expression of denitrification pathway genes. *Water Res* **47**: 7087-7097.

Van Dongen U, Jetten MS & Van Loosdrecht M (2001) The SHARON®-Anammox® process for treatment of ammonium rich wastewater. *Water Sci Technol* **44**: 153-160.

van Kessel MA, Speth DR, Albertsen M, Nielsen PH, den Camp HJO, Kartal B, Jetten MS & Lücker S (2015) Complete nitrification by a single microorganism. *Nature* **528**: 555-559.

van Niftrik L & Jetten MS (2012) Anaerobic ammonium-oxidizing bacteria: unique microorganisms with exceptional properties. *Microbiol Mol Biol Rev* **76**: 585-596.

van Niftrik L, Geerts WJ, van Donselaar EG, Humbel BM, Webb RI, Fuerst JA, Verkleij AJ, Jetten MS & Strous M (2008) Linking ultrastructure and function in four genera of anaerobic ammonium-oxidizing bacteria: cell plan, glycogen storage, and localization of cytochrome c proteins. *J Bacteriol* **190**: 708-717.

Van Niftrik L, Van Helden M, Kirchen S, Van Donselaar EG, Harhangi HR, Webb RI, Fuerst JA, Op den Camp HJ, Jetten MS & Strous M (2010) Intracellular localization of membrane-bound ATPases in the compartmentalized anammox bacterium '*Candidatus* Kuenenia stuttgartiensis'. *Mol Microbiol* **77**: 701-715.

Virdis B, Rabaey K, Yuan Z & Keller J (2008) Microbial fuel cells for simultaneous carbon and nitrogen removal. *Water research* **42**: 3013-3024.

Virdis B, Rabaey K, Rozendal RA, Yuan Z & Keller J (2010) Simultaneous nitrification, denitrification and carbon removal in microbial fuel cells. *Water research* **44**: 2970-2980.

Vitousek PM, Aber JD, Howarth RW, Likens GE, Matson PA, Schindler DW, Schlesinger WH & Tilman DG (1997) Human alteration of the global nitrogen cycle: sources and consequences. *Ecol Appl* **7**: 737-750.

Wallis P, Haynes R, Hunter C & Morris C (2010) Effect of land use and management on soil bacterial biodiversity as measured by PCR-DGGE. *Applied Soil Ecology* **46**: 147-150.

Wan Y, Lean Zhou SW, Liao C, Li N, Liu W & Wang X (2018) Syntrophic growth of *Geobacter sulfurreducens* accelerates anaerobic denitrification. *Front Microbiol* **9**.

Wang X & Seed B (2006) High-throughput primer and probe design. *Real-time PCR* **1**: 93-106.

Wang Y, Chen Y & Wen Q (2018) Microbial fuel cells: enhancement with a polyaniline/carbon felt capacitive bioanode and reduction of Cr (VI) using the intermittent operation. *Environ Chem Lett* **16**: 319-326.

Wang Y, Ma L, Mao Y, Jiang X, Xia Y, Yu K, Li B & Zhang T (2017) Comammox in drinking water systems. *Water Res* **116**: 332-341.

Ward B (2015) Bacterial energy metabolism. In: *Molecular Medical Microbiology,*(Tang Y-W, ed.) 201-233. Elsevier.

Ward MH, DeKok TM, Levallois P, Brender J, Gulis G, Nolan BT & VanDerslice J (2005) Workgroup report: drinking-water nitrate and health—recent findings and research needs. *Environ Health Perspect* **113**: 1607-1614.

Ward MH, Jones RR, Brender JD, De Kok TM, Weyer PJ, Nolan BT, Villanueva CM & Van Breda SG (2018) Drinking Water Nitrate and Human Health: An Updated Review. *Innt J Environ Res Public Health* **15**: 1557.

Webster G, Yarram L, Freese E, Köster J, Sass H, Parkes RJ & Weightman AJ (2007) Distribution of candidate division JS1 and other Bacteria in tidal sediments of the German Wadden Sea using targeted 16S rRNA gene PCR-DGGE. *FEMS Microbiol Ecol* **62**: 78-89.

Wickham H (2017) ggplot2: elegant graphics for data analysis. *J Stat Softw* **77**.

Wickham H (2019) stringr: Simple, Consistent Wrappers for Common String Operations. Vol. 1.4.0 p.^pp.

Wiegel J (2006) The genus Xanthobacter. *The prokaryotes* **5**: 290-314.

Wieringa EB, Overmann J & Cypionka H (2000) Detection of abundant sulphate-reducing bacteria in marine oxic sediment layers by a combined cultivation and molecular approach. *Environ Microbiol* **2**: 417-427.

Wietz M, Hall MR & Høj L (2009) Effects of seawater ozonation on biofilm development in aquaculture tanks. *Syst Appl Microbiol* **32**: 266-277.

Wimpenny J (2000) An overview of biofilms as functional communities. In: *Community Structure and Co-operation in Biofilms,*(Allison D, Gilbert P, Lappin-Scott H & Wilson M, eds.), 1-24. Cambridge University Press, Cambridge.

Winiwarter W, Grizzetti B & Sutton MA (2015) Nitrogen pollution in the EU: best management strategies, regulations, and science needs. *AWMA EM magazine* **September 2015**: 18-23.

World Health Organization (2004) *Guidelines for drinking-water quality*. World Health Organization.

Wricke B (2014) Wasseraufbereitung. In: *Mutschmann/Stimmelmayr Taschenbuch der Wasserversorgung,*(Fritsch P, Knaus W, Merkl G, Preininger E, Rautenberg J, Weiß M & Wricke B, eds.), 237-397. Springer.

Wrighton KC, Virdis B, Clauwaert P, Read ST, Daly RA, Boon N, Piceno Y, Andersen GL, Coates JD & Rabaey K (2010) Bacterial community structure corresponds to performance during cathodic nitrate reduction. *ISME J* **4**: 1443-1455.

Xu G, Fan X & Miller AJ (2012) Plant nitrogen assimilation and use efficiency. *Annu Rev Plant Biol* **63**: 153-182.

Yang D-C, Im W-T, Kim MK & Lee S-T (2005) *Pseudoxanthomonas koreensis* sp. nov. and *Pseudoxanthomonas daejeonensis* sp. nov. *Int J Syst Evo Microbiol* **55**: 787-791.

Yang Y, Li X, Yang X & He Z (2017) Enhanced nitrogen removal by membrane-aerated nitritation-anammox in a bioelectrochemical system. *Bioresour Technol* **238**: 22-29.

Yılmaz M, Ozic C & Gok İ (2012) Principles of nucleic acid separation by agarose gel electrophoresis. *Gel Electrophoresis–Principles and Basics* **33**.

Zekker I, Rikmann E, Tenno T, Loorits L, Kroon K, Fritze H, Tuomivirta T, Vabamäe P, Raudkivi M & Mandel A (2015) Nitric oxide for anammox recovery in a nitrite-inhibited deammonification system. *Environ Technol* **36**: 2477-2487.

Zhang Y & Angelidaki I (2013) A new method for in situ nitrate removal from groundwater using submerged microbial desalination–denitrification cell (SMDDC). *Water Res* **47**: 1827-1836.

Zumft WG (1997) Cell biology and molecular basis of denitrification. *Microbiol Mol Biol Rev* **61**: 533-616.

Zumft WG (2005) Nitric oxide reductases of prokaryotes with emphasis on the respiratory, heme–copper oxidase type. *J Inorg Biochem* **99**: 194-215.

Erklärung

Hiermit versichere ich, dass ich die vorliegende Arbeit mit dem Titel

„Nitrogen cycling in technical water systems”

selbst verfasst und keine außer den angegebenen Hilfsmitteln und Quellen benutzt habe und dass die Arbeit in dieser oder ähnlicher Form noch bei keiner anderen Universität eingereicht wurde.

Königstein, Oktober 2020

Danksagung

Mein besonderer Dank gilt Prof. Dr. Rainer Meckenstock, der mir die Möglichkeit gab, meine Arbeit in seiner neu etablierten Arbeitsgruppe in Essen zu schreiben. Danke, Rainer, dass du mich für diese spannenden Themen (vor allem dem Aquaponik) begeistert hast. Danke, für all die Diskussionen in unseren Science Meetings und die Ideen, die meine Arbeiten weiter vorangebracht haben.

Ich möchte der gesamten Arbeitsgruppe für die gemeinsame Zeit im Labor, im Büro und auch außerhalb der Uni danken! Ein ganz besonderer Dank geht dabei an Meike Arnold, Dr. Ivana Kraiselburd und Astrid Dannehl für ihre stetige Unterstützung. Ich konnte immer auf eure Hilfe zählen. Danke, Dr. Martin Mackowiak, Mark Pannekens, Dr. Philip Weyrauch und Dr. Janina Kölschbach für die wundervolle Atmosphäre im Büro. Unsere wissenschaftlichen Diskussionen beim Kaffee halfen mir sehr bei den Entwicklungen der Experimente. Auch die vielen privaten Gespräche und eure Späße werde ich sehr vermissen. Danke, Dr. Marcel Schulte, für deine Hilfe beim Aufbau der bioelektrochemischen Systeme und Dr. Verena Brauer, für deine Hilfe bei den Auswertungen der Sequenzierdaten.

Ihr alle seid nicht nur wundervolle Arbeitskollegen gewesen, sondern auch Freunde geworden. Vielen Dank dafür!

Prof. Dr. Martin Denecke möchte ich für die Übernahme des Zweitgutachtens danken. Martin, ich danke dir ebenfalls für die wissenschaftlichen Gespräche, auch wenn es leider nicht sehr viele waren. Thank you, Dr. Leon Steuernagel, Dr. Erika de León Gallegos, and Dr. Mohammad Azari for your technical and scientific support regarding the bioelectrochemical systems, the qPCR analyses and for providing the inoculums.

I also gratefully acknowledge Prof. Dr. Ir. Korneel Rabaey at the Center of Microbial Ecology and Technology (CMET) at Ghent University, Belgium, for his help and support. Special thanks are contributed to Dr. Sunil A. Patil, who designed the batch reactor systems used in this study and who helped me to build them up and to run the systems, as well as Dr. Kristof Verbeeck, who showed me to build and to run

the upflow cells I worked with. I also would like to thank Dr. Antonin Prévoteau for his help in electrochemistry and Dr. Jan Arends for his support.

Während meiner Zeit in Essen konnte ich immer auf die Unterstützung meiner Familie bauen. Ich danke euch, Mama und Papa, für eure Geduld, für eure Aufmunterungen in stressigen Zeiten und dafür, dass ihr immer für mich da gewesen seid.

Zu guter Letzt möchte ich auch Stefanie Sand, Kira Giebler, Helena Pannekens, Julia Raab, and Annika Uphoff danken. Wir hatten eine wunderbare Zeit zusammen im Studium und ich bin froh, dass wir Freunde geworden sind, die versuchen, sich immer mal wieder zu treffen. Ein besonderer Dank geht an dich Steffi, dafür, dass du mich immer wieder aufgebaut hast, wenn alles einfach mal gar nicht lief.

Danke!